

LOAD-DEFORMATION BEHAVIOR
OF SATURATED CLAYS
DURING UNDRAINED SHEAR

by

EDWARD BROOKS KINNER

B.C.E., Rensselaer Polytechnic Institute
(1961)

S.M., Massachusetts Institute of Technology
(1967)

Submitted in Partial Fulfillment of
the Requirements for the Degree

DOCTOR OF SCIENCE

at the

MASSACHUSETTS INSTITUTE OF TECHNOLOGY

June, 1970

Signature of Author

Department of Civil Engineering, May 4, 1970

Certified by

Thesis Supervisor

Accepted by

Chairman, Departmental Committee
on Graduate Students



ABSTRACT

LOAD-DEFORMATION BEHAVIOR OF SATURATED CLAY
DURING UNDRAINED SHEAR

by

EDWARD BROOKS KINNER

Submitted to the Department of Civil Engineering on
May 4, 1970 in partial fulfillment of the requirement for the
degree of Doctor of Science in Civil Engineering.

Comparisons are made between the predicted and observed behavior of a strip footing during undrained loading for the purpose of gaining additional insight into how improved engineering estimates of undrained stability and initial settlements can be made for structures that are to be placed on deposits of saturated clay.

Undrained load-deformation and bearing capacity data for idealized "field" conditions were obtained with the aid of model footing tests on Boston Blue Clay. The model footing tests were conducted at overconsolidation ratios of one, two, and four on undisturbed soil samples that had been one dimensionally consolidated from dilute slurries in the laboratory. Plane strain conditions were approximated in the tests by the use of a rectangular footing having a length to breadth ratio of eight.

Consolidated undrained plane strain, triaxial, and direct-simple shear tests were conducted for the purpose of obtaining information on the undrained strength, stress-strain modulus, E ; and K_0 , the coefficient of lateral stress at rest of the soil. These data were used in making theoretical predictions of the footing performance.

Undrained bearing capacity predictions were made with a bearing capacity theory in which strength anisotropy of the soil during undrained shear can be considered. Load-deformation predictions for the model footing were made with a bi-linearly elastic finite element program.

It is concluded that reasonable predictions of undrained bearing capacity for a strip footing on Boston Blue Clay can only be made if the effects of sample disturbance and strength anisotropy are considered.

The predicted load-deformation behavior of the model footing was dependent on the values of undrained shear strength, K_0 , and E that were specified in the analysis. Parametric studies

showed that average values of K_0 and of undrained strength from plane strain tests for each overconsolidation ratio could be used in making final correlations with the model test results. However, with the bi-linearly elastic finite element analysis it was not possible to make an a priori prediction of the modulus at all values of overconsolidation ratio that would lead to a good prediction of the model footing performance for the full range of loading. Rather, the choice of the best modulus value was dependent on consideration of the stress-strain properties of the soil for each stress history.

Thesis Supervisor:
Title:

Charles C. Ladd
Associate Professor of
Civil Engineering

ACKNOWLEDGEMENTS

The author is indebted to many individuals who have assisted him in his graduate studies and thesis research.

Professor Charles C. Ladd was the author's faculty advisor and thesis supervisor. His encouragement, interest, and advice throughout the author's graduate work is gratefully acknowledged.

Professor John T. Christian was a member of the author's doctoral committee. His assistance, particularly in the theoretical aspects of this research, was most helpful.

The work of Professor David J. D'Appolonia in the development of finite element program FEAST III and his advice during this research are appreciated.

Professor Anwar E.Z. Wissa made valuable suggestions concerning the design and development of equipment that was used in this investigation and provided helpful assistance concerning the experimental program.

Professors E.H. Davis and H.G. Poulos of the University of Sidney contributed valuable suggestions to this research.

Thanks is given to all other members of the Soil Mechanics faculty, both present and past, who contributed to this effort through their classroom instruction.

The assistance of Ernest Schmid and Ross T. McGuillivary in the design of equipment used in this investigation was most helpful.

The perseverance and cheerful assistance of Richard B. Bovee is gratefully acknowledged. Much of the test data discussed in this report

was obtained by others. Among these are W.A. Bailey, N.F. Braathen, J.W. Dickey, J.J. Rixner, and T. Okumura. Their efforts are appreciated.

Juraj Bajgar assisted the author in the performance of several of the model footing tests.

Elin Braathen drafted most of the figures in this thesis and Mrs. Erika Babcock typed the final draft.

Through a N.S.F. Traineeship, the National Science Foundation provided financial support to the writer for one year. Funds for the research and financial support for the other years of the writer's graduate studies were provided by the U.S. Army Waterways Experiment Station, Vicksburg, Mississippi.

Finally, the author is grateful to his wife, Judith, for her patience, guidance, and support during his graduate work. Her assistance was indeed invaluable.

TABLE OF CONTENTS

	<u>Page No.</u>
Title Page	1
Abstract	2
Acknowledgements	4
Table of Contents	6
List of Tables	9
List of Figures	11
CHAPTER 1 INTRODUCTION	18
1.1 Background	18
1.2 Purpose	19
1.3 Scope	20
CHAPTER 2 THEORETICAL CONSIDERATIONS AND REVIEW OF MODEL FOOTING TESTS	22
2.1 Theoretical Considerations	22
2.1.1 Initial Settlements	22
2.2.2 Undrained Stability	26
2.2 Review of Model Footing Tests	29
CHAPTER 3 MODEL FOOTING TESTS	37
3.1 Introduction	37
3.2 Test Procedures and Equipment Used for Model Footing Tests	37
3.3 Model Footing Tests	40
CHAPTER 4 UNDRAINED SHEAR TESTS	44
4.1 Introduction	44
4.2 Strength and Modulus Data From Plane Strain Tests	45
4.3 K_o Determinations	50

TABLE OF CONTENTS (Continued)

		<u>Page No.</u>
4.4	Triaxial Compression Tests	51
4.5	Direct-Simple Shear Tests	56
4.6	Comparison of Selected Data from Plane Strain, Triaxial Compression, and Direct-Simple Shear Tests	59
CHAPTER 5	CORRELATION OF PREDICTED AND OBSERVED BEHAVIOR	64
5.1	Introduction	64
5.2	Undrained Bearing Capacity Predictions	64
5.3	Influences of Soil Parameters on Predicted Load-Deformation Behavior	69
	5.3.1 Discussion of Finite Element Program FEAST III and the Finite Element Grids That Were Used	69
	5.3.2 Parametric Study Using Selected Soil Parameters	72
5.4	Finite Element Correlations of Predicted and Observed Behavior	80
	5.4.1 Presentation of Final Correlations	81
	5.4.2 Preliminary Considerations With Respect to the Choice of Modulus	84
	5.4.3 Discussion of the Final Correlation for an Overconsolidation Ratio of Four	89
	5.4.4 Discussion of the Final Correlation for an Overconsolidation Ratio of Two	92
	5.4.5 Discussion of the Final Correlation for an Overconsolidation Ratio of One	94
	5.4.6 Summary Remarks Concerning the Choice of Modulus Values for Use in Final Correlations	99
5.5	Additional Comments Concerning Finite Element Correlations	101
CHAPTER 6	SUMMARY, CONCLUSIONS, AND RECOMMENDATIONS	106

TABLE OF CONTENTS (Continued)

		<u>Page No.</u>
6.1	Summary and Conclusions	106
6.2	Recommendations for Further Research	109
CHAPTER 7	BIBLIOGRAPHY	112
CHAPTER 8	LIST OF NOTATION	118
TABLES		124
FIGURES		132
APPENDIX A	INDEX PROPERTIES OF BOSTON BLUE CLAY USED FOR PLANE STRAIN, DIRECT-SIMPLE SHEAR, AND MODEL FOOTING TESTS	177
APPENDIX B	DESCRIPTION OF MODEL TEST EQUIPMENT AND EXPERIMENTAL PROCEDURES	183
APPENDIX C	TABULATED TEST RESULTS AND OTHER INFORMATION ON MODEL FOOTING TESTS	213
APPENDIX D	MISCELLANEOUS INFORMATION ON PLANE STRAIN TESTS AND MEASUREMENTS OF K_o	240
APPENDIX E	MISCELLANEOUS INFORMATION ON \overline{CU} TRIAXIAL COMPRESSION TESTS	253
APPENDIX F	MISCELLANEOUS INFORMATION FOR CONSTANT VOLUME GEONOR DIRECT-SIMPLE SHEAR TESTS	260
APPENDIX G	FACTORS INFLUENCING FINITE ELEMENT CORRELATIONS	265
BIOGRAPHICAL NOTE		303

LIST OF TABLES

<u>Table No.</u>	<u>Title</u>	<u>Page No.</u>
4-1	Comparison of Normalized Modulus Values from Plane Strain, Triaxial, and Direct-Simple Shear Tests	124
5-1	Comparison of Measured Values of Ultimate Bearing Capacity and Those Predicted by Davis and Christian (1970) on the Basis of Anisotropic Undrained Shear Strength	125
5-2	Comparison of Measured Values of Ultimate Bearing Capacity and Those Predicted on the Assumption of Isotropic Undrained Shear Strength	126
5-3	Summary Information All Three Overconsolidation Ratios	127
5-4	Summary Information OCR = 1.0	128
5-5	Summary Information OCR = 2.0	129
5-6	Summary Information OCR = 4.0	130
5-7	Comparison of Strains After Yield With Failure Strains of Plane Strain Active Tests	131
A-1	Index Properties and Batch Information for Boston Blue Clay Used in Plane Strain and Direct-Simple Shear Tests	178
A-2	Index Properties of Boston Blue Clay Used in Several Model Tests	180
A-3	Approximate Mineralogical Data on Boston Blue Clay	181
C-1	Sample Preparation History	230
C-2	Elapsed Time for Secondary Compression for the Last 235 Normally Consolidated Increment	

LIST OF TABLES (Continued)

<u>Table No.</u>	<u>Title</u>	<u>Page No.</u>
C-3	Model Test Water Contents	236
D-1	Summary of Plane Strain Active Tests on Boston Blue Clay Summary of Plane Strain Passive Tests on Boston Blue Clay	241
D-2	K_o Determinations	243
E-1	Miscellaneous Information on \overline{CU} Triaxial Tests: Boston Blue Clay	254
E-2	Summary of \overline{CKU} Triaxial Compression Tests on Boston Blue Clay - 1968 Earth Physics Research	255
E-3	Summary of \overline{CIU} Triaxial Tests on Boston Blue Clay - Bailey (1961)	256
E-4	Summary of \overline{CU} Triaxial Tests on Boston Blue Clay - Braathen (1966)	258
F-1	Results of Constant Volume Direct-Simple Shear Tests on Boston Blue Clay	262
F-2	Constant Volume Direct-Simple Shear Tests on Recompressed, Overconsolidated Samples of Boston Blue Clay	264
G-1	Normally Consolidated Soil Properties Used In Comparative Study of Grids 1, 2, and 4	277
G-2	Soil Properties for the Evaluation of the Performance of Grid 4 for Use in Overconsolidated Correlations	278

LIST OF FIGURES

<u>Figure No.</u>	<u>Title</u>	<u>Page No.</u>
2-1	Elliptical Strength Plot for Anisotropic Clay Proposed by Davis and Christian (1970)	132
2-2	Bearing Capacity Factor Versus b/a Ratio	133
3-1	Equipment Arrangement at Final Consolidation - Bin One	134
3-2	Equipment Arrangement at Final Consolidation - Bin Two	135
3-3	Membrane for Bin Two	136
3-4	Bin Two at Time of Test	137
3-5	Model Footing Tests: Normally Consolidated Tests, Stress Ratio Versus Normalized Displacement	138
3-6	Model Footing Tests: Overconsolidation Ratio = 2. Stress Ratio Versus Normalized Displacement	139
3-7	Model Footing Tests: Overconsolidation Ratio = 4. Stress Ratio Vs Normalized Displacement	140
3-8	Stress Ratio Versus Normalized Displacement: Normally Consolidated Model Footing Tests	141
3-9	Stress Ratio Versus Normalized Displacement for Model Footing Tests at Three Overconsolidation Ratios	142
3-10	Ratio $\frac{\text{Average Applied Footing Stress}}{\text{Maximum Past Pressure}}$ Versus Normalized Displacement for Model Footing Tests at Three Overconsolidation Ratios	143
4-1	$s_u / \bar{\sigma}_{vc}$ and K_s Versus Log OCR: Plane Strain Tests Boston Blue Clay	144
4-2	Normalized Secant Modulus: Plane Strain Tests	145

LIST OF FIGURES (Continued)

<u>Figure No.</u>	<u>Title</u>	<u>Page No.</u>
4-3	Coefficient of Lateral Stress at Rest Versus Log Overconsolidation Ratio Boston Blue Clay	146
4-4	$s_u/\bar{\sigma}_{vc}$ Vs $\bar{\sigma}_{vc}$ for Normally Consolidated Boston Blue Clay Sheared in Triaxial Compression $s_u/\bar{\sigma}_{vc}$ Vs Preshear Consolidation Time for Normally Consolidated Boston Blue Clay Sheared in Triaxial Compression	147
4-5	$s_u/\bar{\sigma}_{vc}$ Vs $\bar{\sigma}_{vc}$ for Normally Consolidated Boston Blue Clay Sheared in Triaxial Compression	148
4-6	$s_u/\bar{\sigma}_{vc}$ Vs Log OCR, \overline{CIU} and \overline{CK}_oU Triaxial Compression Tests Boston Blue Clay	149
4-7	Normalized Secant Modulus Versus Time for Last Consolidation Increment for Normally Consolidated Triaxial Compression Tests	150
4-8	Normalized Secant Modulus Versus Consolidation Stress for Normally Consolidated Triaxial Compression Tests	151
4-9	Normalized Secant Modulus Versus Log OCR for Triaxial Compression Tests Boston Blue Clay	152
4-10	$(\tau_{h\max})/\bar{\sigma}_{vc}$ Vs Log OCR \overline{CUDSS} Tests	154
4-11	Normalized Pseudo Secant Modulus Versus Maximum Consolidation Stress Direct-Simple Shear Tests OCR = 1 and 8	155
4-12	Normalized Pseudo Secant Modulus Versus Log OCR Direct-Simple Shear Tests Boston Blue Clay	156
4-13	Comparison of $s_u/\bar{\sigma}_{vc}$ Vs Log OCR for Boston Blue Clay as Measured in Plane Strain, Triaxial Compression, and Direct-Simple Shear Tests	157

LIST OF FIGURES (Continued)

<u>Figure No.</u>	<u>Title</u>	<u>Page No.</u>
4-14	$\frac{s_u \text{ at } \bar{\sigma}_{vc}}{s_u \text{ at } \bar{\sigma}_{vm}}$ Vs Log OCR for Plane Strain, Triaxial Compression, and Direct-Simple Shear Tests	158
4-15	Comparison of Normalized Secant Moduli as Measured in Several Undrained Shear Tests	159
4-16	E/s_u Versus OCR Plane Strain, Triaxial Compression, and Direct-Simple Shear Tests at a Factor of Safety = 3	161
5-1	Comparison of Three Hypothetical Variations of Strength Anisotropy for $K_s = 0.6$	162
5-2	Effect of Variation on K_o on the Predicted Load-Deformation Behavior for Normally Consolidated Boston Blue Clay	163
5-3	Effect of Variation in K_o on the Predicted Load-Deformation Behavior for Boston Blue Clay OCR = 2	164
5-4	Effect of Variation in K_o on the Predicted Load-Deformation Behavior for Boston Blue Clay OCR = 4	165
5-5	Effect of Variation in Undrained Shear Strength on the Predicted Load-Deformation Behavior for Normally Consolidated Boston Blue Clay	166
5-6	Effect of Variation in Undrained Shear Strength on the Predicted Load-Deformation Behavior for Boston Blue Clay OCR = 2	167
5-7	Effect of Variation in Undrained Shear Strength on the Predicted Load-Deformation Behavior of Boston Blue Clay OCR = 4	168
5-8	Hypothetical Distributions of Undrained Shear Strength, $s_{u\alpha}$	169

LIST OF FIGURES (Continued)

<u>Figure No.</u>	<u>Title</u>	<u>Page No.</u>
5-9	Load-Deformation Predictions Obtained With Hypothetical Distributions of Undrained Shear Strength, s_{u0}	170
5-10	Comparison of Finite Element Prediction and Model Footing Tests for Normally Consolidated Boston Blue Clay	171
5-11	Comparison of Finite Element Prediction and Model Footing Test Results for Boston Blue Clay at an Overconsolidation Ratio of Two	172
5-12	Comparison of Finite Element Predictions and Model Footing Test Results for Boston Blue Clay at an Overconsolidation Ratio of Four	173
5-13	Comparison of Bi-Linear Elastic and Measured Stress-Strain Curves: Plane Strain Active Condition	174
5-14	Comparison of Bi-Linear Elastic and Measured Stress-Strain Curves: Plane Strain Passive Condition	175
5-15	Normally Consolidated Model Footing Tests Normalized With Respect to Stress Ratio for $\bar{\sigma}_{vc} = 3.38 \text{ kg/cm}^2$	176
A-1	Grain Size Distribution Boston Blue Clay	182
B-1	Vacuum Apparatus: Bin Two	205
B-2	Consolidation Plate with Removable O-Ring Feature	206
B-3	Linear Bushing Assembly for Guiding Consolidation Plate	207
B-4	Surcharge Bag: Bin One	208
B-5	Surcharge Membrane: Bin Two	209

LIST OF FIGURES (Continued)

<u>Figure No.</u>	<u>Title</u>	<u>Page No.</u>
B-6	Final Consolidation: Bin Two	210
B-7	Apparatus Arrangement at Time of Test: Bin One	211
B-8	Apparatus Arrangement at Time of Test: Bin Two	212
C-1	Void Ratio Versus Vertical Consolidation Stress for Model Loading Tests	237
C-2	C_{α} Values for the Last Normally Consolidated Increment of Each Test	238
C-3	Change in Void Ratio During Secondary Compression of the Last Normally Con- solidated Increment Versus Vertical Con- solidation Stress	239
D-1	Stress-Strain Curves Normally Consolidated Plane Strain Active Tests Boston Blue Clay	245
D-2	Stress-Strain Curves Normally Consolidated Plane Strain Passive Tests Boston Blue Clay	246
D-3	Stress-Strain Curves Plane Strain Active Tests Boston Blue Clay OCR = 2	247
D-4	Stress-Strain Curve Plane Strain Passive Test Boston Blue Clay OCR = 2	248
D-5	Stress-Strain Curves Plane Strain Active Tests Boston Blue Clay OCR = 4	249
D-6	Stress-Strain Curves Plane Strain Passive Test Boston Blue Clay OCR = 4	250
D-7	Normalized Secant Modulus Versus Applied Shear Stress Ratio for Plane Strain Active Tests with Boston Blue Clay	251
D-8	Normalized Secant Modulus Versus Applied Shear Stress Ratio for Plane Strain Passive Tests with Boston Blue Clay	252

LIST OF FIGURES (Continued)

<u>Figure No.</u>	<u>Title</u>	<u>Page No.</u>
E-1	Normalized Secant Modulus Versus Time for Last Consolidation Increment for Normally Consolidated \overline{CIU} Triaxial Compression Tests (Bailey 1961)	259
G-1	Finite Element Grid 1	279
G-2	Finite Element Grid 2	280
G-3	Finite Element Grid 4	281
G-4	Finite Element Grid 4A	282
G-5	Vertical Stress Distributions Under the Edge of a Uniformly Loaded Flexible Strip	283
G-6	Comparison of Results of Finite Element Predictions Employing Displacement and Stress Controlled Loading of the Footing, OCR = 4	284
G-7	Vertical Stress Distributions Under Footing for Two Finite Element Grids	285
G-8	Normalized Lateral Displacement With Depth for Nodes Under Edge of Footing, Grid 1	286
G-9	Normalized Lateral Displacement With Depth for Nodes Under Edge of Footing, Grid 2	287
G-10	Normalized Lateral Displacement With Depth for Nodes Under Edge of Footing, Grid 4	288
G-11	Normalized Lateral Displacement With Depth for Nodes B/4 From Side of Footing, Grid 1	289
G-12	Normalized Lateral Displacement With Depth for Nodes B/4 From Side of Footing, Grid 2	290
G-13	Normalized Lateral Displacement With Depth for Nodes B/4 From Side of Footing, Grid 4	291
G-14	Comparison of Yielded Zones for Three Finite Element Grids at Similar Normalized Displacements	292

LIST OF FIGURES (Continued)

<u>Figure No.</u>	<u>Title</u>	<u>Page No.</u>
G-15	Comparison of Yielded Zones for Three Finite Element Grids at Similar Normalized Displacements	293
G-16	Yielded Zone for Grid 2 Run With Isotropic Undrained Shear Strength	294
G-17	Comparison of Finite Element Predictions Obtained with Different Grids Using the Same Soil Properties	295
G-18	Normalized Lateral Displacements With Depth for Nodes Under Edge of Footing, Grid 4, OCR = 2	296
G-19	Normalized Lateral Displacement With Depth for Nodes B/4 From Side of Footing, Grid 4, OCR = 2	297
G-20	Normalized Lateral Displacement With Depth for Nodes Under Edge of Footing, Grid 4, OCR = 4	298
G-21	Normalized Lateral Displacement With Depth for Nodes B/4 From Side of Footing, Grid 4, OCR = 4	299
G-22	Yielded Zones Near Failure for Over-consolidated Cases: Grid 4	300
G-23	Influence of Size of Load Increment on Load-Settlement Predictions Using FEAST III	301
G-24	Comparison of Finite Element Predictions Obtained With Grids 4 and 4A	302

CHAPTER 1

INTRODUCTION

1.1 BACKGROUND

Estimates of two major factors, stability and settlement, are usually required when designing earth structures and foundations that are to be placed on deposits of saturated clay.

Stability calculations are made to ascertain the safety of the structure with regard to ultimate collapse. Emphasis in stability calculations is normally given to the most critical condition occurring during or following construction. For many foundations problems on clay deposits, this critical period occurs at the end of construction for nearly undrained conditions, when little if any dissipation of excess pore pressures has occurred, Bishop and Bjerrum (1960).

Estimates of total settlements are made so that the structure may be designed for anticipated movements. The total settlement that a foundation may experience is generally considered to consist of three components:

- a. The first, an initial or immediate settlement, is caused by deformation of the soil at constant volume (undrained conditions) under the imposed shear stresses.
- b. A time-dependent settlement, commonly known as primary consolidation, occurs as the volume of the clay mass changes due to increasing effective stress upon dissipation of the excess pore pressure.
- c. A settlement known as secondary compression or secondary consolidation occurs wherein the volume

of the clay changes under conditions of apparent constant effective stress.

This report is concerned with the undrained stability and initial settlements of foundations on saturated clay. Estimating the undrained stability of a foundation is very important for in many cases this is the most critical condition from the standpoint of safety. Estimating initial settlement is important because the existence of large initial settlements may indicate an approaching undrained failure. Furthermore, initial settlements are the starting point from which to analyze primary and secondary consolidation.

Direct observations of undrained stability in the field must either be made with special load tests or test embankments or after unexpected failures. Therefore, observations of undrained stability in the field require either special and expensive procedures or undesirable conditions. An analysis of the initial settlements in the field is desirable so that the reliability of the predictions that had been made might be ascertained. Complicated field conditions frequently make this analysis difficult. For these reasons, it is desirable that the engineer have reference "field" data upon which to judge the reliability of his predictions of undrained stability and settlement. These reference "field" data may be obtained with the aid of model footing tests.

1.2 PURPOSE

The research described in this report was conducted for the purpose of making comparisons between the predicted behavior of a

strip footing and the measured "field" behavior of the footing as simulated in the laboratory model footing tests. The intent of the research was to develop a body of knowledge that might be utilized to make improved engineering estimates of undrained stability and initial settlements for plane strain foundation problems on saturated clays.

1.3 SCOPE

Undrained stability and initial settlements were studied with the aid of model footing tests in the laboratory under carefully controlled conditions. The equipment that was developed employed a rectangular footing having a length to breadth ratio of eight. This permitted simulating plane strain foundation conditions that are frequently encountered in practice.

A comprehensive series of undrained model footing tests was conducted on samples of Boston Blue Clay (liquid limit approximately 40 percent) having overconsolidation ratios of one, two, and four. Normally consolidated tests at three values of effective stress were conducted for the purpose of observing normally consolidated "field" behavior over a range of consolidation stresses.

Undrained strength and stress-strain data (normally consolidated and overconsolidated) from plane strain, triaxial, and direct-simple shear tests on Boston Blue Clay were compiled, analyzed, and compared for use in making theoretical predictions of the performance of the model footing.

Undrained stability predictions were made using a bearing capacity

theory developed for application to cohesive soils that exhibit anisotropic undrained shear strength. Load-deformation predictions, throughout the full range of loading, were made with the aid of a bi-linearly elastic finite element program in which anisotropic initial stresses and strength anisotropy could be specified. Detailed studies were made of the influence that variations in undrained strength, stress-strain modulus, and the coefficient of lateral stress at rest have on the predicted performance of the model footing.

It is shown that stability calculations for undrained bearing capacity conditions can be greatly in error unless anisotropy with respect to undrained strength is considered. Recommendations are made concerning how improved predictions of initial settlements in the field can be made with the aid of finite element techniques. Suggestions are presented for additional laboratory and analytical effort that this research has shown to be desirable.

CHAPTER 2

THEORETICAL CONSIDERATIONS AND REVIEW OF MODEL FOOTING TESTS

2.1 THEORETICAL CONSIDERATIONS

Consideration is given in this section to methods by which the initial settlements and undrained stability may be estimated for foundations such as the model footing employed in this research. Initial settlements will be discussed in Section 2.1.1 and undrained stability will be considered in Section 2.1.2.

2.1.1 Initial settlements

Several theoretical approaches may be employed to estimate the initial settlements of foundations on clay. Elastic solutions are frequently used. If the soil is reasonably homogeneous, it may be possible to characterize the deposit as a single elastic layer. The initial settlement can then be estimated using an equation of the form:

$$\rho = \sigma \frac{B}{E} I \quad (1)$$

where

ρ is the initial settlement of the foundation

σ equals the average stress imposed on the soil by the foundation

B is a convenient foundation dimension (usually the width in the case of a rectangular footing)

E is the undrained Young's modulus of the soil and

I is an appropriate influence factor determined for Poisson's ratio equal to 0.5.

Influence values are presented by several authors. Poulos (1967), for example, gives influence values that can be used to calculate the settlement of a strip footing resting on an elastic layer of finite depth underlain by a rough rigid base. Influence values presented by Janbu, et al. (1956) can be used to estimate initial settlements for a range of foundation embedments, strata thicknesses, and footing shapes.

For cases where the underlying clay is composed of several layers or in cases where it is desirable to divide a homogeneous deposit into several layers, Davis and Poulos (1968) proposed using a numerical integration approach to compute the immediate settlements. In this approach, the footing settlement is calculated by summing the strains of the individual layers using an expression of the form:

$$\rho = \sum \frac{1}{E} \left[\sigma_z - 0.5 (\sigma_x + \sigma_y) \right] \delta h \quad (2)$$

where δh is the thickness of each layer, and representative increments of vertical and horizontal total normal stress are given by σ_z , and σ_x and σ_y respectively.

Classical elastic stress distribution theories are employed in determining the influence values for use in equation (1) and the stress increments used with equation (2). For the stress ranges usually encountered in practice, soils do not behave as linearly elastic

materials. Methods that retain a portion of the classical elastic theory but that include consideration of the aforementioned non-linear behavior have been presented for estimating initial settlements.

Lambe (1964) used elasticity theory to compute the increments of normal stress that were imposed at selected points below the foundation. However, in this method, the strains determined in laboratory tests on soil specimens subjected to these representative field stresses are integrated over the depth of the soil to estimate the initial settlement.

Davis and Poulos (1968) retained the use of equations (1) and (2). The non-linear behavior of the soil is considered in their method by using modulus values that are determined in undrained shear tests on soil samples subjected to stresses representative for the problem under consideration.

Both methods were developed for axi-symmetric foundation problems. However, the principles of the methods are applicable to plane strain conditions.

Both approaches are subject to the limitation that the strains and redistribution of stress that accompany yielding of the soil cannot be considered in the estimate of initial settlement. Thus if significant yielding occurs in the soil it is expected that neither approach will yield accurate predictions of the initial settlement. In their paper, Davis and Poulos show that the foundation stress required to cause first yield is dependent on the undrained strength and coefficient of lateral stress at rest of the clay. It is shown for

normally consolidated clays, that the factor of safety with respect to undrained bearing capacity failure for a strip footing at first yield is typically greater than four. The corresponding factors of safety for lightly overconsolidated clays are shown to be from two to four. Thus, since local yielding occurs in most foundation problems on clay, it is desirable that methods be employed that consider this behavior.

Recently, theoretical methods have been developed that can be utilized to estimate initial settlements, even though local yielding occurs. Christian (1966), and Hoëg, et al. (1968), used a lumped parameter model to predict the load-deformation behavior of a strip footing resting on an elastic-plastic soil which yielded in accordance with the Tresca yield criterion.

Foundation performance after first yield can be studied with the aid of finite element techniques. Plane strain problems can be studied with finite element program PLASAD, MIT (1968). As with the lumped parameter model, it is assumed with this program that the soil exhibits an isotropic shear strength that is characterized by the Tresca yield criterion.

Finite element program FEAST III, D'Appolonia (1968) and D'Appolonia and Lambe (1970), employs a bi-linearly elastic stress-strain relationship. In this approach, the elastic properties of the soil are modified when the imposed shear stresses in an element equal or exceed the specified yield stress. Although this stress-strain relationship can closely approximate elastic-perfectly plastic behavior, stress and strain remain uniquely related after yield. Program FEAST III

has been employed extensively in the research described in this report.

2.2.2 Undrained Stability

It has long been recognized that clays can exhibit anisotropic strength. An early mention of this fact was made by Casagrande and Carrillo (1944), and Hansen and Gibson (1949) made theoretical predictions of its influence. But only recently has considerable effort been devoted to the study of the magnitude and causes of strength anisotropy and to the solution of engineering problems that consider this behavior. Several reviews of the state-of-the-art concerning anisotropic strength in clays have recently been made: Ladd and Varallyay (1965), Bishop (1966), Duncan and Seed (1966) and Baker and Krizek (1970). The causes of strength anisotropy have been categorized as follows:

- a) anisotropy of the effective stress-strength parameters
- b) anisotropy with respect to pore pressure development
- c) rotation or reorientation of the principal stresses during shear.

It is difficult, if not impossible, at the present time to isolate and study the effects of the individual sources of strength anisotropy when dealing with the solution of stability problems in the field. Nevertheless, it is important that the net effect of this physical behavior be considered.

The implications of strength anisotropy were outlined by Ladd and Bailey (1964). The results of undrained triaxial tests on Boston Blue Clay were presented to demonstrate that significant differences

in undrained shear strength can occur when samples of this clay are subjected to a reorientation of principal stresses during shear. Based on the results of these tests, Ladd and Bailey pointed out that due to differences in total stress paths, it was possible that variations in undrained strength could occur along potential failure surfaces below footings and foundations on normally consolidated deposits of clay. Hence, the average undrained strength along potential failure surfaces would be a function of the strength anisotropy.

Ladd and Bailey further noted that when the results of vane and unconfined tests are used in making predictions of undrained stability, satisfactory predictions might be made because of compensating errors. For instance, Bishop and Bjerrum (1960) used the results of these tests to analyze several end of construction failures of fills and footings resting on saturated clays. Factors of safety of approximately one were obtained. Ladd and Bailey suggested that the lower measured strengths of the unconfined and vane tests, relative to $\overline{CK}_0 UC$ triaxial tests,¹ resulted from sample disturbance and reorientation of principal stresses respectively. Satisfactory stability predictions might be obtained since use of these low strengths was offset by the presence of a low average insitu strength, relative to the $\overline{CK}_0 UC$ strength, because of anisotropic strength behavior.

Numerous solutions to engineering problems that consider strength anisotropy have been proposed. For example Hansen (1952)

¹ $\overline{CK}_0 UC$ Anisotropically consolidated triaxial compression test.

formulated solutions for passive earth pressure and bearing capacity problems on anisotropic clays. Duncan and Seed (1965), Lo (1965), Rangantham and Matthai (1967), and others have considered slope stability problems for cases of anisotropic strength. Of particular interest to the research described in this report is the work of Davis and Christian (1970) and D'Appolonia (1968).

Davis and Christian (1970) presented a method that can be employed to estimate the undrained bearing capacity of a strip footing resting on an anisotropic clay. They assumed that the strength anisotropy of a clay can be characterized by an elliptical strength plot as shown in Figure 2-1. s_{uv} in the figure is the undrained shear strength for vertical compression, i.e. the major principal stress, σ_1 , is in the insitu vertical direction. s_{uh} and $s_{u\theta}$ are the undrained strengths measured when σ_1 is oriented horizontally and θ degrees from the vertical respectively at failure. Using the method of stress characteristics, Davis and Christian determined that N_c , the bearing capacity factor, varied as b/a , the ratio of the half axes of the elliptical strength plot. N_c for a surface strip footing varies as shown in Figure 2-2. Once the appropriate N_c value of the soil has been determined, the bearing capacity of a strip footing is estimated as N_c times the average of s_{uv} and s_{uh} . Davis and Christian noted for most clays that N_c could be expected to be between 4.75 and 5.14. This represents an eight percent variation in the ultimate bearing capacity for the same average of s_{uv} and s_{uh} . The Davis and Christian theory is employed later in this report to predict the

undrained bearing capacities of the model footing tests.

The capability to consider strength anisotropy was incorporated in finite element program FEAST III, D'Appolonia (1968). Therefore, when use of this program is made, predictions of both load-deformation behavior and bearing capacity can be made for an anisotropic clay. As noted earlier, this program is employed extensively in the research described in this report. Anisotropic strength is assumed to vary in the program in accordance with the distribution proposed by Casagrande and Carrillo (1944).

2.2 REVIEW OF MODEL FOOTING TESTS

Small scale footing tests have been employed extensively in soil mechanics research. A comprehensive survey of footing tests conducted prior to 1959 was made by Roberts (1961). Six references were cited that dealt with tests on cohesive soils. All laboratory programs cited considered either remolded clays or "undisturbed" samples from the field that were placed in containers for testing. One interesting observation from these early footing tests was that the ultimate bearing capacity for a strip footing was found to be approximately equal to 5.1 times the shear strength of the soil measured in unconfined tests.¹ Roberts pointed out that very little effort had been made in

¹ Laboratory model footing tests on remolded or compacted clays have continued. Among these are Young, et al. (1966), Goodman, et al. (1966), Perloff and Rahim (1966), and Brown (1967). The investigation by Brown concerned layered clays.

these investigations to study footing behavior as a function of the stress-strain characteristics of the soil.

Recently, emphasis in model tests has been directed toward more fundamental studies of footing behavior for idealized "field" conditions in which anisotropically consolidated deposits of saturated clay are simulated in the laboratory. A review of some of this work is presented here.

Model footing tests on Spestone Kaolin, liquid limit 74 percent, were conducted by Burland (1967). A detailed description of the equipment and a review of a preliminary portion of the research is given by Burland and Roscoe (1969). Emphasis in the research to date has been directed toward making comparisons of predicted and observed behavior during periods of primary consolidation subsequent to the application of footing loads. Relatively little effort has been given toward the study of initial settlements. Thus, most of the work is not directly applicable to the research described in this report. However, a brief description of the tests is given here for they are considered to be of general interest with respect to equipment development and testing procedures for model footing investigations of the type described in this report.

The tests were conducted for the purpose of evaluating a theory for the stress-strain behavior of "wet" clay that is under development at Cambridge University. Rectangular footing were employed with widths of one and two inches and a length of six inches. The soil to be tested was anisotropically consolidated, under a back pressure, from a slurry

having an initial water content of about twice the liquid limit. Lead shot were placed in the slurry prior to consolidation so that observations of subsurface movements could be made. Initial consolidation increments were performed with a hydraulically actuated piston operating from the bottom of the container and final consolidation was conducted with a rubber membrane that enclosed the footing at the top of the unit. All tests reported have been on normally consolidated samples that were consolidated to the same initial vertical effective stress.

A stress controlled loading of the footing was employed. In both of the tests reported to date, three load increments were used with 24 hour intervals being allowed for consolidation between them. The nominal factor of safety with respect to undrained bearing capacity failure for the first load increments was greater than 2.9. No bearing capacity tests were reported. Rather, the bearing capacity was calculated to be 5.14 times the undrained shear strength determined from simple shear tests. Settlement occurring within 10 seconds of the load application was assumed to be initial settlement. This initial settlement was noted to always be less than 10 percent of the final settlement that existed after primary consolidation was complete. For a factor of safety of three, the ratio of the consolidation settlement to footing width was 0.04. Hence, the initial settlement for this test was less than about 0.004 times the footing width.

Model footing tests conducted at the University of Sidney are described by Poulos (1964) and Davis and Poulos (1968). The tests were conducted to aid in the development and evaluation of a method for

predicting the initial and total final settlements and the rate of consolidation settlement under three dimensional conditions for foundations on clay soils. Tests were conducted on two normally consolidated clays: a kaolin with a liquid limit of 55 percent and Hurstville Clay with a liquid limit of 43 percent.

A soil container 12 inches in diameter was used. Circular footings of 1, 2, and 5 inches were employed for most tests. The different footing sizes permitted observation of footing behavior for various ratios of foundation width to strata thickness. Apparatus construction and experimental procedures permitted footing behavior to be studied for a wide range of hydraulic boundary conditions.

The soil was placed in the apparatus at a water content within a few percent of the liquid limit. The footing was placed on the slurry surface prior to consolidation. Consolidation stresses were then applied to the top surface of the sample with a rubber membrane pressurized by water. The pretest vertical effective stress was about 30 psi, and a back pressure of 20 psi was employed. Most of the tests were stress controlled wherein the footing was loaded instantaneously with dead weights. Observations of footing settlement with time were then made. At the time of load application, the nominal factor of safety against undrained bearing capacity failure varied from approximately 4 to 16. The undrained bearing capacity was estimated to be N_c times the undrained shear strength of the soil determined from anisotropically consolidated triaxial compression tests.

Of particular interest is the fact that comparisons were made

between the measured and predicted initial settlements of the model footings. Initial settlements were predicted from three dimensional elastic displacement and stress distribution theory, as discussed in the previous section, using undrained stress-strain modulus data from anisotropically consolidated triaxial compression tests. The predicted values were consistently from three to 73 percent greater than the observed values. The primary reason for the reported discrepancies arose from the values of undrained modulus used in making the predictions. Values of strain for the modulus calculations were taken when the pore pressures in the stress controlled triaxial tests had equalized and become stationary. The authors reported that a considerable amount of creep occurred in the triaxial tests by this point. In contrast they stated that the same amount of creep could not have occurred during the few seconds which elapsed in the model tests before the readings of initial settlement were taken. These observations point out the considerable influence that the choice of the modulus value has on predictions of footing performance.

It is also of interest to note that the authors conducted three displacement controlled tests, two on Kaolin and one on Hurstville Clay to study the load-settlement behavior of footings under conditions where no appreciable excess pore pressures developed. The two Kaolin tests employed very different sized footings. A two inch diameter footing was used in one test and a half inch diameter one was used in the second. When plotted in terms of normalized displacement¹, the tests exhibited

¹ Normalized displacement is defined as the footing penetration divided by the footing diameter.

almost identical behavior. This suggests that any edge effects that existed in the test with the half inch diameter footing were no more severe than those for the test with the two inch diameter footing.

Model footing tests are currently being employed in research in Japan. Aboshi, Yoshikuni, and Uchibayashi (1969) report the results of studies that were conducted to examine the stability of foundations in which consolidation is accelerated by the use of vertical cardboard drains. A highly plastic clay from the Inland Sea of Japan is being used. Considerable emphasis to date has been given to observing the pattern of subsurface movements during the tests. Since no load-deformation behavior, bearing capacity values, or undrained shear strength data on the clay used in the above tests have been reported, information from these tests is of little direct benefit to the research described in this report. However, mention is made of this work since effort is currently being directed toward the measurement of excess pore pressures, total stresses, and subsurface strains during the footing tests. These results should be of interest to any one engaged in model footing studies in the future.

Model footing tests have been conducted at M.I.T. for the purpose of investigating the load-settlement-time behavior of circular footings on normally consolidated Boston Blue Clay. This work is described in detail by Alvarez-Stelling (1966) and Gicot (1966). A review of some of the research is given by Perez-La Salvia, et al. (1966).

A circular footing 2 inches in diameter was used for all tests. All samples were consolidated in a 12 inch diameter bin to a vertical

effective stress of two kg/cm². An initial slurry water content of about 75 percent was used. Consolidation to 1.75 kg/cm² was performed with an air driven hydraulic ram and a consolidation plate. The footing was placed in the apparatus for the final consolidation increment that was performed with a rubber surcharge bag pressurized by air. Stress controlled tests were conducted by Alvarez-Stelling in which the footing was loaded instantaneously with dead weights. Values of initial settlement were obtained by extrapolating the plots of footing settlement versus the square root of time to zero time. Predictions of initial settlement were made using solutions from elasticity theory and the stress path method, Lambe (1964). In general, agreement between the predicted and observed values was not good. Initial settlements when expressed in terms of normalized displacement varied from 7.5×10^{-4} to 1×10^{-2} as the approximate factor of safety with respect to bearing capacity failure decreased from 4 to 1.3. Thus, the initial settlement increased by a factor of 13 as the factor of safety decreased by a factor of three.

Gicot consolidated piezometers in the clay in order to observe excess pore pressure behavior at selected locations under the footing. Interpretation of the pore pressure data is somewhat difficult because of the experimental techniques which were employed.

Both Alvarez-Stelling and Gicot conducted bearing capacity tests. Increments of load were applied to the footing over a period of several minutes. Interpretation of these bearing capacity data is somewhat difficult because of the testing procedures that were adopted.

Several observations can be drawn from this review. Model footing

tests have only recently been employed in efforts to study footing behavior for idealized field cases in which anisotropically consolidated deposits of saturated clay are simulated in the laboratory. Primary emphasis in these investigations has been given to studies of the time rate of settlement of the footings or to observations of subsurface movements. Although initial settlements have been studied, no detailed investigation has yet been made of the magnitude of initial settlements throughout the full range of loading, from zero load to failure. Consideration in several of the studies has been given to correlating the observed initial settlements with the undrained stress-strain behavior of the soil. However, it is evident that much is still unknown concerning how the stress-strain behavior of a soil as measured in undrained shear tests can be utilized to accurately predict footing performance.

Laboratory bearing capacity studies have been made with compacted, remolded, and "undisturbed" field samples of clay. However, no program (other than that reported here) is known to exist wherein bearing capacity observations have been made for both normally consolidated and overconsolidated samples of a completely undisturbed, one dimensionally consolidated clay that is known to be highly anisotropic with respect to undrained shear strength.

In each of the programs reviewed, all of the normally consolidated tests employed approximately the same vertical consolidation stress. Therefore, observations have not been made of normally consolidated "field" behavior on the same clay for a range of vertical consolidation stresses.

CHAPTER 3

MODEL FOOTING TESTS

3.1 INTRODUCTION

A comprehensive series of model footing tests was conducted for the purpose of observing the "field" performance of a strip footing for undrained loading conditions on saturated clay. Tests at over-consolidation ratios of one, two, and four were performed on "undisturbed" samples of Boston Blue Clay that were one dimensionally consolidated from dilute slurries. Boston Blue Clay is a silty clay of moderate plasticity with typical index properties as follows: liquid limit 40 percent, plasticity index 20 percent, and activity 0.4. Detailed classification data for this soil are presented in Appendix A.

A description of the test procedures and equipment is given in Section 3.2. The model footing test results are presented in Section 3.3.

The results of 14 tests, each requiring about two weeks' work are reported here. Eight to ten other tests were conducted before perfecting the test procedures and equipment.

3.2 TEST PROCEDURES AND EQUIPMENT USED FOR MODEL FOOTING TESTS

The test procedures and equipment used during the model footing tests are described in this section. The intent of this investigation was to obtain high quality load-deformation and bearing capacity data for a strip footing during undrained loading conditions under idealized

field conditions. Plane strain conditions for the strip footing were approximated by the use of a rectangular footing having a length to breadth ratio of eight (length five inches, width 0.625 inches). Completely undisturbed, anisotropically consolidated samples of clay were used to simulate idealized field conditions. The undisturbed samples of clay that were employed were obtained by consolidating soil in 12 inch diameter bins.

The soil was placed in the bins under a partial vacuum at a water content of 100 percent, about two and a half times the liquid limit. Consolidation to the desired pretest effective stress was performed in several increments in two stages. The initial consolidation was performed with a stainless steel consolidation plate and a 5000 pound capacity air operated Karol Warner Conbel loader. After this stage, the plate was removed and the footing placed in the bin. Depending on the apparatus being used, consolidation was then continued with either a latex surcharge bag or a latex membrane, pressurized by water. Both the bag and membrane were specifically developed for this investigation. Bin One used the surcharge bag. The equipment arrangement for final consolidation and testing is shown in Figure 3-1. Bin Two, Figure 3-2, employed a latex membrane. A rectangular recess was formed in both the surcharge bag and membrane to house the footing. This is illustrated for the membrane with Bin Two in Figure 3-3.

At least one additional increment of virgin compression, and all the overconsolidated increments, were conducted with the surcharge bag or membrane. Except for one test, the ratio of the total increment ($\Delta\bar{\sigma}_v$) of virgin compression under the bag or membrane to that with the

consolidation plate varied from 0.6 to 1.25. Thus, the samples of clay were completely undisturbed at the time of testing.

Standardized procedures were followed throughout the experimental program. Particularly close control was maintained of initial slurry water contents, batch consolidation, and times of "aging" at the maximum past pressure, $\bar{\sigma}_{vm}$. The ratio (T_s/T_p) of the time permitted for secondary compression to the time for primary consolidation at $\bar{\sigma}_{vm}$, varied from 2.16 to 6.15. As will be seen in the following chapter, this range of T_s/T_p is comparable to that for the plane strain tests that were used extensively in the analysis of the model test results.

Detailed information for each of the tests is given in Appendix C. This includes data on consolidation, initial and final water contents, aging, secondary compression, and tabulated test results.

Observations of footing load and settlement were made during the tests. The footing load was monitored with a load cell and the displacement obtained with a linear displacement transducer. Data from these devices were collected on an X-Y recorder. During the tests the footing was advanced into the clay at a constant rate. Undrained tests were performed wherein the footings were taken to failure within about 15 seconds.

A photograph of the equipment arrangement for Bin Two at the time of the test is shown in Figure 3-4. Of particular interest in this photograph is the loading system that was employed. The load cell, with which the footing load was applied, was screwed into a horizontal cross arm that was restrained to move in a vertical direction by two

one inch diameter shafts passing through linear bushings. The dead weight of these components was supported by two springs. The cross arm was connected to a worm gear screw jack that was advanced at a constant rate by the electric motor shown resting on the stand at the left of the figure. The electric motor was connected to the jack with a universal joint linkage and reduction gear.

Additional information is given in Appendix B concerning the test equipment and experimental procedures that were employed. This includes supplementary photographs of the equipment.

3.3 MODEL FOOTING TEST RESULTS

Normally consolidated model footing tests were conducted at three vertical consolidation pressures: 1.0, 2.0, and 3.38 kg/cm². The overconsolidated tests had a maximum past pressure of 3.38 kg/cm².

The test results are presented in terms of $\sigma/\bar{\sigma}_{vc}$ versus ρ/B . The stress ratio, $\sigma/\bar{\sigma}_{vc}$, is equal to the average net applied footing stress, σ , divided by the vertical effective consolidation stress at the time of the test, $\bar{\sigma}_{vc}$ ¹. The normalized displacement, ρ/B , equals the footing displacement, ρ , divided by the footing width, B .

A composite plot of the normally consolidated tests is given in Figure 3-5. It is of particular interest to note in this figure that

1

The surcharge pressure during undrained shear was maintained equal to the vertical consolidation stress $\bar{\sigma}_{vc}$.

very reproducible results were obtained at each consolidation stress. Seating effects occurred occasionally. These were eliminated in the figure by defining zero normalized displacement to be at a factor of safety of five for each test.¹ The factor of safety was computed relative to $\sigma/\bar{\sigma}_{vc}$ at $\rho/B = 0.1$.

Examination of Figure 3-5 shows that the tests did not exhibit normalized behavior. The load-settlement behavior and ultimate bearing capacities for each stress level fall within distinct bands. At $\rho/B = 0.1$, the $\sigma/\bar{\sigma}_{vc}$ value for the tests with $\bar{\sigma}_{vc} = 1.0 \text{ kg/cm}^2$ is about six percent greater than that for the tests at $\bar{\sigma}_{vc} = 3.38 \text{ kg/cm}^2$. This indicates a slight reduction in the normalized strength, $s_u/\bar{\sigma}_{vc}$, with increasing consolidation stress. The data indicate that the normalized stress-strain modulus of the clay in undrained shear, $E/\bar{\sigma}_{vc}$, is not unique and is affected more significantly by the magnitude of $\bar{\sigma}_{vc}$ than is the normalized strength $s_u/\bar{\sigma}_{vc}$. Modulus data for tri-axial and direct-simple shear tests that are cited in the next chapter also show decreasing normalized moduli with increasing effective stress.

The non-uniqueness in the load-deformation behavior has important practical application. It has been recommended, Ladd and Lambe (1963), that "undisturbed" samples obtained from the field be consolidated to stresses greater than the insitu stresses and normalized parameters used in order to minimize the effects of sample disturbance. This sampling and consolidation process may destroy the soil structure that originally existed insitu, Bjerrum (1967). In addition to this problem, the data in Figure 3-5 suggest that by virtue of the differing

¹ The maximum adjustment to the "measured" ρ/B was 0.0027.

effective stresses, the measured stress-strain modulus of the laboratory specimen can be significantly different from that exhibited insitu. Fortunately, changes in undrained strength arising from the differences in $\bar{\sigma}_{vc}$ are not as large, at least for this particular clay.

The test results for overconsolidation ratios of two and four are given in Figures 3-6 and 3-7 respectively. Once again it is seen that excellent agreement existed among the tests at each stress history.

Plane strain conditions did not exist near the ends of the footing. The predictions of footing behavior that will be discussed in Chapter Five were made for plane strain conditions. Accordingly, the $\sigma/\bar{\sigma}_{vc}$ values of the model tests have been reduced by approximately 2.5 percent to correspond to plane strain stresses. The guidelines of Meyerhof (1951) were followed and are discussed in Appendix B.

Average curves for each stress level or stress history were prepared after the data were adjusted by 2.5 percent to be comparable to plane strain conditions. The average curves for the three normally consolidated stress levels are shown in Figure 3-8. The average curves for the overconsolidated tests and the normally consolidated tests at $\bar{\sigma}_{vc} = 3.38 \text{ kg/cm}^2$ are given in Figure 3-9.

The modulus that was effective for each overconsolidation ratio prior to first yield was calculated from the theory of elasticity using the method proposed by Janbu, et.al. (1956).¹ When normalized with respect to the vertical undrained plane strain strength² the computed

¹ Determination of first yield was made with the aid of finite element predictions discussed in Chapter Five.

² The vertical undrained plane strain strength is discussed in Chapter Four.

moduli, E/s_u , are 950, 815, and 610 for overconsolidation ratios of one, two, and four respectively. The decreasing ratio of modulus to s_u with increasing overconsolidation ratio means that the modulus decreases more rapidly upon rebound than does the strength.¹

The changes in the absolute values of modulus and strength that occur upon rebound are illustrated in Figure 3-10. The data in this figure have been replotted from Figure 3-9 by normalizing the average footing contact stress (plane strain conditions) with respect to the maximum past pressure, $\bar{\sigma}_{vm}$. This is a particularly informative plot, for it is seen that at any ρ/B value, $\sigma/\bar{\sigma}_{vm}$ decreases as the overconsolidation ratio increases.

Predictions of the model footing behavior will be made in Chapter Five. The model footing tests will be considered again there.

¹ Similar observations are made in Chapter Four with respect to E/s_u values computed from undrained plane strain, triaxial, and direct-simple shear tests.

CHAPTER 4

UNDRAINED SHEAR TESTS

4.1 INTRODUCTION

In order to make correlations between the measured performance of the model tests and those predicted by theoretical methods, information is needed concerning the behavior of Boston Blue Clay in undrained shear following one dimensional consolidation. The following soil parameters must be specified when making a load-deformation prediction with a finite element analysis: s_{uv} , K_s , K_o , and E . Information is needed concerning s_{uv} and K_s for making undrained bearing capacity predictions. The parameter s_{uv} is defined as the undrained shear strength ($\tau_{max} = q_f$) of the soil specimen, determined from a test in which the major principal stress is in the insitu vertical direction at failure. The parameter K_s is a measure of the strength anisotropy of the soil. It is equal to the ratio s_{uh}/s_{uv} where s_{uh} represents the undrained shear strength (q_f) resulting from a test wherein the major principal stress at failure is in the direction coincident with the insitu horizontal plane. The ratio $\bar{\sigma}_{hc}/\bar{\sigma}_{vc}$ represents the coefficient of lateral stress at rest, K_o . Young's modulus, E , is used to characterize the stress-strain behavior of the soil.

The engineer frequently encounters problems that approximate plane strain conditions. The model tests performed during this investigation employed a rectangular footing having a length to breadth ratio of eight. This is a good approximation to plane strain conditions. The results from undrained shear tests in a plane strain device are therefore of direct interest in this investigation. Since plane strain equipment is only beginning to become available to the practicing engineer, it is useful to compare the

results of triaxial tests with those from plane strain tests. The Norwegian Geotechnical Institute direct-simple shear device is easier to use than plane strain equipment, and it models a horizontal failure surface. It is therefore of interest to compare test results determined with this equipment with those from plane strain and triaxial tests.

Test data from the three types of equipment are summarized and compared in this chapter. Throughout this discussion emphasis is placed on data from those tests that have direct applicability when making bearing capacity predictions and finite element analyses of the load-deformation behavior of the model footing tests described in this report. The range of overconsolidation ratios for the three classes of tests is not constant, and in the case of the triaxial and direct-simple shear tests exceeds that of the model tests. Information has been included for these higher overconsolidation ratios, since it was deemed useful to compile these data in one reference.

4.2 STRENGTH AND MODULUS DATA FROM PLANE STRAIN TESTS

Plane strain data cited here were obtained with the M.I.T. plane strain device described by Dickey, Ladd, and Rixner (1968) and Bovee and Ladd (1970). Data reported by Rixner (1967); Dickey, Ladd, and Rixner (1968); and Bovee, Kinner, and Ladd (1970) are discussed here. Tests have been conducted for overconsolidation ratios of one, two, and four.

The M.I.T. plane strain device uses a sample 3.5 inches wide by 3.5 inches high by 1.4 inches deep and has the following capabilities: (1) K_0 consolidation with removable side platens; (2) measurement of K_0 ; (3) vertical and horizontal stresses, σ_v and σ_h , can be varied independently; (4) the sample can be sheared by increasing or decreasing σ_v or by increasing or

decreasing σ_h . All tests reported herein were strain controlled with σ_v being either increased or decreased to produce failure.

The Boston Blue Clay samples used in these tests were consolidated from dilute slurries in the laboratory using procedures similar to those discussed in Appendix B for preparation of the soil in the model tests. Prior to use, the consolidated batches of clay were stored in oil. Classification data and batch information on the soil are given in Appendix A.

Plane strain active (compression) tests yield strength and stress-strain data corresponding to s_{uv} . All tests conducted to date have had K_o values less than one. Therefore, these active test results correspond to conditions where the orientation of the major principal stress during consolidation and shear has been constant. Plane strain passive (extension) tests yield strength and stress-strain data corresponding to s_{uh} . Because of the aforementioned K_o conditions, all passive tests conducted to date have experienced a reorientation of the major principal stress during shear. Two types of passive tests have been employed. The first is the vertical K_o test in which the sample is trimmed in the conventional manner and consolidated with $\bar{\sigma}_{1c}$ in the vertical direction. A passive (extension) test is performed by reducing the vertical stress on the specimen. The second type is the horizontal K_o test.¹ The sample is trimmed from the batch of clay at an orientation 90° from that employed for the active and vertical K_o passive tests. The sample is consolidated with $\bar{\sigma}_{1c}$ in the horizontal direction in the apparatus. The horizontal direction in the apparatus, therefore, corresponds to the insitu vertical direction. Undrained shear is conducted by increasing the vertical stress in the apparatus. Thus, the sample experiences a reorientation of the principal stresses during shear. The stress-strain modulus computed from this test,

¹Consolidation and subsequent shear of this type were reported by Duncan and Seed (1966 b).

when multiplied by $(1-\nu^2) = 0.75$, is a measure of E_h , Young's modulus in the insitu horizontal direction.

Summary tables of the tests are contained in Appendix D. Representative stress-strain curves for the active and passive tests at OCR's of one, two, and four are presented in Figures D-1 through D-6. Detailed plots illustrating the effective stress behavior of these tests during shear are given in Bovee, Kinner, and Ladd (1970). This information has been studied to assess the reliability of the data. However, since correlations employing total stress parameters have been made, the effective stress plots for these tests are not duplicated in this report. Modulus data for several of the tests are given in Figures D-7 and D-8.

The variation of $s_{uv}/\bar{\sigma}_{vc}$, $s_{uh}/\bar{\sigma}_{vc}$, and K_s with overconsolidation ratio for Boston Blue Clay in plane strain shear are shown in Figure 4-1. The values of $s_{uv}/\bar{\sigma}_{vc}$ for the three overconsolidation ratios are considered to be reliable. The effective stress paths to the maximum stress difference for overconsolidation ratios of one and four compare favorably, geometrically, with those for \overline{CK}_0U triaxial compression tests. No \overline{CK}_0U triaxial tests at an overconsolidation ratio of two were available for comparison. It will be shown later that the average $s_{uv}/\bar{\sigma}_{vc}$ curve in Figure 4-1 and a similar curve for \overline{CK}_0U triaxial compression tests are in good agreement.

Difficulties have been encountered with the passive tests. The most persistent problem has been that of computed obliquities that were too high at strains greater than about two percent. In those tests where this problem existed, undrained failure was defined to have occurred at $\text{ARCSIN } q/\bar{p} = 40^\circ$. It is recognized that highly overconsolidated soils can exhibit high obliquities at low strains. This point was borne in mind so as to avoid a premature definition of undrained failure in the case of

the overconsolidated samples. Furthermore, in those vertical K_o tests where necking may have been a problem, undrained failure was defined to occur at the point of inflection of the stress strain curve.¹ The steps taken to resolve these problems are discussed in detail in Bovee and Ladd (1970).

The plot of K_s in Figure 4-1 is based on the average $s_{uv}/\bar{\sigma}_{vc}$ curve and the curve shown for the passive tests. For overconsolidation ratios from one to four, the K_s values indicate that Boston Blue Clay is highly anisotropic when subjected to a reorientation of principal stresses during undrained shear in plane strain.

Values of normalized secant modulus were computed from the test results. These plane strain moduli, adjusted by the factor $(1-\nu^2) = 0.75$ to permit comparison with undrained triaxial data, are shown in Figure 4-2 for three factors of safety. The factor of safety is defined as the ratio of the change in shear stress required to cause failure at q_f to the total change in shear stress at the point in the test under consideration, $\Delta q_f / \Delta q$.

Ladd (1964) has discussed how the measured stress-strain modulus of a soil can be dependent on such factors as aging, strain rate, and environment. Using a viscoelastic model, Watt (1969) has shown how the stress-strain modulus of a soil determined from a laboratory test can be dependent on strain rate. Using creep data typical of moderately

¹ This was done for two tests, P-1 and P-2. The computed values of $\bar{\phi}$ at the points of inflection were 25.3 and 28.3 degrees respectively.

plastic clays (San Francisco Bay Mud) Watt predicted that the secant modulus of an isotropically consolidated sample sheared at a strain rate of 1.0 percent per hour would be four percent greater at 2.5 percent axial strain than that of a sample tested at 0.6 percent per hour. Strain rates of 0.5 and 1.0 percent per hour were used in the plane strain tests. Differences in the computed moduli arising from this difference in strain rate are considered minimal, if existent at all. Batch preparation procedures were standardized early in the testing program to minimize variations in the test results due to preparation factors.

A deliberate effort was made to minimize the effect of variations in aging time. A standard 24 hour period for the last normally consolidated consolidation increment was adopted. This criterion was met for all the tests plotted in Figure 4-2, except for one of the two active tests at an OCR = 2. Therefore, the tests had times of secondary compression of from 16 to about 22 hours under the last normally consolidated increment.

Secondary compression was computed from the time the side platens were released for those tests in which they were used. One of the two tests at an OCR = 2 had six hours of secondary compression. The ratio of the time for secondary to the time for primary consolidation, T_s/T_p , thus varied from two to seven.

All tests had a nominal maximum past pressure, $\bar{\sigma}_{vm}$, of 4 kg/cm² except for the two active tests at an OCR = 4. These tests had $\bar{\sigma}_{vm}$ values of 2.9 and 5.8 kg/cm². The effect that the magnitude of $\bar{\sigma}_{vm}$ has on the measured modulus will be discussed in relation to the triaxial and CUDSS tests.

Even though scatter does exist in the data in Figure 4-2, trends with increasing overconsolidation ratio have been indicated wherever possible. Secant modulus values for the full range of loading during these tests are given in Figures D-7 and D-8.¹

At factors of safety of three and four, the passive moduli at each OCR are approximately equal to or greater than the active moduli. This behavior is reasonable in spite of the much larger values of Δq , since at the early stages of the passive tests the shear stresses acting on the samples are being released. By $\Delta q_f / \Delta q = 2$, the $E_s / \bar{\sigma}_{vc}$ values from the passive tests are less than those for the active. This is attributed to the much larger strains exhibited by the passive tests prior to failure.

4.3 K_o DETERMINATIONS

Many measurements of K_o for Boston Blue Clay have been made with the plane strain device. Other determinations have been made during anisotropically consolidated triaxial tests. Triaxial and plane strain K_o determinations are reported here for OCR's of one, two, and four. Square oedometer tests described by R. Ladd (1965) were used to make the first determinations of K_o for overconsolidated Boston Blue Clay. He reported K_o values for OCR's up to 96.

A summary plot of K_o measurements from several sources is given in Figure 4-3. Table D-2, Appendix D, lists K_o values for several

¹ Modulus data from two passive tests at an OCR = 4 are given in Figures 4-2 and D-8, while strength data from only one test are reported in Table D-1. The Δq_f value for test PSP-12 was used to plot the modulus information for the second test.

triaxial and plane strain tests. All K_0 values noted for the plane strain device were computed on the basis of the lateral stress applied to the cell membranes.

The results reported by R. Ladd (1965) are from one sample which was subjected to two cycles of virgin compression and overconsolidation. The ranges of virgin compression were from 2 to 8 and from 10 to 12 kg/cm². His measurements did not indicate that K_0 was dependent upon stress level in the normally consolidated range. Likewise, no dependence of K_0 on $\bar{\sigma}_{vc}$ is seen in Table D-2 for virgin compression. At an OCR = 4, K_0 as measured in the plane strain device is about 15 percent lower than the values determined from triaxial and square oedometer tests. The reason for this is not clear.

4.4 TRIAXIAL COMPRESSION TESTS

An extensive review of existing triaxial compression test data on Boston Blue Clay was undertaken for the primary purpose of developing relationships for the variation of undrained strength, measured at maximum stress difference, and stress-strain modulus with overconsolidation ratio. Factors such as the reproducibility of test results, the effects of the magnitude of preshear consolidation stresses, and aging were considered. Data obtained at M.I.T. from 1961 to 1968 were used. These included tests reported by Bailey (1961), Ladd and Varallyay (1965), and Braathen (1966). Other data from Earth Physics research which have not been previously reported were also included. Summary information for these tests is given in Appendix E, Table E-2. Summary data from Bailey (1961) and Braathen (1966) are given in Tables E-3 and E-4 respectively.

All these tests were performed on clay which had been consolidated from dilute slurries in the laboratory and stored in oil before use. The index properties and other information about the samples are listed in Appendix E, Table E-1. Data from "undisturbed" natural samples were not employed since it was desired to work with a family of tests for which the stress history, origin, and other factors such as environment were as well defined as possible.¹ This discussion is limited to tests wherein the pore fluid salt concentration was constant throughout batch preparation, consolidation, and shear. Triaxial extension tests were not considered, since no overconsolidated extension data exist.

In Figure 4-4 the $s_u/\bar{\sigma}_{vc}$ ratios for the normally consolidated tests are plotted versus the preshear consolidation stress and time. No dramatic trend exists in the data as a result of the variations in index properties, pore fluid salt concentrations, or batch preparation procedures of the clay over the period of research under consideration.

The data have been replotted in Figure 4-5 in a manner permitting study of the combined effect of $\bar{\sigma}_{vc}$ and of T_s . For a constant $\bar{\sigma}_{vc}$ there is a fairly consistent increase in $s_u/\bar{\sigma}_{vc}$ with increasing T_s . This is particularly apparent at $\bar{\sigma}_{vc} = 6 \text{ kg/cm}^2$. A similar trend for Drammen Clay was reported by Bjerrum (1967).

The average $s_u/\bar{\sigma}_{vc}$ ratio for the \overline{CIU} tests with $\bar{\sigma}_{vc}$ greater than two kg/cm^2 is 0.308. That for the \overline{CK}_0U tests is 0.323. It has

¹ However, the \overline{CU} triaxial data on Boston Blue Clay from the M.I.T. campus show very similar behavior to that of resedimented BBC, Ladd and Luscher (1965).

been shown previously that the difference in the above undrained strength ratios for $\overline{CK}_O U$ and \overline{CIU} triaxial compression tests is not large, Ladd (1965).

The shear strength ratio, $s_u / \bar{\sigma}_{vc}$ versus the log of the overconsolidation ratio for the tests is shown in Figure 4-6.¹ Insufficient data are available to permit making a distinction between the overconsolidated $\overline{CK}_O U$ and \overline{CIU} tests.

As with the plane strain tests, the stress-strain moduli for the tests were studied by considering how the normalized secant modulus, $E_s / \bar{\sigma}_{vc}$, varied with stress level, $\Delta q_f / \Delta q$, and overconsolidation ratio. The strain rates for the triaxial tests reported here varied from 0.68 to 1.2 percent per hour. Differences in the computed moduli arising from this range of strain rates are not considered significant.

As seen in Figure 4-4, the differing environment between the "salt" and "water" samples employed by Bailey (1961) did not result in a consistent difference in the undrained strengths of the two types of samples. This has been discussed in detail by Ladd and Kinner (1967). This difference in environment was also found not to have had any dramatic effect on the stress strain moduli computed from Bailey's tests. (See Appendix E, Figure E-1.) This observation plus those made with respect to Figure 4-4 suggest that differences in the stress-strain behavior

¹ The void in the strength data between OCR's of 1 and 4 is not as large as it first appears. The author had access to strength data on overconsolidated BBC in this region which are not cited here. This information was used as a general guide to locating the curves in this region.

among the batches of clay as reflected by computed values of $E_s/\bar{\sigma}_{vc}$, arising from variations in preparation procedures are small.

The normalized secant moduli at $\Delta q_f/\Delta q = 2$ for the normally consolidated samples are plotted in Figure 4-7 versus the time allowed under the last consolidation increment, T_s . Even though scatter exists, an increase in the normalized secant modulus for Boston Blue Clay with increased aging is indicated. D'Appolonia (1968) reached similar conclusions for Boston Blue Clay aged up to a maximum of about 100 hours. An increase in the stress-strain modulus with aging for other soils has been reported by Wissa (1961), Bjerrum and Lo (1963), and Ladd (1964).

It is often assumed for normally consolidated clays that the modulus is proportional to the consolidation stress, i.e. a constant normalized modulus. The influence of the magnitude of the preshear consolidation stress on the normalized secant moduli for the normally consolidated samples is illustrated in Figure 4-8.¹ While conflicts in the data do exist, it is concluded from the \overline{CIU} tests in this figure that the normalized secant modulus for Boston Blue Clay is not necessarily constant but may decrease with increasing consolidation pressure for a fixed time of aging. The effect may be more important with lower times of T_s . It also may be more important for \overline{CIUC} than for \overline{CK}_oUC tests.

¹ The number of tests in Figure 4-8 is less than those in Figure 4-4 and 4-5. Difficulty was encountered in interpreting the initial modulus data for some tests. The strength data have been used for those tests where the uncertainty concerning $(\sigma_1 - \sigma_3)_{max}$ was small.

Data presented by Lambe and Whitman (1969)¹ indicate that a similar conclusion can be drawn for at least one other clay, Lagunillas Clay. Data which they present show a downward curvature of strain contours drawn through effective stress paths of $\overline{\text{CIU}}$ tests at different values of $\bar{\sigma}_{\text{vc}}$. Working at much smaller strains than those existing here, Hardin and Black (1968) found that the shear modulus, G, for normally consolidated clay varied (at constant void ratio) as $\sqrt{\bar{\sigma}_{\text{vc}}}$ rather than $\bar{\sigma}_{\text{vc}}$. The observation concerning the data in Figure 4-8 is not for a case where changes in void ratio have been isolated.

These observations indicate that attention should be given to the magnitude of the preshear effective stress for normally consolidated samples and to the maximum past pressure for overconsolidated samples in any study involving comparisons of soil behavior, particularly modulus, with overconsolidation ratio.

Ten of the twelve overconsolidated triaxial tests studied had a $\bar{\sigma}_{\text{vm}}$ equal to six kg/cm². Accordingly, whenever possible with the $\overline{\text{CIU}}$ tests, the variation in $E_s/\bar{\sigma}_{\text{vc}}$ with OCR has been compared with normally consolidated samples having $\bar{\sigma}_{\text{vc}} = 6 \text{ kg/cm}^2$. Owing to the limited number of tests, no such distinction could be made with the $\overline{\text{CK}_0\text{U}}$ samples.

The resulting variations in normalized secant modulus with overconsolidation ratio are shown in Figure 4-9 for three factors of safety, $\Delta q_f/\Delta q$, with respect to undrained shear failure. To eliminate the effects of aging as much as possible, only those normally consolidated tests having T_s of four days or less have been used. All known T_s values at $\bar{\sigma}_{\text{vm}}$ for the overconsolidated tests were from one to four

¹ Page 457.

days. The normalized modulus relationship for the \overline{CIU} tests reaches a maximum at an OCR from six to eight depending on the factor of safety under consideration. For overconsolidation ratios of one and four the normalized modulus values for the \overline{CK}_0U tests are on the average about twice those for the \overline{CIU} tests.

4.5 DIRECT-SIMPLE SHEAR TESTS

An extensive series of constant volume shear tests has been performed on samples of Boston Blue Clay using the direct-simple shear device described by Bjerrum and Landva (1966). Some of these tests have been reported by Edgers (1967). A description of the equipment, its calibration, and the testing procedures that are employed are given by Edgers. The results of all the constant volume tests conducted by Edgers plus several of the tests conducted subsequently are summarized in Table F-1. A brief summary of tests on recompressed, overconsolidated samples is also contained in Appendix F. All tests reported here were performed on samples which were trimmed from batches of clay previously consolidated from dilute slurries in the laboratory. Classification data and batch information on the soil are given in Appendix A.

The exact meaning of the strength measurements obtained with the apparatus is not yet known. This is the subject of current research. An axi-symmetric, linearly elastic, finite element analysis is being made of the cylindrical sample which is used in the apparatus.

Accordingly, no attempt has been made to date to adjust the measured values of maximum horizontal shear stress to arrive at the value of maximum shear stress needed for making direct comparisons with triaxial

and plane strain undrained strength data.

Duncan and Dunlop (1969) attempted such a comparison. They applied the results of a finite element analysis made for a prismatic simple shear sample patterned after Roscoe (1953) to the cylindrical Geonor direct-simple shear sample. They assumed that the imposed simple shear stresses could be approximated by an increment of pure shear. Their approach yielded a reasonable value for the undrained strength of Manglerud Clay. However, an examination of their method in terms of effective stresses showed that the required $\bar{\phi}$ was greater than 45° . The assumption that the imposed shear stresses are those of pure shear can not be correct for normally consolidated Boston Blue Clay since this assumption leads to computed values of $\bar{\sigma}_3$ that are negative at $(\tau_h)_{\max}/\bar{\sigma}_{vc}$ and $(\tau_h/\bar{\sigma}_v)_{\max}$.

Even in view of the unknowns concerning the measured strength values, it is of interest to compare the $\overline{\text{CUDSS}}$ results, in terms of $(\tau_h)_{\max}$, with those obtained from triaxial and plane strain tests. Modulus data obtained from this device are also of considerable interest.

The variation of $(\tau_h)_{\max}/\bar{\sigma}_{vc}$ with overconsolidation ratio for OCR's up to eight is shown in Figure 4-10. A comparison of these data with triaxial and plane strain results will be made in the next section.

The $\overline{\text{CUDSS}}$ sample undergoes a shear strain during the test wherein the base of the sample is held stationary and the top is translated horizontally. The modulus computed from this test is not a shear modulus in the strict sense of the word, since the sample does not experience a pure distortional deformation at constant volume under a

fixed net normal load. Nevertheless, the computed modulus, τ_h/γ , is considered to be a first approximation to the shear modulus in the vertical plane, G_{vh} . For an undrained soil possessing isotropic elastic properties $E = 2G(1+\nu) = 3G$.

Examination of the plane strain test results has already shown that moduli in the horizontal and vertical directions are unequal. However, if the assumption of isotropy is invoked, a comparison of moduli can be made among the three types of tests by using a value of E computed from the equation above for the \overline{CUDSS} tests. In the following discussion, the modulus so computed will be called a pseudo-secant modulus.

The modulus information obtained from the \overline{CUDSS} tests is very consistent. Consolidation times of from 18 to 24 hours were allowed at $\bar{\sigma}_{vm}$ for all tests. The values of T_s/T_p varied from about 9 to 11.

Strain rate effects with this device were investigated by Edgers (1967). He conducted tests at 2.5 to 20 percent per hour. (See tests 201 through 204, Table F-1.) No dramatic strain rate effects were observed. Except for tests 201, 202, and 204 all constant volume tests have been conducted at a strain rate of five percent per hour.

The normalized pseudo-secant moduli for the tests with OCR's of one and eight are plotted in Figure 4-11 for a factor of safety, $(\tau_h)_{max}/\tau_h$ equal to two. Numbers beside the symbols denote the strain rates for the three "non-standard" strain rate tests. As with the triaxial data in the previous section, a decreasing normalized modulus with increasing $\bar{\sigma}_{vm}$ is observed. The data in this figure are particularly revealing, for the same trend is seen for both stress histories. This observation underlines the point made in the previous

section concerning the importance of standardizing of the maximum past pressure in studies involving normally consolidated and overconsolidated samples.

The variation in the normalized pseudo-secant modulus with overconsolidation is shown in Figure 4-12 for three factors of safety. With the exception of one sample, all tests used to prepare this figure had $\bar{\sigma}_{vm} = 4 \text{ kg/cm}^2$. The normalized pseudo-secant modulus reaches a maximum value at an OCR of about four.

4.6 COMPARISON OF SELECTED DATA FROM PLANE STRAIN, TRIAXIAL COMPRESSION, AND DIRECT-SIMPLE SHEAR TESTS

Strength and modulus data from the plane strain, triaxial, and direct-simple shear tests are compared in this section for the purposes set forth at the beginning of the chapter. A comparison was made in Section 4-3 of K_o data obtained from \overline{CK}_oU triaxial and plane strain tests. It will be recalled for overconsolidation ratios of one and two that K_o values measured in the two apparatus were in general agreement with those reported by R. Ladd (1965). For an overconsolidation ratio of four the plane strain results were somewhat lower than the triaxial and oedometer data.

Comparisons of strength data from the several types of undrained shear tests are given in Figure 4-13. For purposes of the comparison s_u for the \overline{CUDSS} tests has been defined as $(\tau_h)_{max}$. The average curves developed earlier for each stress system have been plotted. The average values of $s_u/\bar{\sigma}_{vc}$ from the plane strain active tests are about five percent greater than the triaxial compression

values. Thus as a first approximation, the engineer could, in the absence of plane strain equipment, use triaxial compression tests at the appropriate OCR to estimate the value of $s_{uv}/\bar{\sigma}_{vc}$ for Boston Blue Clay.¹

At overconsolidation ratios from approximately four to six, K_o is close to one. It might be expected that the strength measured in plane strain active and passive tests would be approximately equal for these OCR's. They are not. This indicates that the soil has anisotropic properties, perhaps arising from the fabric of the soil which is developed during one dimensional consolidation, Martin and Ladd (1970).

General agreement between the plane strain passive and direct-simple shear tests is also noted in Figure 4-13 for OCR's up to four. This agreement should be considered somewhat fortuitous since the \overline{CUDSS} test has never been shown to correspond to the plane strain passive condition, and $(\tau_h)_{max}$ was defined as s_u in the figure. It should also be remembered that some difficulty has been experienced with the plane strain passive tests.² However, in the absence of a plane strain device, the engineer can obtain an approximation to $s_{uh}/\bar{\sigma}_{vc}$ for Boston Blue Clay for overconsolidation ratios up to four by using the \overline{CUDSS} strength, $(\tau_h)_{max}/\bar{\sigma}_{vc}$. It should be noted that a \overline{CUDSS} test is easier, faster, and hence, less costly to run than either a $\overline{CK_U}$ triaxial or

¹ A similar observation can be made with respect to normally consolidated Weald Clay, Henkel and Wade (1966).

² The influence that uncertainties in $s_{uh}/\bar{\sigma}_{vc}$ have on load-deformation predictions are discussed in the following chapter.

plane strain test.

Data in Figure 4-13 for overconsolidation ratios of one, two, four, and eight have been replotted as appropriate in Figure 4-14. This figure expresses the strength at any overconsolidation ratio as a fraction of that existing at the maximum past pressure, $\bar{\sigma}_{vm}$. As expected, the triaxial and plane strain active tests are in good agreement.

The relative positions of the data in Figure 4-14 for the four types of tests are considered correct. With increasing OCR, the effect of the reorientation of the principal stresses during shear should decrease as K_o approaches one. It is expected that continuation of these curves to higher overconsolidation ratios would ultimately lead to a computed K_s greater than 1. Bishop (1966) and D'Appolonia (1968) present triaxial data for London Clay and Boston Blue Clay respectively which indicate that this is possible. Unconsolidated-undrained triaxial compression data reported by D'Appolonia indicate that K_s equals one at an OCR = 16. Additional research is needed to define the overconsolidation ratio at which this will occur under plane strain conditions for Boston Blue Clay. The intermediate position of the \overline{CUDSS} curve in Figure 4-14 is expected since the samples tested in this apparatus experience a reorientation of principal stresses at failure that is probably between about 30 and 60°. As explained in Section 4.2, all active and passive tests to date have experienced 0 and 90 degrees reorientation of the principal stresses during shear respectively.

Normalized secant moduli from the three shear devices are compared in Table 4-1 and Figure 4-15 for three factors of safety with

respect to undrained shear failure. The best estimate of the average value for each factor of safety and test condition has been listed. Better agreement in some cases between the \overline{CK}_0U triaxial and plane strain active tests could be achieved if the triaxial data were reduced to the same time at $\bar{\sigma}_{vm}$ as existed for the plane strain and \overline{CUDSS} tests. However, this was not done in view of the scatter in the data and the averaging required to develop the table and figure.

In general, normalized moduli from the \overline{CK}_0U triaxial tests are equal to or greater than the plane strain active moduli. As expected, the larger axial strains in the \overline{CIU} tests yielded secant modulus values which were lower than those of the \overline{CK}_0U triaxial compression and plane strain active tests. For the factors of safety and overconsolidation ratios considered, the normalized secant moduli for the \overline{CIU} tests are typically from 1.5 to 2.5 times lower than those computed from plane strain active tests. This approximate relationship might be used to estimate modulus values for plane strain active conditions when plane strain and \overline{CK}_0U triaxial compression test data are not available.

The agreement between the \overline{CIU} and \overline{CUDSS} moduli is fortuitous since in the \overline{CIU} tests no reorientation of stresses occurred, whereas they were reoriented in the \overline{CUDSS} device. Additionally $q = 0.5(\sigma_1 - \sigma_3)$ was employed in the \overline{CIU} computations, whereas τ_h was used for the \overline{CUDSS} tests. The principal stresses are rotated in the passive test as well. However, this occurs as the shear stresses pass through zero. The high initial passive moduli are associated with this stress release.

An entirely different situation exists in the $\overline{\text{CUDSS}}$ test since the principal stresses are rotated in the company of shear stresses.¹ Such a condition occurs at many points in the soil underlying a strip footing.

No approximately constant relationship is seen among the modulus values from plane strain passive tests and other test data that have been studied. However, it is seen that for factors of safety greater than about three, the normalized moduli from plane strain passive tests are greater than the values from $\overline{\text{CK}}_0\text{U}$ triaxial compression or plane strain active tests. At lower factors of safety, the much larger strains in the passive tests result in normalized secant modulus values that are lower than those for these other tests.

Examination of the data shows that the ratio E_s/s_u for each test decreases with increasing overconsolidation ratio. This is illustrated in Figure 4-16 at a factor of safety for each test of three. This indicates that the decrease in the absolute value of the modulus is greater at a given overconsolidation ratio than is the decrease in the absolute value of undrained strength. A similar observation was made with respect to the values calculated from the model tests prior to first yield.

¹ Other factors as yet undefined may also contribute to the low modulus values of the anisotropically consolidated $\overline{\text{CUDSS}}$ tests.

CHAPTER 5

CORRELATION OF PREDICTED AND OBSERVED BEHAVIOR

5.1 INTRODUCTION

The results of correlations between the ultimate bearing capacity and load-deformation behavior observed during the model footing tests and those predicted by theoretical methods are presented in this chapter. The values of undrained bearing capacity measured in the tests are considered in Section 5.2. Stability predictions are made there for cases of both anisotropic and isotropic undrained shear strength. With the aid of finite element program, FEAST III, a parametric study was performed to investigate the influences that variations in soil parameters have on the predicted load-deformation behavior of the model footing. This study is discussed in Section 5.3. Final finite element correlations with the model tests are discussed in Section 5.4. Additional factors concerning the finite element correlations are discussed in Section 5.5.

5.2 UNDRAINED BEARING CAPACITY PREDICTIONS

The bearing capacity measurements obtained during the model footing tests presented in Chapter Three are the first undrained bearing capacity determinations that have been made for both normally consolidated and overconsolidated stress histories of a clay that is known to be highly anisotropic with respect to undrained shear in plane strain. The average s_{uh}/s_{uv} ratio for Boston Blue Clay at over-

consolidation ratios of one, two, and four was shown in the previous chapter to be about 0.6.

In this section comparisons are made among the ultimate bearing capacities measured in the model footing tests and those predicted by the Davis and Christian (1970) theory on the basis of anisotropic undrained shear strength. Comparisons are also made among the measured bearing capacities and values predicted under the assumption that Boston Blue Clay exhibits isotropic undrained strength as measured in unconsolidated-undrained triaxial tests and in several of the undrained shear tests discussed in Chapter Four.

With the Davis and Christian method, the ultimate bearing capacity of a surface strip footing is equal to $N_c \left[\frac{s_{uv} + s_{uh}}{2} \right]$. As shown in Figure 2-2, N_c varies from 4.0 to 5.14 depending on the anisotropic strength ellipse of the soil. It will be recalled from the discussion of this theory in Chapter Two that for most clays N_c will not be less than about 4.75.

The parameters s_{uv} and s_{uh} can be determined from plane strain active and passive tests. However, information from other sources is required to define the anisotropic strength distribution of the soil.

D'Appolonia (1968) conducted an extensive series of unconsolidated undrained (UU) triaxial compression tests on samples of Boston Blue Clay cut with their axes inclined at 0° , 30° , 45° , 60° , and 90° from the insitu vertical direction. The purpose of these tests was to establish a variation of undrained strength for this soil with rotation of the principal planes. D'Appolonia (page 146) was unable to draw

conclusions regarding a specific distribution of undrained shear strength for Boston Blue Clay. Therefore, his tests do not provide information that is of direct benefit in the choice of N_c .¹

Other criteria must therefore be used to determine N_c . Hypothetical distributions of strength might be employed and the resulting variations in N_c determined. The Davis and Christian strength ellipse for $K_s = 0.6$ and $N_c = 5.14$ is shown in Figure 5-1. Two other distributions of strength are shown for comparison. Both were prepared for $K_s = 0.6$. The first (shown by the dashed line) is the Casagrande and Carrillo distribution. This is the distribution of strength employed in finite element program FEAST III. Although not elliptical, it is seen that the Casagrande and Carrillo relation for this K_s value yields an N_c value that is approximately 5.14. The third relation in the figure represents the probable lower limit of the anisotropic strength relation for Boston Blue Clay for OCR's from one to four.² This distribution is also not elliptical. However, an approximate b/a ratio for it was determined in order to estimate N_c . The resulting N_c is 5.0. Also shown in the figure is a shaded area that represents the probable range of the \overline{CUDSS} test results. This was determined

¹ Even if a distribution of strength had been observed, it would not necessarily be that existing during the model tests. The UU samples experienced an isotropic preshear stress state. Furthermore, they were subjected to disturbance resulting from trimming and handling, and the release of the anisotropic consolidation stresses that existed during batch consolidation. In comparison, samples in the model tests were undisturbed and subjected to anisotropic consolidation stresses prior to shear.

² This relation will be discussed further in regard to Figure 5-8. It is labeled there as curve 3.

assuming that the reorientation of principal stresses at $(\tau_h)_{\max}$ is from 45 to 60 degrees and that $s_u = (\tau_h)_{\max} / \cos \bar{\phi}$ where $\bar{\phi} = 30$ degrees. The CUDSS results and the three hypothetical distributions of anisotropic strength all indicate that an N_c of approximately 5.14 could be used. Accordingly, the value of 5.14 was chosen for use in making bearing capacity predictions with the Davis and Christian theory.

The values of undrained strength used in making predictions with this theory were taken from Figure 4-1 and are as follows:

<u>OCR</u>	<u>$s_{uv} / \bar{\sigma}_{vc}$</u>	<u>$s_{uh} / \bar{\sigma}_{vc}$</u>	<u>K_s</u>
1	.34	.18	.53
2	.58	.35	.605
4	.94	.58	.617

Comparisons of the observed undrained bearing capacities and those predicted by the Davis and Christian theory are given in Table 5-1. Excellent agreement is seen between the measured and predicted values of bearing capacity at each overconsolidation ratio.

The comparisons that were made among the measured bearing capacity values and those predicted from several undrained shear tests in Chapter Four on the basis of isotropic undrained strength are given in Table 5-2. The undrained strength used in each case was taken from the average curves in Figure 4-13. An additional comparison was made for each OCR using UU test data on vertical samples from D'Appolonia (1968). Specimens were cut from batches of clay prepared in the same fashion as for the model footing tests. These are also given in Table

5.2. An N_c value of 5.14 was used in all cases.

The comparisons in these two tables clearly demonstrate that significant error will result if the anisotropic undrained strength of Boston Blue Clay for these overconsolidation ratios is ignored. The maximum difference between the measured ultimate bearing capacities and those predicted on the basis of anisotropic strength was seven percent. However, only in one case was the percent difference between the observed value and that predicted assuming isotropic undrained strength less than 15 percent. If the soil is assumed to exhibit isotropic undrained shear strength in accordance with either plane strain active or \overline{CIU} triaxial compression tests, the bearing capacity is over predicted from 10 to 28 percent. Conversely, the bearing capacity is under predicted by about 25 percent if direct-simple shear test results are employed.¹ If UU test data are employed, the effects of sample disturbance result in a 25 to 30 percent under prediction in the bearing capacity. Thus, depending on the undrained shear data employed in the analysis, either unconservative or over conservative predictions of undrained stability will result if the soil is assumed to exhibit isotropic strength. From the standpoint of both safety and economics, it is desirable that the strength anisotropy of the soil and the effects of sample disturbance be considered when making bearing capacity predictions. To achieve this end, a theory that considers strength anisotropy should be combined with laboratory tests that are

¹ If the mean τ_h from the \overline{CIU} tests is increased by 15 percent to yield an estimated q_f , then the error is about 10 percent on the low side.

performed to determine the necessary anisotropic strength parameters of the soil.

In the case of the Davis and Christian theory, it is desirable that plane strain active and passive tests be conducted to determine s_{uv} and s_{uh} for use in the analysis. However, as noted earlier, the results of plane strain tests are not sufficient to choose N_c . Other test data, trial and error procedures, or some additional criterion might be used to choose this parameter.

5.3 INFLUENCES OF SOIL PARAMETERS ON PREDICTED LOAD-DEFORMATION BEHAVIOR

Finite element program FEAST III was utilized in predicting the load-deformation behavior of the model footing. This program and the finite element grids that were used are discussed in Section 5.3.1.

It is necessary to specify several soil parameters when making predictions of load-deformation behavior with this program. The influences that variations in selected soil parameters have on the predicted load-deformation behavior are considered in Section 5.3.2.

5.3.1 Discussion of Finite Element Program FEAST III and the Finite Element Grids that Were Used.

Predictions of the load-deformation behavior of the model footing were made with finite element program FEAST III developed by D'Appolonia (1968). As used here, the program employs a total stress analysis for a nearly incompressible soil that is assumed to yield in accordance with the Tresca yield criterion $(\frac{\sigma_1 - \sigma_3}{2})_f = s_u$. The program

uses a piecewise linear analysis with incremental loads for a bi-linearly elastic material. The elastic properties of an element are changed when the imposed shear stresses reach or exceed the specified yield stress. Stress and strain remain uniquely related both prior to and following yield.

Anisotropic strength may be specified. The program was written on the assumption that the anisotropic strength of the purely cohesive soil varies as $s_{u\alpha} = s_{uv} [K_s + (1-K_s) \sin^2\alpha]$ where $s_{u\alpha}$ is the undrained strength of an element that yields when the major principal stress is oriented α degrees from the horizontal. This distribution of undrained shear strength was proposed by Casagrande and Carrillo (1944). Other distributions of anisotropic strength were considered, and are discussed in Section 5.3.2.

In addition to the yield criterion, the following soil parameters must be specified when using this program: the yield stress, s_{uv} ; the yield factor, K_s ; the coefficient of lateral stress at rest; modulus of elasticity; Poisson's ratio; yielded modulus ratio; and yielded Poisson's ratio.¹ Values of Poisson's ratio were chosen to simulate undrained loading conditions as closely as possible. Two values were used, 0.49 and 0.495. The effect of the resulting volume compressibility was assessed and found to be insignificant. The yielded modulus ratio, the ratio of the yielded modulus to the

¹ Anisotropic elastic properties prior to yield may be specified. However, all predictions in this report employed isotropic elastic properties.

initial modulus was taken as 0.001. In order to maintain constant bulk modulus, the yielded Poisson's ratios were made equal to 0.49999 and 0.499995 respectively. The influence that the remaining soil parameters (s_{uv} , K_s , K_o , and E) have on the predicted load-deformation behavior will be considered in Section 5.3.2.

All finite element predictions were made for a soil body existing under initial K_o stresses that were constant with depth. This is the same condition existing in the model footing tests.¹ Unless otherwise noted, the footing was subjected to a uniform vertical displacement and the average stress under it calculated.

Three basically different finite element grids were employed during the course of this research. These are numbered 1, 2, and 4.² Grid 4 was modified slightly to achieve better performance. This modified grid is termed grid 4A. Grids 1, 2, 4, and 4A are shown in Figures G-1 through G-4, Appendix G. The reader is referred to Appendix G for a comparative discussion of the grids. Greatest reliance can be attached to the correlations obtained with grids 4 and 4A. It is shown in Appendix G that the predictions with these two are similar. Unless otherwise noted, grid 4 was used in the parametric study discussed in Section 5.3.2. Grid 4A was used in making the final correlations with the model tests that are discussed in Section 5.4.

¹ The average soil height during the tests was four inches, and the minimum σ_{vc} was 0.844 kg/cm². Therefore the influence of the unit weight of the soil on σ_v was insignificant.

² Another grid, number 3, was not used extensively and is not considered here. It was very similar to grid 2.

5.3.2 Parametric Study Using Selected Soil Parameters

One of the major objectives of the research described in this report was to obtain correlations between the measured load-deformation behavior of the model footing during undrained loading and that predicted by the finite element method. These correlations were made using soil properties determined from the undrained shear tests discussed in Chapter Four. Prior to making final correlations, it was found desirable to have information concerning the influence that variations in these soil properties had on the predicted behavior. This information is developed in this section for the three over-consolidation ratios employed in the model footing tests. The soil parameters to be considered are E , the modulus of elasticity; s_{uv} , the vertical undrained strength; K_s , the ratio $\frac{s_{uh}}{s_{uv}}$; and the coefficient of lateral stress at rest, K_o . The effect of varying the undrained shear strength distribution, $s_{u\alpha}$, for a given value of K_s will also be discussed.

For the conditions considered here, D'Appolonia (1968) illustrated that the displacements computed with this program at any load are inversely proportional to $E/\bar{\sigma}_{vc}$, to within about five percent in the region corresponding to contained plastic flow.¹ Accordingly, except near the ultimate load, the predicted load-deformation behavior

¹ This point has been known for some time. Christian (1966) derived incremental stress-strain relations for an elastic, perfectly plastic material. He demonstrated that E could be factored out of the incremental relations. This is the reason for the proportionality condition.

varies inversely as $E/\bar{\sigma}_{vc}$.

The soil properties s_{uv} and K_o , and to a lesser degree $K_s = \frac{s_{uh}}{s_{uv}}$ and $s_{u\alpha}$, influence the predicted load-deformation since they determine when an element will first yield. In any parametric study concerned with these properties, it must be remembered that their influence on the predicted load-deformation behavior is interrelated. For example, the increment of shear stress required to cause yielding, $\Delta q/\bar{\sigma}_{vc}$, is controlled by both s_{uv} and K_o . A greater increment of $\Delta q/\bar{\sigma}_{vc}$ is required to cause yielding if K_o is increased at constant $\frac{s_{uv}}{\bar{\sigma}_{vc}}$. Conversely, a similar increase in $\frac{\Delta q}{\bar{\sigma}_{vc}}$ would be required if $s_{uv}/\bar{\sigma}_{vc}$ were increased appropriately at constant K_o . Even though the effect of these properties is interrelated, it is desirable to have information concerning the variation of the individual parameters at the three overconsolidation ratios. This information is helpful, for entirely reproducible results were not always obtained in the undrained shear tests. Furthermore, in field situations, some uncertainty will always exist concerning values of the soil properties that should be used for making predictions of foundation performance. Under these conditions it is desirable that the engineer have information concerning the effects that uncertainties in the individual parameters will have on the predicted behavior.

Variations in K_o at each overconsolidation ratio are considered first. This is followed by a discussion of the effects of uncertainties in s_{uv} and s_{uh} . Lastly, variations in the $s_{u\alpha}$ distribution at a fixed K_s value are considered for an overconsolidation ratio of

one.

Figure 5-2 shows what effect a 10 percent variation in K_0 has on the predicted load-deformation behavior for the normally consolidated case. The range of K_0 used in preparing the figure equals the range of K_0 values that is usually encountered for normally consolidated Boston Blue Clay in the laboratory. (See Chapter Four and its related Appendices). Note that the ordinates of this and other figures in this section have been expanded relative to those of the model test results presented in Chapter Three. The strength and modulus values for the runs in the figure are representative of normally consolidated Boston Blue Clay. These values will be considered further in Section 5.4. To provide perspective, model test data have been included in the figure. The shaded area is bounded by the average curves from the model tests for $\bar{\sigma}_{vc}$ values of 2.0 and 3.38 kg/cm². The test results for $\bar{\sigma}_{vc} = 1.0$ kg/cm² in general lie above curve 1. Differences in load-deformation behavior existed in the two runs from a factor of safety of about 3.4 for the model tests. Throughout this chapter, the factors of safety of the model tests are reckoned from $\sigma/\bar{\sigma}_{vc}$ values for $\rho/B = 0.1$. On the average, differences in the two predictions are equal to or less than the observed variations in the model test results.

The effect of at least a 10 percent variation in K_0 is shown in Figures 5-3 and 5-4 for overconsolidation ratios of two and four respectively. As with the normally consolidated case, the ranges of K_0 values shown in these figures are approximately equal to or somewhat greater than those encountered in laboratory tests for Boston Blue Clay.

The strength values noted in these figures are typical for these stress histories. The average test curves are shown in the figures to offer perspective concerning K_o effects for these stress histories. It is apparent from the figures that errors in load-deformation predictions arising from uncertainties in K_o decrease as the overconsolidation ratio increases. As the value of K_o (and $\frac{s_{uv}}{\bar{\sigma}_{vc}}$) increases with overconsolidation ratio, a greater increment of shear stress, $\Delta q/\bar{\sigma}_{vc}$, is required to cause first yielding. Hence, the factor of safety at which differences in K_o become apparent decreases with increasing overconsolidation ratio. For an OCR = 2, the effects of K_o do not become evident until a factor of safety of 1.5 is reached. At an OCR = 4, a 13 percent variation in K_o does not have any dramatic effect even at a factor of safety for the model tests as low as 1.3.

The effect that specifying different values of undrained shear strength has on the predicted load-deformation behavior for the normally consolidated case is illustrated in Figure 5-5. A value of $K_o = 0.53$ was used. It is intermediate between the K_o values used in Figure 5-2. Curve 1 was prepared using $s_{uv}/\bar{\sigma}_{vc}$ equal to the largest value that has been measured to date for normally consolidated Boston Blue Clay in undrained plane strain active shear. The value of $s_{uh}/\bar{\sigma}_{vc}$ used in this run was somewhat larger than the maximum value reported in Table D-1. Curve 2 was prepared using the lowest values of $s_{uv}/\bar{\sigma}_{vc}$ and $s_{uh}/\bar{\sigma}_{vc}$ that could be considered for later correlations. Relative to the strength values for curve 1, these curves represent a 10 percent difference in $s_{uv}/\bar{\sigma}_{vc}$ and about a 23 percent variation in $s_{uh}/\bar{\sigma}_{vc}$.

As in Figure 5-2, the shaded area shown is bounded by the average model test curves at $\bar{\sigma}_{vc} = 2.0$ and 3.38 kg/cm^2 . The average test curve for $\bar{\sigma}_{vc} = 1.0 \text{ kg/cm}^2$ in general lies above curve 1. The combined differences in $s_{uv}/\bar{\sigma}_{vc}$ and $s_{uh}/\bar{\sigma}_{vc}$ resulted in a larger divergence of the curves than existed in Figure 5-2 for a 10 percent variation in K_o . At $\sigma/\bar{\sigma}_{vc} = 1.15$, curve 2 has a ρ/B value 1.6 times that of curve 1.

The effects that differences in undrained shear strength have on the predicted load-deformation behavior for an $OCR = 2$ are shown in Figure 5-6. Here there is about a five percent variation in both $s_{uv}/\bar{\sigma}_{vc}$ and $s_{uh}/\bar{\sigma}_{vc}$ between the two predictions. The values of $s_{uv}/\bar{\sigma}_{vc}$ are both within a few percent of those used in the final correlations for this overconsolidation ratio. In both cases the value of $s_{uh}/\bar{\sigma}_{vc}$ is larger than that finally used. Some difficulty was encountered in the plane strain passive tests at this overconsolidation ratio. The value of $s_{uh}/\bar{\sigma}_{vc}$ used for curve 2 is for the extreme case of no reduction in the passive strength upon rebound. Therefore, from the standpoint of strength, curve 2 represents an upper limit for this stress history. The combined effect of changes in $s_{uv}/\bar{\sigma}_{vc}$ and $s_{uh}/\bar{\sigma}_{vc}$ are evident for factors of safety of 1.6 or less as compared with a factor of 3.4 for the normally consolidated case. This is expected since similar observations were made concerning K_o effects with increasing overconsolidation ratio.¹ While not within the scope of the present discussion, it

¹ More dramatic effects were encountered in the normally consolidated case for another reason. The differences in the undrained strengths for the $OCR = 2$ case were less, percentage wise, than were those for the normally consolidated case.

should be noted that the $E/\bar{\sigma}_{vc}$ values used for these predictions did not yield as good agreement with the average test curve as did the modulus values shown in Figure 5-3. Modulus values appropriate to each overconsolidation ratio will be considered in Section 5.4.

The continued insensitivity of initial load-deformation predictions to small uncertainties in undrained strength which accompanies increasing overconsolidation is seen in Figure 5-7 for an OCR = 4. The two predictions did not employ the same value of K_o . However, in view of the observations made with respect to Figure 5-4, any difference in behavior arising from the unequal K_o values is small. There is about a five percent difference in both $s_{uv}/\bar{\sigma}_{vc}$ and $s_{uh}/\bar{\sigma}_{vc}$ between the two runs. This is comparable to the differences in strength employed in the preparation of Figure 5-6. The two predictions were identical until a factor of safety relative to the model tests of 1.35 was reached.

Important conclusions can be drawn from the above observations. It is seen that errors in load-deformation predictions arising from inaccurately estimating K_o decrease with increasing overconsolidation ratio. Likewise, differences in initial load-deformation predictions arising from some uncertainty concerning s_u decrease as the overconsolidation ratio increases. However, it should be remembered that calculations of the ultimate bearing capacity are still proportional to estimates of the strength.

With the assistance of D.J. D'Appolonia of M.I.T., the author modified FEAST III to investigate the influences that different

distributions of undrained shear strength, $s_{u\alpha}$, for the same K_s value, have on the predicted load-deformation behavior. Only the normally consolidated case was investigated. This work employed grid 1 and used a uniformly loaded flexible footing. All runs employed identical load increments. The load-deformation plots that follow are based on the normalized displacement of the centerline of the footing. The results are presented for the purpose of making qualitative observations concerning the effects of differing distributions of $s_{u\alpha}$. Before extensive quantitative conclusions are drawn concerning this effect, it is recommended that additional runs be made with a grid such as 4A.

The distributions of undrained strength that were used are shown in Figure 5-8 along with the algebraic expressions by which they are defined. Curve 1 is the basic undrained shear strength distribution of FEAST III. As noted earlier, this is based on the earlier work of Casagrande and Carrillo (1944). Curves 2, 3, and 4 were chosen for two reasons. Their algebraic expressions were easily programmed. Additionally, they have other interesting properties. Curve 2 represents a case where the undrained strength at yield is approximately constant for the first 20 degrees of reorientation of the major principal stress.¹ Curve 3 represents a case where the undrained strength at yield is approximately constant for a reorientation of principal stresses greater than 70 degrees, but changes rapidly during the early stages of reorientation. Curve 4 is a linear relationship which under certain

¹ Throughout this discussion K_o is assumed to be less than or equal to 1.

circumstances might be easier to remember and use. These curves are not based on further theoretical or experimental grounds.

The load-deformation predictions made with these distributions are shown in Figure 5-9. The numbering of the predicted curves corresponds to the numbering of the distributions in Figure 5-8. The shaded area in the figure is bounded by the average test curves at $\bar{\sigma}_{vc} = 2.0$ and 3.38 kg/cm^2 .

The relative positions of the load-deformation curves look reasonable intuitively. At any α greater than 20° , curve 2 in Figure 5-8 has the largest $s_{u\alpha}$ value. This curve experienced the smallest normalized displacement at any ρ/B value. Curves 3 and 4 both exhibit larger ρ/B values relative to curve 1, for $\sigma/\bar{\sigma}_{vc}$ less than 1.4. Curve 4 lies below curve 3 for $\sigma/\bar{\sigma}_{vc}$ less than 1.3 and then intersects curve 1 at $\sigma/\bar{\sigma}_{vc} = 1.43$. This suggests that, except near failure, most of the elements in the grid that yielded, did so for α values greater than 45 degrees.

One quantitative observation will be made. At $\sigma/\bar{\sigma}_{vc} = 1.3$, the ratio of ρ/B for curve 3 to that for curve 2 is 1.24. If the two curves had had identical $s_{u\alpha}$ distributions, this displacement ratio could be explained on the basis of a 25 percent difference in modulus. This is not a large effect. Furthermore, as the overconsolidation ratio increases, K_s will increase. As this occurs, the importance of the specific $s_{u\alpha}$ distribution will decrease. Additionally, it has been shown that uncertainties in the values of undrained strength have less effect on the predicted load-deformation behavior

as the overconsolidation ratio increases. For these reasons, the Casagrande and Carrillo relationship, curve 1 Figure 5-8, was used in making final correlations at all overconsolidation ratios.

5.4 FINITE ELEMENT CORRELATIONS OF PREDICTED AND OBSERVED BEHAVIOR.

The final finite element correlations that were made with the model footing test results are discussed in this section. Emphasis is given to choosing those soil properties that lead to good agreement between the predicted and observed load-deformation curves for the full range of loading. Observations that were made in the previous section for overconsolidation ratios of two and four showed that for the ranges of strength and K_0 values that are obtained in laboratory tests for these stress histories, the predicted load-deformation behavior is not dramatically effected until a factor of safety of about 1.5 or less is reached. Therefore, one set of average strength and K_0 properties was used in final correlations for each of these overconsolidation ratios.

For the normally consolidated case it was shown that a similar range of strength and K_0 values will lead to different predictions at factors of safety less than about 3.5. Instead of making final correlations with such a range of values, it was found useful to choose average properties for this stress history as well.

After the values of strength and K_0 have been fixed, the only soil parameter left that will influence the finite element prediction

is the modulus. An investigation was undertaken to ascertain which modulus values yielded the best predictions for each case. The explanation for the choice of these values is the main topic of this section.

5.4.1 Presentation of Final Correlations

The average model test curves and the best finite element correlations are shown in Figures 5-10, 5-11, and 5-12 for overconsolidation ratios of one, two, and four respectively.¹ The value of $\bar{\sigma}_{vm}$ for the overconsolidated tests was 3.38 kg/cm². Therefore, initial correlations have been obtained for the normally consolidated tests at $\bar{\sigma}_{vm} = 3.38$ kg/cm². Observations are then made with respect to the soil properties needed for correlations with the other normally consolidated tests.

The $s_{uv}/\bar{\sigma}_{vc}$ value for the normally consolidated case is the average value shown in Figure 4-1. A $K_s = 0.588$ was employed, which is larger than that in Figure 4-1. This gives a $\frac{s_{uh}}{\bar{\sigma}_{vc}} = 0.20$. It will be recalled that failure in two of the normally consolidated plane strain passive tests was defined at the point of inflection of the stress-strain curve. This is considered to have resulted in a computed average strength for the tests which is somewhat low. A K_o value of 0.51 was used for this stress history. Examination of the data in

¹ Two predicted curves are shown in each figure. The curves labeled "Adjusted Prediction" will be considered later in this section. The circled numbers denote the total number of yielded elements at the indicated values of $\sigma/\bar{\sigma}_{vc}$.

Figure 4-3 and Table D-2, Appendix D, will show that this value is reasonable.

The two plane strain active tests at an OCR of two had $s_{uv}/\bar{\sigma}_{vc}$ values that differed by three percent. The lower of the two values was chosen for the final correlations. The value of $s_{uh}/\bar{\sigma}_{vc}$ was taken from the average curve in Figure 4-1 at this OCR. The value of $K_o = 0.72$ was taken from the relationship presented by R. Ladd (1965) and replotted in Figure 4-3.

The $s_{uv}/\bar{\sigma}_{vc}$ values for the two active tests at an OCR = 4 differed by 10 percent. A $s_{uv}/\bar{\sigma}_{vc}$ value was used that was approximately equal to the average of the two tests. It was noted in Chapter Four that the square oedometer, \overline{CK}_oU triaxial, and plane strain K_o values were not in complete agreement for this overconsolidation ratio. The K_o value of 0.93 is taken from the midpoint of the range of the data.

A normalized modulus of 400 was used for making final the correlation with the normally consolidated tests. An $E/\bar{\sigma}_{vc} = 300$ was used for the two overconsolidated cases.

In the normally consolidated case, Figure 5-10, the footing displacement is slightly under predicted initially. For $\sigma/\bar{\sigma}_{vc}$ values from 0.6 to about 1.15 the footing displacements are overpredicted somewhat and at low factors of safety ρ/B is once again under predicted.¹ Footing displacements at high factors of safety are over

¹ During the final load increment for this run, several additional elements yielded. If the prediction had been continued beyond $\rho/B = 0.04$, it would have exhibited increased non-linear behavior.

predicted in both overconsolidated cases and are under predicted at low factors of safety, Figures 5-11 and 5-12.

It might at first appear odd to the reader that an $E/\bar{\sigma}_{vc} = 400$ was used for the normally consolidated correlation, whereas a value of 300 was found best for the overconsolidated tests. The reasons for choosing these $E/\bar{\sigma}_{vc}$ values will become clear later in this discussion.

Consolidation settlements due to a high value of c_v , the coefficient of consolidation, during recompression in the overconsolidated stress range is not considered to have necessitated use of the lower $E/\bar{\sigma}_{vc}$ value for the overconsolidated tests. The average times to $\rho/B = 0.02$ and 0.10 in all tests were 3.1 and 15.6 seconds respectively. Calculations were made of the percent consolidation and the magnitude of consolidation settlement that could have occurred during the tests. At $\rho/B = 0.02$ the maximum computed percent consolidation was approximately one percent for the overconsolidated tests when a very conservatively high value of c_v was used, $150 \times 10^{-4} \text{ cm}^2/\text{sec}$. This corresponds to a consolidation settlement of less than $\rho/B = 0.0005$. The maximum computed consolidation settlement at $\rho/B = 0.10$ was less than $\rho/B = 0.002$.

It is concluded that for practical purposes both the normally consolidated and overconsolidated tests were completely undrained. Additional information concerning these calculations is given in Appendix B.

5.4.2 Preliminary Considerations with Respect to the Choice of Modulus.¹

In order to understand why a lower $E/\bar{\sigma}_{vc}$ value was needed in the overconsolidated cases than for the normally consolidated case, it is necessary to compare the stress-strain curves specified in the computer predictions with those obtained from laboratory tests. Before making comparisons among predicted and measured stress-strain curves, a determination must first be made concerning what stress-strain curves to compare. Two obvious choices are available: comparison of the predicted and measured plane strain active curves or comparison of curves for the plane strain passive condition.

The non-linear behavior of the predicted load-deformation curves is the result of the yielding of elements in the finite element grid. One is then lead to consider the orientation of the principal stresses prior to and at yield, for the elements in the grid that ultimately yield. If the average α value is nearer 90° than 0° , then primary attention can be directed to the plane strain active stress-strain curves. Conversely if the average α valve is close to 0° the passive tests should be given primary consideration. At the same time however, it should be remembered that the behavior of those elements that never yield also influence the predicted load-deformation behavior, for these elements do experience strain.

An examination of the orientation of the principal stresses at yield, for the yielded elements in the runs at each OCR has shown

¹ A summary concerning the choice of the modulus value for use in the final correlations is presented in section 5.4.6.

that primary consideration for most of the loading in each case can be given to comparisons of the stress-strain curves for the plane strain active case. The results of this study are as follows:

Direction of σ_1 at Yield Measured From the Horizontal, α (Degrees)		
OCR = 1	OCR = 2	OCR = 4
78% > 80°	69% > 70°	43% > 70°
	78% > 50°	75% > 50°

The tabulated values are for a $\rho/B = 0.022$ for an OCR = 1 and $\rho/B = 0.018$ for the two overconsolidated cases. The percentages are based on the total number of yielded elements in the runs at the indicated values of normalized displacement.

Comparisons are made in Figure 5-13 among the stress-strain curves obtained during the plane strain active tests and those employed in the finite element analyses.¹ In the figure the test curves at each overconsolidation ratio are the average curves of those presented in Appendix D. The slopes of the yielded portions of the computer stress-strain curves have not been indicated in the figure. They are approximately horizontal, since the yielded modulus ratio was 0.001 in all cases.

Figure 5-13 shows that the stress-strain curves of the finite

¹ Comparisons between the finite element stress-strain curves and those measured in the plane strain passive tests are also shown for each OCR in Figure 5-14. This figure will be considered later in the section.

element model are not coincident with the measured plane strain active stress-strain curves. For an OCR = 1, strains are under predicted in the finite element analysis for values of $\Delta q/\Delta q_f$ greater than about 0.4. At an OCR = 2 strains are slightly over predicted for $\Delta q/\Delta q_f$ less than 0.55 and are underestimated thereafter. For an OCR = 4 strains are overestimated in the finite element analysis for $\Delta q/\Delta q_f$ less than about 0.75 and under predicted thereafter.

In view of these observations, it is necessary to consider the distribution of stress and strain in the finite element grids throughout loading in order to understand why the particular modulus values were employed. Emphasis throughout this discussion is given to comparing the strains in the bi-linear finite element model with those measured in the plane strain active tests at equal stress levels, $(\Delta q/\Delta q_f)$. It is these comparisons of strain that are used to explain the choices of the modulus values for the final correlations. The fact is first illustrated that the distributions of stress and strain in the finite element grids change throughout the loading sequence. This is discussed in relation to Table 5-3 for all three OCR's. Comparisons of strain between the bi-linear model and the plane strain active test curve at each OCR are then made to explain the final correlations.

With each overconsolidation ratio, attention was directed to the stresses and strains that existed throughout the loading sequence for those elements that yielded at ρ/B equal to or less than 0.04. The total number of elements considered was 185, 153, and 123 for OCR's of one, two, and four respectively. Summary information from this study

for the three overconsolidation ratios is given in Table 5-3. More detailed information for each overconsolidation ratio is given in Tables 5-4 through 5-6. With respect to these tables, it is to be noted that primary attention was given to those elements at each load increment that had experienced less than 20 degrees of reorientation of the major principal stress, i.e. $|\alpha| > 70^\circ$. This range of α (70° to 90°) permitted making direct comparisons between the $\Delta q/\Delta q_f$ and strain values for the elements and those of the plane strain active stress-strain curves. Note also that the percentages listed in Table 5-3 are with respect to the total number of elements that yielded in each of the runs by $\rho/B = 0.04$, irrespective of α .

Table 5-3 was prepared to illustrate two points. First, there are differences in the extent of yielding among the runs for the three OCR's at the same value of $\sigma/\bar{\sigma}_{vm}$. Secondly, the distributions of stress and strain of the elements in the grids change throughout the loading sequence in each case.

Consider the second column for each OCR in Table 5-3. It is apparent that considerably more yielding occurred at low values of $\sigma/\bar{\sigma}_{vm}$ for an OCR = 1 than occurred for the overconsolidated cases. For example, by $\sigma/\bar{\sigma}_{vm} = 0.46$, 52 elements had yielded in the normally consolidated run as opposed to only 4 at $\sigma/\bar{\sigma}_{vm} = 0.531$ for an OCR = 2. Likewise, at $\sigma/\bar{\sigma}_{vm} = 0.7$, 81 elements had yielded in the normally consolidated case as opposed to only 31 at $\sigma/\bar{\sigma}_{vm} = 0.77$ at an OCR = 4. These observations suggest that more attention should be directed to the agreement between the unyielded portion of the specified bi-linear

stress-strain curve and the plane strain active stress-strain curve as the overconsolidation ratio increases.

The changing distribution of stress and strain in the finite element grid during loading is further illustrated in the third column for each OCR. There a summary is given of the total number of elements that exhibited $\Delta q/\Delta q_f$ values for the region on the finite element stress-strain curve where the predicted strains could be less than the strain measured in the undrained plane strain active tests. For example, the listing for OCR = 1 is for those elements (yielded and unyielded with $|\alpha| > 70^\circ$) that had $\Delta q/\Delta q_f$ values greater than 0.4.

It is seen that strains can be underestimated in many elements, and that the number of elements for which this occurs changes during loading.¹ At $\sigma/\bar{\sigma}_{vm} = 0.35$, 72 elements in the normally consolidated case have $\frac{\Delta q}{\Delta q_f} > 0.4$. At $\sigma/\bar{\sigma}_{vm} = 0.7$, the number had increased to approximately 100 even though only a total of 81 elements had yielded. At $\sigma/\bar{\sigma}_{vm} = 0.43$ for an OCR = 2, only about 15 elements exhibited an underestimate of strain relative to the plane strain active test. However, by $\sigma/\bar{\sigma}_{vm} = 0.65$, strains were underestimated in more than 60 unyielded elements with $|\alpha| > 70^\circ$. The same behavior existed for an OCR = 4. For example at $\sigma/\bar{\sigma}_{vm} = 0.77$ strains were underestimated in at least the 20 unyielded elements with $|\alpha| > 70^\circ$.

The agreement between the predicted and measured footing

¹ It will be shown later that strains in many elements can be overestimated as well.

performance for each OCR will now be considered. As noted above, emphasis throughout loading in each case is directed to comparing the strains from the bi-linear finite element model with those measured in the plane strain active tests at equal values of $\Delta q/\Delta q_f$. The most dramatic effects occurred for an OCR = 4. The prediction for this OCR will be considered first. Discussions of the predictions at OCR's of two and one will then be presented.

5.4.3 Discussion of the Final Correlation for an Overconsolidation Ratio of Four.

Consider Table 5-6 and Figures 5-12 and 5-13. The present discussion only concerns the prediction shown by the upper dashed line in Figure 5-12. The curve labeled "Adjusted Prediction" will be considered later. For purposes of this discussion, the elements in Table 5-6 having $\Delta q/\Delta q_f \geq 0.69$ are considered to form a group for which an underestimate of strain relative to the plane strain active curve is possible.¹

At $\sigma/\bar{\sigma}_{vc} = 1.39$ only one element had a $\Delta q/\Delta q_f$ value for which there existed an underestimate of strain. Strains were overestimated in 28 elements having $\frac{\Delta q}{\Delta q_f} \geq 0.38$ (and for about 45 with $\frac{\Delta q}{\Delta q_f} < 0.38$). These overestimates of strain resulted in the over prediction of footing displacement seen in Figure 5-12 for low values of $\sigma/\bar{\sigma}_{vc}$.

As loading continued in the finite element analysis, the

¹ A value of 0.75 would be more reasonable based on Fig. 5-13.

predicted footing displacement curve intersected and then underestimated the model test curve until low factors of safety were reached. Further examination of Table 5-6 shows why this happened. At $\sigma/\bar{\sigma}_{vc} = 2.27$, 11 (7+3+1=11) unyielded elements exhibited an underestimate of strain. At $\sigma/\bar{\sigma}_{vc} = 3.07$ strains were under predicted in 38 unyielded elements. Furthermore, the average strain of the yielded elements at this point was only 0.52 percent, as compared with a failure strain in the plane strain test of about 1.7 percent. (See Figure 5-13). The underestimate of strain for this large a number of elements lead to the divergence of the predicted and measured curves.

Even more divergent behavior existed at $\sigma/\bar{\sigma}_{vc} = 3.52$ where strains were underestimated for about 60 elements since the average strain of yielded elements is less than 0.6 percent.¹

The average strain for the yielded elements increased rapidly after this point. At $\sigma/\bar{\sigma}_{vc} = 3.92$ the average strain of the 52 yielded elements in Table 5-6 was 1.25 percent. It is seen that the predicted load-deformation curve is "breaking" rapidly at this $\sigma/\bar{\sigma}_{vc}$ and is beginning to "catch-up" with the model test curve.

An adjustment to the prediction in Figure 5-12 will now be considered. With program FEAST III, the yielded values of the elastic constants of an element are employed for loading subsequent to the load increment in which the specified yield stress is equaled or exceeded. After yield the shearing resistance of an element increases from the

¹ The largest strain of the yielded elements was 1.4 percent.

value existing at yield in accordance with the specified yielded modulus. Economics dictates the use of a limited number of load increments. Therefore, it is unavoidable that the apparent shear strength of some of the yielded elements will be larger, following yield, than desired. The cumulative effect of the overestimate of strength could affect interpretation of the prediction.

An approximate correction has been applied to the prediction in Figure 5-12. This was determined as follows. A cumulative average of the yield ratios at yield, q/q_f , for all the yielded elements in the grid at each load increment was computed. For example it is seen in Table 5-3 that this average was determined for eight elements at $\sigma/\bar{\sigma}_{vm} = 0.576$ and for 72 elements at $\sigma/\bar{\sigma}_{vm} = 0.88$. At $\sigma/\bar{\sigma}_{vc} = 4.1$ ($\rho/B = 0.04$) it was determined for a total of 123 elements.

A pro-rated correction to the original prediction was calculated at each load increment on the basis of the average yield ratio and the percentage of the total number of yielded elements at that point. For example, if at some $\sigma/\bar{\sigma}_{vc}$ the cumulative average yield ratio at yield for the 61 yielded elements was 1.05, the adjustment to the prediction would be:

$$5 \left(\frac{61}{123} \right) = 2.5 \text{ percent}$$

Approximate corrections of this type were determined throughout the loading sequence.¹ The resulting corrected curve is labeled "Adjusted

¹ This correction procedure is approximate for it does not consider the different sizes of elements in the grid. Furthermore, increases in the shearing resistance of the yielded elements following yield are not considered. Error from this point is small since the yielded modulus ratio was 0.001 and large strains were confined to the region near the footing.

Prediction" in Figure 5-12. It is seen that the adjusted curve does not really improve matters very much.

It should now be evident why $E/\bar{\sigma}_{vc} = 300$ was used for this OCR. The intent of the correlation was to achieve general agreement with the test curve throughout the full range of loading. If a higher $E/\bar{\sigma}_{vc}$ had been employed, excellent agreement would have been achieved initially but even poorer agreement would have been obtained at low factors of safety. Conversely, a lower $E/\bar{\sigma}_{vc}$ would have yielded better agreement at low factors of safety, but poorer agreement early in loading.

5.4.4 Discussion of the Final Correlation for an Overconsolidation Ratio of Two.

The final correlation for an overconsolidation ratio of two will now be considered.¹ See Table 5-5 and Figures 5-11 and 5-13. It should be noted that for elements with $\Delta q/\Delta q_f$ greater than about 0.55, strains can be underestimated relative to the plane strain active undrained shear tests. At $\sigma/\bar{\sigma}_{vc} = 0.855$ strains were underestimated in only 13 elements while they were overestimated in 70 to 80 elements. Up to this value of $\sigma/\bar{\sigma}_{vc}$, it is seen that the finite element prediction slightly overestimates the load-deformation behavior observed in the model tests. The magnitude of this over prediction is less than for the OCR = 4 since the magnitude of the overestimate of strain is less. (See Figure 5-13.) At $\sigma/\bar{\sigma}_{vc} = 1.07$ strains are underestimated

¹ The basic FEAST III prediction will be considered first. A discussion of Adjusted Prediction follows.

in 50 elements and overestimated in 30 elements. The finite element analysis is beginning to under predict the footing settlement at this point. Divergence of the two curves continues because of the under prediction of strain in the finite element analysis. At $\sigma/\bar{\sigma}_{vc} = 1.98$, strains are underestimated in 21 unyielded elements and the average strain of the yielded elements is only 0.56 percent as opposed to a failure strain in the plane strain test of about 1.2 percent. Beyond this point the average strain of the yielded elements with $|\alpha| > 70^\circ$ increases rapidly. At $\sigma/\bar{\sigma}_{vc} = 2.26$ it was 1.4 percent, and the predicted curve had converged with the model test results.

The same type of adjustment was applied to this prediction as was discussed with regard to the correlation for an overconsolidation ratio of four. As before, it is seen that the "overshoot" of the yield stress in the computer prediction does not invalidate the observations made concerning the effect of the distribution of stress and strain in the grid.

The prediction of footing displacement at $\sigma/\bar{\sigma}_{vc}$ values greater than about 2.0 for the adjusted curve is explained by consideration of the average strain for the yielded elements. As noted earlier, at $\sigma/\bar{\sigma}_{vc} = 1.98$ (unadjusted) the average strain was 0.56 percent. This is still less than the failure strain in the plane strain active test. The corresponding adjusted value while closer to the model test curve, is still above it. The adjustment from $\sigma/\bar{\sigma}_{vc} = 2.26$ lies below the model test, but the average strain of the yielded elements for this load increment was greater than average failure strain of the plane strain

active test. For intermediate values, the failure strain of the undrained shear test and the average strains for the yielded elements were approximately equal. Additionally, $s_{uv}/\bar{\sigma}_{vc} = 0.56$ was used in the prediction. This is the minimum vertical strength that has been measured at this OCR. Therefore, it maybe somewhat low.

The reasons for using $E/\bar{\sigma}_{vc} = 300$ with this OCR should again be clear. The intent of the correlation was to obtain general agreement between the predicted and measured load-deformation curves for the full range of loading. As with the OCR = 4, use of higher or lower values of $E/\bar{\sigma}_{vc}$ would have resulted in improved agreement at specific $\sigma/\bar{\sigma}_{vc}$ values. However, agreement elsewhere would have been sacrificed and would have resulted in poorer overall agreement.

5.4.5 Discussion of the Final Correlation for the Normally Consolidated Case.

The final correlation for the normally consolidated case will now be considered.¹ Refer to Table 5-4 and Figures 5-10 and 5-13. For $\Delta q/\Delta q_f$ greater than about 0.4, strains can be under predicted in the finite element analysis. It will be recalled that extensive yielding occurs at low values of $\sigma/\bar{\sigma}_{vc}$ for this stress history. Hence, much more of the predicted load-deformation behavior is controlled by contained plastic flow for this stress history than for the over-consolidated cases.

¹ This portion of the discussion is limited to the unadjusted prediction for the test curve at $\bar{\sigma}_{vc} = 3.38 \text{ kg/cm}^2$.

At $\sigma/\bar{\sigma}_{vc}$ values less than or equal to about 0.7, the finite element prediction is slightly above or coincident with the model test results. Even though 52 elements had yielded by $\sigma/\bar{\sigma}_{vc} = 0.46$, the average strain of these yielded elements was only 0.07 percent, as compared with about 0.55 percent for the failure strain in the plane strain active test. This explains the under prediction of footing displacement for high factors of safety. The magnitude of the discrepancy between the two curves is not large in this region. However, even the differences in the failure strains between the computer and test curves is not as large in this case as in the others. For example in the normally consolidated case yielding occurs at 0.035 percent in the bi-linear model and the average failure strain in the plane strain active test is about 0.55 percent. Thus the difference in failure strains is approximately 0.5 percent. For an OCR = 4 yielding occurs in the computer prediction at 0.45 percent, as compared with failure at 1.7 percent in the soil test. Thus the difference in failure strains for this OCR is 1.2 percent, much larger than in the normally consolidated case.

At $\sigma/\bar{\sigma}_{vc} = 0.7$ the average strain of the yielded elements was 0.31 percent, very close to the failure strain in the active test. At about this point the two curves crossed. By $\sigma/\bar{\sigma}_{vc} = 1.056$, the average strain of the yielded elements had increased to 0.81 percent, and the predicted results agree well with the measured curve.

Reasons for the divergent behavior of the predicted curve for $\sigma/\bar{\sigma}_{vc}$ values greater than about 1.2 are not entirely clear. However,

when an adjustment is made for the overestimate of yielded stress, more reasonable performance is observed.¹

The above behavior is perhaps partially explained by comparing the predicted and measured stress-strain curves for the plane strain passive case, Figure 5-14. The finite element stress-strain curves under predict the plane strain passive strains beyond a certain point at all values of OCR, but the problem is most severe for the normally consolidated stress history. In this case strains are under predicted for $\Delta q/\Delta q_f$ greater than 0.3 and for practical purposes are never over predicted. By comparison, in both overconsolidated cases the strains are over predicted up to $\Delta q/\Delta q_f$ equal to about 0.5 and are under predicted thereafter. The normally consolidated prediction experienced the least abrupt "break" in relation to the model test results. However as seen above, the problem of under predicting strains in passive failure is most severe for this stress history.

As with the overconsolidated cases, the $E/\bar{\sigma}_{vc}$ that was used in the prediction was employed to obtain general agreement throughout the full range of loading. It is evident that different values of $E/\bar{\sigma}_{vc}$ would have lead to improved agreement locally at the expense of general agreement throughout loading.

¹ Approximately 40 additional elements yielded during the last load increment for this run. If the prediction had been continued, the predicted curves would have exhibited increased non-linear behavior. Drawing on experience from other runs, the approximate behavior of the adjusted curve has been indicated for further displacement of the footing.

The next point to be considered in regard to the normally consolidated tests is the choice of the modulus value needed for good predictions with the tests at $\bar{\sigma}_{vc} = 1.0$ and 2.0 kg/cm^2 . The normally consolidated tests have been replotted in Figure 5-15. The curves in the figure for $\bar{\sigma}_{vc} = 1.0$ and 2.0 kg/cm^2 have been normalized with respect to the ultimate bearing capacity of the test curve for $\bar{\sigma}_{vc} = 3.38 \text{ kg/cm}^2$. For example, at $\rho/B = 0.1$ in Figure 5-10, the ratio of $\sigma/\bar{\sigma}_{vc}$ for the tests at 3.38 kg/cm^2 to those at 1.0 kg/cm^2 is 0.945. The $\sigma/\bar{\sigma}_{vc}$ value at any ρ/B for the $\bar{\sigma}_{vc} = 1.0 \text{ kg/cm}^2$ curve in Figure 5-10 has been multiplied by this factor to prepare Figure 5-15.¹ The ratio for $\bar{\sigma}_{vc} = 2.0 \text{ kg/cm}^2$ is 0.986.

It is evident in Figure 5-15 that when the data are normalized with respect to the ultimate bearing capacity, significant differences still exist among the load-deformation curves.² The model footing tests at $\bar{\sigma}_{vc} = 1.0 \text{ kg/cm}^2$ exhibited a much more abrupt break in the load-settlement curve than did the tests at the other two effective stresses. This may be due to some difference in soil structure at this low effective stress. While variations in K_o with $\bar{\sigma}_{vc}$ may

¹ No distinction has been made among the three consolidation stresses for $\sigma/\bar{\sigma}_{vc}$ less than about 0.5.

² Differences in sample preparation procedure are not considered to have caused these differences in behavior. The ratio of the increment of consolidation stress under the surcharge bag to that with the consolidation plate was 1.0, 0.6, and 1.25 for the tests at $\bar{\sigma}_{vc} = 1.0, 2.0, \text{ and } 3.38 \text{ kg/cm}^2$ respectively. If disturbance effects due to removal of the consolidation plate and placement of the footing on the soil surface existed then the tests at $\bar{\sigma}_{vc} = 2.0 \text{ kg/cm}^2$ would not be expected to occupy the intermediate position that they do.

be possible, they are not considered very probable. It will be recalled that in Chapter Four an examination was made of the dependence of K_o on the magnitude of $\bar{\sigma}_{vc}$. For $\bar{\sigma}_{vc}$ equal to or greater than 2 kg/cm², no dependence was seen between the value of K_o and the magnitude of $\bar{\sigma}_{vc}$ in the normally consolidated region.

It was observed in Chapter Four that the normalized stress-strain modulus of Boston Blue Clay did decrease with increasing $\bar{\sigma}_{vc}$. This was observed for anisotropically consolidated \overline{CUDSS} tests; see Figure 4-11. Data in Figure 4-8 for \overline{CIU} triaxial compression tests also indicate that the normalized stress-strain modulus resulting from this type of undrained shear is not necessarily constant but may decrease with increasing $\bar{\sigma}_{vc}$.

If the relationships between normalized modulus and $\bar{\sigma}_{vc}$ in Figures 4-8 and 4-11 are extrapolated to 1.0 kg/cm², the normalized moduli at 1.0 kg/cm² are calculated to be from 35 to 40 percent greater than those at 3.4 kg/cm². In the range $\sigma/\bar{\sigma}_{vc} = 0.8$ to 1.2, the effective normalized modulus of the footing test curve at $\bar{\sigma}_{vc} = 1.0$ kg/cm² is from 35 to 100 percent greater than that for the curve at $\bar{\sigma}_{vc} = 3.38$ kg/cm². Thus, the increases in normalized modulus that were observed over the same range of $\bar{\sigma}_{vc}$ in the direct simple-shear and \overline{CIU} triaxial tests might explain much of the observed difference in footing behavior.

For the same range of $\sigma/\bar{\sigma}_{vc}$, the effective normalized modulus of the model test curve at $\bar{\sigma}_{vc} = 2.0$ kg/cm² is 10 to 30 percent greater than that for $\bar{\sigma}_{vc} = 3.38$ kg/cm². The normalized moduli at 2.0 kg/cm²

in Figures 4-8 and 4-11 are 27 and 20 percent greater respectively than those at $\bar{\sigma}_{vc} = 3.38 \text{ kg/cm}^2$. The differences in normalized moduli for this range of $\bar{\sigma}_{vc}$ in the three types of tests are remarkably similar.

5.4.6 Summary Remarks Concerning the Choice of Modulus Values for Use in Final Correlations

The important findings of these correlations of load-deformation behavior will now be reviewed.

A bi-linear finite element analysis was used to predict the behavior of the model footing. The effects that variations in strength and K_o at each OCR had on the predicted load-deformation behavior were investigated. Following this study, values of these parameters for each OCR were chosen for use in making the final predictions of footing behavior. An investigation was then conducted to ascertain what values of modulus yielded a good prediction of footing behavior throughout loading in each case.

For the rigid footing considered here, the choice of the modulus value at each OCR was explained by comparing the strains in the bi-linear finite element model with those measured in the plane strain active test at equal values of $\Delta q/\Delta q_f$. No single factor of safety with respect to the choice of the modulus value was found applicable for the three stress histories. The bi-linear stress-strain curves yielding the best correlations intersected the plane strain active stress-strain curves as follows: (See Figure 5-13)

<u>OCR</u>	<u>$E/\bar{\sigma}_{vc}$</u>	<u>$\Delta q/\Delta q_f$ for intersection</u>
1	400	approx. tangent to curve at less than 0.4
2	300	.55
4	300	.75

The point at which extensive yielding occurred varied with the overconsolidation ratio and played an important role in the choice of the modulus. In the normally consolidated case extensive yielding occurred at high factors of safety. Thus most of the load-deformation behavior was controlled by contained plastic flow. The factor of safety at which extensive yielding occurred decreased as the OCR increased. Hence, more of the load-deformation behavior was controlled by "elastic or prefailure" strains as the overconsolidation ratio increased. Thus, use of a constant E prior to yield, to approximate the actual curved stress-strain behavior of the soil lead to larger differences between the predicted and measured footing behavior as the OCR increased.

At high factors of safety in the normally consolidated case the bi-linear model slightly underpredicted the footing displacement. Then as the strains of the yielded elements increased, good agreement existed for most of the remaining loading sequence.

In the overconsolidated cases, the bi-linear model resulted in over predictions of footing displacement at high factors of safety since the model overestimated strains compared to the plane strain active test. Conversely, at low factors of safety where the bi-linear

model underestimated the plane strain active strains, the footing displacements were under predicted.

5.5 ADDITIONAL COMMENTS CONCERNING FINITE ELEMENT CORRELATIONS

In this section several additional factors concerning the finite element correlations will be discussed. These include observations concerning the development of a tri-linear finite element analysis, strain rate effects with regard to the choice of modulus, strain softening, and observations concerning other improvements to finite element analyses that may be desirable. These will be discussed in the order listed above.

An important conclusion resulting from the correlations in the previous section is that with the bi-linear finite element analysis, it is difficult to make an a priori statement concerning the modulus value that leads to general agreement with the model footing test results. At each overconsolidation ratio, it was necessary throughout loading, to study the states of stress and strain of many of the elements in the finite element grid. A comparison then had to be made with regard to the plane strain active stress-strain curve of the soil, to determine whether, on the average, the bi-linear stress-strain curve predicted the soil's behavior adequately throughout loading.

The bi-linear finite element analysis is a very powerful tool. However, this study has shown that a modification to it is desirable. As a first step, finite element programs employing tri-linear stress-strain curves should be developed. Development of these programs will actually make it easier to obtain good predictions. As it now

stands, one is forced to over predict strains for one range of $\Delta q/\Delta q_f$ and to under predict strains for the remainder of the loading. Then in order to estimate the potential error in the prediction, it is necessary to go through the laborious task of compiling the distribution of stress and strain for elements in the grid so that a comparison can be made with respect to the stress-strain curve for the soil.¹ With a tri-linear model the net effect of overestimating and underestimating strains will be reduced. Thus, better agreement will be achieved initially without having to make a detailed study of the distribution of stress and strain in the grid.

Mention was made in Chapter Four that the strain rate employed in an undrained shear test can have an influence on the stress-strain modulus that is measured. Strain rates of 1.0 percent per hour or less were employed in the plane strain tests. The model footing tests were performed within about 15 seconds. The question might be raised concerning why "slow" plane strain tests can be used to analyze "fast" model tests. No specific answer to this question is possible. However it should be noted that it was not necessary to resort to strain rate effects to explain the results. Using the plane strain data, a cogent explanation for the agreement between the observed and predicted behavior was presented for each overconsolidation ratio. For those cases where significant overestimates of strain existed in the finite element model, the finite element analyses over predicted the footing behavior. Conversely, under predictions of footing displacement occurred for

¹ In the future it is recommended that subroutines be written to perform this task.

cases where the strains in the "slow" plane strain tests were underestimated in the bi-linear model.

It will be recalled that the yielded portion of the stress-strain curve specified in the computer prediction has a small positive slope. The point to be considered now is how closely does this specified behavior approximate soil behavior after yield. Strain softening, a decrease in the stress difference after failure, occurred in some of the undrained shear tests studied in Chapter Four. For example, strain softening occurred in the plane strain active tests at all three overconsolidation ratios. Conversely, no significant strain softening was observed during the plane strain passive tests. Is the divergence of the yielded portion of the stress-strain curve used in the finite element analysis from the strain softening behavior of the plane strain active tests important? At the present time strain softening is not considered in any finite element analysis. Therefore, no definite answer to the question can be made. However, it is possible to consider how well the average behavior of the bi-linear analysis approximates the behavior of Boston Blue Clay.

The plane strain active test results suggest that if strain softening did occur in the model tests, it should be most predominant in those areas under the footing that experienced little if any re-orientation of the principal stresses. The distribution of strain for the yielded elements with $|\alpha| > 70^\circ$ was examined for the largest $\sigma/\bar{\sigma}_{vc}$ value tabulated for each overconsolidation ratio in Tables 5-4 through 5-6. This information is tabulated in Table 5-7.

The average strain of the yielded elements, ϵ_y , was greater than ϵ_f , the failure strain in the plane strain active test, for OCR's of one and two. However, there is no problem with regard to strain softening since significant strain softening did not occur immediately in the plane strain tests. (See Figures D-1 and D-3). At the $\sigma/\bar{\sigma}_{vc}$ studied for an OCR = 4, there is no strain softening problem since ϵ_y is less than ϵ_f .

As with the discussion in the previous section, it is necessary to consider the overall behavior of the grid, rather than the behavior of the "outlying elements". Therefore, while some elements at each OCR experienced large strains, the effects of these elements can only be considered significant from the standpoint of how they influence the average strain. Since the average strains in the above listing do not indicate extensive strain softening of the soil, the average behavior of the bi-linear analysis is acceptable in this regard at the indicated stress levels.

A second point to be considered with respect to strain softening is the matter of changes in shearing resistance after yield due to continued reorientation of principal stresses. At the present time, no specific guidance in this area can be obtained from laboratory data. However, the FEAST III solutions were examined in this regard in order to obtain some insight into the problem. There appears to be little concern with respect to this question since less than five percent of the yielded elements experienced more than five degrees additional reorientation of the principal stresses after yield.

Further research in the area of strain softening may be warranted. However, before an extensive effort is expended, a tri-linear finite element program should be developed. Better agreement between the model tests results and these finite element predictions is anticipated. The importance of strain softening can then be re-examined in light of the new correlations.

In Appendix G the patterns of subsurface movements at hypothetical slope indicator positions were examined for three different finite element grids. At normalized footing displacements greater than 0.02, erratic subsurface movements were occasionally observed. These erratic subsurface movements are the result of large strains that existed in the grids at large footing displacements. Small strain theory was employed in the development of the finite element program. If the coordinates of the nodal points are updated after each load increment, the small strain theory of the analysis may be able to better handle the large strains that develop.

CHAPTER 6

SUMMARY, CONCLUSIONS, AND RECOMMENDATIONS

6.1 SUMMARY AND CONCLUSIONS

A comprehensive series of model footing tests on normally consolidated and overconsolidated Boston Blue Clay was conducted. These tests were performed for the purpose of observing the ultimate bearing capacity and load-deformation behavior of a strip footing for undrained loading under carefully controlled laboratory conditions where the stress history, stress state, strength and other properties of the soil were well known. Strength and modulus parameters were obtained from consolidated-undrained ($\overline{\text{CU}}$) plane strain, triaxial compression, and direct-simple shear tests. Values of K_0 , the coefficient of lateral stress at rest, were determined from plane strain, triaxial, and square oedometer tests. These soil parameters were used in theoretical analyses to predict the performance of the model footing. An analysis of the correlation between the predicted and observed behavior was made for the purpose of gaining additional insight into how improved engineering estimates of the undrained stability and initial settlements of structures in the field can be achieved. It has been shown that good estimates of footing performance for undrained shear are possible if the appropriate soil parameters are employed.

The important points resulting from this research are:

1. The model footing test results obtained during this research demonstrate that the anisotropic undrained

strength of Boston Blue Clay must be considered if reasonable estimates of undrained bearing capacity are to be achieved for overconsolidation ratios of one, two, and four. The maximum difference between the ultimate bearing capacities measured in this testing program and that predicted by the Davis and Christian (1970) theory using anisotropic strengths based on \overline{CU} plane strain tests was only seven percent. If the effects of strength anisotropy and sample disturbance were ignored, predicted undrained bearing capacities were typically in error by ± 15 to 30 percent.

2. Analysis of the load-deformation behavior of the model footing tests with finite element program FEAST III showed the following:
 - a. The load-deformation behavior for the normally consolidated case was found to be very dependent on the accurate assessment of the vertical undrained strength, s_{uv} , and of K_o . The strength anisotropy of the soil, K_s and $s_{u\alpha}$, while also important, did not dramatically affect the predicted performance at factors of safety greater than about two.
 - b. Error in the predicted behavior arising from moderate uncertainties in s_{uv} , K_s , and K_o of the soil, decreased as the overconsolidation ratio increased.
 - c. At all overconsolidation ratios the predicted load-settlement behavior was found to be very dependent on the modulus employed in the analysis.

3. With the bi-linearly elastic finite element analysis used in this research, it was not possible to make an a priori prediction of the modulus value at all OCR's that would lead to a good prediction of model footing performance for the full range of loading. Rather, choice of the best modulus value was dependent on consideration of the stress-strain properties of the soil at each stress history.
 - a. In the normally consolidated case extensive yielding occurred at high factors of safety and most of the load-deformation behavior was controlled by contained plastic flow. The bi-linear model in this case predicted the footing behavior quite well until just before failure. Strains in plane strain compression prior to failure were under predicted by the bi-linear model (see Figure 5-13) and thus at high factors of safety there was a very slight underprediction of footing displacement (Figure 5-10). There was general agreement throughout most of the remaining loading sequence as the strains of the yielded elements increased.
 - b. As the overconsolidation ratio increased the factor of safety at which extensive yielding occurred decreased. Thus more of the load-deformation behavior was controlled by "elastic or pre-failure" strains. Consequently the bi-linear stress-strain curve was less able to model the actual non-linear stress-strain behavior of the soil

(see Figure 5-13). Differences between the predicted and measured load-deformation behavior became larger as the OCR increased. At high factors of safety in both overconsolidated cases, the footing displacement was over predicted. Conversely, at low factors of safety, the finite element method underestimated the footing displacement (see Figures 5-11 and 5-12).

4. The normally consolidated model footing tests did not exhibit truly normalized behavior. The normalized modulus $E/\bar{\sigma}_{vc}$ was found to decrease with increasing $\bar{\sigma}_{vc}$ (Figure 5-10). Similar behavior was observed in direct simple-shear and CIU triaxial compression tests. (Figures 4-8 and 4-11).
5. This research has demonstrated that an integrated approach to the solution of engineering problems is fruitful. The correlations that were obtained demonstrated that the results of laboratory measurements can be used with theoretical methods to achieve good predictions of undrained "field" behavior as measured in model footing tests.

6.2 RECOMMENDATIONS FOR FUTURE RESEARCH

The following laboratory research is recommended:

1. Research on the undrained shear strength behavior of Boston Blue Clay under plane strain conditions should be extended to higher overconsolidation ratios.
2. Model footing tests should be conducted at higher

overconsolidation ratios concurrently with additional undrained plane strain tests. Both groups of data are needed for making reliable predictions of load-deformation behavior at overconsolidation ratios greater than four.

3. Model footing tests having extended times of aging should be conducted to compare aged "field" behavior with that observed in other laboratory tests.
4. Larger sized model footing apparatus should be developed and instrumented so that effective stress analyses of load-deformation behavior can be studied. A method for observing sub-surface movements should also be developed and incorporated in this equipment.
5. Reference data for undrained stability conditions starting from K_0 stresses now exist. The area of strength-increases-with-consolidation has received very little attention. The laboratory equipment and techniques for model tests which now exist make it possible to consider research in this area. Much laboratory and theoretical effort will be required.
6. As time permits, research in the following areas would be beneficial:
 - a. A concurrent program of drained plane strain and model footing tests.
 - b. A concurrent program of plane strain and model footing tests on overconsolidated recompressed samples.

The following analytical effort is recommended:

1. A tri-linearly elastic (or bi-linearly elastic perfectly

plastic) finite element program should be developed.

2. Another analysis of the model footing tests should be conducted with the program that is developed. Emphasis in this analysis should be directed to two areas. The first would be the establishment of general guidelines that could be employed in choosing modulus values for differing over-consolidation ratios. This is considered possible for the tri-linear analysis since the net error of underestimating and/or overestimating strains will be smaller than with the bi-linear analysis. Secondly, based on the resulting correlations an assessment should be made of the effects (if any) of strain softening in the model tests. If strain softening is considered to be of significance, then a finite element program having a strain softening capability should be developed.
3. Existing finite element programs should be modified to update the nodal point coordinates following each load increment. This should improve the performance of elements that are subjected to large strains.

CHAPTER 7

BIBLIOGRAPHY

Note: ICSMFE - International Conference Soil Mechanics and
Foundation Engineering
JSMFD - Journal of Soil Mechanics and Foundation Divisions

1. Aboshi, H., H. Yoshikuni, and T. Uchibayashi (1969):
"Stability of Soft Foundations Underneath Embankment, Consolidated by Means of Card-Board Drains", Soil and Foundations, Vol. IX, No. 2.
2. Alvarez-Stelling, J., (1966): "Settlement of Footings on Clay", S.M. Thesis, Dept. of Civil Engineering, M.I.T., Cambridge, Massachusetts (unpublished).
3. Bailey, W.A. (1961): "Effects of Salt on the Shear Strength of Boston Blue Clay", S.B. Thesis, Dept. of Civil Engineering, M.I.T., Cambridge, Massachusetts (unpublished).
4. Baker, W.H. and R.J. Krizek (1969): "Mohr-Coulomb Strength Theory for Anisotropic Soils", ASCE JSMFD, Vol. 96, SM 1, pp. 269-292.
5. Bishop, A.W. (1966): "The Strength of Soils as Engineering Materials", Geotechnique, Vol. XVI, No. 2, pp. 91-128.
6. Bishop, A.W. and L. Bjerrum (1960): "The Relevance of the Triaxial Test to the Solution of Stability Problems", ASCE Research Conference on the Shear Strength of Cohesive Soils, Boulder, Colorado, pp. 437-501.
7. Bjerrum, L. (1967): "Engineering Geology of Norwegian Normally-Consolidated Marine Clays as Related to Settlements of Building", Geotechnique, Vol. XVII, No. 2, pp. 81-118.
8. Bjerrum, L. and A. Landva (1966): "Direct Simple Shear Tests On a Norwegian Quick Clay", Geotechnique, Vol. XVI, No. 1, pp. 1-20.
9. Bjerrum, L. and K.Y. Lo (1963): "Effect of Aging on the Shear Strength Properties of a Normally Consolidated Clay", Geotechnique, Vol. XIII, No. 2, pp. 147-157.

10. Braathen, N.F. (1966): "Investigation of Effects of Disturbance on Undrained Shear Strength of Boston Blue Clay", S.M. Thesis, Dept. of Civil Engineering, M.I.T., Cambridge, Massachusetts, (unpublished).
11. Bovee, R.B. and C.C. Ladd (1970): "M.I.T. Plane Strain Device", M.I.T. Research Report, Department of Civil Engineering (in preparation).
12. Bovee, R.B., E.B. Kinner, and C.C. Ladd (1970): "Plane Strain Test Data on Boston Blue Clay", M.I.T. Research Report, Department of Civil Engineering (in preparation).
13. Brown, J.D. (1967): "The Ultimate Bearing Capacity of Layered Clay Foundations", Ph. D. Thesis, Nova Scotia Technical College, Halifax, Nova Scotia (unpublished).
14. Burland, J.B. (1967): "Deformation of Soft Clay", Ph.D. Thesis, Cambridge University, London (unpublished).
15. Burland, J.B. and K.H. Roscoe (1969): "Local Strains and Pore Pressures in a Normally Consolidated Clay Layer During One Dimensional Consolidation", Geotechnique, Vol. XIX, No. 3, pp. 335-356.
16. Carrier, W.D. III (1968): "Lunar Soil Mechanics: Distribution of Contact Stress Beneath a Rigid Plate Resting on Sand", Sc.D. Thesis, Dept. of Civil Engineering, M.I.T., Cambridge, Massachusetts (unpublished).
17. Casagrande, A. and N. Carrillo (1944): "Shear Failure of Anisotropic Materials", Contributions to Soil Mechanics, 1941-1953, Boston Society of Civil Engineers, Boston, Massachusetts.
18. Christian, J.T. (1966): "Plane-Strain Deformation Analysis of Soil", Ph.D. Thesis, Dept. of Civil Engineering, M.I.T., Cambridge, Massachusetts (unpublished).
19. D'Appolonia, D.J. (1968): "Predictions of Stress and Deformation For Undrained Loading Conditions", Ph.D. Thesis, Dept. of Civil Engineering, M.I.T., Cambridge, Massachusetts (unpublished).
20. D'Appolonia, D.J. and T.W. Lambe (1970): "Method for Predicting Initial Settlement", ASCE JSMFD, Vol. 96, No. 2, pp. 523-544.
21. D'Appolonia, D.J. and H.G. Poulos (1970): "Initial Settlement of Structures on Clay" (in preparation).

22. Davis, E.H. and H.G. Poulos (1968): "The Use of Elastic Theory for Settlement Prediction Under Three-Dimensional Conditions", Geotechnique, Vol. XVIII, No. 1, pp. 67-91.
23. Davis, E.H. and J.T. Christian (1970): "Anisotropic Strength and Bearing Capacity" (in preparation).
24. Dickey, J.W., C.C. Ladd, and J.J. Rixner (1968): "A Plane Strain Shear Device for Testing Clays", M.I.T. Research Report R 68-3.
25. Duncan, J.M. and H.B. Seed (1965): "The Effect of Anisotropy and Reorientation of Principal Stresses on the Shear Strength of Saturated Clay", Report TE 65-3, College of Engineering, University of California, Berkeley, California.
26. Duncan, J.M. and H.B. Seed (1966a): "Anisotropy and Stress Reorientation in Clay", ASCE JSMFD, Vol. 92, SM5, pp. 21-49.
27. Duncan, J.M. and H.B. Seed (1966b): "Strength Variation Along Failure Surfaces in Clay", ASCE JSMFD, Vol. 92, SM6, pp. 81-104.
28. Duncan, J.M. and P. Dunlop (1969): "Behavior of Soils in Simple Shear Tests", 7th ICSMFE, Vol. 1, pp. 101-109.
29. Edgers, L. (1967): "The Effect of Simple Shear Stress System On the Strength of Saturated Clay", S.M. Thesis, Dept. of Civil Engineering, M.I.T., Cambridge, Massachusetts (unpublished).
30. Gicot, O. (1966): "Small Scale Footing Tests on Clay", S.M. Thesis, Dept. of Civil Engineering, M.I.T., Cambridge, (unpublished).
31. Goodman, L.J., E. Hegedus, and P.W. Haley (1966): "Small Scale Footing Studies on Sand and Clay", Highway Research Record No. 108.
32. Hansen, J.B. (1952): "A General Plasticity Theory for Clay", Geotechnique, Vol. 3, No. 4, pp. 154-164.
33. Hansen, J.B. and R.E. Gibson (1949): "Undrained Shear Strengths of Anisotropically Consolidated Clays", Geotechnique, Vol. 1, No. 3, pp. 189-204.

34. Hardin, B.O., and W.L. Black (1968): "Vibration Modulus of Normally Consolidated Clay", ASCE JSMFD, Vol. 94, SM2, pp. 353-369.
35. Henkel, D.J. and N.H. Wade (1966): "Plane Strain Tests On a Saturated Clay", ASCE JSMFD, Vol. 92, SM6, pp. 67-80.
36. Hoëg, K., J.T. Christian, and R.V. Whitman (1968): "Settlement of Strip Load on Elastic-Plastic Soil", ASCE JSMFD, Vol. 94, SM2, pp. 431-445.
37. Janbu, N., L.Bjerrum, and B. Kjaernsli (1956): "Veiledning ved Losning au Fundamenteringsoppgauer", Norwegial Geotechnical Institute No. 16.
38. Ladd, C.C. (1964): "Stress-Strain Modulus of Clay from Undrained Triaxial Tests", Proceedings of the ASCE Soil Mechanics and Foundations Division Conference on "The Design of Foundations for Control of Settlements", Evanston, Illinois, pp. 127-156.
39. Ladd, C.C. (1965): "Stress-Strain Behavior of Anisotropically Consolidated Clays During Undrained Shear", 6th ICSMFE, Vol. 2, pp. 282-286.
40. Ladd, C.C. and T.W. Lambe (1963): "The Strength of 'Undisturbed' Clay Determined from Undrained Tests", National Research Council - American Society of Testing Materials Symposium on Laboratory Shear Testing of Soils, ASTM Special Technical Publication No. 361, pp. 342-371.
41. Ladd, C.C. and W.A. Bailey (1964): Discussion Geotechnique, Vol. 14, No. 4, pp. 353-358.
42. Ladd, C.C. and U. Luscher (1965): "Engineering Properties of Soils Underlying the M.I.T. Campus", M.I.T. Research Report R65-58.
43. Ladd, C.C. and W.B. Preston (1965): "On the Secondary Compression of Saturated Clays", M.I.T. Research Report R65-59.
44. Ladd, C.C. and J. Varallyay (1965): "The Influence of Stress System on the Behavior of Saturated Clays During Undrained Shear", M.I.T. Research Report, R 65-11.
45. Ladd, C.C. and E.B. Kinner (1967): "The Strength of Clays at Low Effective Stress", M.I.T. Research Report R67-4.
46. Ladd, R.S. (1965): "Use of Electrical Pressure Transducers to Measure Soil Pressure", M.I.T. Research Report R65-48.

47. Lambe, T.W. (1964): "Methods of Estimating Settlement", ASCE JSMFD, Vol. 90, SM5, pp. 43-67.
48. Lambe, T.W. and R.V. Whitman (1969): Soil Mechanics, John Wiley and Sons, New York.
49. Lo, K.Y. (1965): "Stability of Slopes in Anisotropic Soils", ASCE JSMFD, Vol. 91, SM4, pp. 85-106.
50. Martin, R.T. and C.C. Ladd (1970): "Fabric of Consolidated Kaolinite", M.I.T. Research Report (in preparation).
51. Meyerhof, G.G. (1951): "The Ultimate Bearing Capacity of Foundations", Geotechnique, Vol. II, No. 4, pp. 301-332.
52. Mitchell, J.K. (1956): "The Importance of Structure to the Engineering Behavior of Clay", Sc.D. Thesis, Dept. of Civil Engineering, M.I.T., Cambridge, Mass. (unpublished).
53. M.I.T. (1968): "Prediction Of The Deformation Of a Levee On A Soft Foundation", M.I.T. Research Report R 69-18.
54. Norwegian Geotechnical Institute (1969): "Some Experiences From Stress Calculations Using Finite Elements", Internal Report F 358-4, October.
55. Perez-La Salvia H., J. Alvarez-Stelling, T.W. Lambe, and U. Luscher (1966): "A Model Study: Settlement of Footings on Clay", Proceedings ASCE Structural Engineering Conference, January-February 1966.
56. Perloff, W.H. and K.S.A. Rahim (1966): "A Study of Pressure Penetration Relationships for Model Footings", Highway Research Record, No. 145.
57. Poulos, H.G. (1964): "Analysis of Settlement of Foundations on Clay Soils Under Three-Dimensional Conditions", Ph.D. Thesis, University of Sidney, Sidney (unpublished).
58. Poulos, H.G. (1967): "Stresses and Displacements in an Elastic Layer Underlain by a Rough Rigid Base", Geotechnique, Vol. XVII, No. 4, pp. 378-410.
59. Rangantham, B.V. and A.C. Matthai (1967): "Effect of Anisotropy on the Stability of Earth Masses Under $\phi = 0$ Condition", Proceedings 3rd Asian Regional Conference on Soil Mechanics and Foundation Engineering, Haifa, Israel, pp. 348-352.

60. Rixner, J.J. (1967): "The Influence of Plane Strain Conditions on the Strength Behavior of a Saturated Clay", S.M. Thesis, Dept. of Civil Engineering, M.I.T., Cambridge, Massachusetts (unpublished).
61. Roberts, J.E. (1961): "Small-Scale Footing Studies: A Review of the Literature", M.I.T., Department of Civil and Sanitary Engineering, Soil Engineering Division, Publication 108.
62. Roscoe, K.H. (1953): "An Apparatus for the Application of Simple Shear to Soil Samples", 3rd ICSMFE, Vol. 1, pp. 186-191.
63. Roscoe, K.H. (1968): "Soils and Model Tests", Journal of Strain Analysis, Vol. 3, No. 1, pp. 57-64.
64. Watt, B.J. (1969): "Analysis of Viscous Behavior in Undrained Soils", Sc.D. Thesis, Dept. of Civil Engineering, M.I.T., Cambridge, Massachusetts (unpublished).
65. Wissa, A.E.Z.(1961): "A Study of the Effects of Environmental Changes on the Stress-Strain Properties of Kaolinite", S.M. Thesis, Dept. of Civil Engineering, M.I.T., Cambridge, Massachusetts (unpublished).
66. Young, R., G.M. Peck, and H.C. Leitch (1963): "Model Bearing Tests on a Remolded Clay", Second Panamerican Conference on Soil Mechanics and Foundation Engineering, Vol. I, pp. 337-350.

CHAPTER 8

LIST OF NOTATIONS

Note: A bar over a stress indicates an effective stress
Suffix f indicates a failure condition

1. Stresses

$\sigma_1, \bar{\sigma}_1$	Major principal stress
$\sigma_3, \bar{\sigma}_3$	Minor principal stress
$\sigma_v, \bar{\sigma}_v$	Vertical stress
$\sigma_h, \bar{\sigma}_h$	Horizontal stress
$\bar{\sigma}_{vc}$	$\bar{\sigma}_v$ at consolidation
$\bar{\sigma}_{hc}$	$\bar{\sigma}_h$ at consolidation
$\bar{\sigma}_c$	Consolidation stress for $\overline{CIU C}$ triaxial test
$\bar{\sigma}_{vm}$	Maximum past vertical effective stress
σ	Average footing contact stress
$\Delta\sigma_v$	Change in vertical stress
$\sigma_z, \sigma_y, \sigma_x$	Increments of vertical and horizontal total normal stress for use in calculating the initial settlement of a foundation

q	$(\sigma_1 - \sigma_3)/2$
\bar{p}	$(\bar{\sigma}_1 + \bar{\sigma}_3)/2$
q_f, τ_{\max}	$(\sigma_1 - \sigma_3)/2$ at failure (maximum stress difference)
Δq_f	Change in shear stress required to cause failure
Δq	Change in shear stress at point in test
τ_h	Horizontal shear stress measured in direct-simple shear test

2. Stress Ratios

A	Skempton's A parameter
B	Skempton's B parameter
K_o	Coefficient of lateral stress at rest = $\bar{\sigma}_{hc} / \bar{\sigma}_{vc}$
OCR	Overconsolidation ratio = $\bar{\sigma}_{vm} / \bar{\sigma}_{vc}$
$\sigma / \bar{\sigma}_{vc}$	Model footing test stress ratio

3. Strength and Modulus

s_u	q_f for undrained shear
s_{uv}	q_f for test in which σ_1 at failure is in insitu vertical direction
s_{uh}	q_f for test in which σ_1 at failure is in insitu horizontal direction

$s_{u\alpha}$	q_f for soil when σ_1 at failure is oriented α degrees from the insitu horizontal direction; term referring to the distribution of anisotropic undrained shear strength
$s_{u\theta}$	q_f for soil when σ_1 at failure is oriented θ degrees from the insitu vertical direction
α	Orientation of σ_1 from insitu horizontal direction
θ	Orientation of σ_1 from insitu vertical direction
K_s	s_{uh}/s_{uv}
E	Young's modulus; stress-strain modulus
E_h	Modulus in insitu horizontal plane
E_s	Secant modulus
E_o, E	Initial modulus specified in bi-linearly elastic finite element analysis
E_y	"Yielded" modulus specified in bi-linearly elastic finite element analysis
G_s	Secant shear modulus computed from direct-simple shear test
G_{vh}	Shear modulus in vertical plane

4. Dimensions, Displacements, and Strains

B	Width of Model footing
ρ	Vertical displacement of model footing, initial settlement of a foundation
ρ/B	Normalized footing displacement
ϵ_f	Axial strain at failure in plane strain active test
ϵ_v	Axial strain in triaxial and plane strain tests
ϵ_y	Average vertical strain of yielded elements in finite element grid ($ \alpha > 70^\circ$)
γ	Shear strain in direct-simple shear test
h_f	Model footing test sample height at end of primary compression for the last normally consolidated increment
H_s	Height of solids
δ_h	Thickness of elastic layer
ΔR	Lateral displacement of node in finite element grid

5. Miscellaneous

a,b	Half axes of elliptical strength plot in bearing capacity theory of Davis and Christian (1970)
C_α	Rate of secondary compression

C_c	Compression index
c_v	Coefficient of consolidation
e	Void ratio
Δe_s	Change in void ratio during secondary compression
G_s	Specific gravity
I	Influence factor for computing the initial settlement of a foundation
N_c	Bearing capacity factor
P.I.	Plasticity Index
T_p	Time required for primary consolidation
T_s	Time allowed for secondary compression at $\bar{\sigma}_{vm}$ for model footing, plane strain, and direct-simple shear tests
	Time allowed at $\bar{\sigma}_{vm}$ for triaxial compression tests
ν	Poisson's ratio
w_i	Initial water content
w_f	Final water content
w_L	Liquid limit
w_P	Plastic limit

$\bar{\phi}$ ARCSIN q/\bar{p} for plane strain and triaxial tests
 ARCTAN $\tau_h/\bar{\sigma}_v$ for direct-simple shear tests

6. Designation of Undrained Shear Tests

\overline{CIU} C	Isotropically consolidated undrained triaxial compression test with pore pressure measurements
\overline{CK}_o U C	Anisotropically consolidated undrained triaxial compression test with pore pressure measurements
\overline{CK}_o U PSA	Anisotropically consolidated plane strain active (compression) test with pore pressure measurements
\overline{CK}_o U PSP	Anisotropically consolidated plane strain passive (extension) test with pore pressure measurements
\overline{CU} DSS	Anisotropically consolidated constant volume direct-simple shear test
UU	Unconsolidated - Undrained triaxial compression test

Table 4-1

COMPARISON OF NORMALIZED MODULUS VALUES FROM
PLANE STRAIN, TRIAXIAL, AND DIRECT-SIMPLE
SHEAR TESTS

F.S.	OCR	Triaxial		Plane Strain		\overline{CUDSS}^a
		\overline{CIU}	$\overline{CK_o U}$	Active	Passive	
4	1	200	530	410	800±	200
3	1	190	380	350	480	180
2	1	175	290	230	230	125
4	2	275	700	420	800±	390
3	2	270	520	370	530	320
2	2	190	335	290	245	225
4	4	370	850	600	800±	420
3	4	350	650	550	625	350
2	4	215	450	525	350	230

Test	Consolidation Time at $\bar{\sigma}_{vm}$ (days)	$\bar{\sigma}_{vm}$ (kg/cm ²)
Triaxial	~1 to 4	6.0
Plane Strain	1	4.0
\overline{CUDSS}	1	4.0

a.
Normalized pseudo secant modulus

Table 5-1
 COMPARISON OF MEASURED VALUES OF ULTIMATE BEARING CAPACITY AND
 THOSE PREDICTED BY DAVIS AND CHRISTIAN (1970) ON THE BASIS OF
 ANISOTROPIC UNDRAINED SHEAR STRENGTH

OCR	Values of $\frac{\sigma}{\bar{\sigma}_{vc}}$			Predicted/Measured
	Measured at $\rho/B = 0.1$		Predicted	
1	$\bar{\sigma}_{vc} = 1.0 \text{ kg/cm}^2$: 1.42	}	1.34	0.94
	$\bar{\sigma}_{vc} = 2.0 \text{ kg/cm}^2$: 1.36			0.99
	$\bar{\sigma}_{vc} = 3.38 \text{ kg/cm}^2$: 1.34			1.00
2	2.42		2.39	0.98
4	4.20		3.90	0.93

Table 5-2
 COMPARISON OF MEASURED VALUES OF ULTIMATE BEARING CAPACITY AND
 THOSE PREDICTED ON THE ASSUMPTION OF ISOTROPIC UNDRAINED SHEAR STRENGTH

	Values of $\sigma/\bar{\sigma}_{vc}$		
	(Predicted / Measured)	(Predicted / Measured)	(Predicted / Measured)
Measured at $\rho/B = 0.1$	$\frac{OCR = 1}{1.37}$ (Avg.)	$\frac{OCR = 2}{2.42}$	$\frac{OCR = 4}{4.20}$
Predicted: \overline{CK}_O Plane Strain Active $s_{uv}/\bar{\sigma}_{vc}$	1.75 (1.28)	3.0 (1.24)	4.85 (1.15)
\overline{CIU} Triaxial Compression	1.66 (1.21)	2.85 (1.18)	4.62 (1.10)
\overline{CK}_O DSS	1.03 (.75)	1.9 (.785)	3.06 (.73)
UU (D'Appolonia 1968)	.925 (.675)	1.83 (.725)	3.08 (.735)

Table 5-3

SUMMARY INFORMATION ALL THREE OVERCONSOLIDATION RATIOS

Note: All percents based on total number of yielded elements at $\rho/B = 0.04$

Nominal $\sigma/\bar{\sigma}_{vm}$	OCR = 1 Total Yielded = 185			OCR = 2 Total yielded = 153			OCR = 4 Total Yielded = 123		
	Actual $\sigma/\bar{\sigma}_{vm}$	Total No. of Yielded Elements (%)	No. of Elements $\frac{\Delta q}{\Delta q_f} > 0.40$ $ \alpha > 70^\circ$ (%)	Actual $\sigma/\bar{\sigma}_{vm}$	Total No. of Yielded Elements (%)	No. of Elements, $\frac{\Delta q}{\Delta q_f} > 0.58$ $ \alpha > 70^\circ$ (%)	Actual $\sigma/\bar{\sigma}_{vm}$	Total No. of Yielded Elements (%)	No. of Elements $\frac{\Delta q}{\Delta q_f} > 0.69$ $ \alpha > 70^\circ$ (%)
0.35- 0.43	0.35	10 (5)	>72 (>40)	0.43	2 (1)	~15 (~10)	0.346	1 (~0)	<5 (0-2)
0.46- 0.57	0.46	52 (28)	>90 (>50)	0.531	4 (2.6)	50 (33)	0.576	8 (6.5)	13 (11)
0.65- 0.75	0.7	81 (44)	~100 (~55)	0.65	10 (6.5)	69 (45)	0.77	31 (25.2)	51 (42)
0.88- 1.05	0.954	86 (46)	~90 (~50)	0.99	75 (49)	78 (~50)	0.88	72 (58)	61 (50)
	1.05 (10)	91 (49)	96 (52)						

Table 5-4
 SUMMARY INFORMATION OCR = 1.0

$\sigma/\bar{\sigma}_{vc}$	Number of Elements in Indicated Range $\Delta q/\Delta q_f$ (Average Vertical Strain)			
	0 - 0.58	0.58 - 0.84	0.84 - 1.0	> 1.0
0.35	45	33	32	7 (0.04)
0.46	33	23	11	52 (0.07)
0.70	8	15	5	81 (0.31)
1.056	1	3	2	91 (0.81)

Note: $|\alpha| > 70^\circ$ For All Elements Considered
 For $\frac{\Delta q}{\Delta q_f} > 0.4$ the bi-linear model under predicts the plane strain active strains for the unyielded elements.

Table 5-5

SUMMARY INFORMATION OCR = 2.0

$\sigma / \bar{\sigma}_{vc}$	Number of Elements in Indicated Range $\Delta q / \Delta q_f$ (Average Vertical Strain)			
	0 - 0.55	0.55 - 0.71	0.71 - 1.0	>1.0
0.855	70 - 80	8	5	-
1.07	30	40	9	1
1.3	~20	26	37	6 (0.21)
1.98	-	3	18	57 (0.56)
2.26	-	-	1	74 (1.4)

Note: $|\alpha| > 70^\circ$ all elements considered

For $\Delta q / \Delta q_f > 0.55$ the bi-linear model under predicts the plane strain active strains for the unyielded elements.

Table 5-6

SUMMARY INFORMATION OCR = 4.0

$\sigma / \bar{\sigma}_{vc}$	Number of Elements in Indicated Range $\Delta q / \Delta q_f$ (Average Vertical Strain)						
	0.38-0.48	0.48-0.59	0.59-0.69	0.69-0.79	0.79-0.89	0.89-1.0	> 1.0
1.39	23	4	1	1	-	-	-
2.27	13	30	24	7	3	1	2
3.07	-	2	14	9	18	11	13 (0.52)
3.52	-	-	-	8	7	7	39 (0.6)
3.92	-	-	-	-	-	2	52 (1.25)

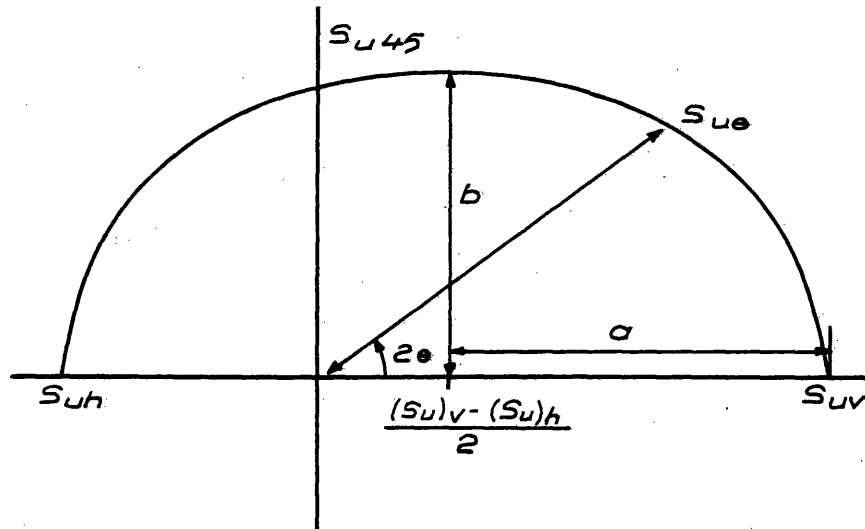
Note: $|\alpha| > 70^\circ$ For all Elements Considered

For $\frac{\Delta q}{\Delta q_f} > 0.75$ the bi-linear model under predicts the plane strain active strains for the unyielded elements.

Table 5--7

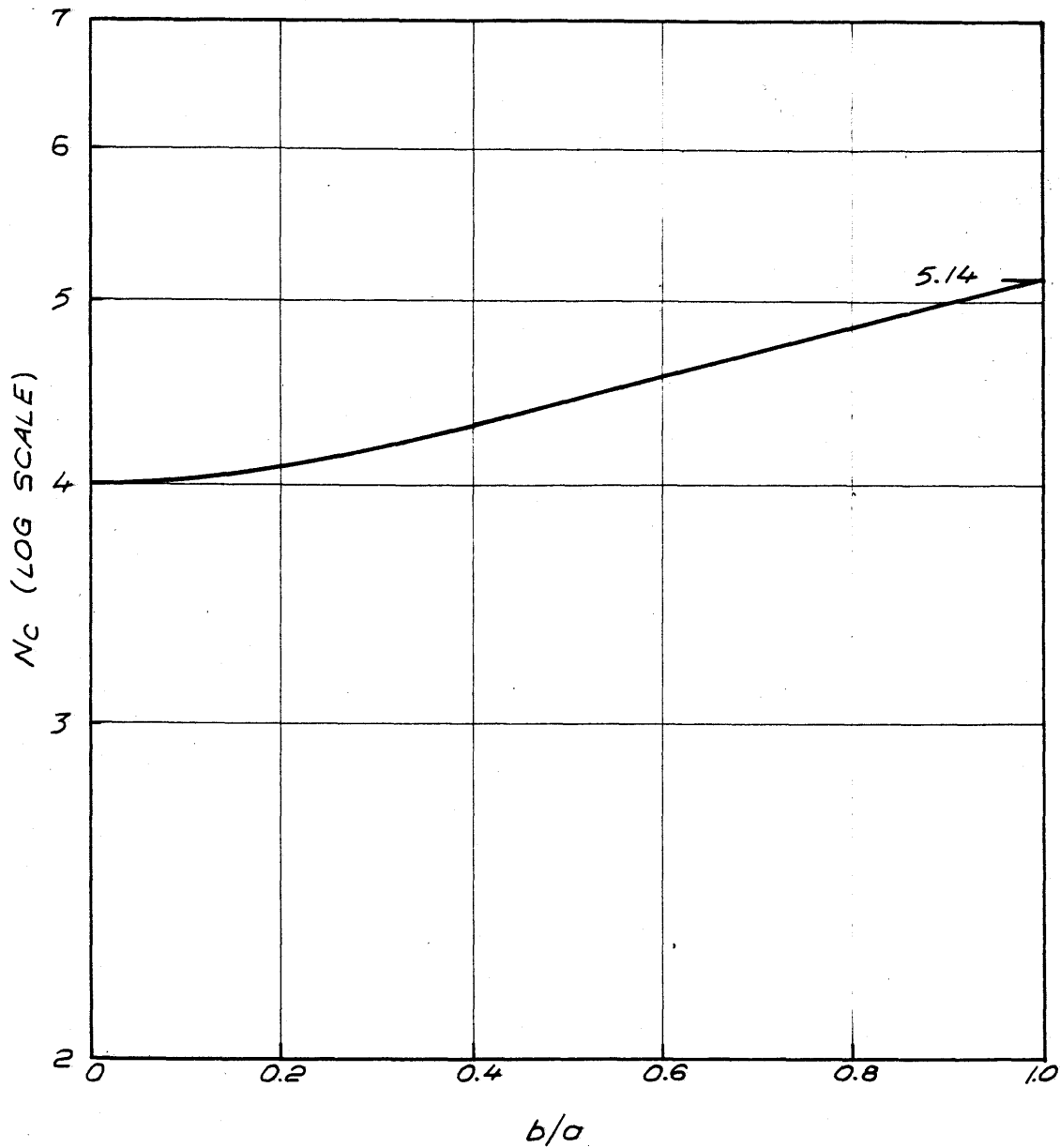
COMPARISON OF STRAINS AFTER YIELD WITH FAILURE STRAINS OF PLANE
STRAIN ACTIVE TESTS

OCR	$\sigma/\bar{\sigma}_{vc}$	Avg. Strain of Yielded Elements $\epsilon_y, \%$	Approx. Active Failure Strain $\epsilon_f, \%$	No. Yielded Elements with Strain Less than, ϵ_f	Total No. Yielded Elements
1	1.06	0.81	0.55	44	91
2	2.26	1.4	1.2	49	74
4	3.92	1.25	1.7	39	52

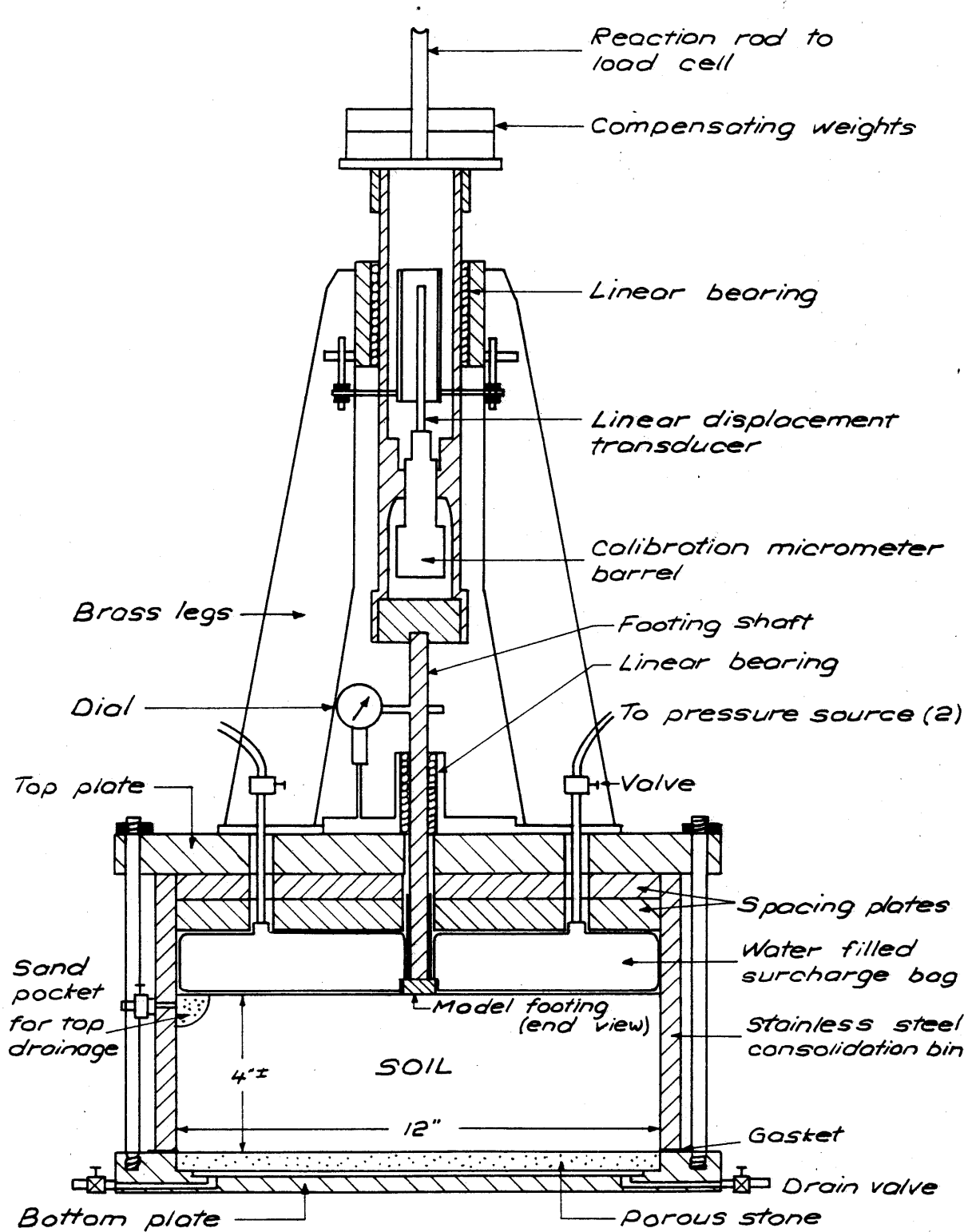


ELLIPTICAL STRENGTH PLOT FOR ANISOTROPIC CLAY
 PROPOSED BY DAVIS AND CHRISTIAN (1970)

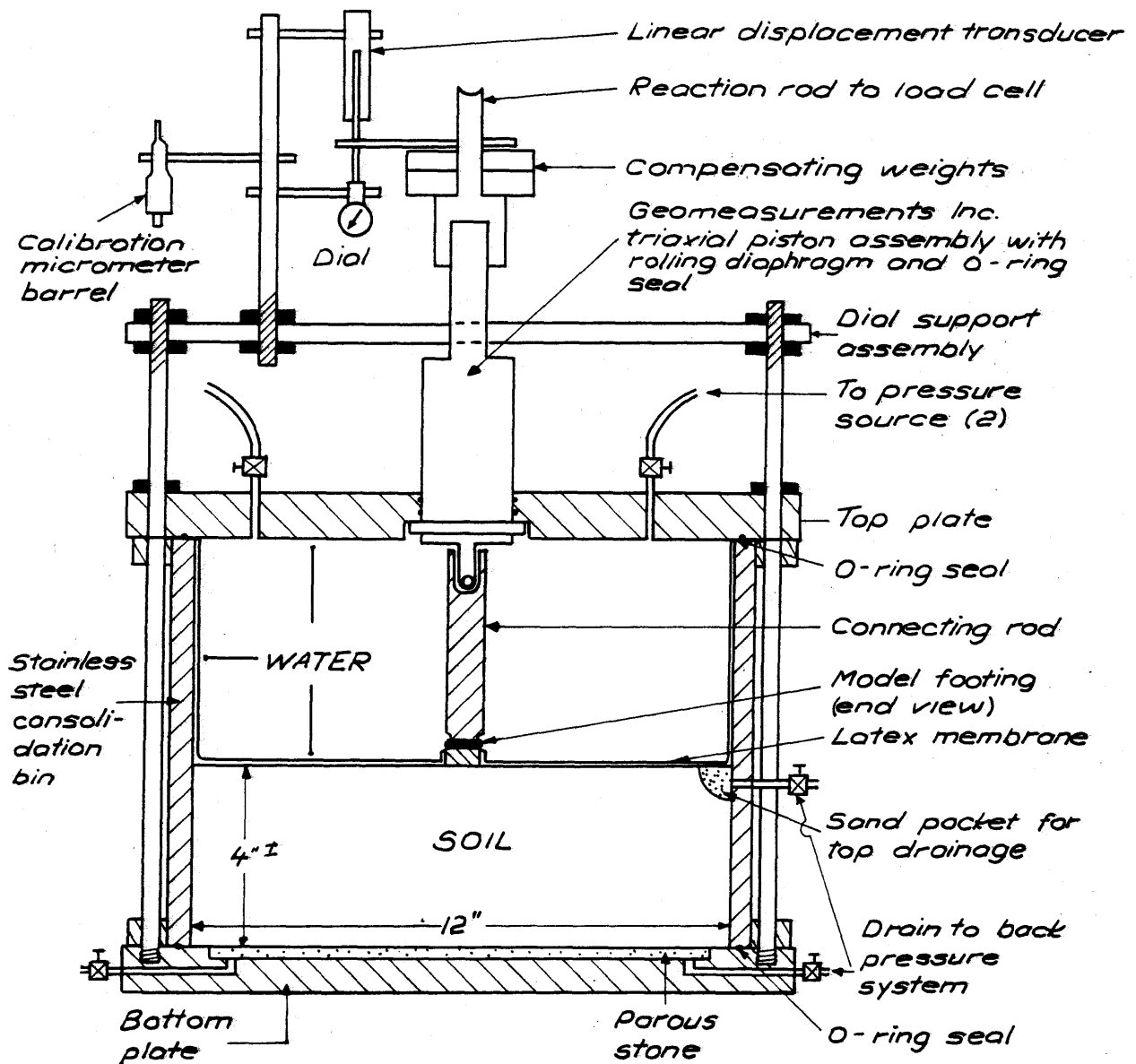
FIGURE 2-1



BEARING CAPACITY FACTOR VERSUS b/a RATIO
 (AFTER DAVIS AND CHRISTIAN 1970)

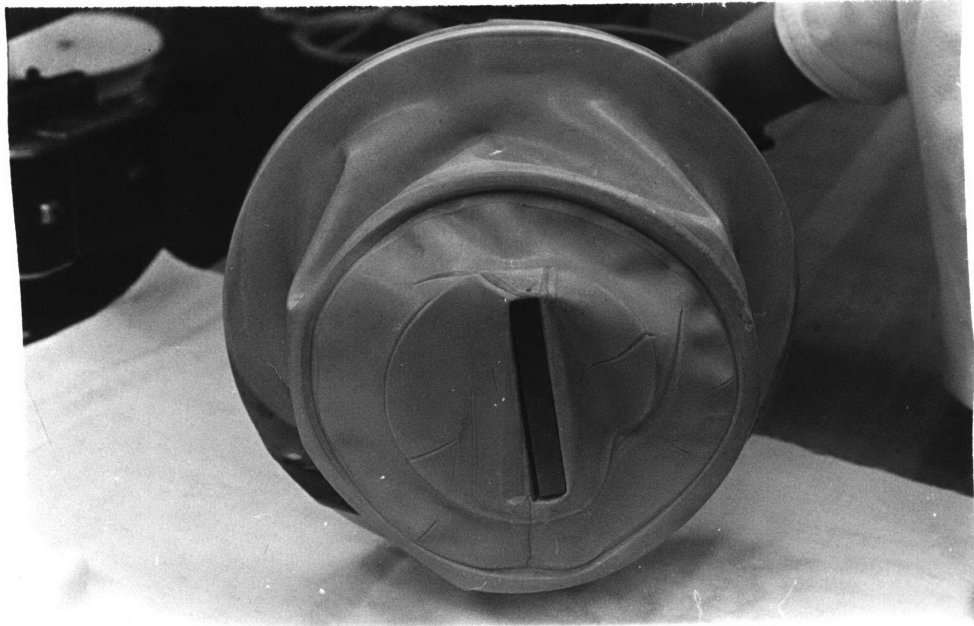


EQUIPMENT ARRANGEMENT AT FINAL CONSOLIDATION -
BIN ONE



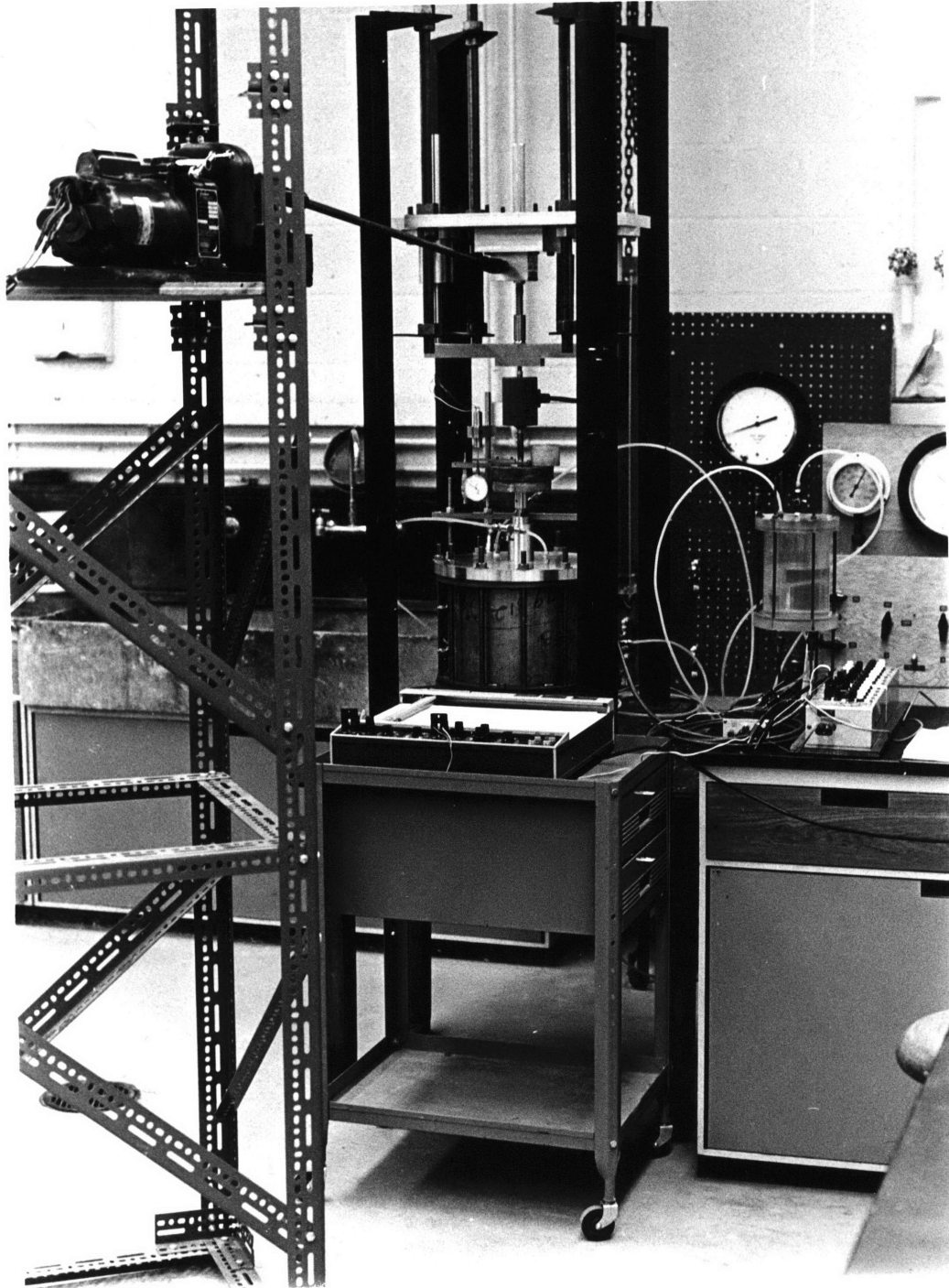
EQUIPMENT ARRANGEMENT AT FINAL CONSOLIDATION - BIN TWO

FIGURE 3-2



Membrane For Bin Two

Figure 3-3



Bin Two At Time Of Test

Figure 3-4

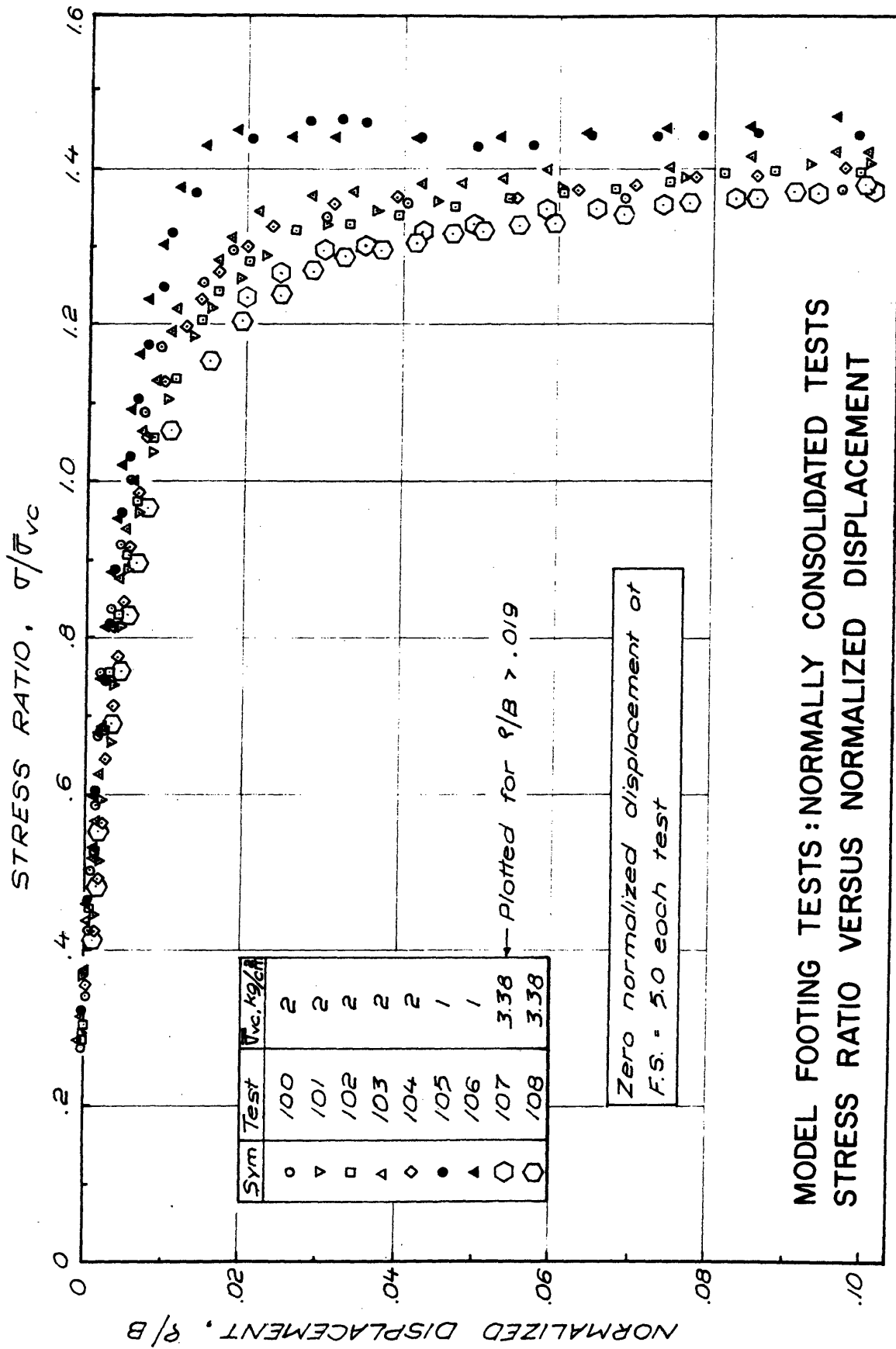
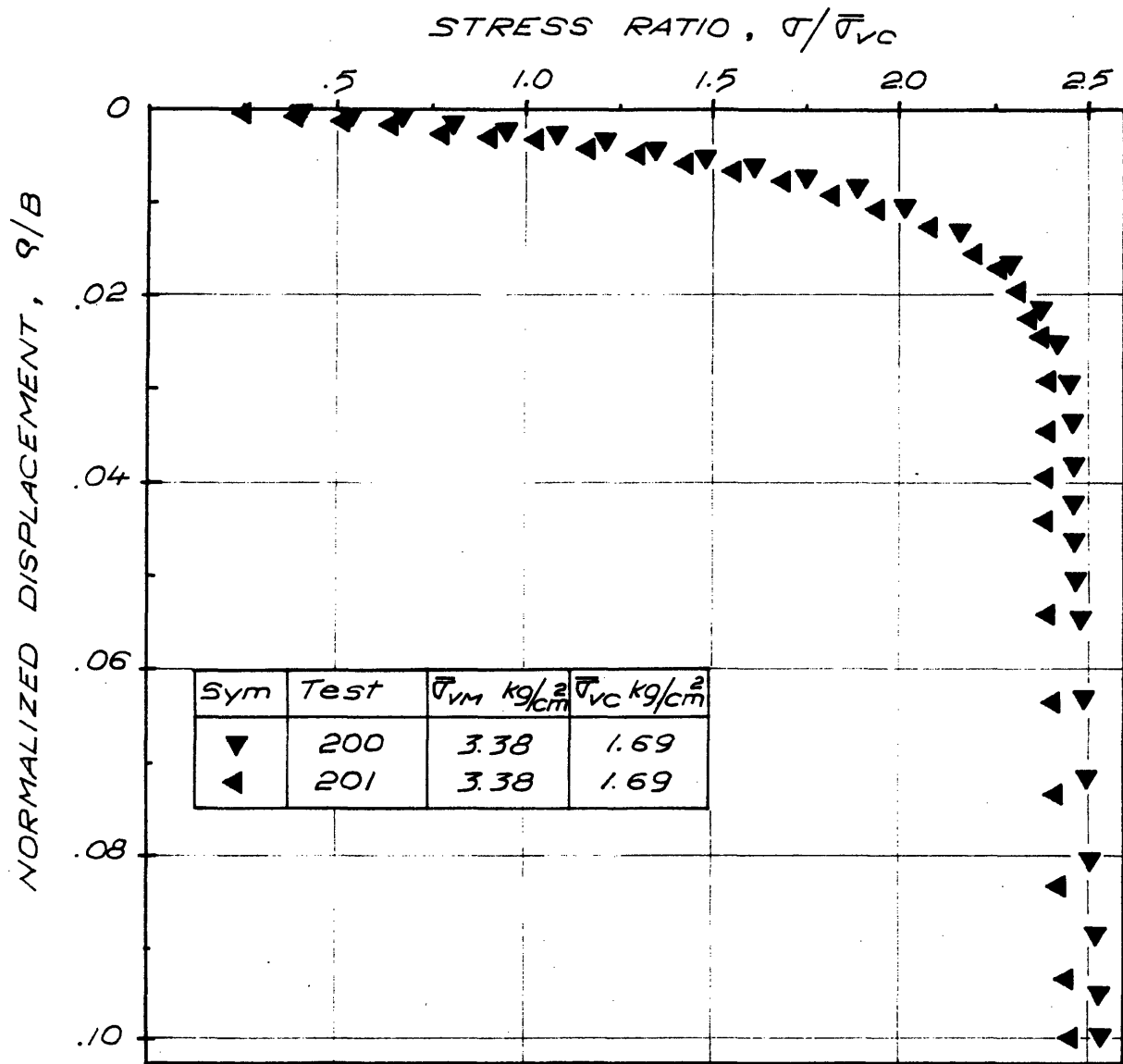
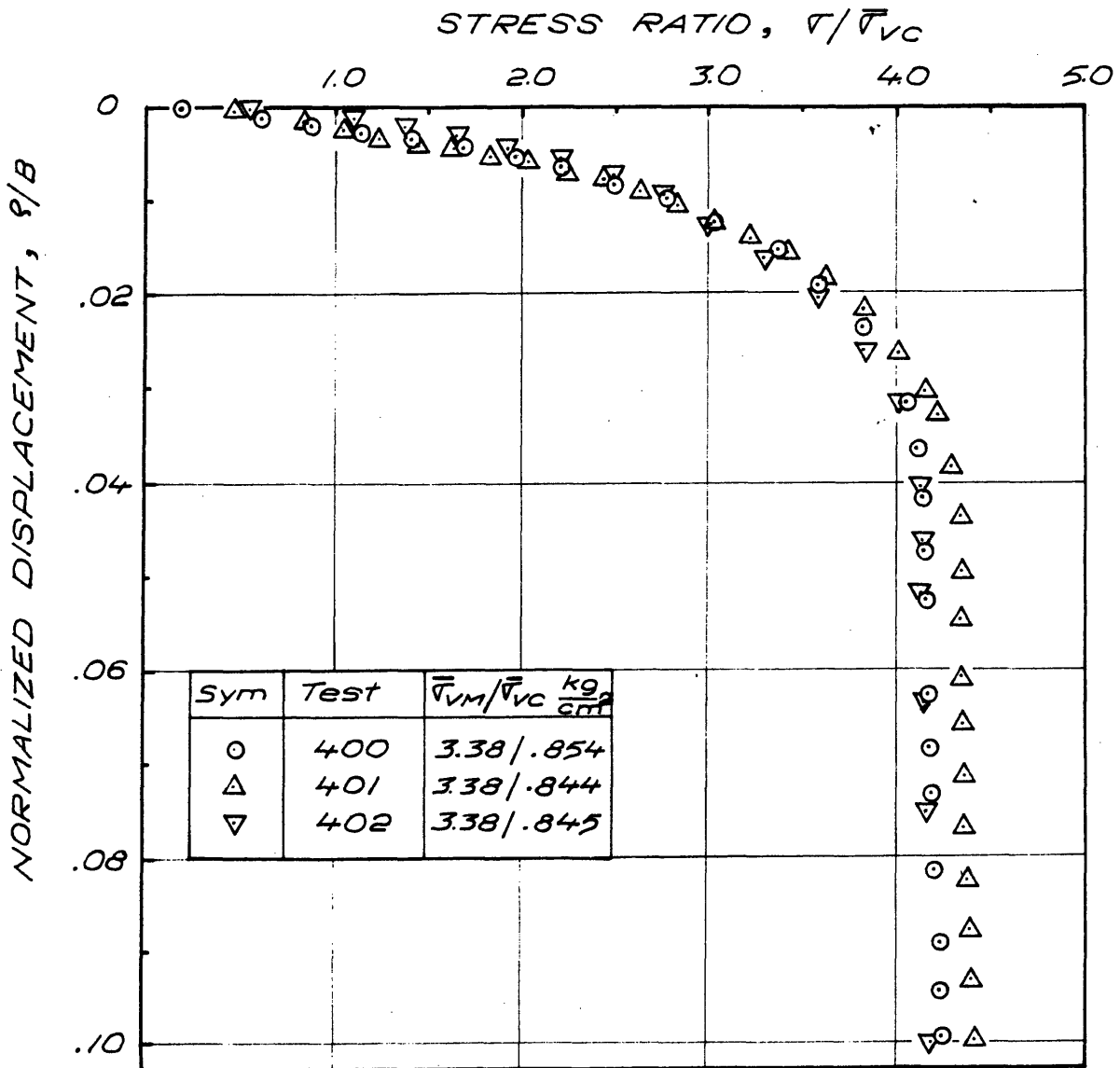


FIGURE 3 - 5

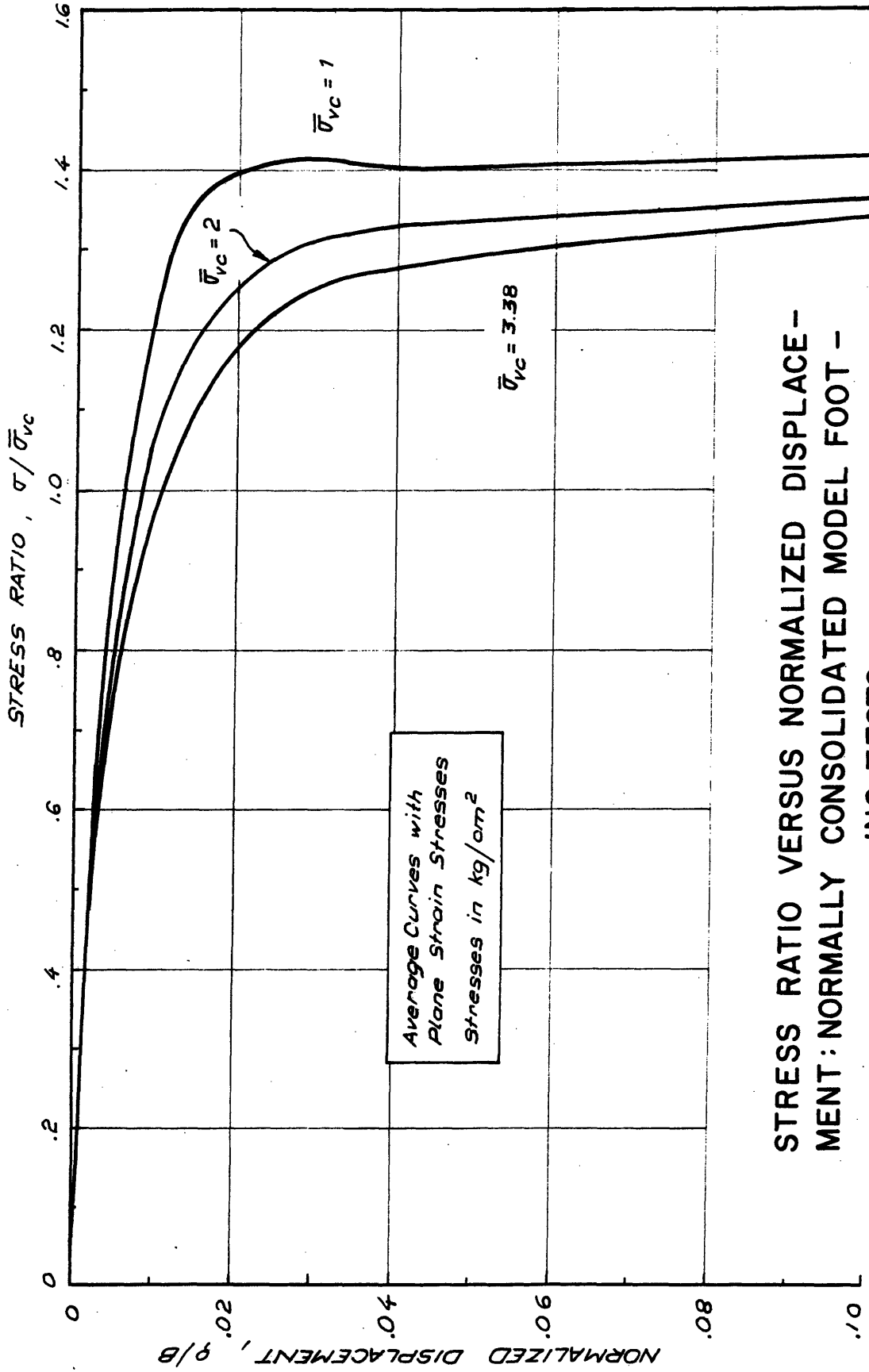


MODEL FOOTING TESTS: OVERCONSOLIDATION RATIO = 2. STRESS RATIO VERSUS NORMALIZED DISPLACEMENT



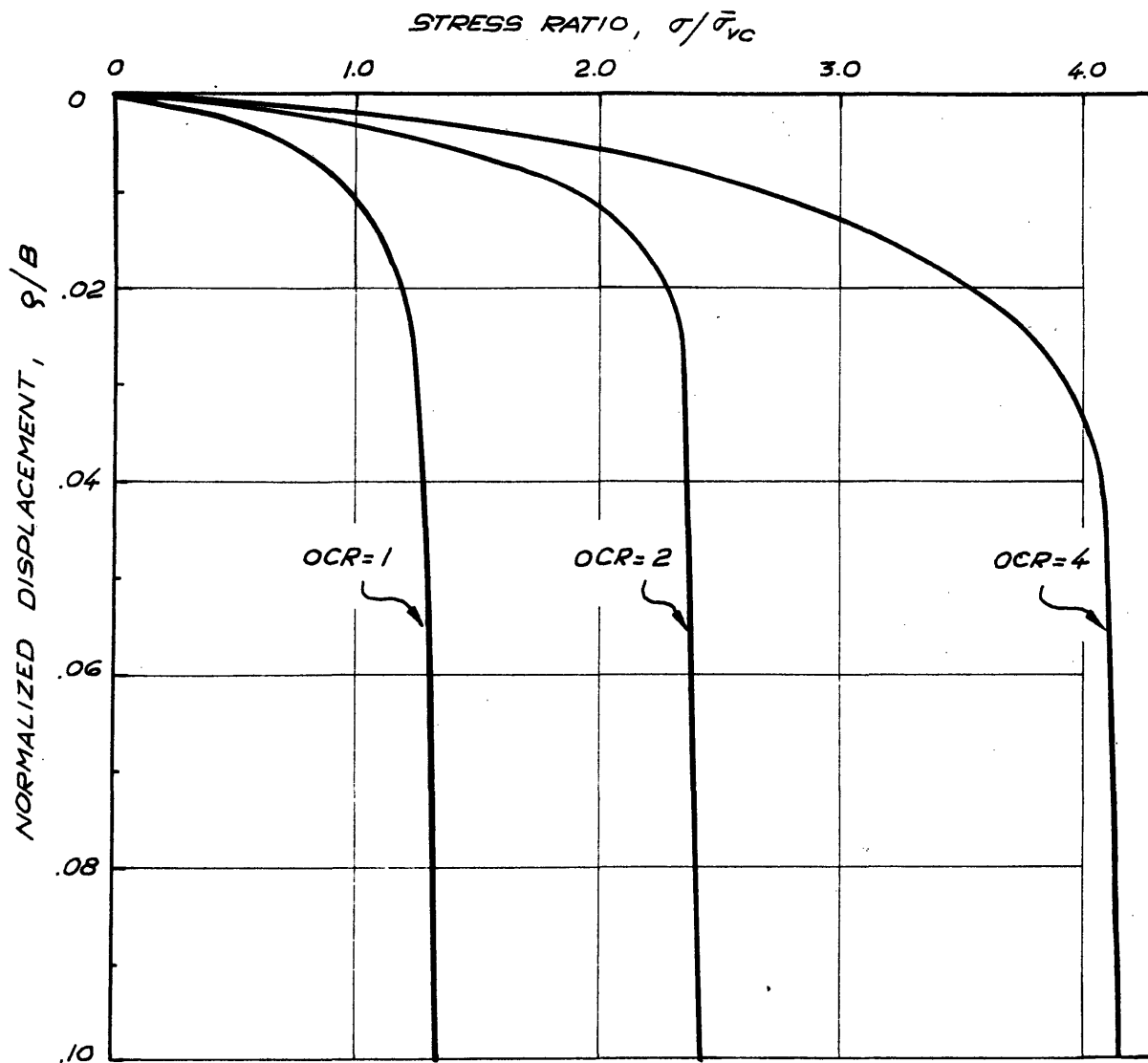
MODEL FOOTING TESTS: OVERCONSOLIDATION RATIO = 4.
STRESS RATIO VS NORMALIZED DISPLACEMENT

FIGURE 3 - 7



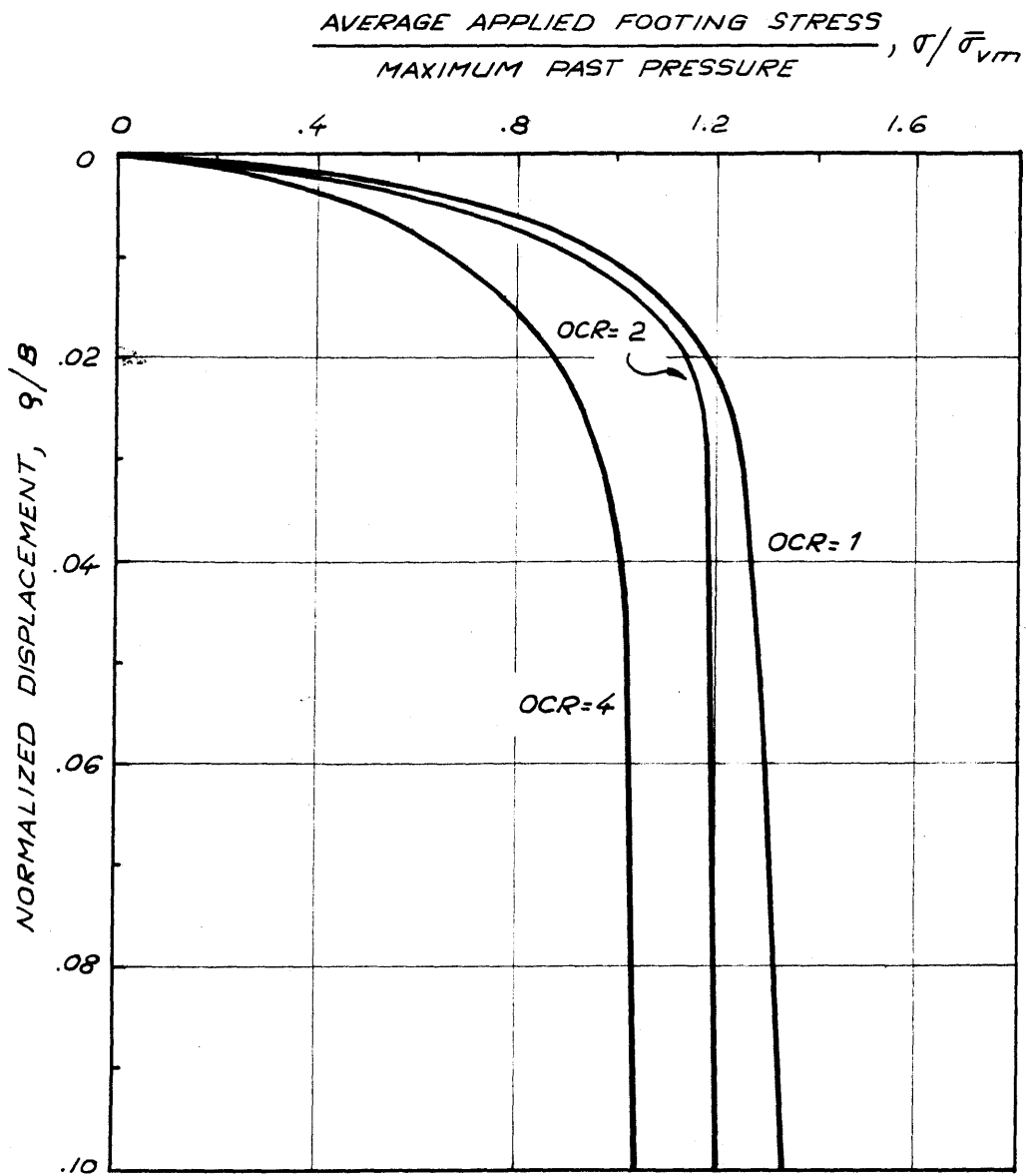
STRESS RATIO VERSUS NORMALIZED DISPLACEMENT: NORMALLY CONSOLIDATED MODEL FOOT -
ING TESTS

FIGURE 3-8



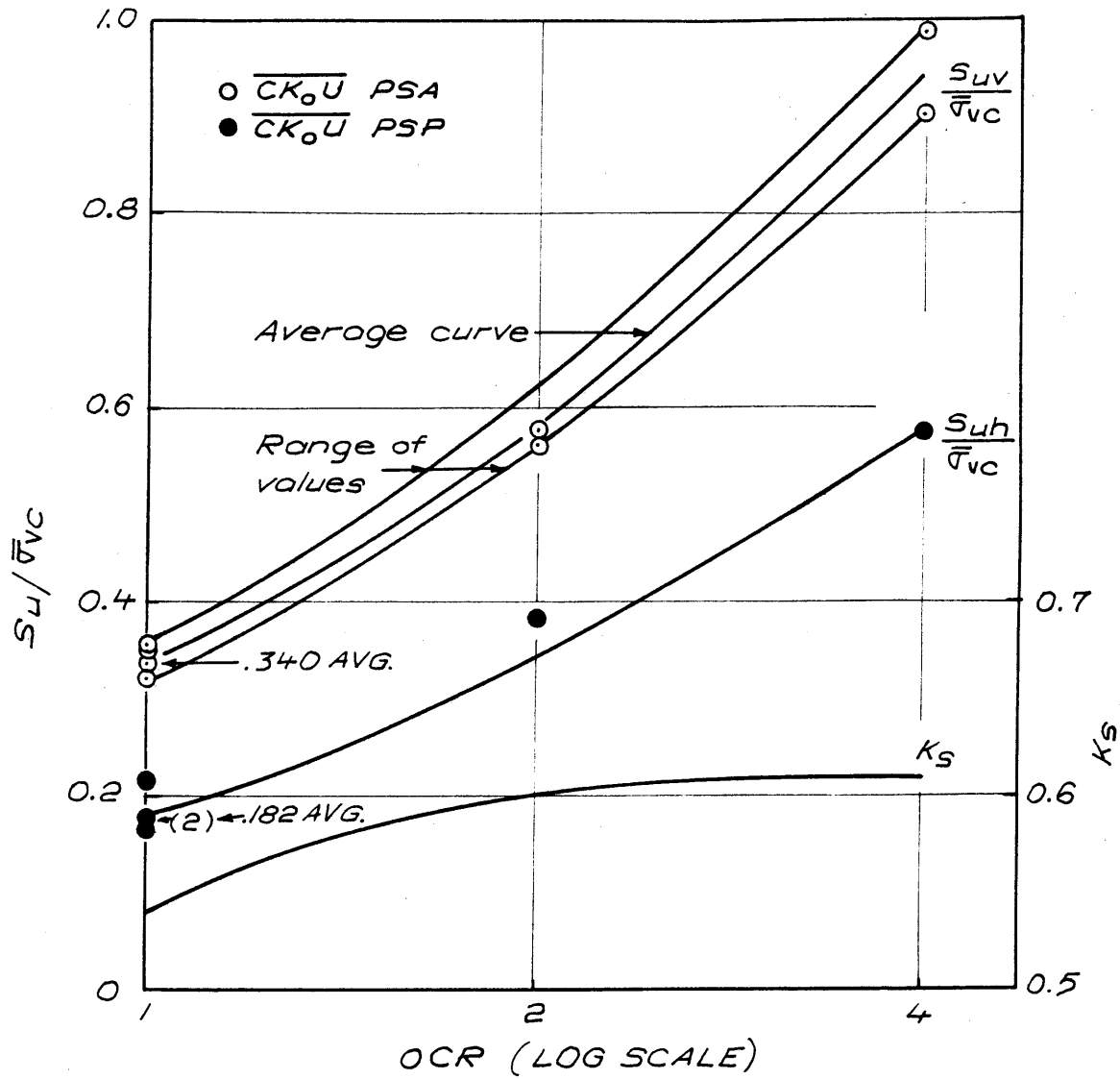
Note: Average Curves with
Plane Strain Stresses
 $\bar{\sigma}_{vm} = 3.38 \text{ kg/cm}^2$

STRESS RATIO VERSUS NORMALIZED DISPLACEMENT FOR MODEL FOOTING TESTS AT THREE OVERCONSOLIDATION RATIOS

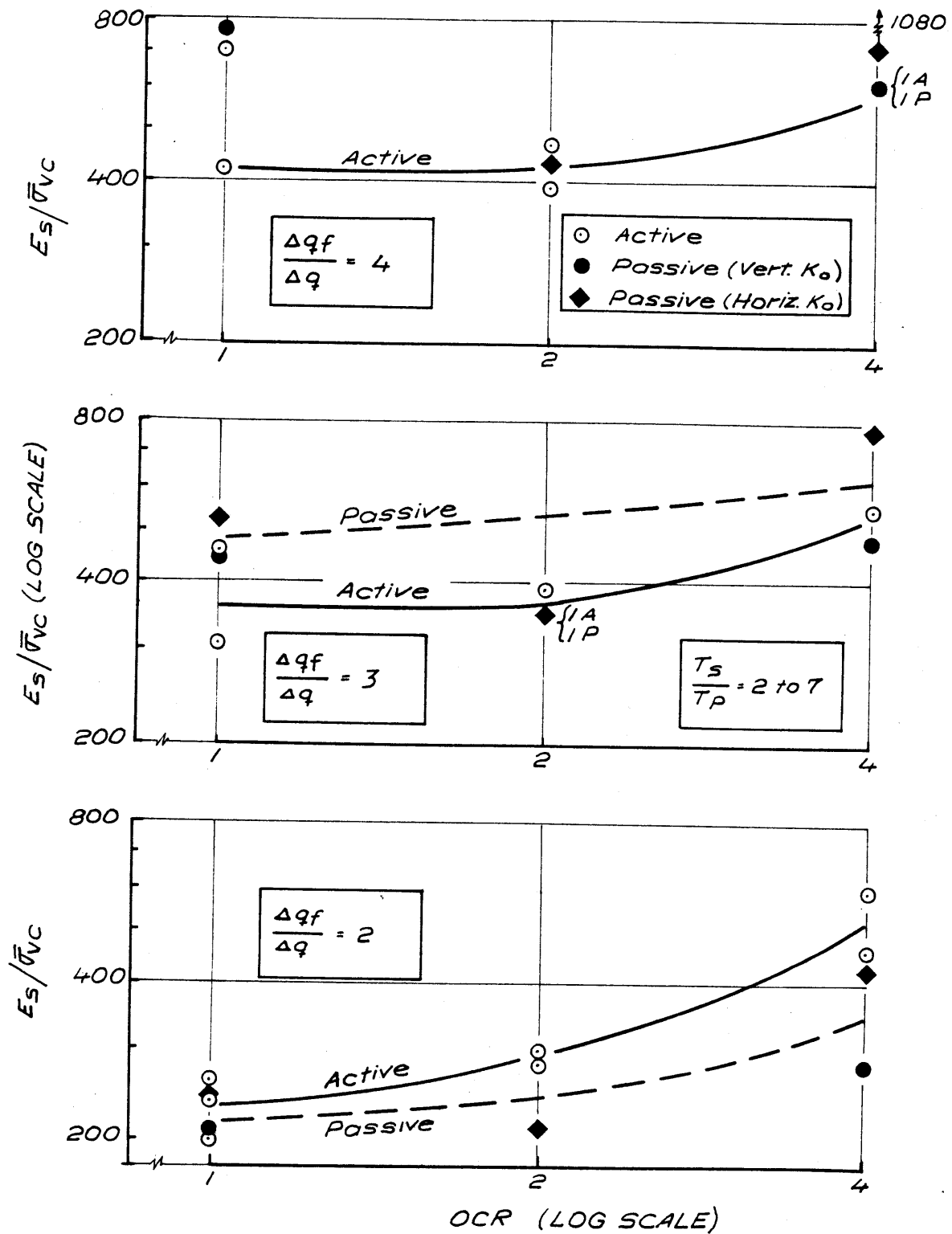


*Average Curves with
Plane Strain Stresses*

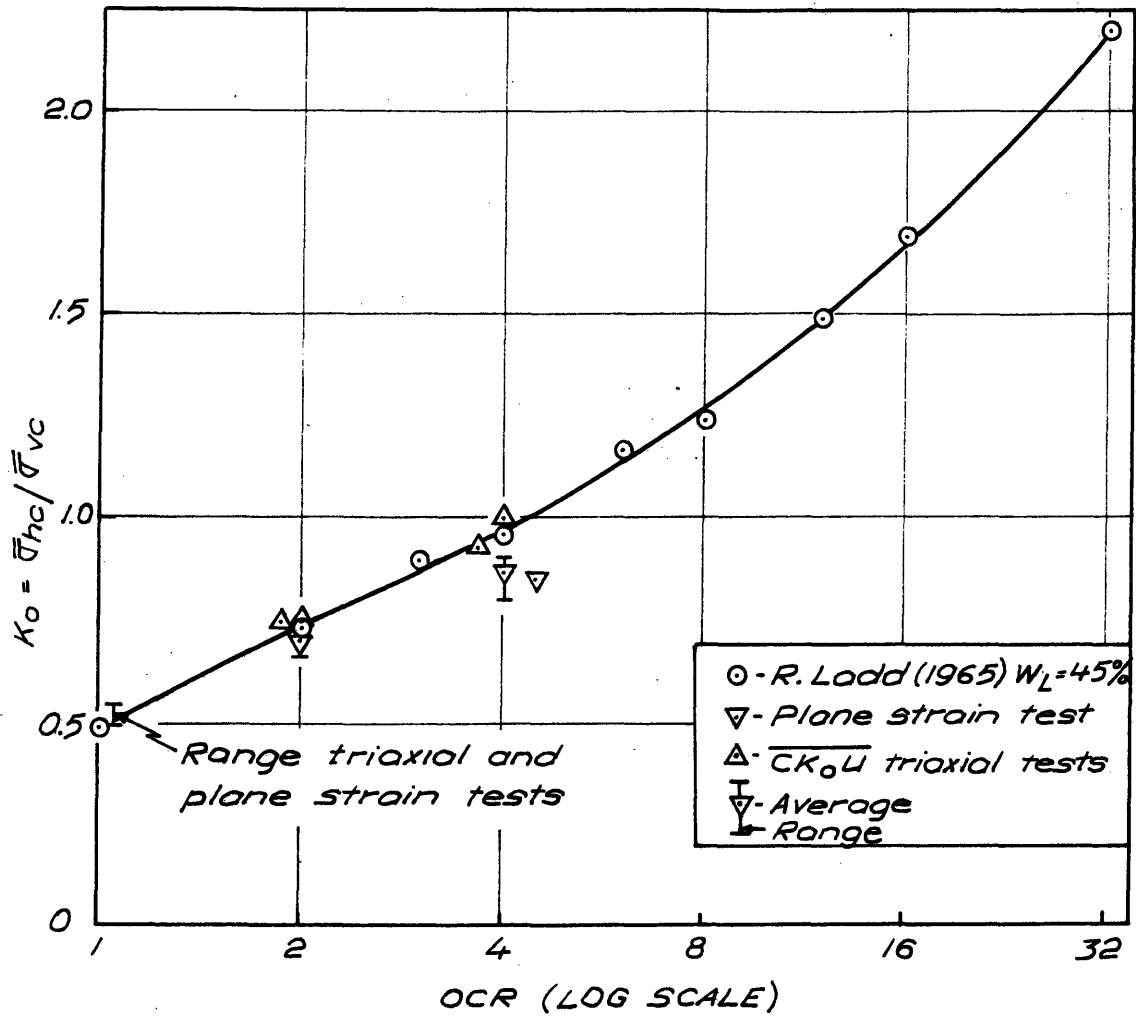
RATIO AVERAGE APPLIED FOOTING STRESS VERSUS
 MAXIMUM PAST PRESSURE
 NORMALIZED DISPLACEMENT FOR MODEL FOOTING
 TESTS AT THREE OVERCONSOLIDATION RATIOS



$\frac{S_u}{\bar{\sigma}_{vc}}$ AND K_s VERSUS LOG OCR PLANE STRAIN TESTS
 BOSTON BLUE CLAY

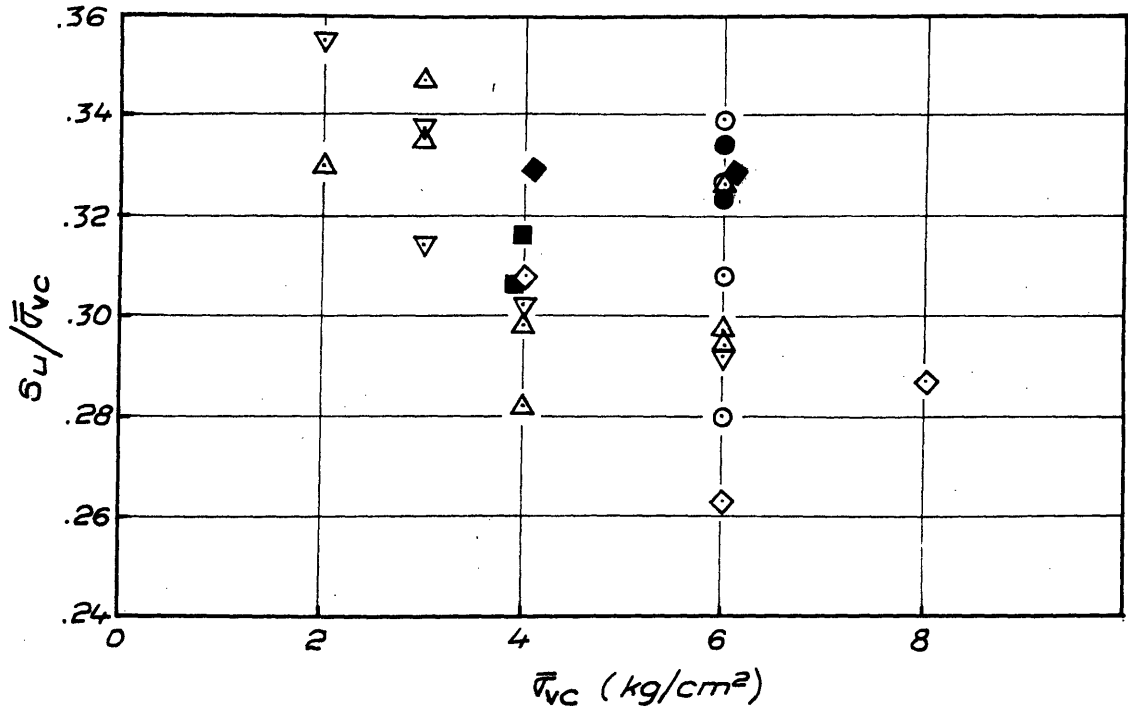


NORMALIZED SECANT MODULUS PLANE STRAIN TESTS

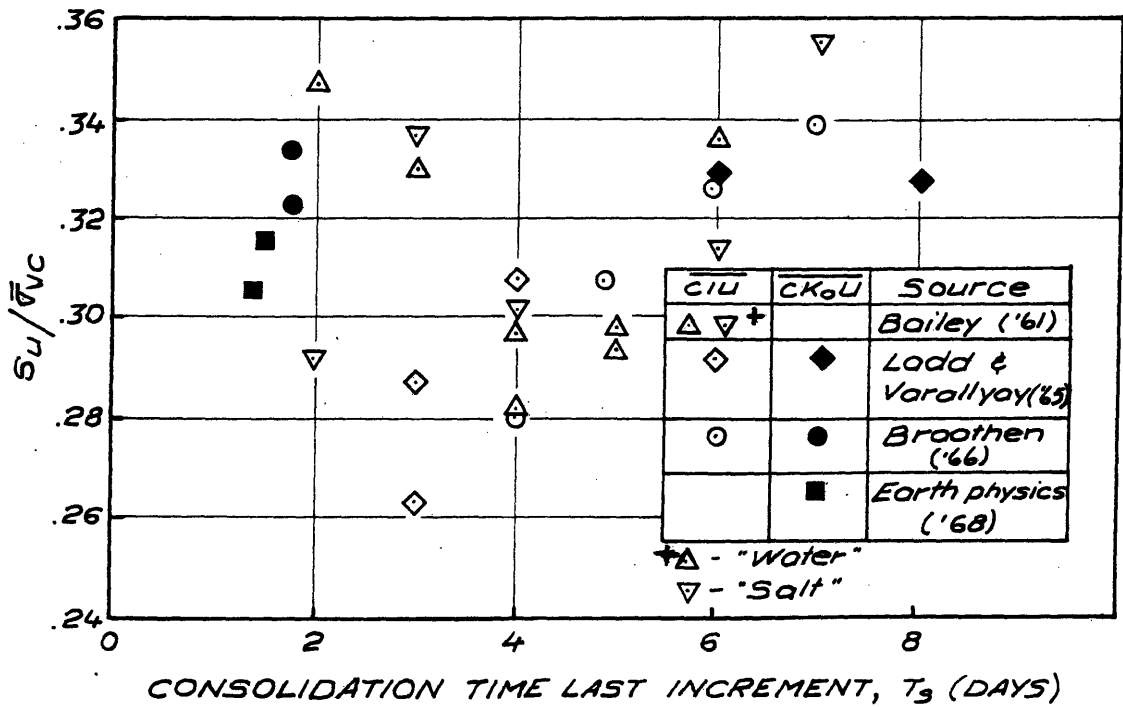


COEFFICIENT OF LATERAL STRESS AT REST VERSUS
 LOG OVERCONSOLIDATION RATIO BOSTON BLUE CLAY

FIGURE 4 - 3

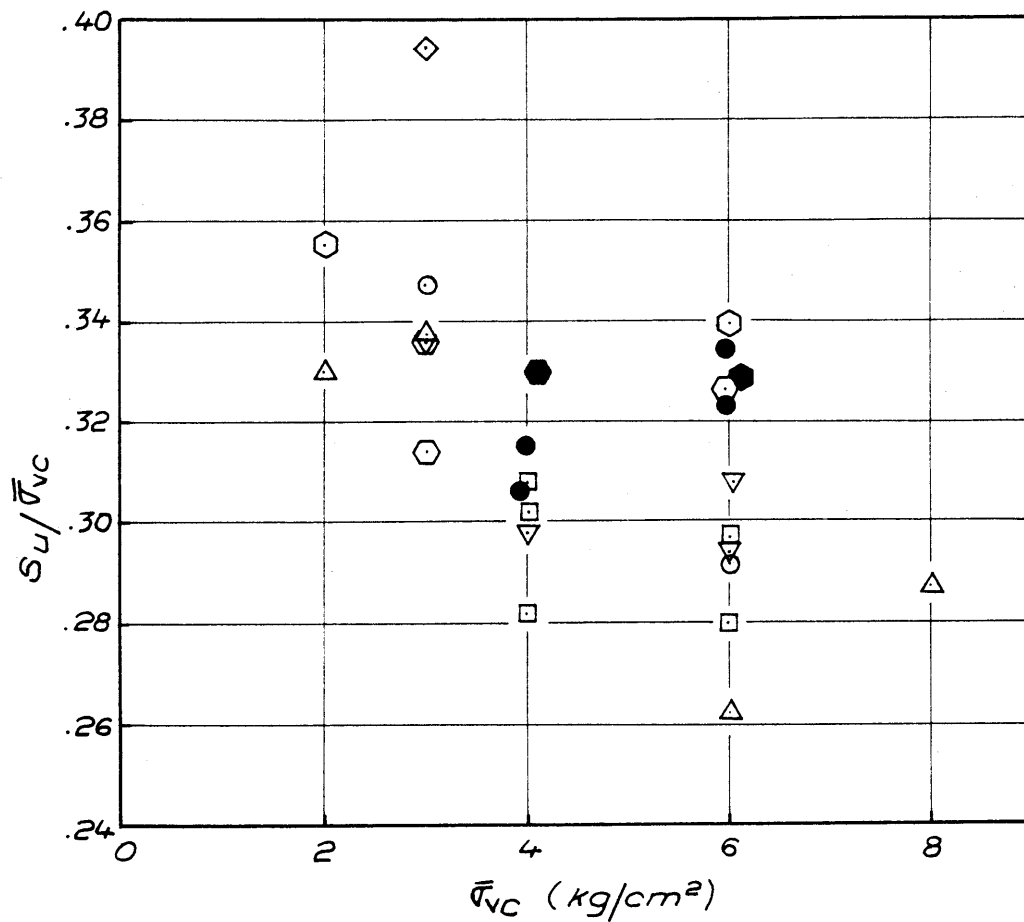


$\frac{s_u}{\bar{\sigma}_{vc}}$ vs $\bar{\sigma}_{vc}$ FOR NORMALLY CONSOLIDATED BOSTON BLUE CLAY SHEARED IN TRIAXIAL COMPRESSION



$\frac{s_u}{\bar{\sigma}_{vc}}$ vs PRESHEAR CONSOLIDATION TIME FOR NORMALLY CONSOLIDATED BOSTON BLUE CLAY SHEARED IN TRIAXIAL COMPRESSION

FIGURE 4-4

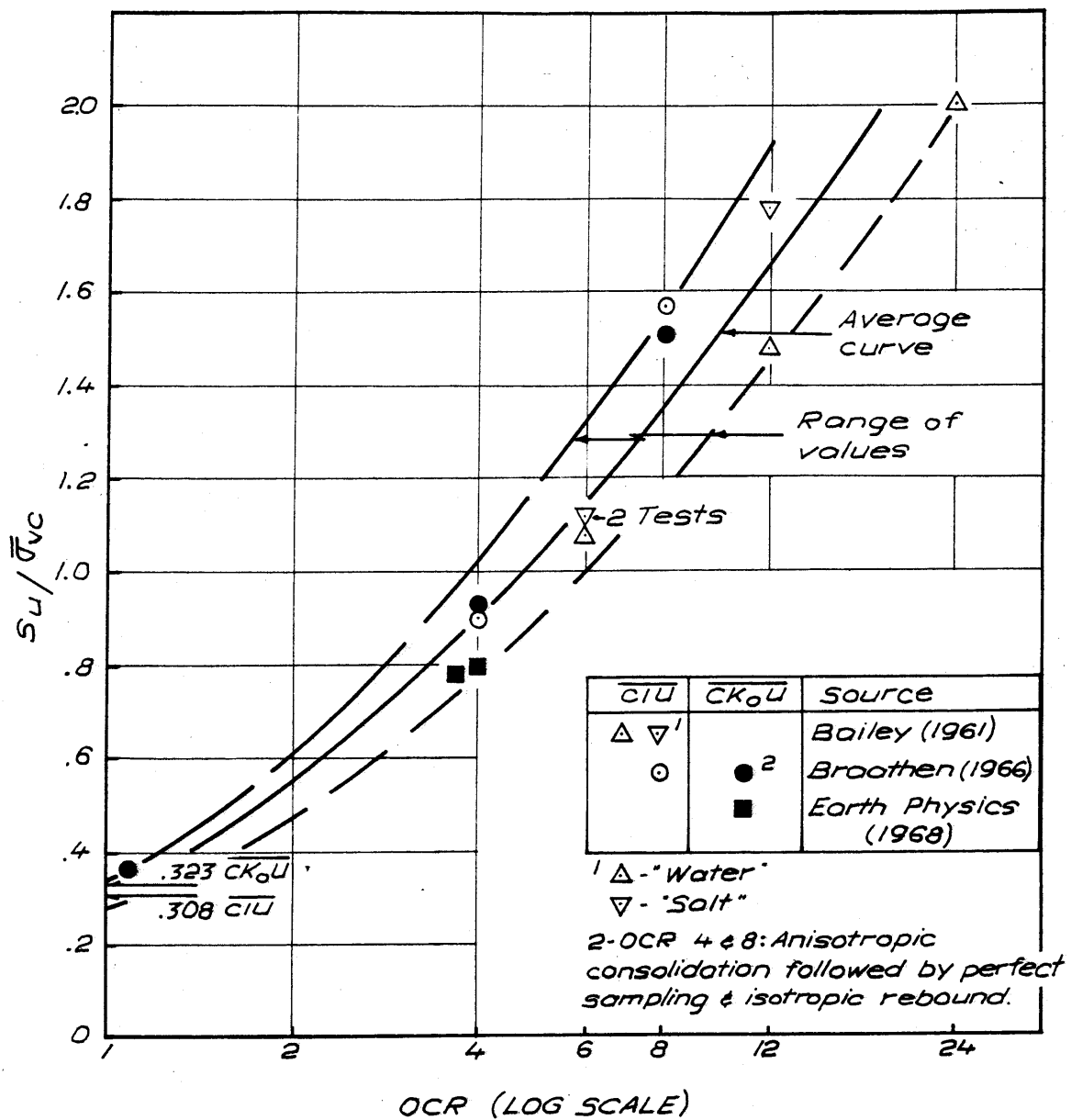


Sym	T_g (days)
○	1-2
△	3
□	4
▽	5
⬡	6
⬢	7-8
◇	46

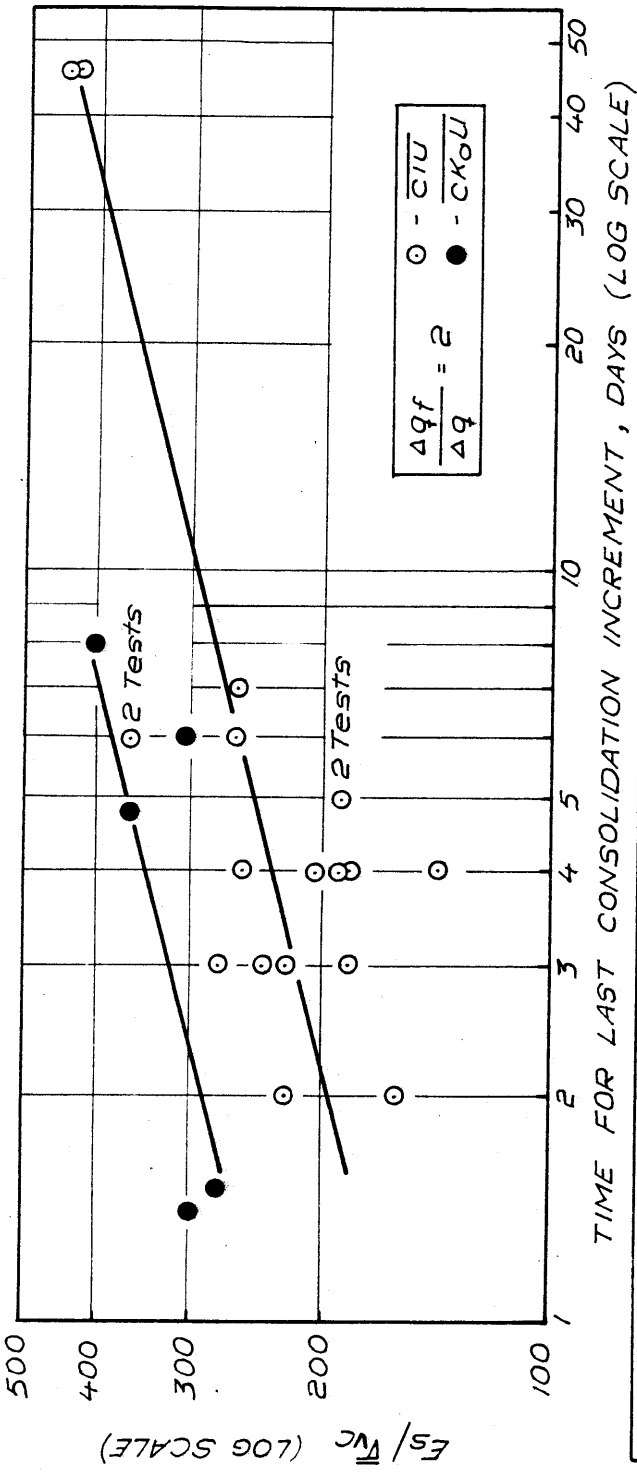
$\overline{CK_0U}$ Darkened

$$\frac{S_u}{\bar{\sigma}_{vc}} \text{ vs } \bar{\sigma}_{vc}$$

FOR NORMALLY CONSOLIDATED BOSTON BLUE CLAY
SHEARED IN TRIAXIAL COMPRESSION



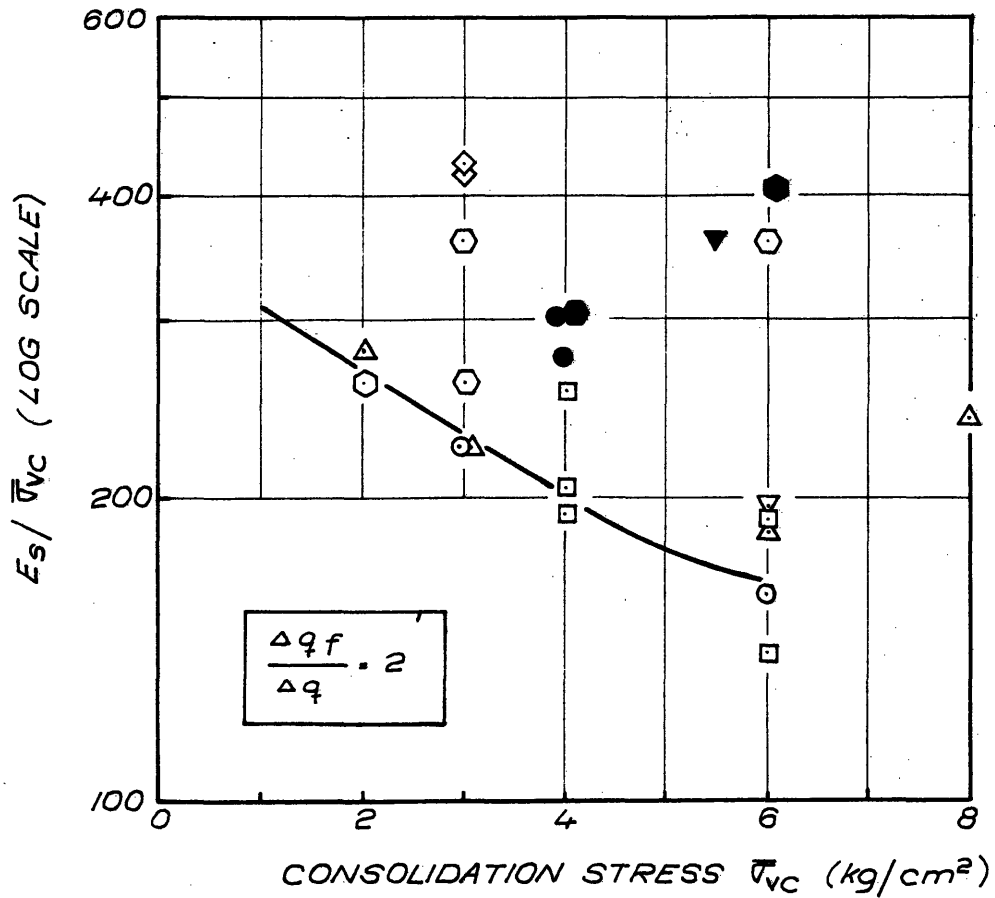
$\frac{S_u}{\bar{\sigma}_{vc}}$ vs LOG OCR, \overline{CIU} AND $\overline{CK_0U}$ TRIAXIAL COMPRESSION TESTS BOSTON BLUE CLAY



Data from Bailey (1961), Braathen (1966) and Earth Physics (1968)

NORMALIZED SECANT MODULUS VERSUS TIME FOR LAST CONSOLIDATION INCREMENT FOR NORMALLY CONSOLIDATED TRIAXIAL COMPRESSION TESTS

FIGURE 4-7

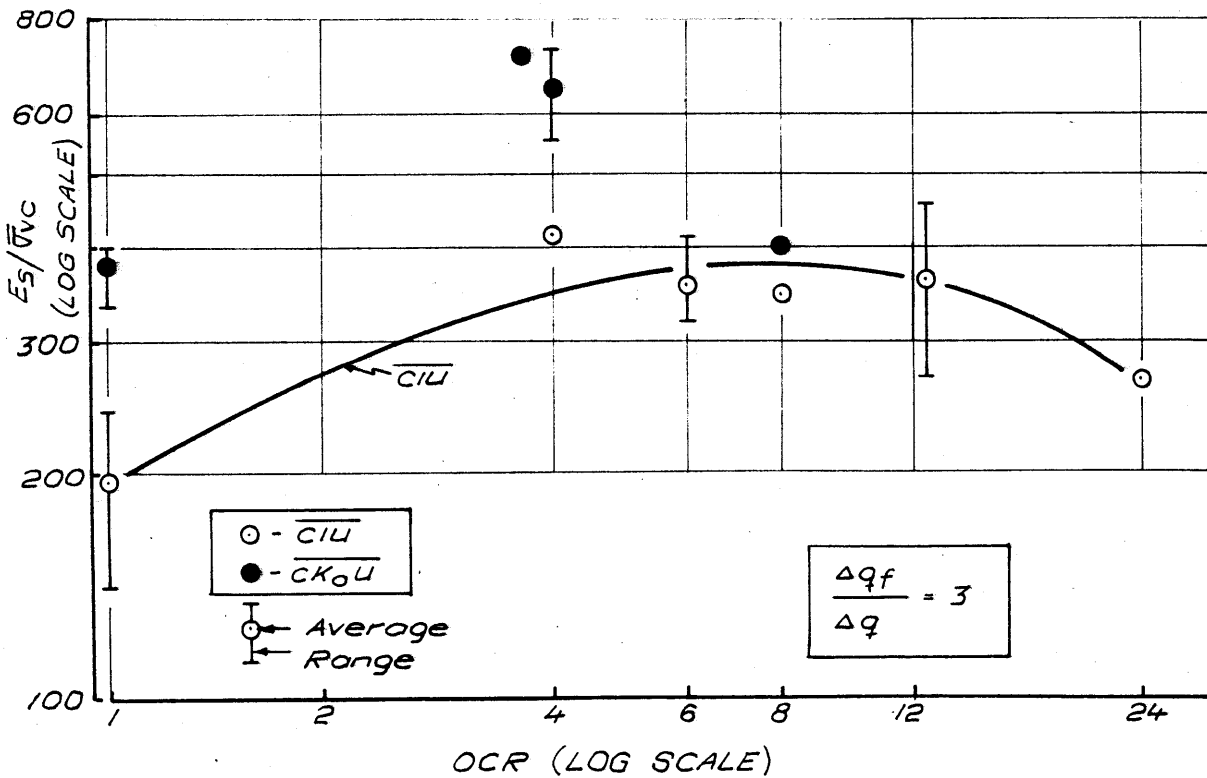
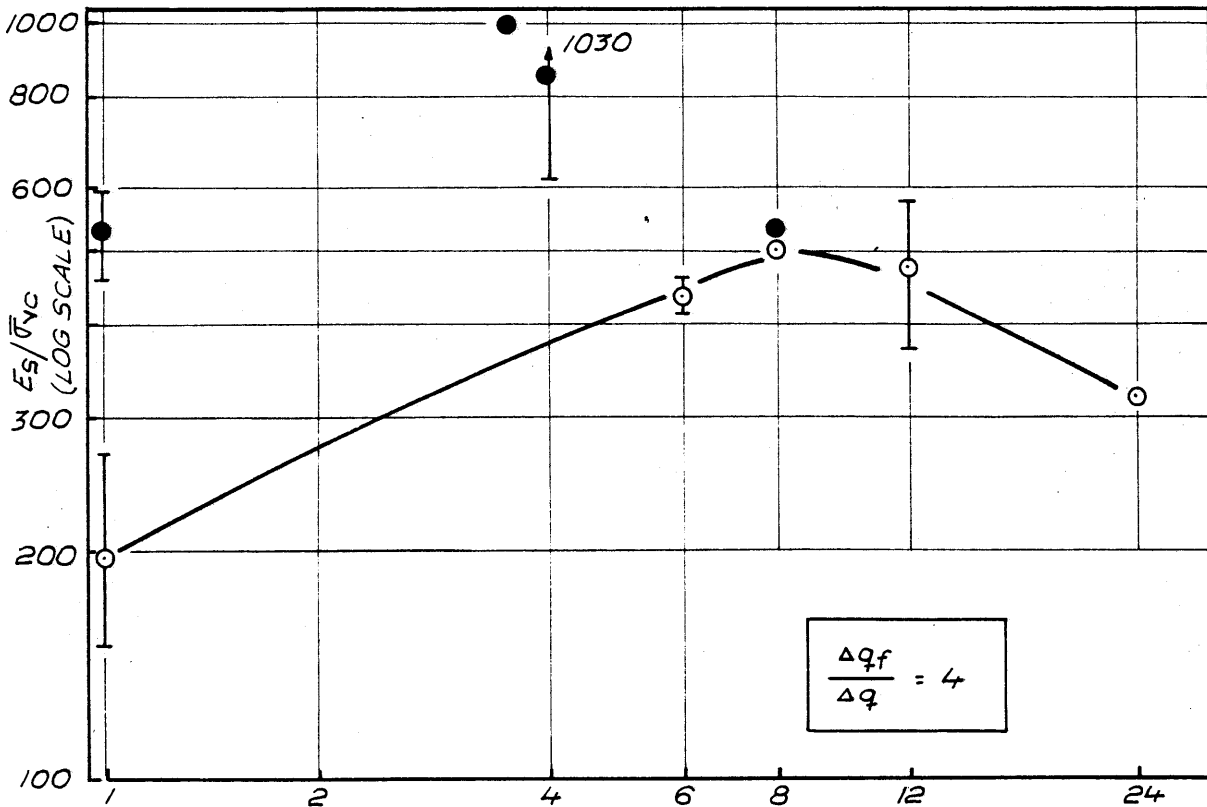


Sym	T_s (days)
○	1-2
△	3
□	4
▽	5
⊙	6
⊕	7-8
◇	46

Data from Bailey (1961),
Broathen (1966) and
Earth Physics (1968)

CK₀U Darkened

NORMALIZED SECANT MODULUS VERSUS CONSOLIDATION STRESS FOR NORMALLY CONSOLIDATED TRIAXIAL COMPRESSION TESTS



NORMALIZED SECANT MODULUS VERSUS LOG OCR FOR TRIAXIAL COMPRESSION TESTS BOSTON BLUE CLAY

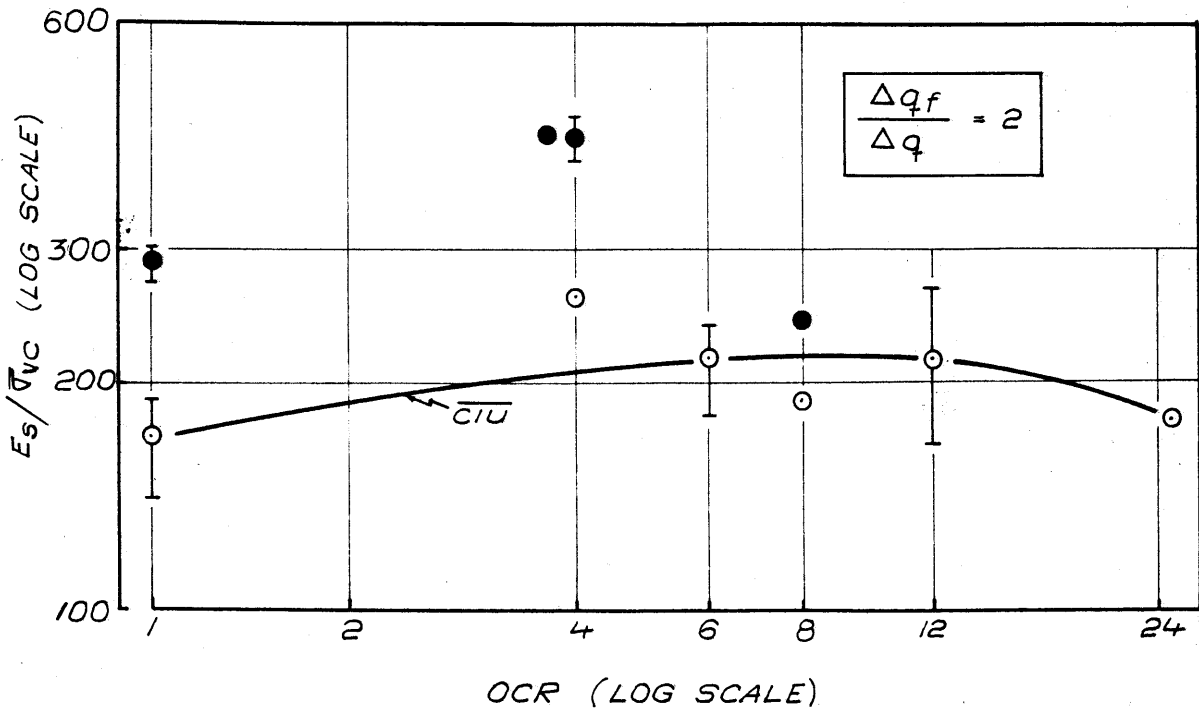
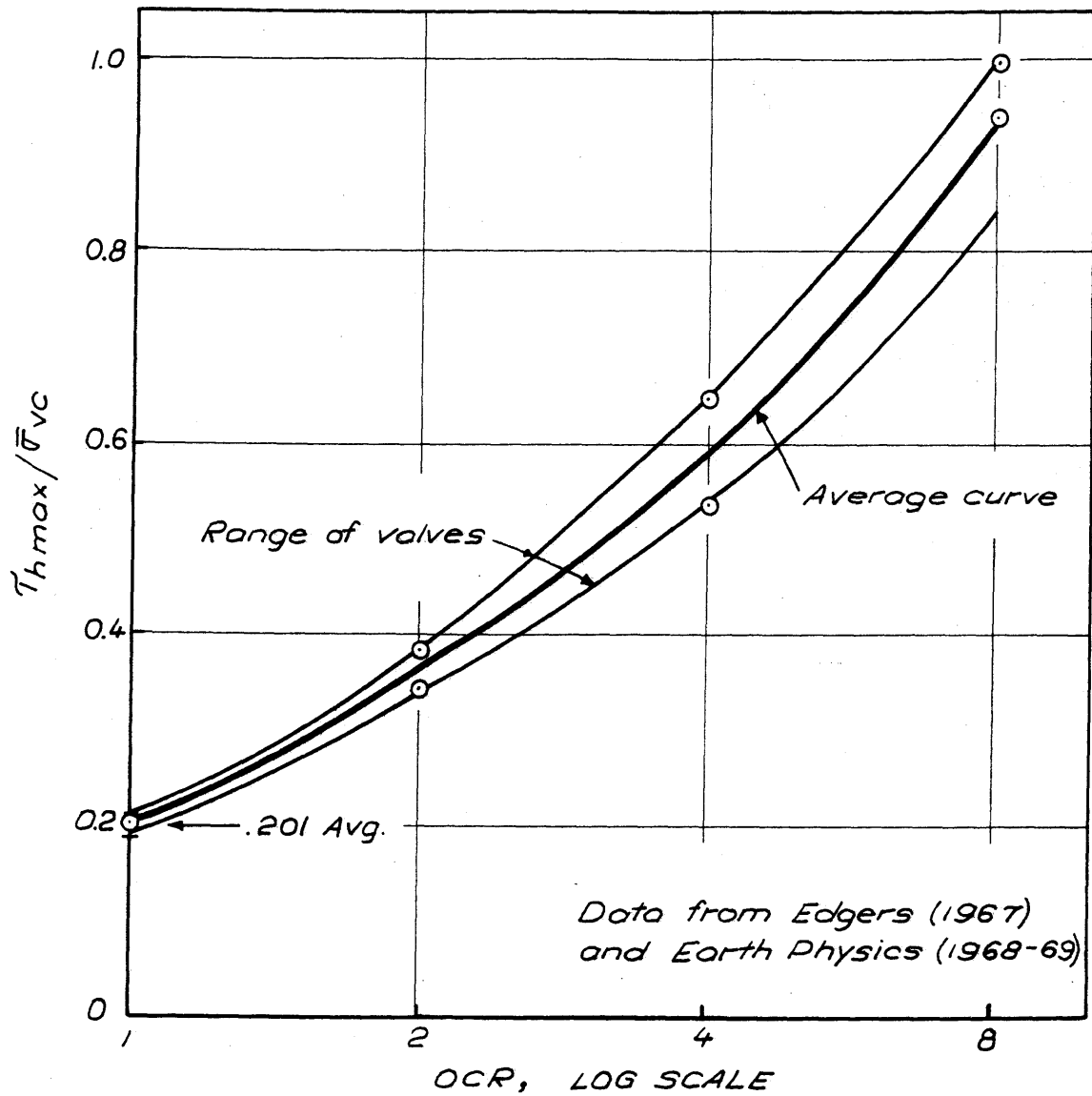
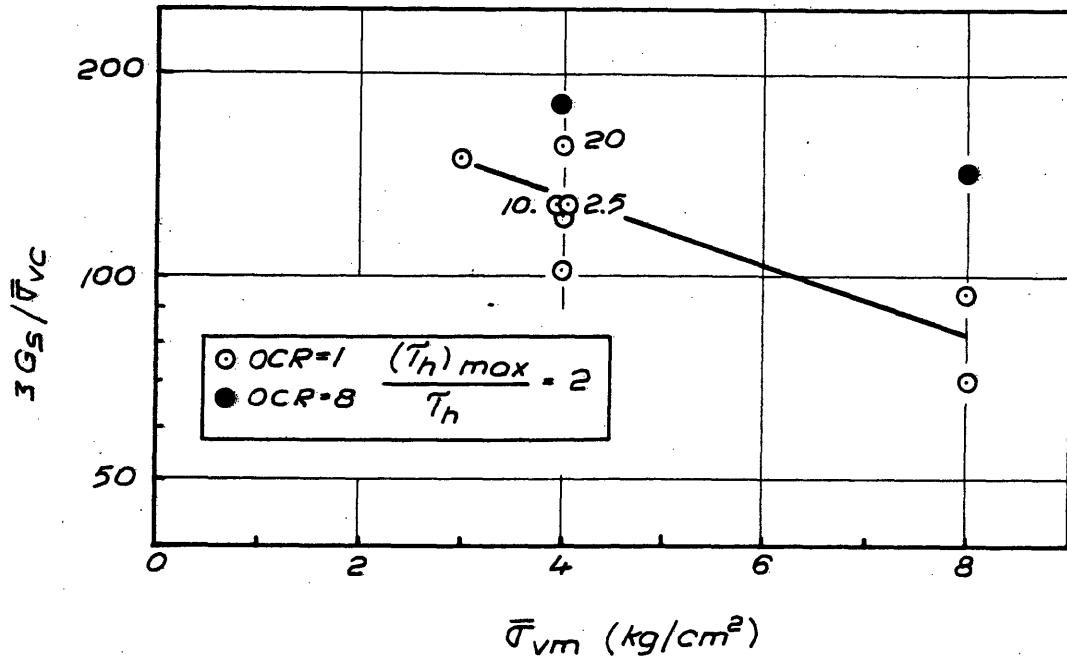


FIGURE 4 - 9
(CONTD.)



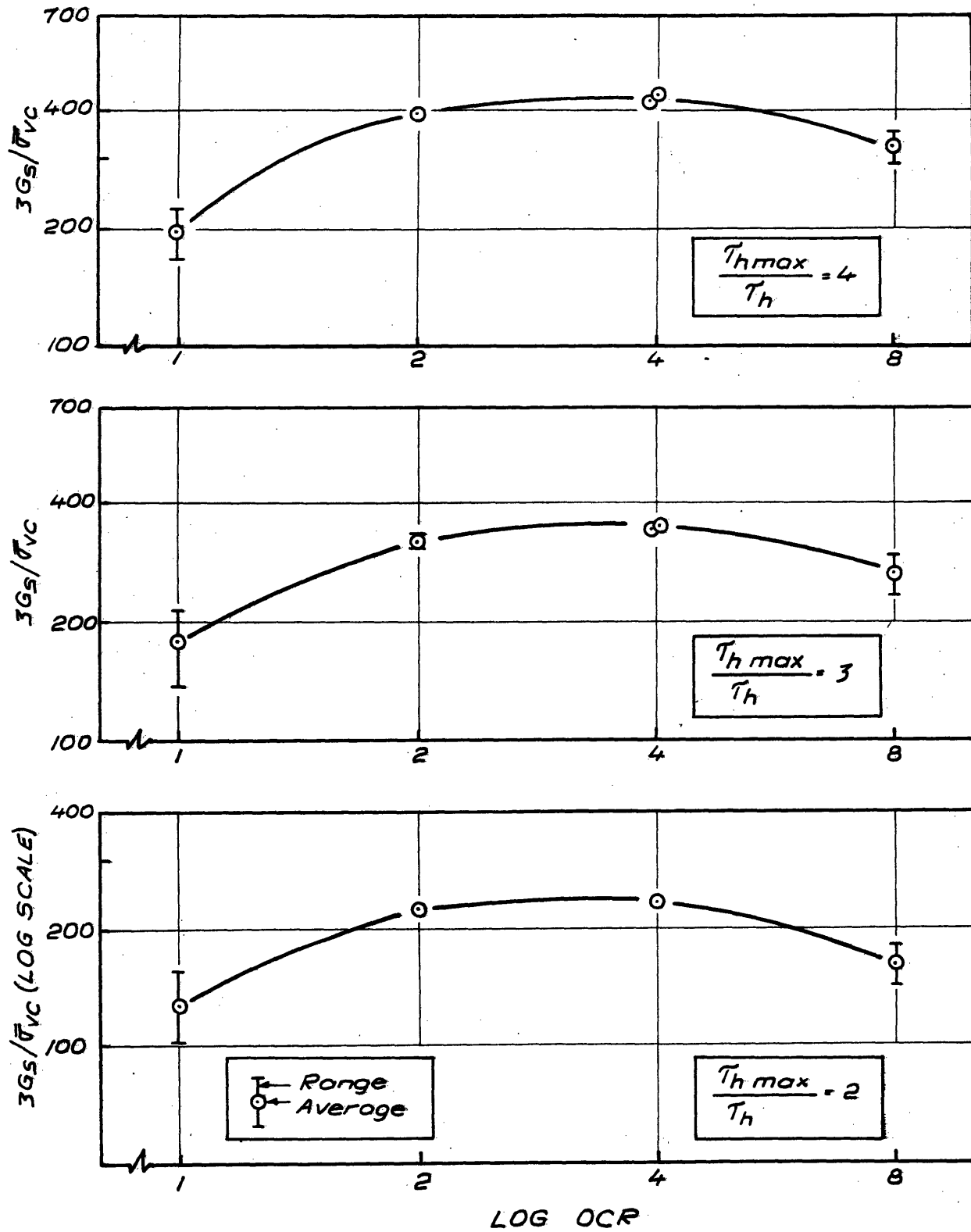
$\frac{T_{h \max}}{\bar{\sigma}_{vc}}$ vs LOG OCR $\bar{\sigma}_{vc}$ DSS TESTS

FIGURE 4-10

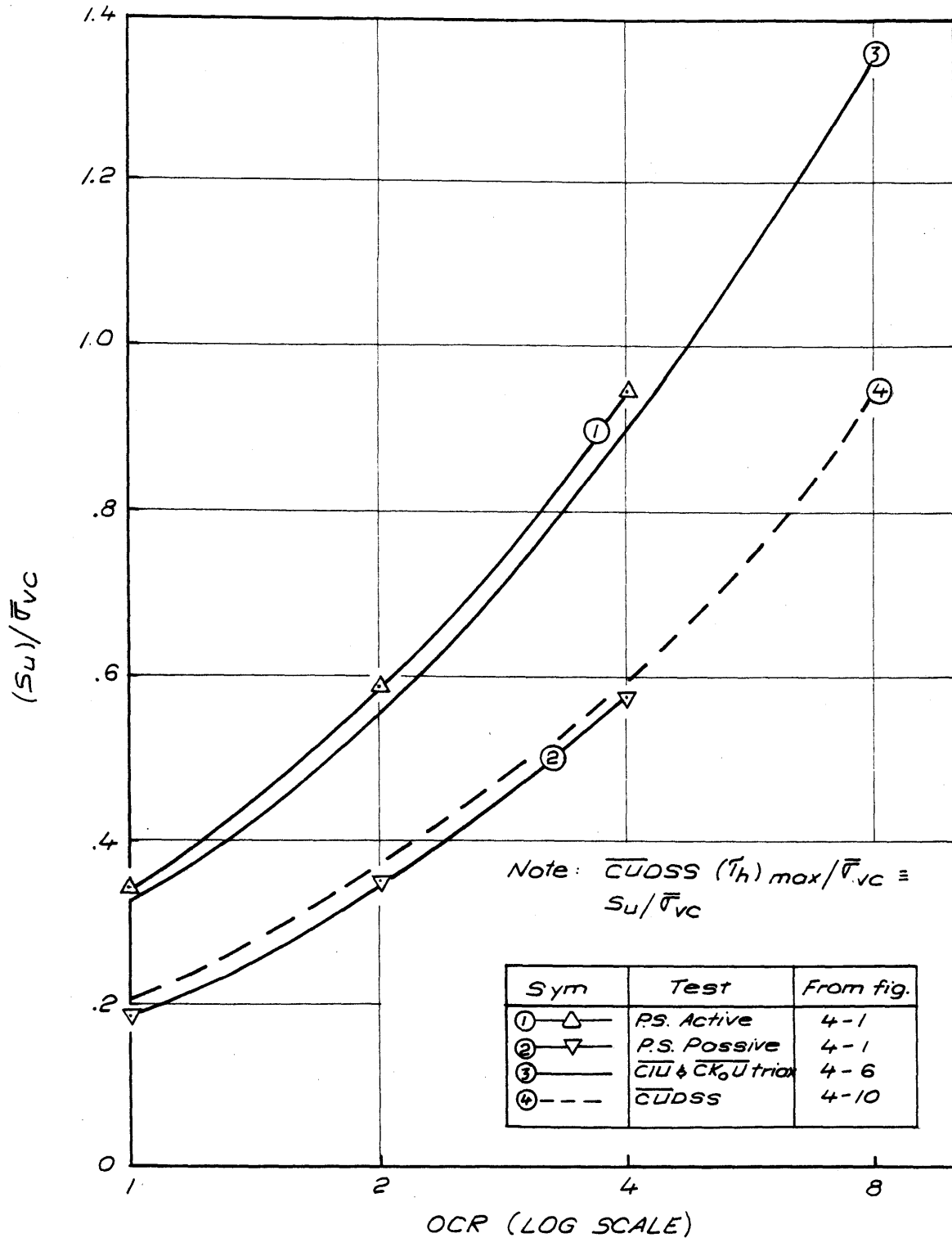


NORMALIZED PSEUDO SECANT MODULUS VERSUS
 MAXIMUM CONSOLIDATION STRESS DIRECT SIMPLE
 SHEAR TESTS OCR = 1 AND 8

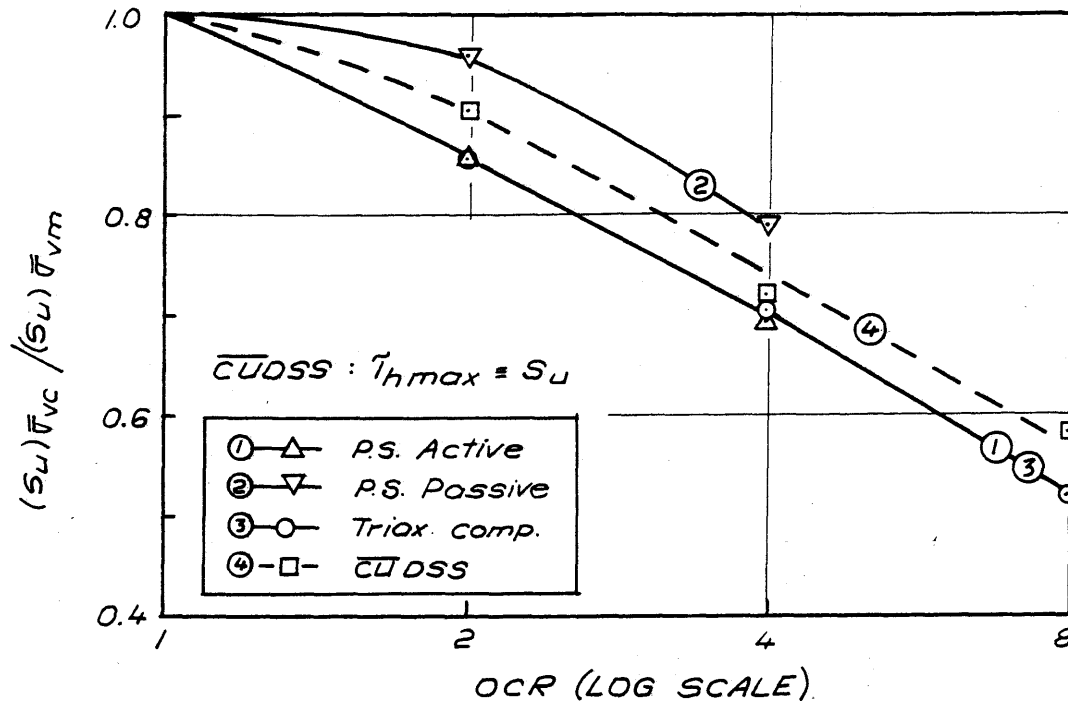
FIGURE 4-II



NORMALIZED PSEUDO SECANT MODULUS VERSUS LOG OCR DIRECT - SIMPLE SHEAR TESTS BOSTON BLUE CLAY



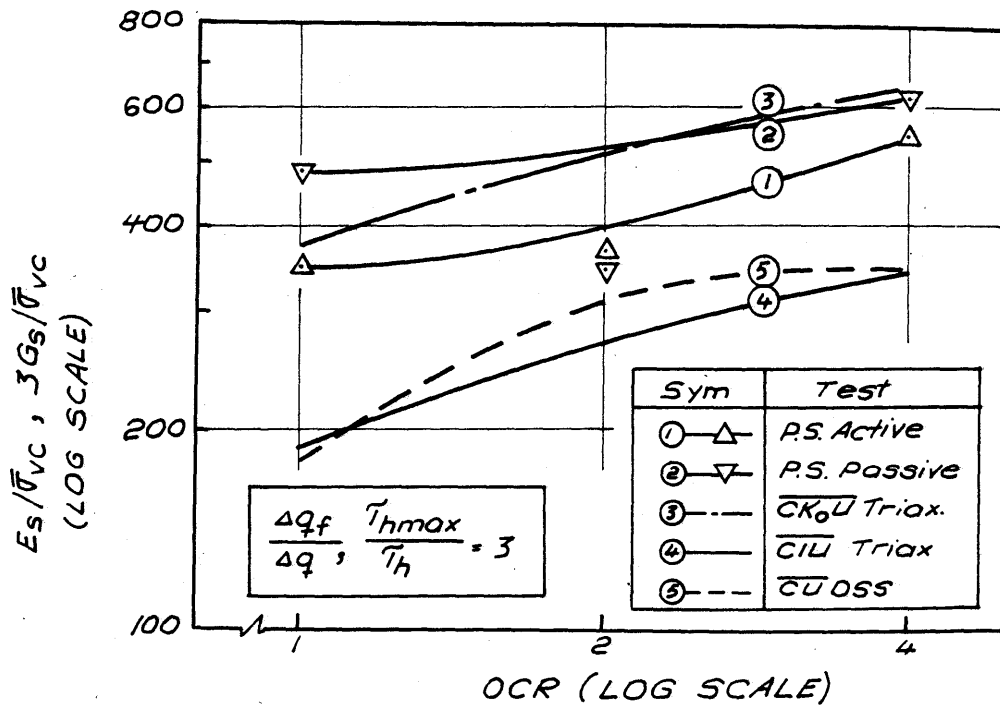
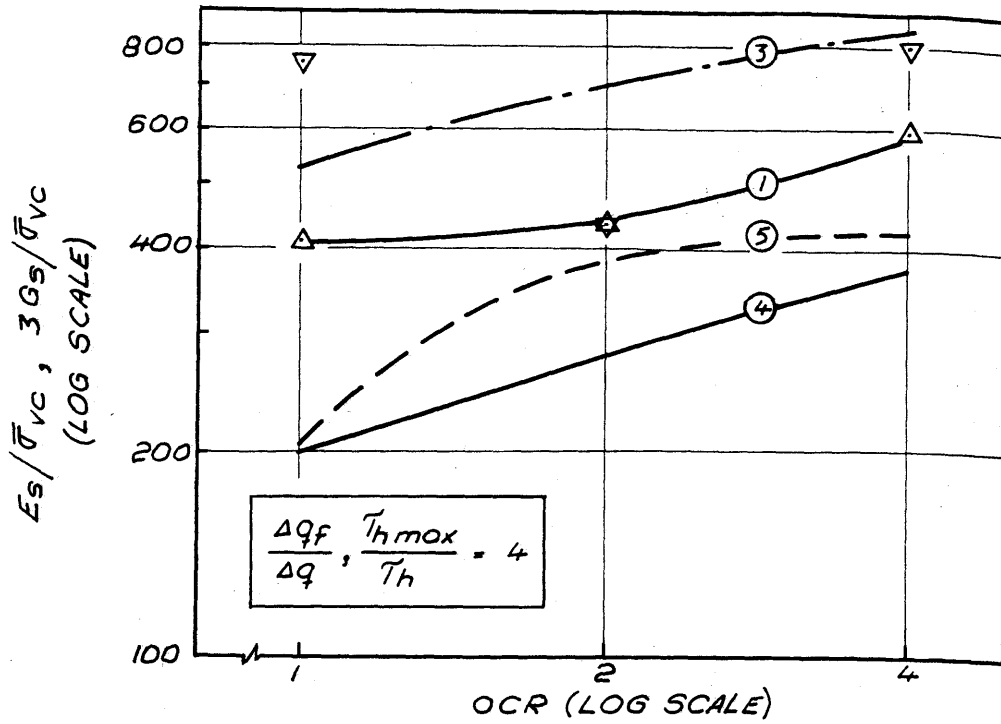
COMPARISON OF $\frac{S_u}{\bar{\sigma}_{vc}}$ VS LOG OCR FOR BOSTON BLUE CLAY AS MEASURED IN PLANE STRAIN, TRIAXIAL COMPRESSION AND DIRECT SIMPLE SHEAR TESTS



Plots determined from figure 4-13

$\frac{S_u \text{ AT } \bar{\tau}_{vc}}{S_u \text{ AT } \bar{\tau}_{vm}}$ VS LOG OCR FOR PLANE STRAIN,
 TRIAXIAL COMPRESSION AND DIRECT SIMPLE SHEAR
 TESTS

FIGURE 4-14



COMPARISON OF NORMALIZED SECANT MODULI AS MEASURED IN SEVERAL UNDRAINED SHEAR TESTS

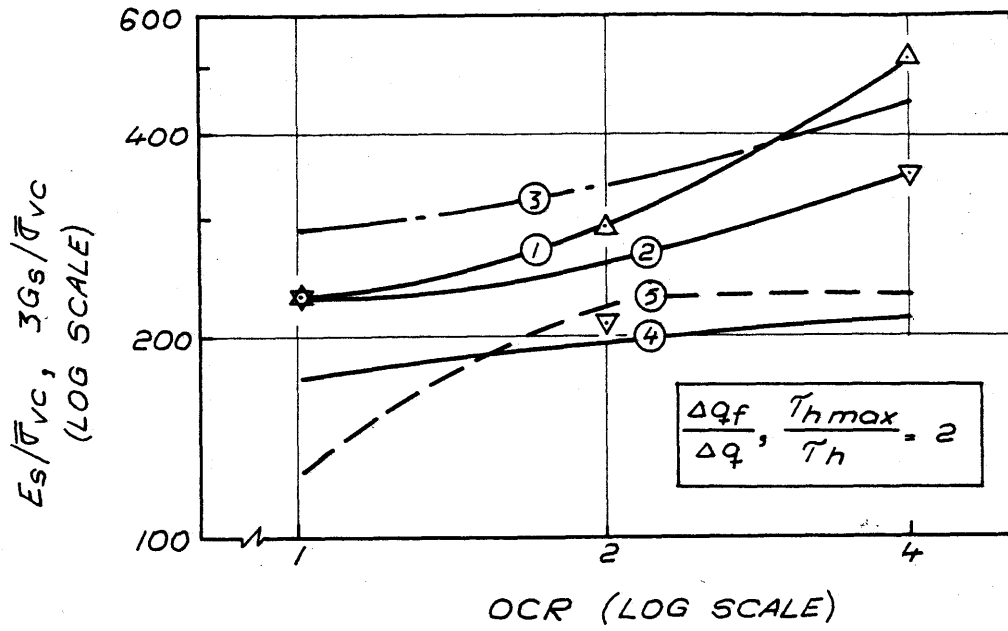
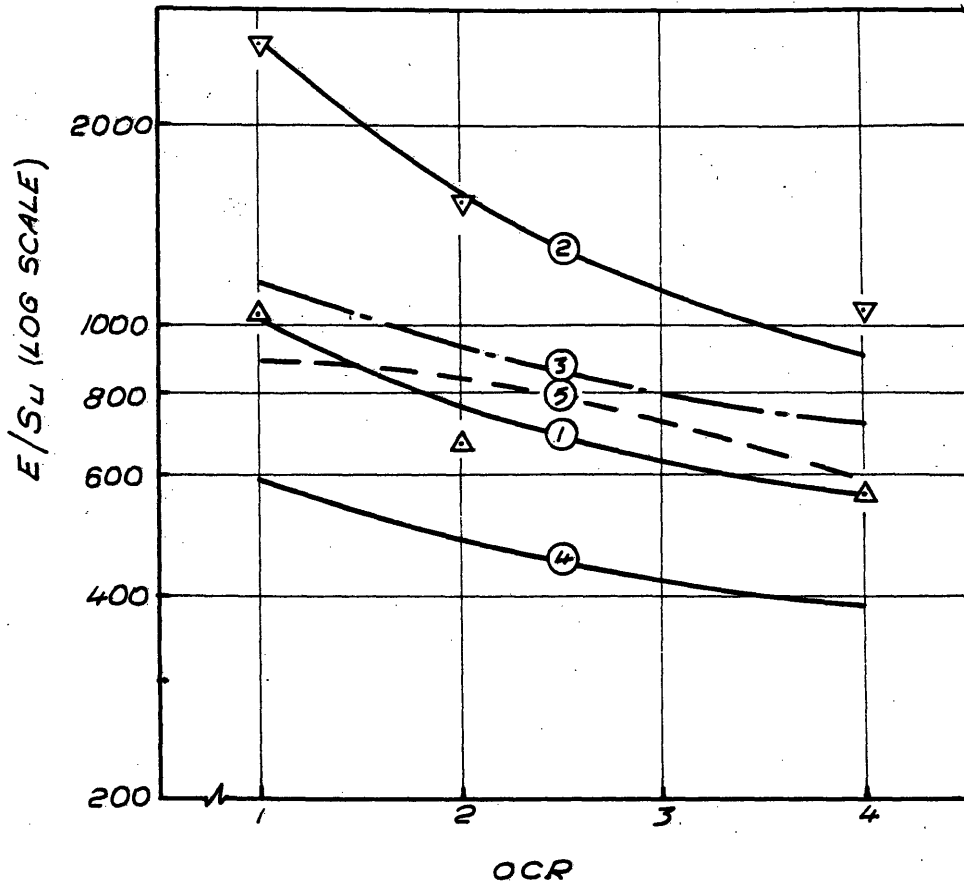


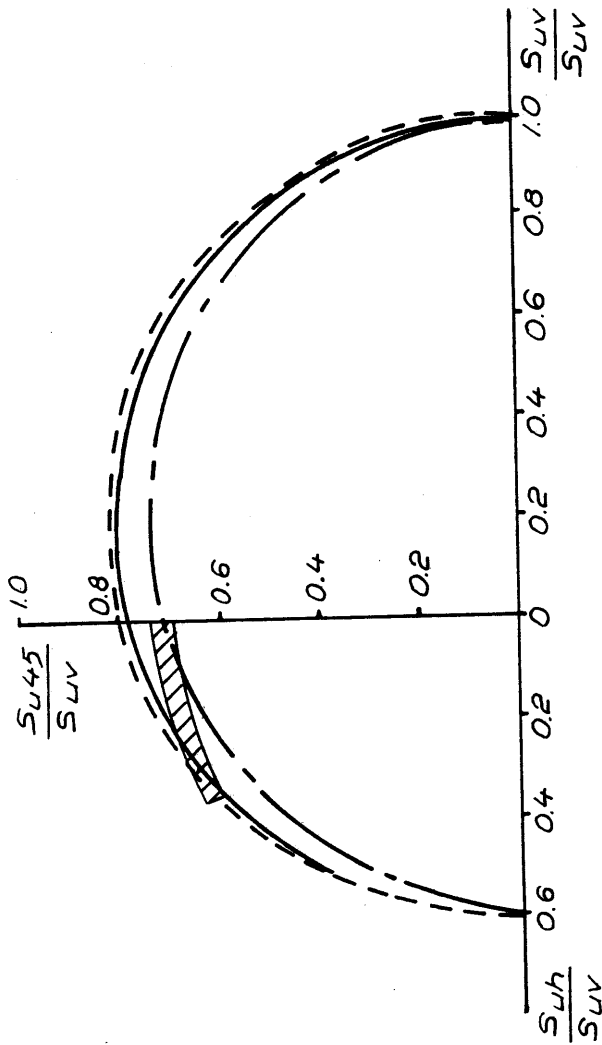
FIGURE 4-15
(CONT.)



Sym	Test
①—△	P.S. Active
②—▽	P.S. Passive
③---○	$\overline{Ck_0U}$ Triax.
④—○	\overline{CIU} Triax.
⑤---○	\overline{CIUSS}

$$F.S. = \frac{\Delta q_f}{\Delta q}, \frac{T_{h \max}}{T_h}$$

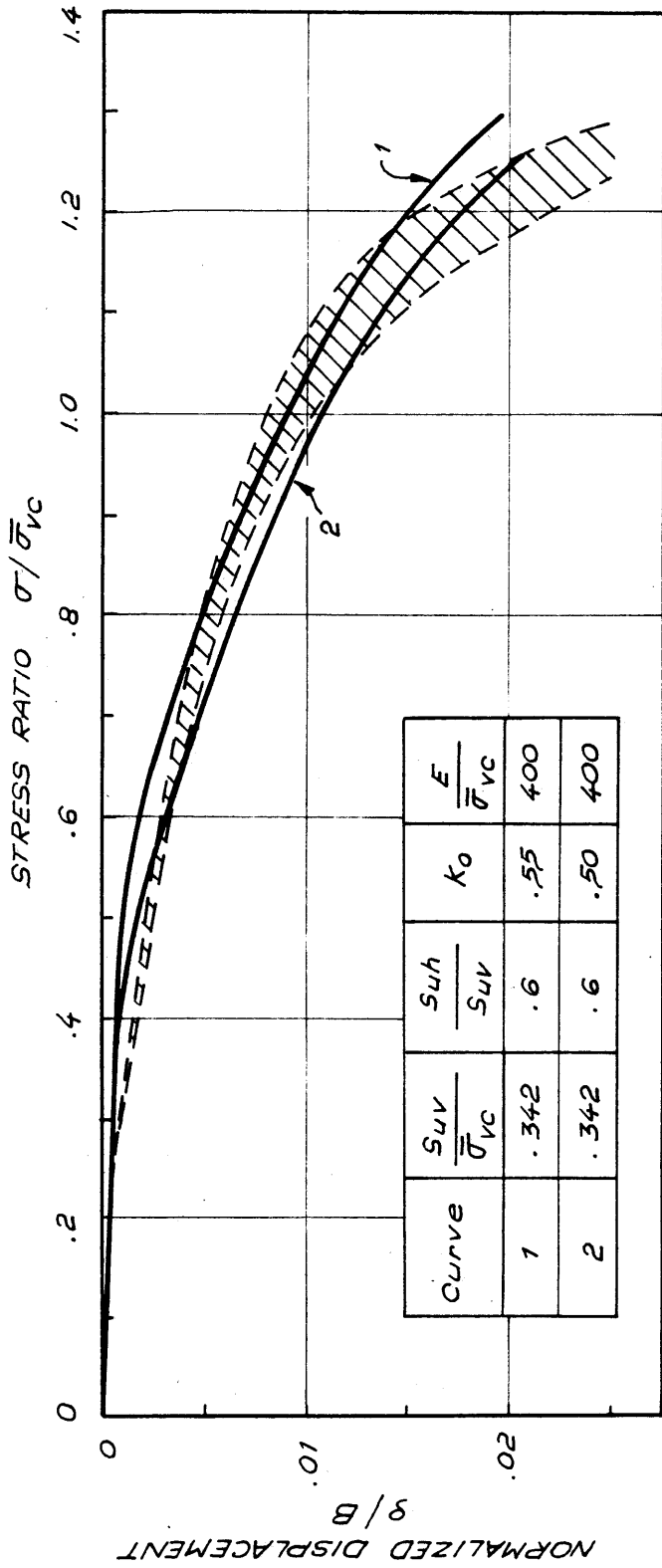
E/S_u VERSUS OCR PLANE STRAIN, TRIAXIAL COMPRESSION AND DIRECT SIMPLE SHEAR TESTS AT A FACTOR OF SAFETY = 3



— Davis and Christian (1970) for $N_c = 5.14$
 - - - Casagrande and Carrillo (1944)
 - · - · Probable lower limit for Boston Blue Clay
 ▨ Probable range : \overline{CROSS} Results (adjusted)

COMPARISON OF THREE HYPOTHETICAL VARIATIONS OF STRENGTH ANISOTROPY FOR $K_s = 0.6$

FIGURE 5 - 1

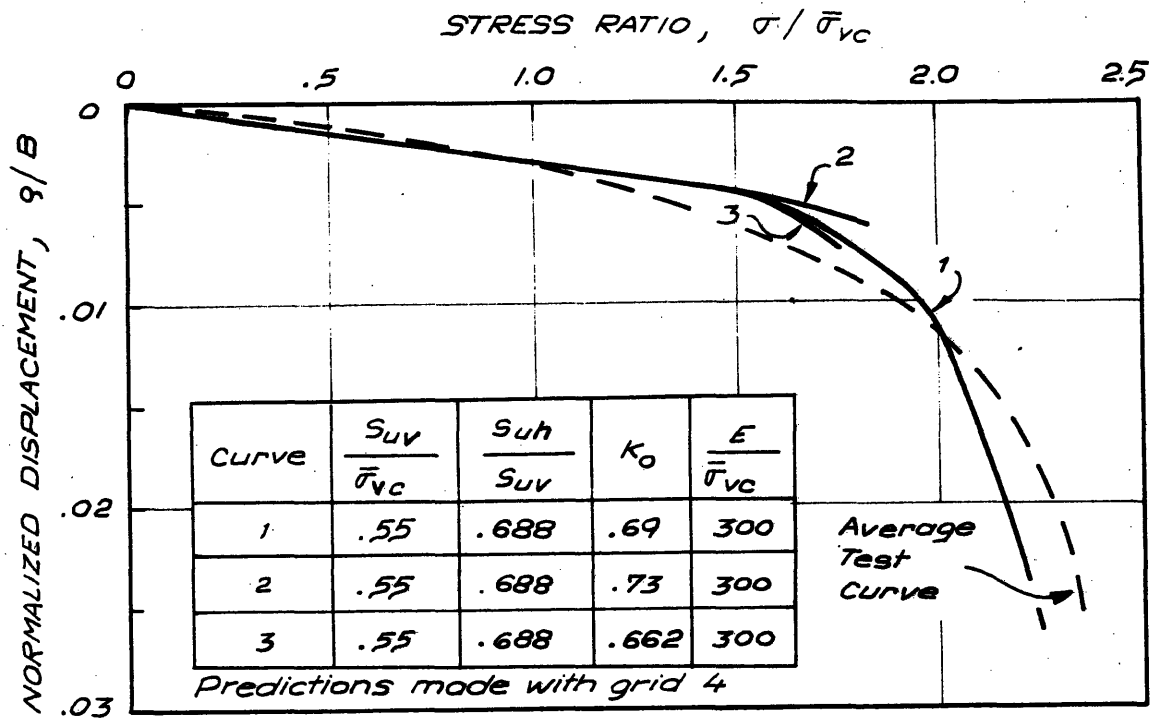


Area Bounded by Average Test Curves $\bar{\sigma}_{vc} = 2 \text{ \& } 3.38 \text{ kg/cm}^2$

Predictions made with grid 4

EFFECT OF VARIATION IN K_0 ON THE PREDICTED LOAD-DEFORMATION BEHAVIOR FOR NORMALLY CONSOLIDATED BOSTON BLUE CLAY

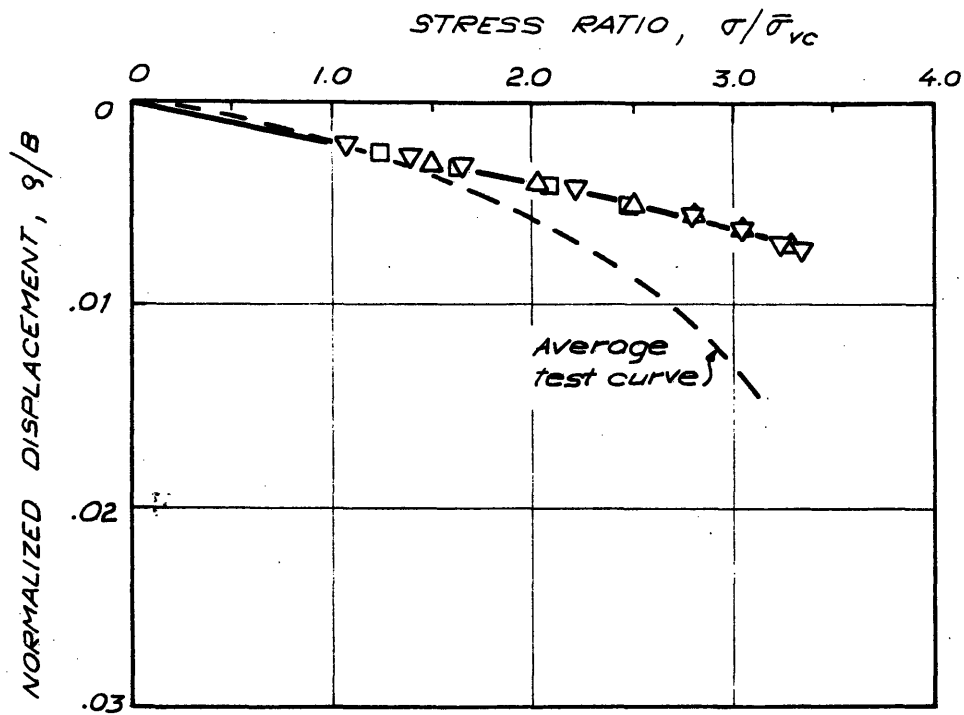
FIGURE 5-2



EFFECT OF VARIATION IN K_0 ON THE PREDICTED LOAD-DEFORMATION BEHAVIOR FOR BOSTON BLUE CLAY

OCR = 2

FIGURE 5-3

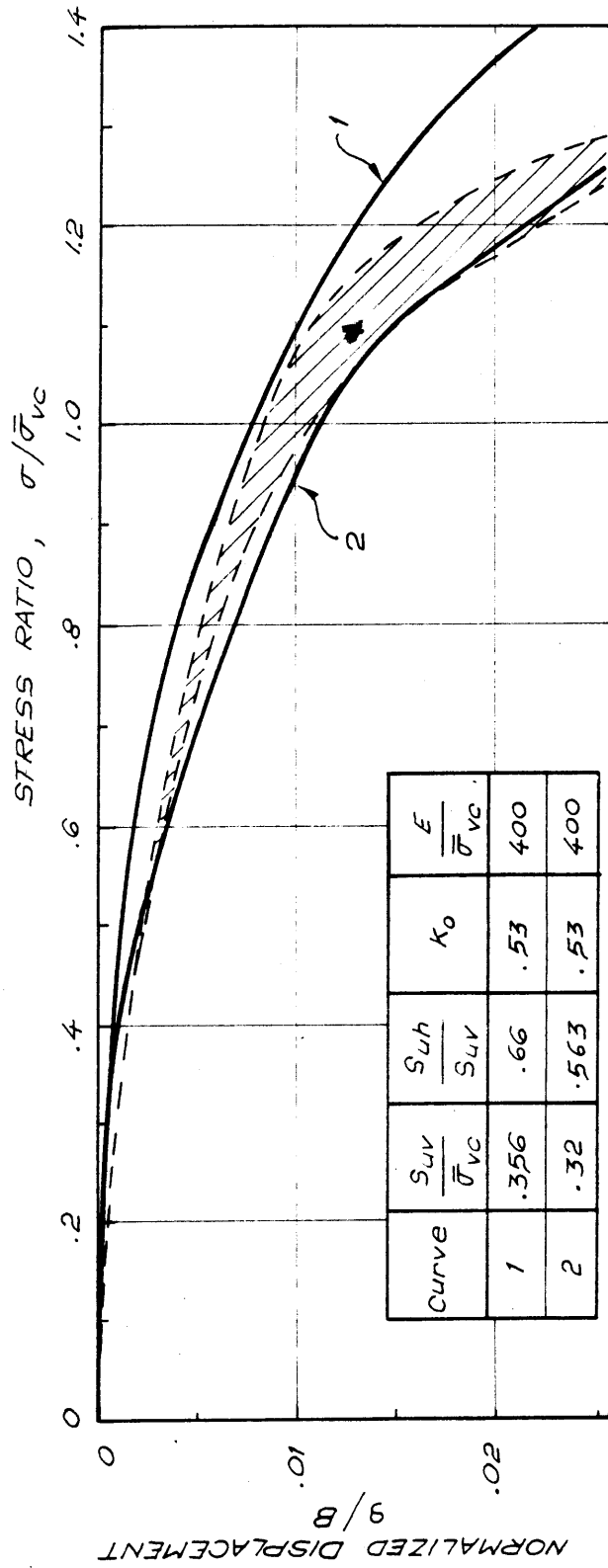


Symbol	$\frac{S_{uv}}{\bar{\sigma}_{vc}}$	$\frac{S_{uh}}{S_{uv}}$	K_0	$\frac{E}{\bar{\sigma}_{vc}}$
□	.9	.64	.8	450
▽	.9	.64	.87	450
△	.9	.64	1.0	450

Predictions made with grid 4

EFFECT OF VARIATION IN K_0 ON THE PREDICTED
LOAD-DEFORMATION BEHAVIOR FOR BOSTON
BLUE CLAY

OCR = 4

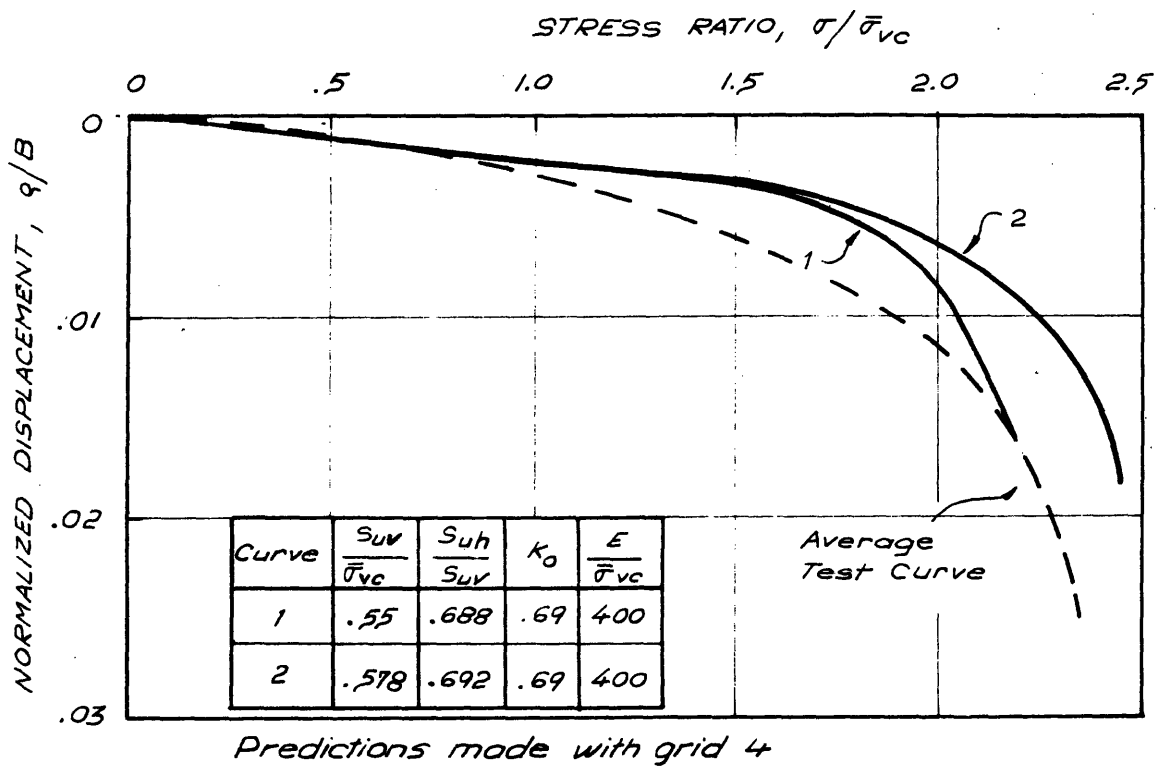


Area Bounded by Average Test Curves $\bar{\sigma}_{vc} = 2 \dot{\epsilon} 3.38 \text{ kg/cm}^2$

Predictions made with grid 4

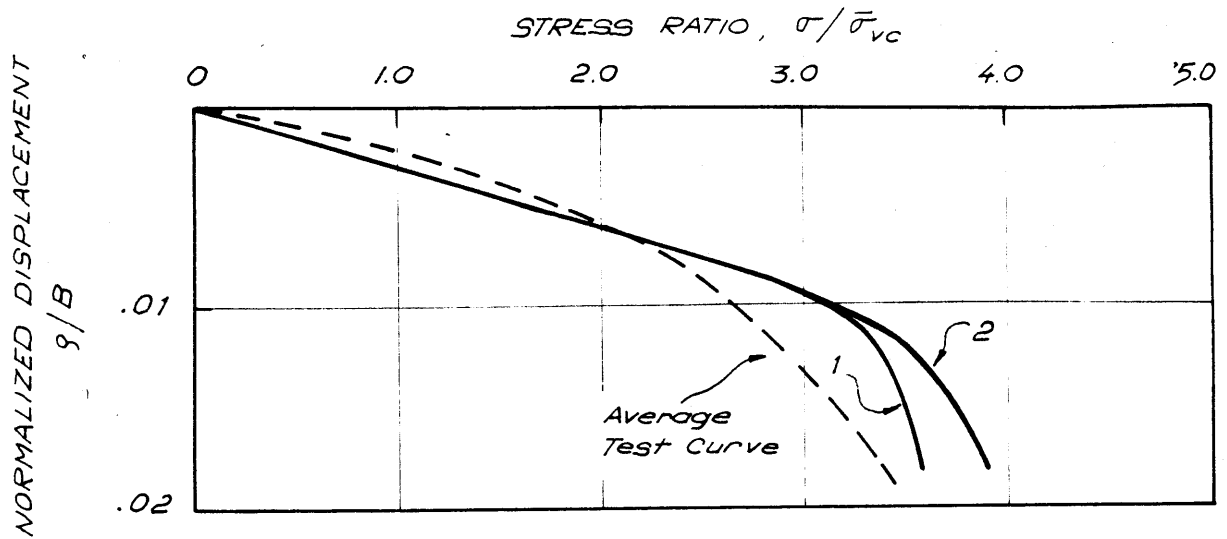
EFFECT OF VARIATION IN UNDRAINED SHEAR STRENGTH ON THE PREDICTED LOAD-DEFORMATION BEHAVIOR FOR NORMALLY CONSOLIDATED BOSTON BLUE CLAY.

FIGURE 5-5



EFFECT OF VARIATION IN UNDRAINED SHEAR STRENGTH ON THE PREDICTED LOAD-DEFOR- MATION BEHAVIOR FOR BOSTON BLUE CLAY

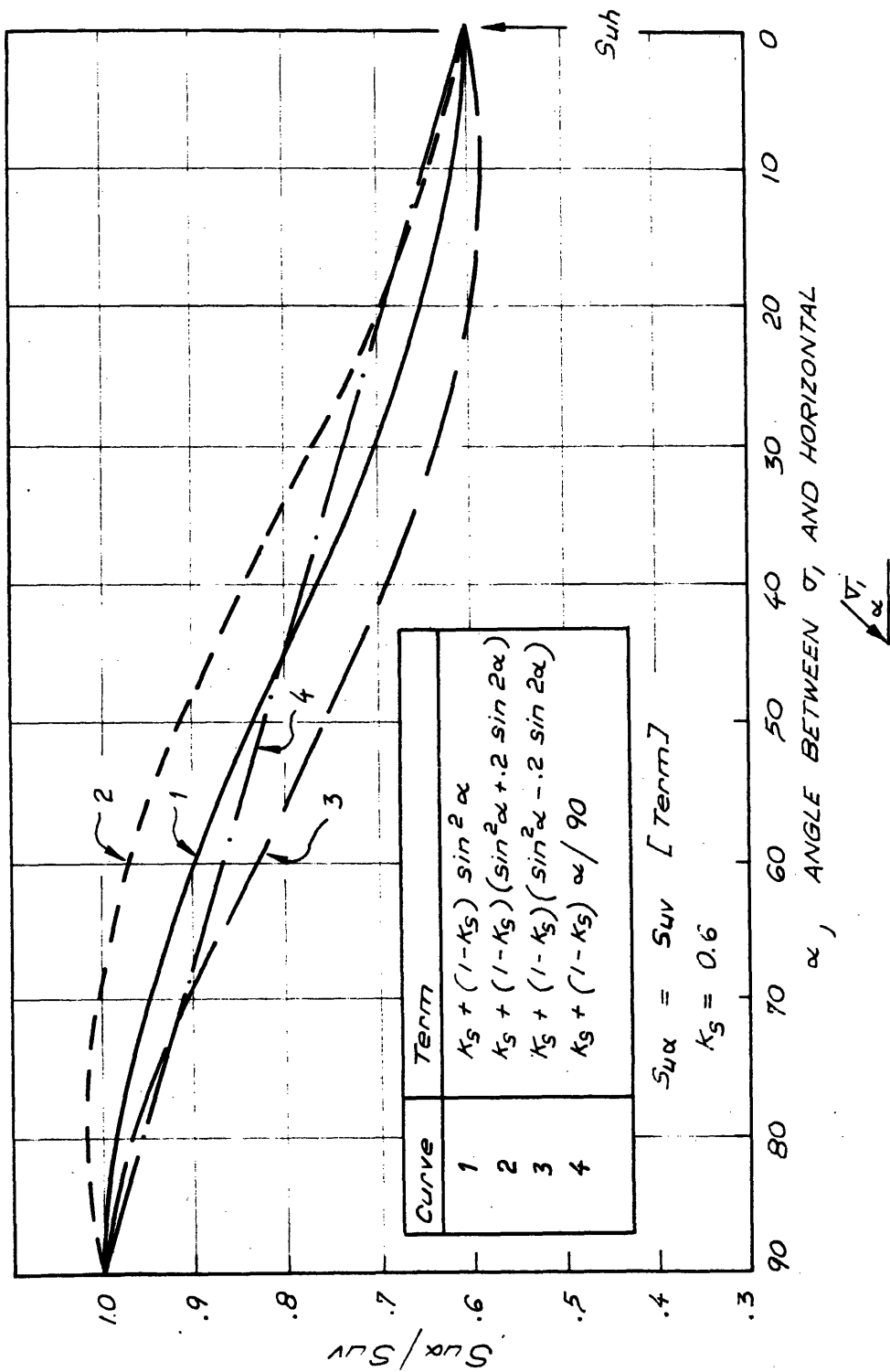
OCR = 2



Curve	$\frac{S_{UV}}{\bar{\sigma}_{vc}}$	$\frac{S_{UH}}{S_{UV}}$	K_0	$\frac{E}{\bar{\sigma}_{vc}}$	Grid
1	.9	.61	.89	300	4
2	.94	.62	.93	300	4A

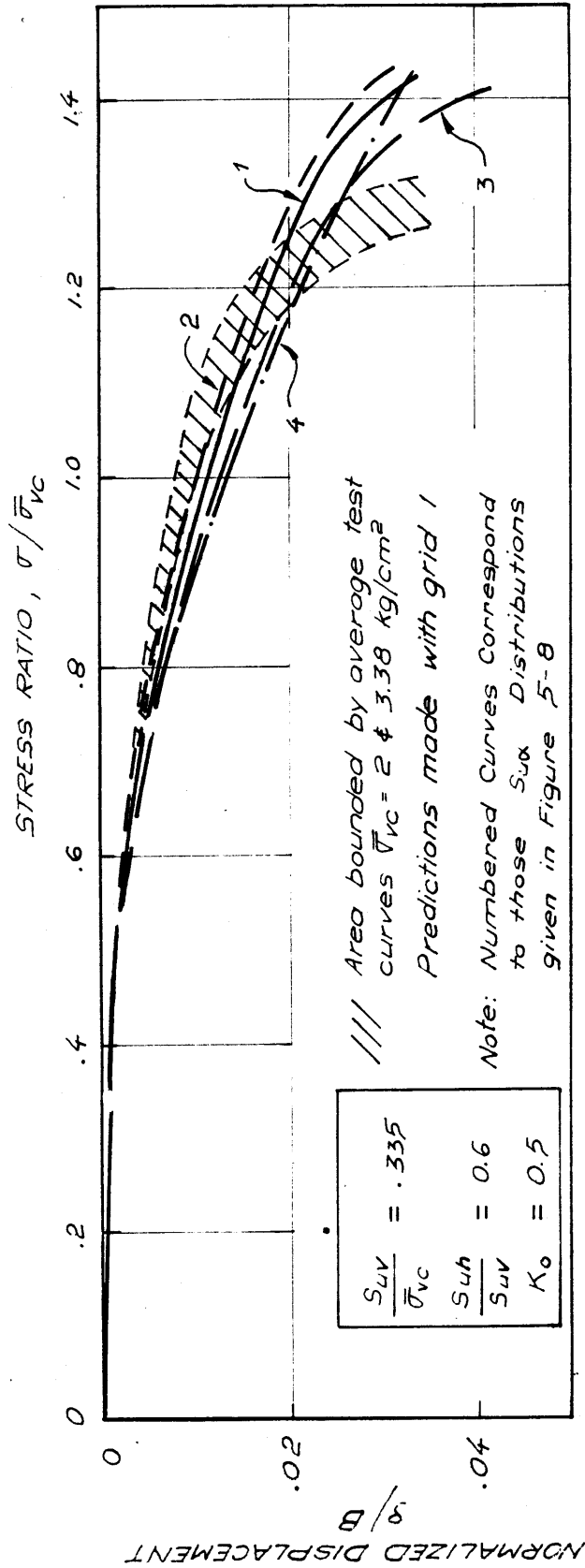
EFFECT OF VARIATION IN UNDRAINED SHEAR STRENGTH ON THE PREDICTED LOAD-DEFOR- MATION BEHAVIOR OF BOSTON BLUE CLAY

OCR = 4



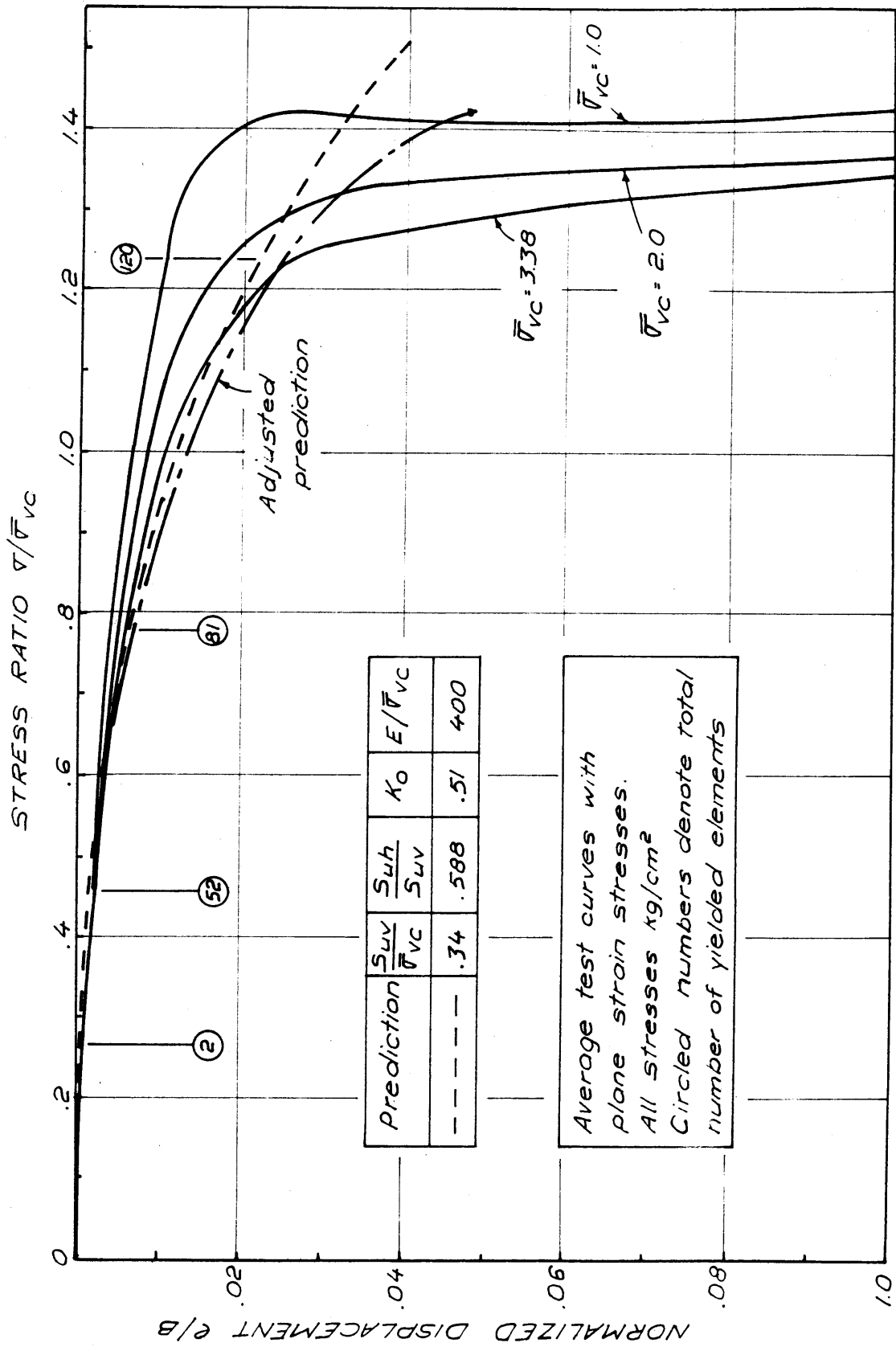
HYPOTHETICAL DISTRIBUTIONS OF UNDRAINED SHEAR STRENGTH, $S_{u\alpha}$.

FIGURE 5-8

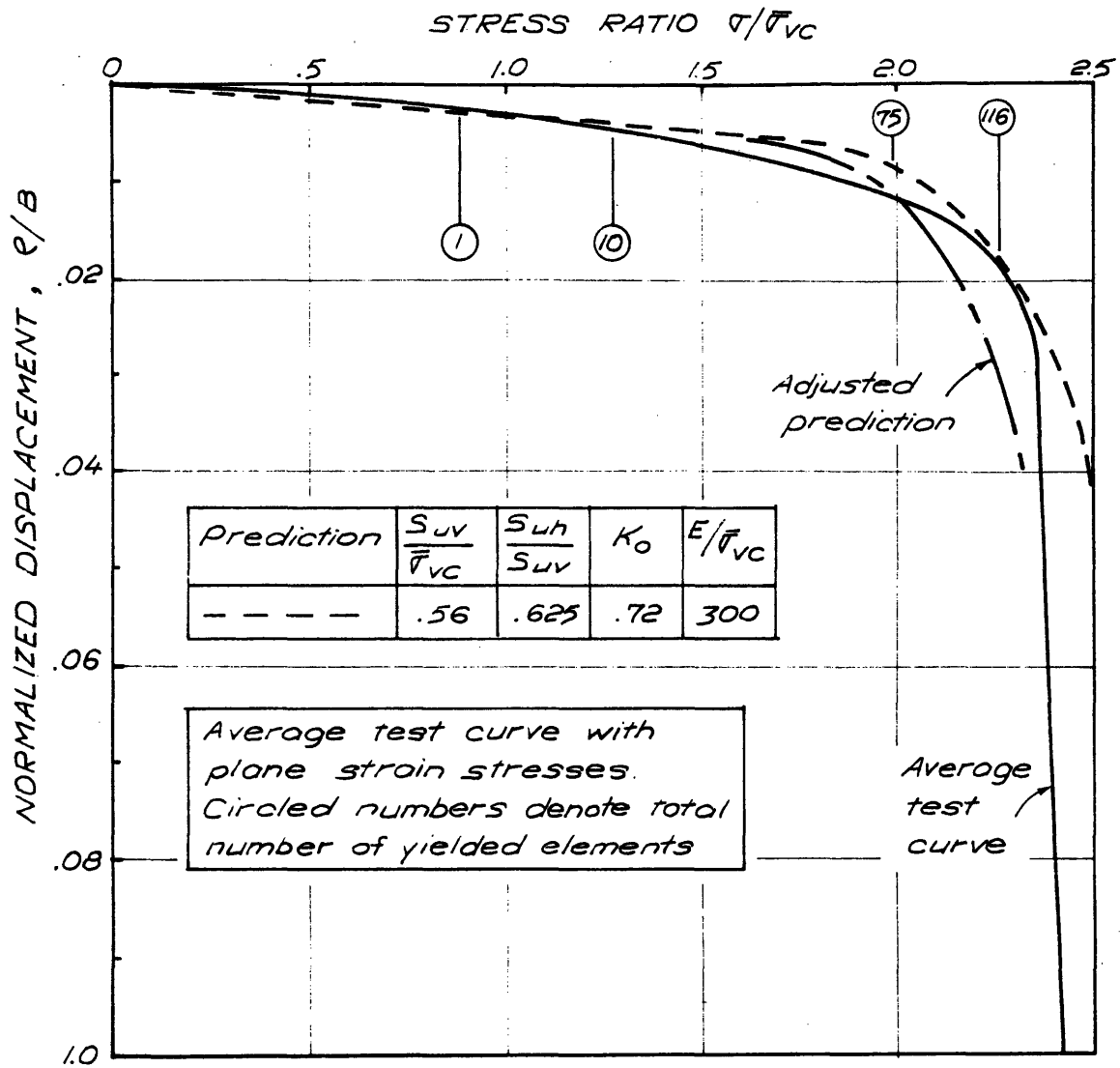


LOAD-DEFORMATION PREDICTIONS OBTAINED WITH HYPOTHETICAL DISTRIBUTIONS OF UNDRAINED SHEAR STRENGTH, S_{ux}

FIGURE 5-9

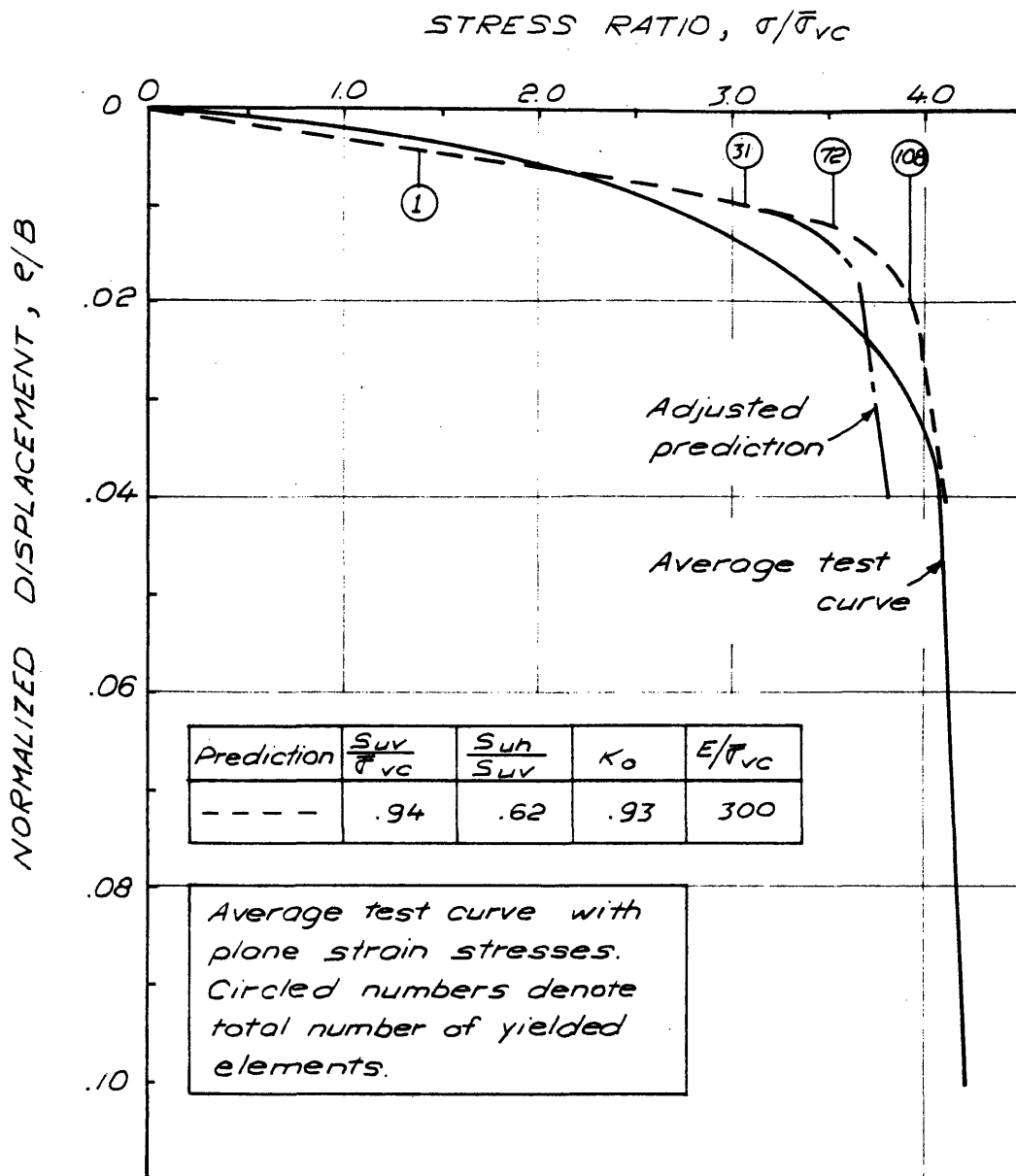


COMPARISON OF FINITE ELEMENT PREDICTION AND MODEL FOOTING TESTS FOR NORMALLY CONSOLIDATED BOSTON BLUE CLAY FIGURE 5-10



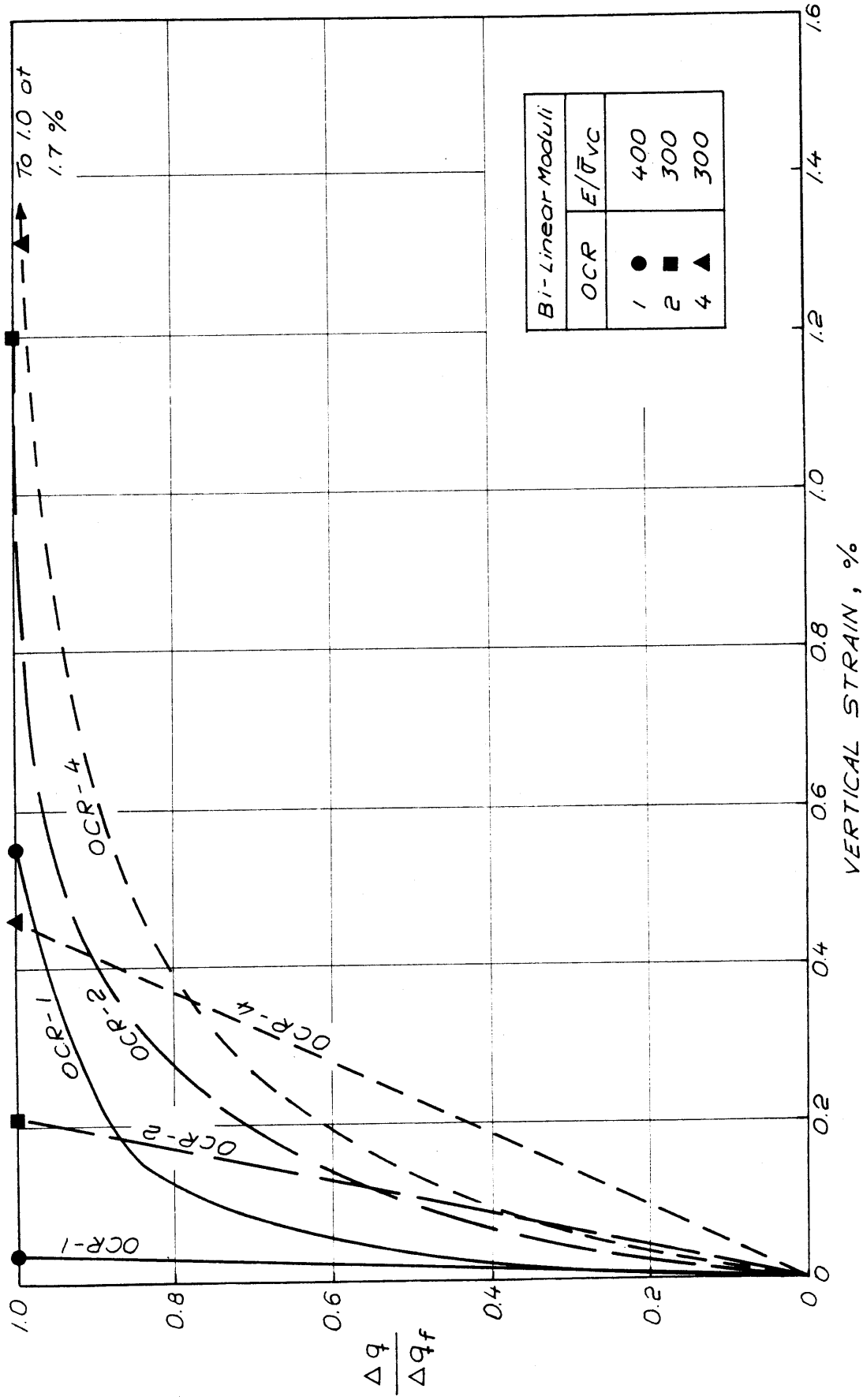
COMPARISON OF FINITE ELEMENT PREDICTION AND MODEL FOOTING TEST RESULTS FOR BOSTON BLUE CLAY AT AN OVERCONSOLIDATION RATIO OF TWO

FIGURE 5-11

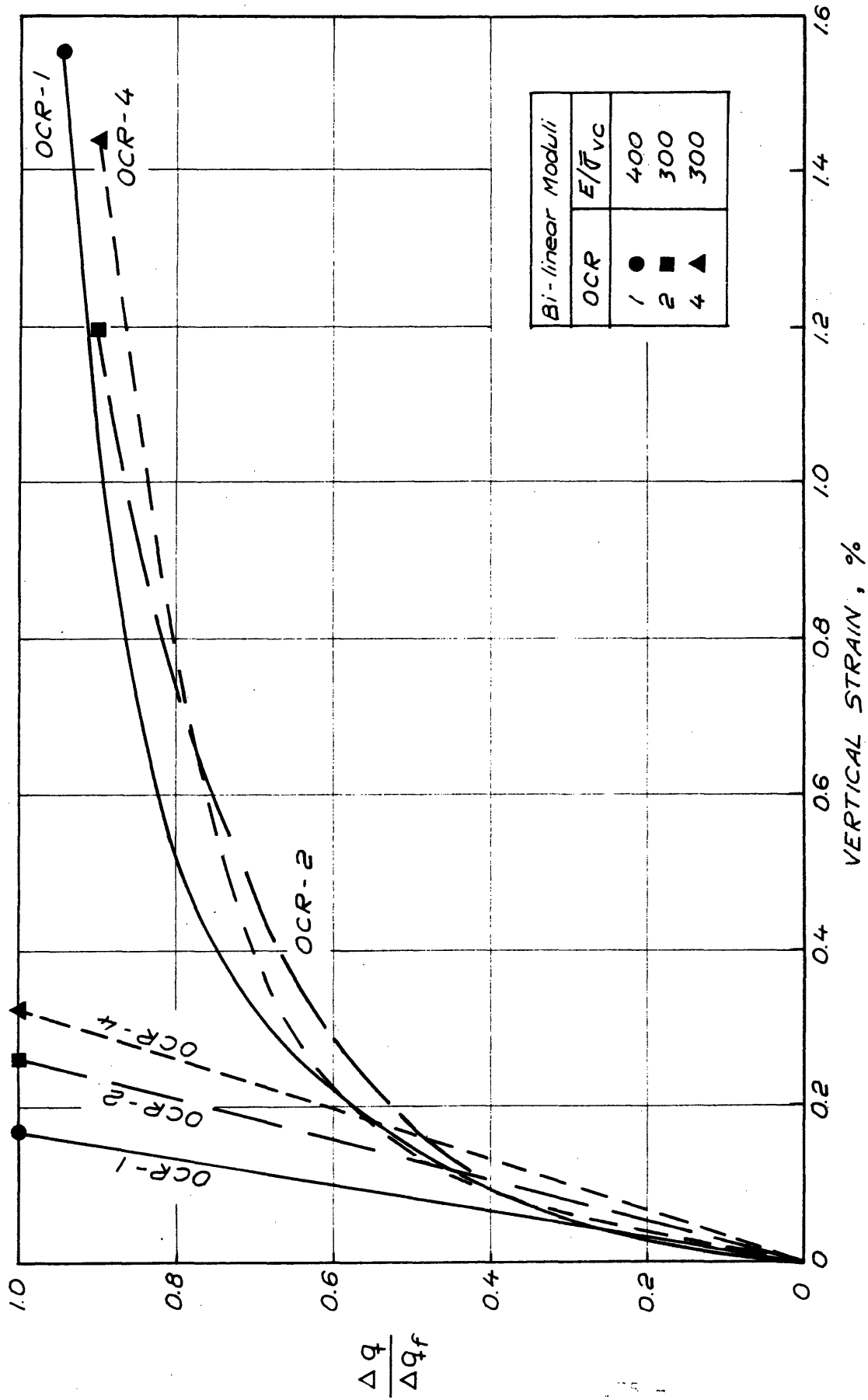


COMPARISON OF FINITE ELEMENT PREDICTIONS AND MODEL FOOTING TEST RESULTS FOR BOSTON BLUE CLAY AT AN OVERCONSOLIDATION RATIO OF FOUR

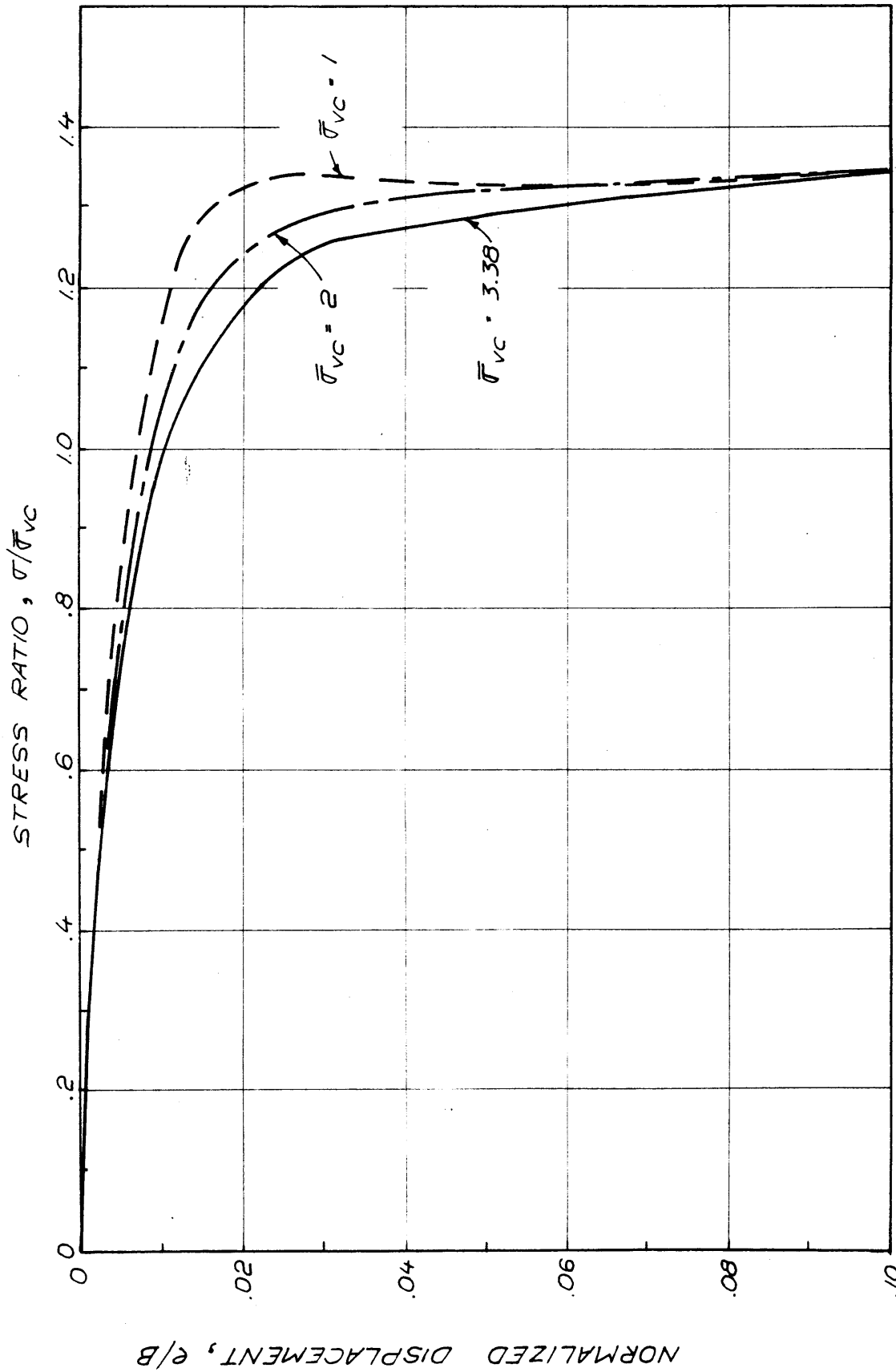
FIGURE 5-12



COMPARISON OF BI-LINEAR ELASTIC AND MEASURED STRESS - STRAIN CURVES :
 PLANE STRAIN ACTIVE CONDITION
 FIGURE 5-13



COMPARISON OF BI-LINEAR ELASTIC AND MEASURED STRESS - STRAIN CURVES:
 PLANE STRAIN PASSIVE CONDITION
 FIGURE 5-14



NORMALLY CONSOLIDATED MODEL FOOTING TESTS NORMALIZED WITH RESPECT TO STRESS RATIO FOR $\bar{\sigma}_{vc} = 3.38 \text{ kg/cm}^2$ FIGURE 5 - 15

APPENDIX A

INDEX PROPERTIES OF BOSTON BLUE CLAY USED FOR PLANE STRAIN, DIRECT-SIMPLE SHEAR, AND MODEL FOOTING TESTS

This appendix presents information on the index properties of the Boston Blue Clay used in the model footing, plane strain, and direct-simple shear tests discussed in this report. Index properties, as well as batch properties, are given in Table A-1 for the plane strain and direct-simple shear soil. Index properties of selected model footing tests are given in Table A-2. A composite plot of the results of hydrometer analyses on several of the batches and tests is given in Figure A-1.

Index properties of each batch or model test were not determined since the soil for the plane strain and direct simple shear tests, from batch 900 on, was taken from the same storage containers as was the soil used in the model tests. Furthermore, as much soil as possible was recycled following use.

The first batch, 100, was prepared in April 1967. Approximate mineralogical data for the clay are given in Table A-3.

TABLE A-1(1)

INDEX PROPERTIES AND BATCH INFORMATION FOR BOSTON BLUE CLAY
USED IN PLANE STRAIN AND DIRECT-SIMPLE SHEAR TESTS

Batch No.	WL %	Wp %	P. I. (activity)	Nominal slurry water content %	Nominal salt concentra- tion g/l	Consolida- tion increments (kg/cm ²)	Time for increment (hr)
100	43.5	19.6	23.9 (.478)	70	?	0 → .5 .5 → 1.5	24 46
150	43.5	19.6	23.9	70	?	0 → .25 .25 → 1.5	24 46
200	38.1	17.8	20.3 (.391)	100	~ 8	0 → .50 .5 → 1.5	24 41
300	39.7	21.6	18.1	100	~ 10	0 → .5 .5 → 1.5	24 45
400	39.4	21.3	18.1 (.351)	100	~ 10	0 → .5 .5 → 1.5	38 48
500				100	~ 10	0 → 1.5	60
600				100	~ 10		
800	41.5	19.5	22.0 (.46)	100	16		

Average specific gravity = 2.788

TABLE A-1 (2)

Batch No.	WL %	WP %	P. I. (activity)	Nominal slurry water content %	Nominal salt concentra- tion, g/l	Consolido- tion increments (kg/cm ²)	Time for increment (hr)
900	41.2	18.7	22.5 (.42)	100	16	0 → .5	4
						.5 → 1.5	168
1000	41.1	19.5	22.6 (.39)	100	16	0 → .25	26
						.25 → .5	12
						.5 → 1.5	47
1100	42.0	20.6	21.4	100	16	0 → .5	-
						.5 → 1.0	144
						1.0 → 1.5	96
1200	40.2	18.6	21.6 (.45)	100	16	0 → .5	228
						.5 → .9	504
						.9 → 1.5	72
1300				100	16	0 → .25	72
						.25 → .5	24
						.5 → 1.0	24
						1.0 → 1.5	27

Average specific gravity = 2.788

Table A-2

INDEX PROPERTIES OF BOSTON BLUE CLAY USED IN
SEVERAL MODEL TESTS

Test No.	w _L %	w _P %	P.I.	Activity
101	40.7	19.6	21.1	.406
104	40.3	19.6	20.7	
107	41.3	19.6	21.7	
200	42.3	18.5	23.8	.458
400	39.8	18.9	20.9	.445

Table A-3

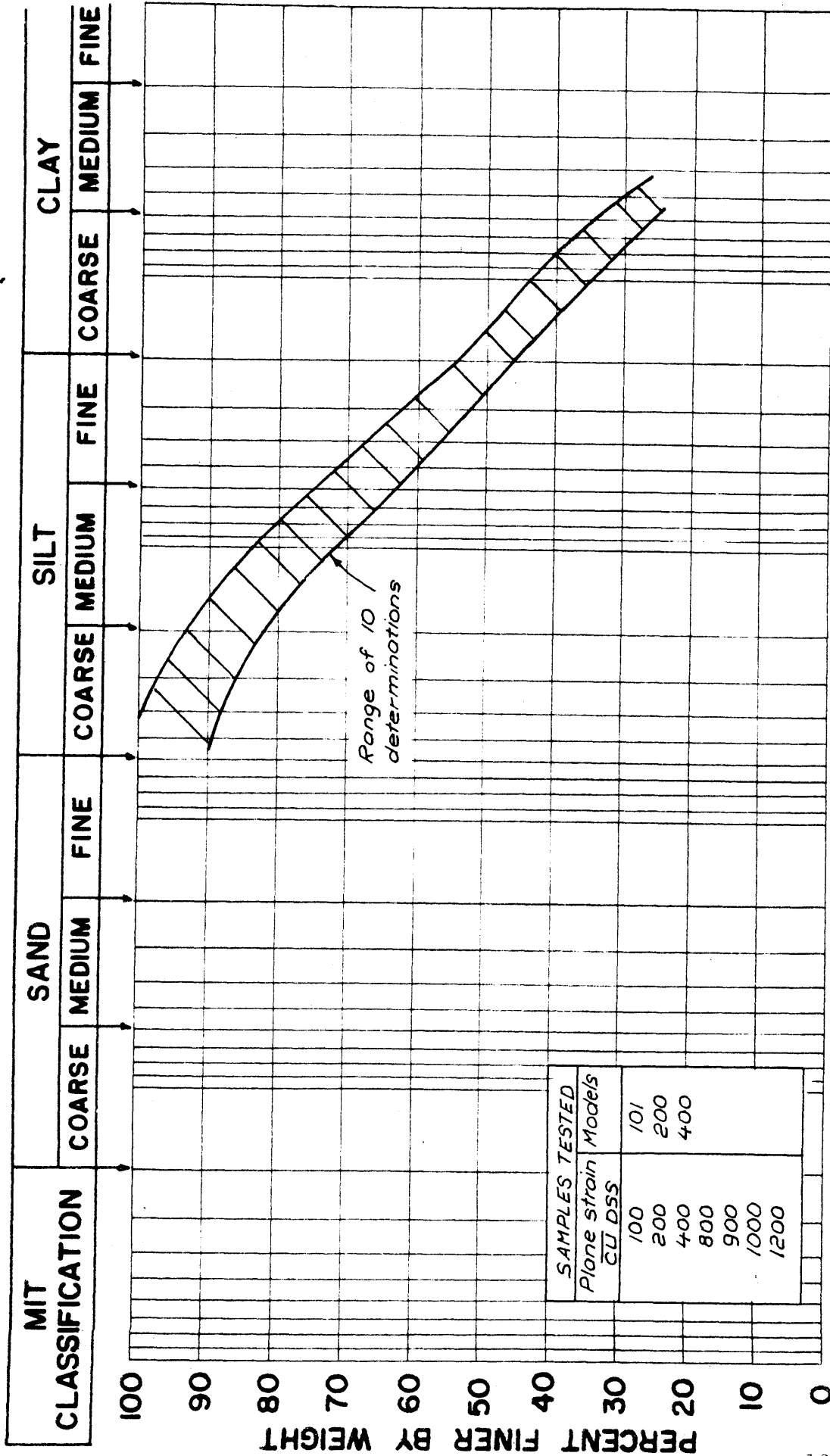
APPROXIMATE MINERALOGICAL DATA ON BOSTON BLUE CLAY

~ 15 - 20 %	Quartz
~ 5 %	Chlorite
~ 30 - 45 %	Illite
~ 1.5 - 3 %	Iron Oxides
< 1 %	Organic Matter

(After Mitchell 1956)

GRAIN SIZE DISTRIBUTION

BOSTON BLUE CLAY



DIAMETER IN MM 0.1 0.01 0.0001
 FIGURE A-1

APPENDIX B

DESCRIPTION OF MODEL TEST EQUIPMENT AND EXPERIMENTAL PROCEDURES

B.1 INTRODUCTION

A detailed description of the test equipment and experimental procedures employed in the performance of the model footing tests is given in this appendix. The equipment is discussed in Section B.2, and the test procedures are outlined in Section B.3. Calibrations, calculations, corrections and other miscellaneous information are considered in Section B.4.

B.2 DESCRIPTION OF TEST EQUIPMENT

B.2.1 Background

Most of the tests conducted during this investigation employed some of the basic equipment used by earlier investigators, Perez La Salvia, et.al. (1966). For brevity in this discussion, this equipment is referred to as Bin One. Bin One is discussed as well as several pieces of apparatus that were developed by the author during this investigation. The model footing apparatus that was designed and constructed during this research is termed Bin Two.¹ The equipment is described in the sequence in which it was employed during the sample

¹ This appendix contains several photographs of Bins One and Two. Schematic diagrams of the bins are given in Figures 3-1 and 3-2, Chapter Three.

preparation and testing.

In summary, the model tests were conducted on samples of normally consolidated and overconsolidated Boston Blue Clay that were one dimensionally consolidated from dilute slurries in 12 inch diameter bins. Rectangular footings having a length to breadth ratio of eight were used. The footings were 5 inches long by 0.625 inches wide. The average soil height at the time of the test was about four inches.

B.2.2 Clay Slurry and Initial Consolidation

The clay was introduced into either Bin One or Bin Two in slurry form under a partial vacuum with the aid of the equipment set-up pictured in Figure B-1. The soil was introduced into the apparatus through a funnel assembly, a portion of which is shown at the top of the photograph. The equipment shown in the figure is that developed by the author for Bin Two. It was developed for the dual purpose of use in the models' program as well as for use as the Soil Mechanics Laboratory's clay batch preparation unit. The depth of the soil container was made greater than that normally needed in the model tests so that batches of clay of approximately seven inches in height can be obtained. This soil height is sufficient to permit several 3.5x3.5x1.4 inch horizontal and vertical specimens to be trimmed from the same cake of soil. All seals between adjacent parts of the apparatus are made with O-rings. The flanges shown on the bin in the figure were press fitted and then welded to the soil container prior to its final machining. In addition to insuring the circularity of the inside diameter of the bin, the flanges also serve to protect the ends of the

unit from damage. The three foot long polyvinyl chloride cylinder that is shown was employed so that after introduction into the chamber, the diffused soil slurry would be fully subjected for a short time to the vacuum existing in the unit. A conically shaped diffuser assembly, not visible in the photograph, was attached to the lucite top plate. It was employed to insure that the soil slurry was atomized prior to its fall through the chamber. The vacuum was applied to the unit with the flask and vacuum pump shown in the background. Vertical tie rods were employed to keep all sections of the apparatus centered and in place. The vacuum apparatus employed with Bin One was similar. Vacuum seals between adjoining pieces of this apparatus were made with rubber gaskets and silicone grease rather than with O-rings.

Initial consolidation of the slurry was performed with the stainless steel consolidation plate shown in Figure B-2. It was loaded by a 5000 pound capacity Karol-Warner Conbel loader. The plate, designed by the author, was constructed with a removal O-ring feature as shown in the photograph. Thus side friction between the plate and the walls of the bin could be reduced as much as possible after the slurry had obtained some rigidity. In order to minimize deflections of the plate, the load from the Conbel loader was transferred to the consolidation plate through a five inch diameter shoulder ring. Double drainage exists during consolidation with the plate. The holes seen in the central region of the plate lead to radial drainage grooves that collect water from the porous stone that is recessed in the bottom surface of the plate.

A plane, level soil surface was achieved by guiding the consolidation plate with the linear bushing assembly shown in Figure B-3. A portion of the Conbel loader is also shown in this figure. The coupling assembly connecting the loader to the consolidation plate shaft, while awkward looking, was extremely versatile and worked well.

Air pressure to the Conbel loader was provided by an air compressor. It is possible that pressure surges could have developed when the air compressor turned on. These were eliminated by placing an air tank in series with the output line of the compressor. The pressure to this tank was maintained at a constant level with a Nullmatic pressure regulator and a Nupro bleed valve. The Conbel was in turn controlled by a second Nullmatic regulator.

B.2.3 Final Consolidation with Surcharge Bag or Membrane

After a desired consolidation stress was reached, the consolidation plate was removed, and subsequent consolidation was performed with the footing apparatus in place. This consolidation was performed in Bin One with a surcharge bag. In Bin Two it was conducted with a surcharge membrane.

In previous work with the Bin One, a circular footing was used. Since the present research employed a rectangular footing, an entirely new surcharge bag was needed. The bag that was developed is shown in Figure B-4. The upper photograph shows the rectangular slot in the bottom of the bag which accommodated the footing. The lower photograph is a view of the top of the bag with the footing installed.

Made from natural latex, the bag was fabricated from three pieces that were formed on separate molds. The top surface, sides, and the outer portion of the bottom of the bag were about 0.030 inches thick. The bottom of the bag adjacent to the rectangular slot for the footing was from 0.010 to 0.015 inches thick. The author found it necessary to make this surcharge bag after a local company experienced difficulty in making a bag with the desired specifications. The diameter of the bag was made greater than the inside diameter of the bin. Thus, its bottom surface was never in tension. This prohibited the rectangular slot from stretching and separating from the sides of the footing. Visual confirmations of this fact were obtained in special experiments at several pressures. A stainless steel collar was slipped over the footing shaft to eliminate friction between the bag and the footing shaft. This is shown in the lower photograph of Figure B-4. The rubber collar fabricated into the bag had a length greater than the bag height. Thus, during the test it was not possible for the collar to stretch and tend to pull the top of the slot off the footing. The rubber slot for the footing was very flexible and had a thickness of from 0.010 to 0.015 inches.

The membrane employed with Bin Two is shown in Figure B-5. This membrane is also made of natural latex. The arrangement illustrated is that existing at the time the footing apparatus is installed in the bin in preparation for the final consolidation increment(s). The footing shaft does not pass through any rubber collar with this apparatus. Instead, the footing, membrane, and the shaft are sealed at the top

of the rectangular slot by an O-ring. However, even with the O-ring, metal to metal contact is still maintained between the footing shaft and the footing. Thus, the unit did not have to be calibrated for the compression of the O-ring. The bottom of the membrane was provided with a convolution to keep it from experiencing tension that would pull it away from the footing. As with the surcharge bag, the slot in the membrane was made very flexible so that it would collapse and follow the footing during the test. The average thickness of the membrane was about 0.015 inches.

At least one increment of virgin compression was conducted with the footing assembly in place. Deaired water was used with both the surcharge bag and membrane. In both cases pressure was applied with the air compressor through an air-water pressure interchange vessel. A long length of polyethylene tubing was used on the outlet of the interchange vessel to retard air flow into the water in the bins.

The equipment set-up during the final consolidation is shown for Bin Two in Figure B-6¹. It should be noted that a Geomeasurements Inc. triaxial piston unit assembly is used for loading the footing. The top one inch thick plate was fabricated from aluminum (copper based alloys would have attacked the latex membrane, a portion of which can be seen in the photograph). Even though the top plate is one inch

¹ Weights are applied to the footing piston during consolidation to compensate for the upward thrust of the pressurized water in the membrane. With Bin One compensating weights are also used during consolidation. In this case they are used to account for the lack of surcharge pressure over the area of the stainless steel collar.

thick, it is still subject to some deflection under pressure, since the span is 12 inches. Accordingly, the dial support was suspended across the bin as shown. The linear displacement transducer employed during the test is attached to the vertical rod that supports the dial. Four Swagelok fittings were installed in the sides of this bin. The upper two are used to vent air from the bin when the membrane is installed. Either one or both of the lower fittings can be used to provide lateral top drainage through a sand pocket. Bin Two is back pressured with a mercury pot system. Back pressure is applied to the soil through the fittings to the bottom porous stone and the sand pocket. Back pressures of up to 2.5 kg/cm^2 have been used.

Volume changes during final consolidation with this bin are monitored with a 200 cc volume change device. The observed volume change can be compared with that computed by multiplying the vertical movement of the footing times the area of the bin.

B.2.4 Apparatus Arrangement at Time of Test

The apparatus arrangements at the time of a test are shown in Figures B-7 and B-8 for Bins One and Two respectively. The 300 pound capacity BLH load cell that records the footing load is suspended from a cross arm. The cross arm is attached to the shaft of a 1000 pound capacity Simplex Uni-Lift Worm Gear Screw Jack. The cross arm is in turn restrained to move only in the vertical direction by two one inch diameter shafts that pass through fixed linear bushings identical to the one shown in Figure B-3. The footing is advanced into

the clay by driving the jack with the aid of a Graham variable speed electric motor that is connected to the jack through a Boston Gear reductor and a universal joint assembly.¹

The wires in the center of Figure B-7 lead to the linear displacement transducer that monitors the footing displacement during the test. This bin is also fitted with a Swagelok fitting so that a sand pocket can be used for top drainage. (See Figure 3-1).

B.3 SAMPLE PREPARATION AND TEST PROCEDURES

B.3.1 Batch Preparation

The Boston Blue Clay used in the model tests was obtained in 1966 during construction operations on the M.I.T. campus. Typical properties of the soil are given in Appendix A. It was stored in galvanized containers at a water content of 60 to 80 percent until the fall of 1968. The soil was sieved through a number 40 sieve prior to use, since in its natural state it contained shells and traces of sand and wood chips. Any soil not used immediately after sieving was stored in 20 gallon plastic containers.

Each batch of clay (approximately 11.25 kg of solids) was mixed to a nominal water content of 100 percent at a NaCl concentration of 16 g/l. The initial water content of the soil to be used was determined the day before sample preparation. Experience showed that

1

The Graham motor and universal joint assembly are shown in Figure 3-4, Chapter Three.

the salt concentration of the raw soil was approximately constant from batch to batch. The salt concentration of the raw soil was therefore checked about every fourth test. Distilled water and reagent quality Na Cl were used to bring the slurry of each batch to the aforementioned nominal water content and salt concentration. The average water content actually achieved for each batch is given along with other test results in Appendix C. The soil was mixed with a hand electric mixer and spoons. Care was exercised to minimize air entrapment during this procedure.

The apparatus comprising the vacuum chamber was assembled and evacuated to an absolute pressure of less than 4 centimeters of mercury. Prior to insertion of the soil, the unit was checked for leaks by isolating it from the vacuum pump and checking for pressure increases with time. The soil was not inserted until all apparent leaks were stopped. The inner surface of the consolidation bin was liberally coated with silicone grease prior to assembly of the vacuum unit so that friction between it and the soil would be minimized during subsequent consolidation.

The soil slurry was inserted into the chamber slowly in several increments. Atomization of the soil was achieved with Bin One by regulating the soil injection valve. The diffuser assembly in Bin Two helped atomize the slurry. Even with diffusion of the slurry it was possible that the excessive air remained in the soil. Accordingly, after every second increment of soil, insertion was discontinued until there was no longer any evidence of air bubbles

escaping from the slurry surface. The total time for insertion varied from batch to batch, but usually took from $1\frac{1}{2}$ to 3 hours.

During insertion of the slurry, the valves at the bottom of the chamber were closed and the vacuum was drawn from the top of the unit through the vacuum valve near the injection valve. Twenty to thirty minutes after soil insertion was completed, the top vacuum valve was closed and the valves at the bottom of the consolidation chamber were opened to the vacuum flask. The soil injection valve was then opened slightly so that the pressure in the cylinder gradually increased to atmospheric pressure. Consolidation of the clay slurry under the resultant seepage force and evacuation of the water from the bottom of the unit continued until the soil surface was about one half inch below the top surface of the bin.

B.3.2 Initial Consolidation

Following disassembly of the vacuum unit, the soil container was transferred to the Conbel loading frame. Several consolidation increments were then performed with the consolidation plate. Both top and bottom drainage existed during this consolidation. All slurries were subjected to an initial consolidation stress of about 0.07 kg/cm^2 for a few hours. The purpose of this increment was to insure that the consolidation plate was well seated on the soil surface before higher stresses were imposed. The consolidation stresses were increased to 0.50 kg/cm^2 in two increments. Except for two tests, the intermediate stress was 0.25 kg/cm^2 . Owing to the extensive time required to complete primary consolidation for the 0.25 kg/cm^2 increment, the

applied stress was increased to 0.50 kg/cm^2 after about 90% consolidation for most tests. The consolidation times allowed for these and other increments for each test are given in Appendix C, Table C-1. Further consolidation with the plate was predicated on the intended use of the clay. Subsequent consolidation for the normally consolidated tests at $\bar{\sigma}_{vc} = 1 \text{ kg/cm}^2$ was performed with the surcharge bag. With the exception of test 100, consolidation for the normally consolidated tests at $\bar{\sigma}_{vc} = 2 \text{ kg/cm}^2$ was continued with the plate to 1.25 kg/cm^2 . Test 100 and all other tests were consolidated to 1.5 kg/cm^2 with the plate.

B.3.3 Final Consolidation and Rebound

Removal of the consolidation plate and insertion of the footing assembly was an operation that required considerable care. It was conducted in the following manner.

Water which had collected on top of the consolidation plate was sponged or siphoned off and the top of the plate thoroughly dried. A fine polyethylene tube was inserted into each of the drainage holes of the consolidation plate and as much water as possible was either siphoned off or blown out of the drainage grooves and porous stone of the plate. The bottom drainage valves were then closed, the consolidation stress from the Conbel released, and the consolidation plate removed as rapidly as possible. The plate was easily removed since the O-ring had been released and thus offered no frictional resistance. Some adhesion between the soil and the plate was observed. Disturbance to the soil surface from this factor was reduced by placing a layer of

filter paper between the soil and the plate when the plate was installed prior to consolidation. Any water that dropped from the porous stone onto the filter paper as the plate was removed was quickly sponged off with a soft cotton towel in order to reduce swelling. Then the filter paper was removed.

After the exposed inner surface of the bin was cleaned of any soil and excess silicone grease, a layer of Saran Wrap was placed over the soil to retard evaporation until the surcharge bag or membrane was installed.

Top and bottom drainage through the consolidation plate and bottom porous stone existed during those consolidation increments with the Conbel. However, with the surcharge bag or membrane only bottom drainage would occur unless special provisions were made. Accordingly, a Swagelok fitting was installed at a location in the bin wall which would be 0.2 inches below the soil surface at the end of consolidation. Prior to insertion of the surcharge bag or membrane a volume of soil one inch long by one inch deep extending one half inch from the bin wall was removed. The plug in the Swagelok fitting was removed and filter paper installed on the inner surfaces of the void. The void was then back filled with sand and the sand densified with a thin rod. The soil adjacent to the sand pocket was undoubtedly disturbed during the process of clay removal and sand backfilling. The sand pocket was therefore located diagonally off one end of the footing, at a distance of more than 5.5 footing widths, in order to prohibit this disturbance from influencing the test results.

The Saran Wrap was removed and two or three layers of filter paper were placed over the soil surface except for the area within about one inch of the footing. After the filter paper had been installed the exposed inner surface of the bin was coated liberally with silicone grease to reduce friction between it and the surcharge bag or membrane.

With Bin One, the surcharge bag, with the footing and stainless steel collar in position, was then placed in the bin. Spacing plates were placed on top of the bag so that when the top plate assembly was installed, the bag was compressed vertically. Enough spacing plates were used so that the bag was compressed more than it would extend during subsequent consolidation.

Placement of the top plate assembly of this apparatus required two people. The footing shaft passed through linear bearings in the assembly. Accordingly, careful alignment of the unit was necessary before it could be lowered into place. The assembly was suspended at the top of the test loading frame by a cable and pulley system leading to a chain fall. While one person controlled the vertical movement of the top plate, the second guided the footing shaft into the bearing housing and held the footing off the soil surface. The footing was not lowered into contact with the soil until the top plate had been lowered into its final position. The unit was then bolted to the consolidation ring and bottom plate. The bolts were tightened uniformly so as not to cock the linear bushing and jam one end of the footing into the soil.

The design of the second apparatus permitted one person to perform the final equipment assembly. The footing shaft was clamped in its retracted position until the top plate was bolted in place.

Thus, if normal caution was exercised, the footing could not damage the soil surface. The retaining nuts with this apparatus were also tightened uniformly to avoid cocking the footing.

Consolidation was continued after water had been siphoned into the bag or membrane. The pressure was increased in steps over about a 30 minute period to the vertical stress to which the clay had been subjected by the Conbel. The next consolidation increment was then applied. Consolidation of the clay was monitored by use of a dial gauge attached to the footing shaft. Weights as necessary were placed on the footing loading assembly to achieve an average stress under the footing equal to the applied fluid pressure.

After the required time of secondary compression at $\bar{\sigma}_{vm}$, the normally consolidated samples were tested and samples for the overconsolidated tests were rebounded. Except for one test, the time for secondary compression at $\bar{\sigma}_{vm}$ varied from 50 to 65 hours. This corresponds to a ratio T_s/T_p from 2.1 to 6.2 as seen in Table C-2, Appendix C. This range of T_s/T_p is similar to that for the plane strain tests reported in Chapter 4. The time of secondary rebound at $\bar{\sigma}_{vc}$ for the overconsolidated tests was never less than 16 hours.

Particular care was exercised during overconsolidation with Bin One to maintain a free flow of water through the sand pocket and filter paper into the bin.

B.3.4 Loading

During the test, the footing load was monitored by a 300 pound BLH load cell and the footing displacement by a 0.625 inch stroke

linear displacement transducer. The test data were recorded on a Hewitt-Packard X-Y Recorder. All electronic equipment was allowed to warm up under the correct input voltage at least 30 minutes prior to the pre-test calibration. The pre-test calibrations of the load cell and transducer were performed on the X-Y recorder. The load cell was calibrated with dead weights and the displacement transducer with a micrometer barrel.

In order to fill the surcharge bag and membrane with water, it was necessary to have two valve connections. This requirement offered a ready made solution to any potential problem of a sudden pressure drop during the test resulting from volume change which accompanied downward movement of the footing. One connection was made to the water side of the air-water pressure interchange vessel while the other was made to the air side. During consolidation the air valve was closed and the water valve open. Before conducting the test the valve positions were reversed. Thus, air was in direct contact with the water in the bin during the test. Hence, any problem with turbulent water flow through valves and fittings, even though remote, was eliminated.

A strain controlled test was conducted using the 1000 lb. capacity jack and variable speed motor mentioned earlier. The load cell was brought into contact with the footing loading assembly prior to the motor being turned on. Thus, while the test was conducted rapidly, an impact loading of the footing was avoided.

With the exceptions noted below, a footing displacement rate

leading to a $\rho/B = 0.1^1$ in 15.6 seconds was used for all tests. Displacement rates of 9.4 and 8.3 seconds for $\rho/B = 0.1$ were used for tests 104 and 105. The choice of this range of displacement rates is discussed in the next section. All drainage valves were closed during the tests.

B.3.5 Post Test Procedures

After the test, the load cell and displacement transducer calibrations on the X-Y recorder were rechecked. No calibration shifts occurred.

With both apparatus, the footing could slip out of the rectangular slot in the bag and membrane unless considerable care was exercised when placing the pressure elements in the bins. Therefore after each test a check was made to determine that the footing had remained in the slot. This was done before either the bag or membrane was removed. No slippage occurred for any test reported here. Final measurements of the sample height were taken after the soil surface was exposed. Water content determinations were then made throughout the sample. The results of these measurements are given in Appendix C.

B.4 CALIBRATIONS, CALCULATIONS, CORRECTIONS, AND OTHER COMMENTS

B.4.1 Calibrations and Calculations

All gauges were calibrated with a deadweight gauge calibrator

1

i.e. $\rho = 0.0625$ inches in 15.6 seconds.

before use. The Conbel loader was calibrated with a 10,000 pound capacity proving ring, the calibration of which had been previously checked with an Instron. Although not used directly, the factory calibrations of the load cell and linear displacement transducer were checked. Both devices were found to meet the manufacturers' specifications.

The sensitivity scales of the X-Y Recorder were set so that each division of the centimeter paper used to record the test data typically represented 0.75 pounds and 0.0003 inches for the calibration factors of the load and displacement axes respectively. Readings to finer values were possible since continuous plots of the data were obtained during the tests.

The test results were calculated from the X-Y Recorder trace as follows:

$$\frac{\sigma}{\bar{\sigma}_{vc}} = \frac{(\text{No. of load divisions})(\text{X-Y Recorder load calib. factor})}{(\text{Footing area}) (\bar{\sigma}_{vc})}$$

$$\frac{\rho}{B} = \frac{(\text{No. of disp. divisions})(\text{X-Y Recorder disp. calib. factor})}{\text{Footing width.}}$$

The $\sigma/\bar{\sigma}_{vc}$ values were adjusted to conform to plane strain conditions as discussed in the following section.

B.4.2 Corrections

Checks were made to determine the frictional resistance of

the linear bushings in the footing loading assemblies. Some frictional resistance between the surcharge bag and the stainless steel collar and footing shaft was possible under certain assumed conditions. Friction tests on latex surfaces coated with silicone grease were conducted. The results of these tests were used to assess the error in the model tests which would occur for a range of conditions considered to be possible, although not necessarily probable. The range of the combined error of bearing friction and surcharge bag-collar-footing shaft friction is as follows:

<u>Pressure at time of test (kg/cm²)</u>	<u>Range of uncertainty in $\sigma/\bar{\sigma}_{vc}$</u>
0.844	-.015 to .0071
1.0	-.013 to .008
2.0	-.009 to .012
3.38	-.007 to .0148

The positive number arises from the fact that if the stainless steel collar lost contact with the footing at any time, then the surcharge pressure would act over a larger area of the footing than anticipated. The test results have not been adjusted for these ranges of error. The data are therefore uncertain to this degree.

The axial compression of the footing loading shaft was calculated to be 0.0003 inches for the largest applied footing load of this test series. This compression corresponds to a normalized displacement of less than 0.0005. Any correction to the recorded

footing displacements for a test would be variable since the load on the footing shaft built up during the experiment. In view of the magnitude of error involved no such corrections have been made.

Following Meyerhof (1951), it was assumed that the bearing stresses at the ends of the model footing approximated those under a square footing. Meyerhof further assumed that the bearing capacity of a square footing is the same as that for a circular footing. The nominal average footing contact stresses computed from the test results were corrected for this effect in order to recover the average plane strain stresses which existed in the central portion of the footing. Using an N_c value of 6.2 for a circular footing, the correction for the footing dimensions used in these tests is -2.6%. This correction has been applied to the average curve for each series of tests. In applying this correction, it has been assumed that it is applicable at all stages of the test, rather than only at the value of the ultimate bearing capacity.

B.4.3 Rate of Loading

The footing displacement rates used during the tests were determined by the fact that undrained conditions were desired. The average times to $\rho/B = 0.02$ and 0.10 were 3.1 and 15.6 seconds. An assessment of the magnitude of the consolidation settlement that could have occurred during the tests was made with the aid of theoretical solutions presented by Poulos (1964). Calculations were made assuming that the full load was applied at time zero. An impermeable footing and bottom boundary were assumed. A fully permeable top

surface was assumed even though the filter paper did not cover the entire soil surface during the tests. Coefficients of consolidation used in the calculations were as follows:

Normally Consolidated : 6 to 30×10^{-4} cm²/sec
Recompression for Overconsolidated range :
37 to 150×10^{-4} cm²/sec

The lower value for each stress history is typical of that determined from $\overline{\text{CUDSS}}$ tests. The upper value in each case represents a very conservative estimate for the largest value that is considered possible.

The vertical stress distribution employed in the calculations of consolidation settlement was taken from a FEAST III run. The Skempton - Bjerrum method was employed to compute the magnitude of the consolidation settlement.

The maximum percent consolidation in the normally consolidated case was 1.1% at 15.6 seconds ($\rho/B = 0.1$). This corresponds to a consolidation settlement of ρ/B less than 0.002. At time 3.1 seconds, the consolidation settlement in the normally consolidated case was approximately zero. Computations for the conservative c_v value in the overconsolidated case yielded consolidation settlements of $\rho/B = 0.0002$ and 0.0016 at 3.1 and 15.6 seconds respectively. It is concluded that for practical purposes the footing tests were completely undrained.

B.4.4 Miscellaneous

The laboratory in which these experiments were conducted was not equipped to maintain constant temperature. Severe temperature

fluctuations, particularly during the summer months, were avoided with the aid of air conditioning.

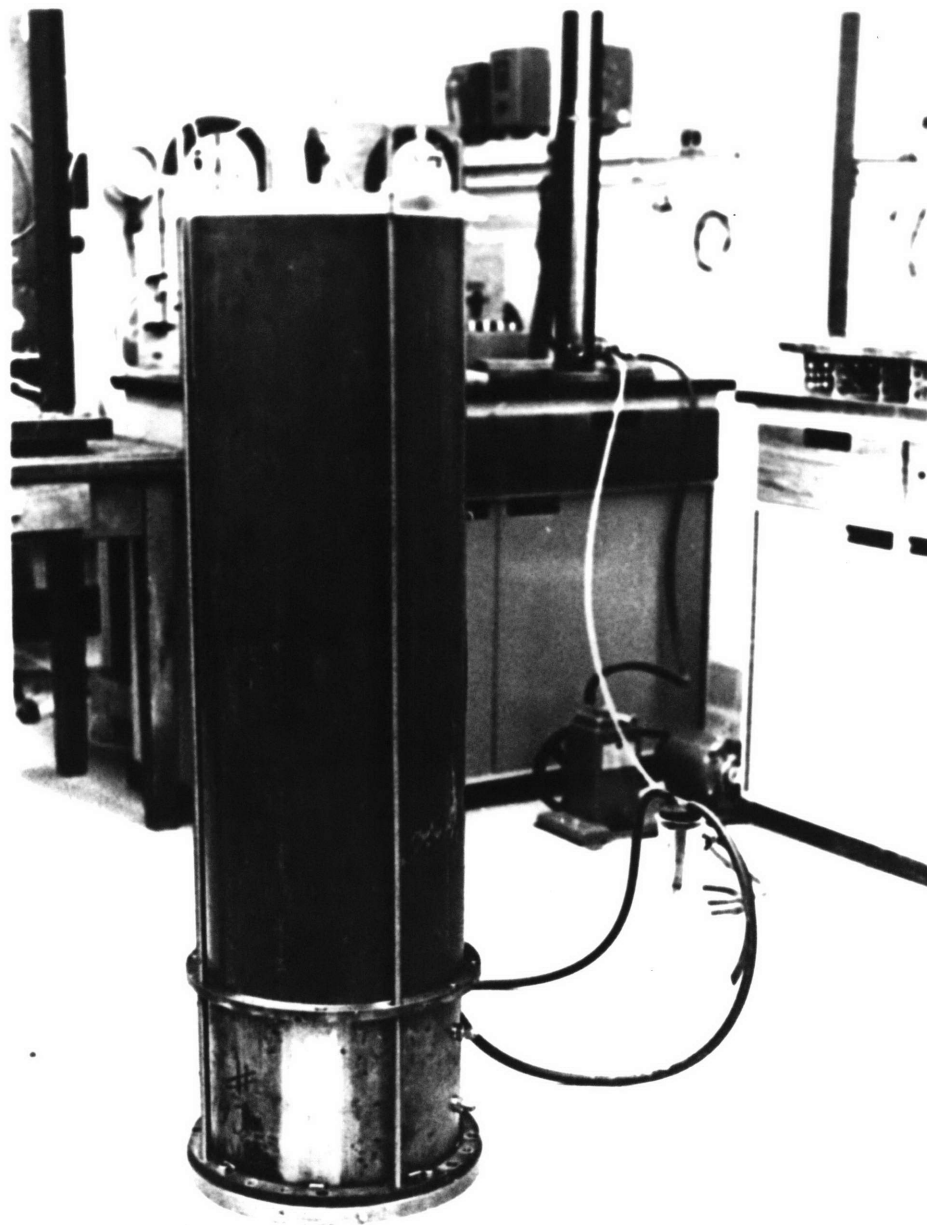
B.4.5 Model Test Similitude

Roscoe (1968) presented a summary of the criteria which must be met to achieve similitude in model tests involving soils. His discussion considers soils, both prototype and model, which exhibit unique stress-strain curves that are effective stress path dependent. The similarity of the model and prototype stress-strain curves for geometrically similar effective stress paths is assumed. Additionally, the stress histories must be identical.

If the above conditions are met then prototype behavior can be predicted by model tests if there is similitude of body stresses, boundary stresses, size, time, and strain between the model and prototype. Roscoe points out that meeting all these criteria can be a difficult task. However, under the conditions employed in the model tests for this research, similitude conditions are easily satisfied.

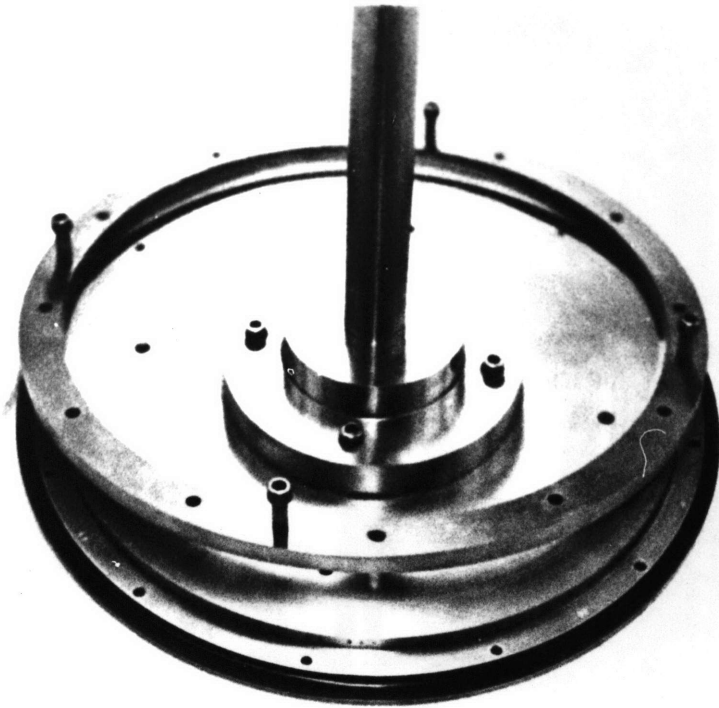
The maximum soil height used in this testing program was less than 4.5 inches. Since the minimum preshear effective stress employed for any bearing capacity test was 0.844 kg/cm^2 , it is seen that body stresses due to soil weight were insignificant. Thus, there is no need to scale either soil or pore fluid unit weights. This permits use of the prototype soil in the model. If the stress state and stress history of the prototype condition are known, these conditions can be duplicated in the model. Thus, the boundary stress scale factor is one. Strain similitude is also achieved since identical soils, stresses,

and stress histories are being used and geometrically similar points in the model and prototype experience identical loading conditions. Dynamic similitude considerations due to pore water flow are of no concern since undrained tests were performed. The size scale is left as the independent variable which can be chosen for convenience. No specific prototype was modelled in the program. However, the footing test results can be applied directly to appropriate field cases on Boston Blue Clay where body forces are relatively small.



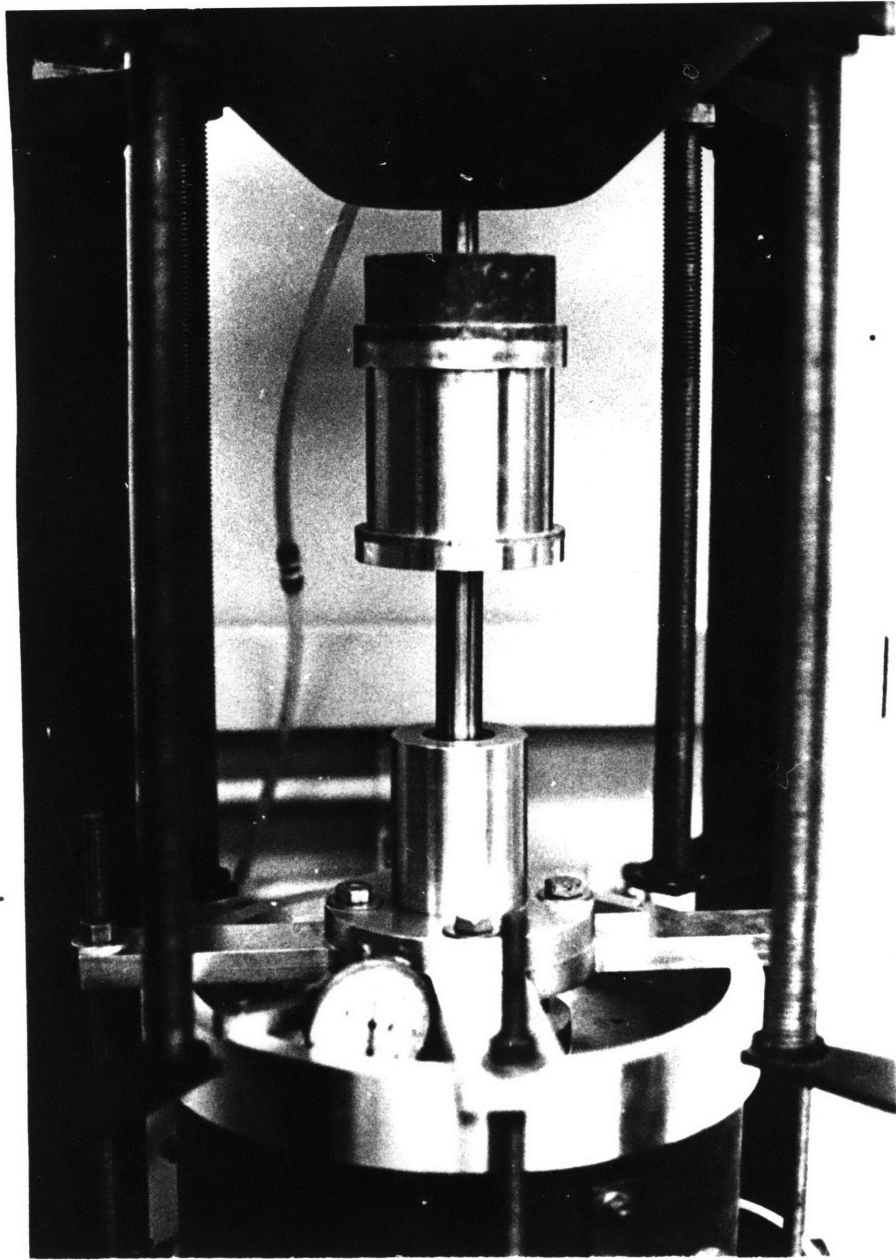
Vacuum Apparatus: Bin Two

Figure B-1



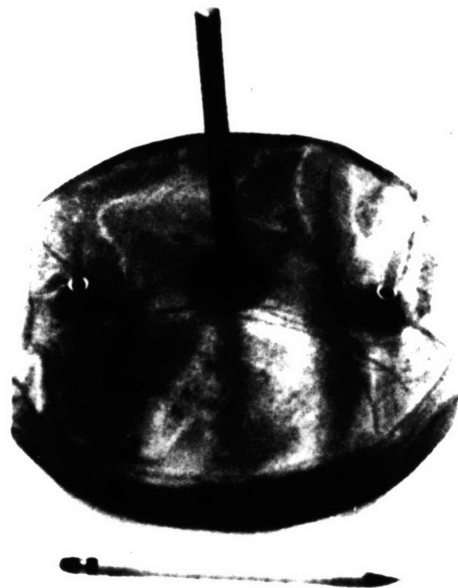
Consolidation Plate With Removable
O-Ring Feature

Figure B-2



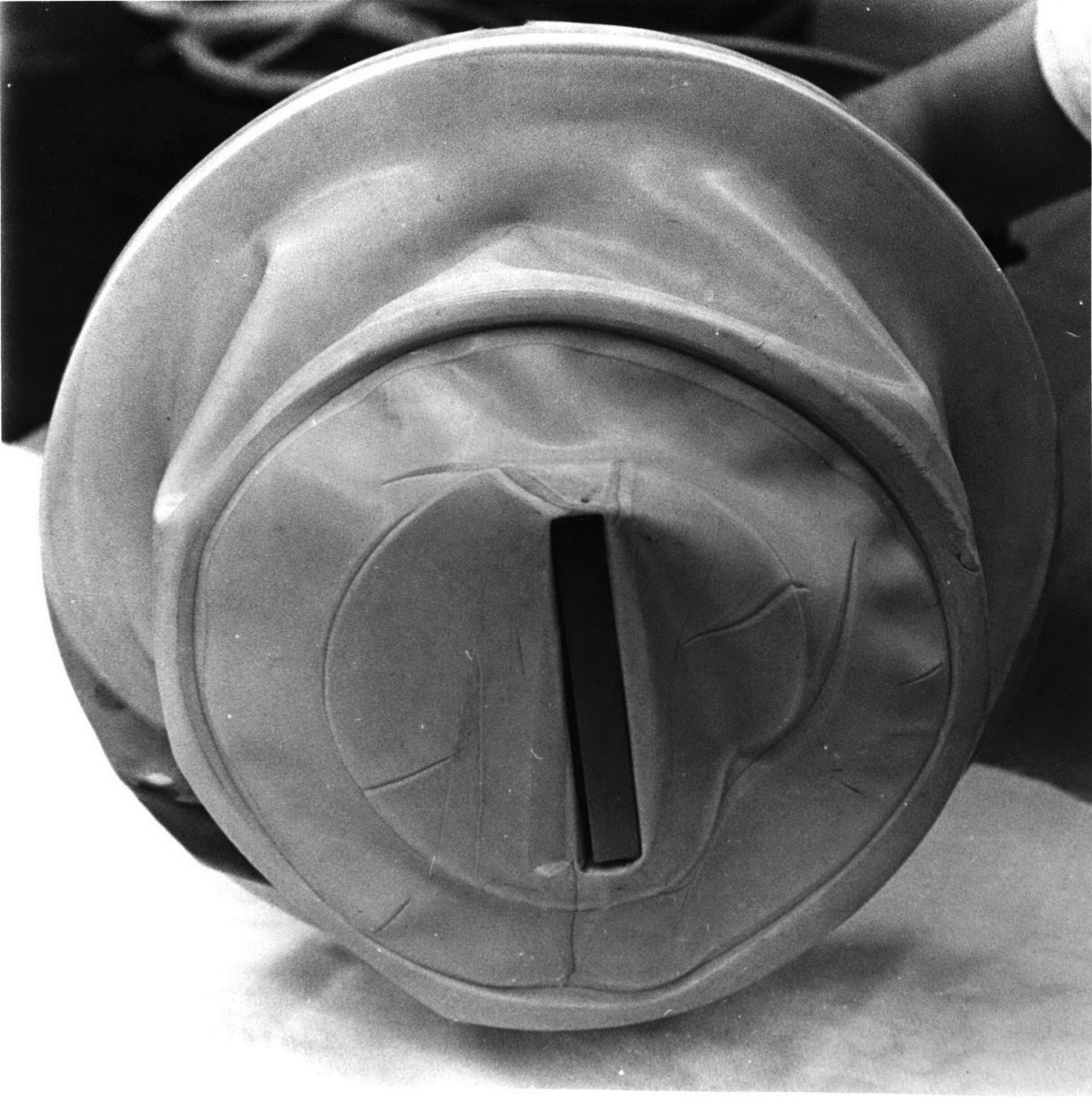
Linear Bushing Assembly For
Guiding Consolidation Plate

Figure B-3

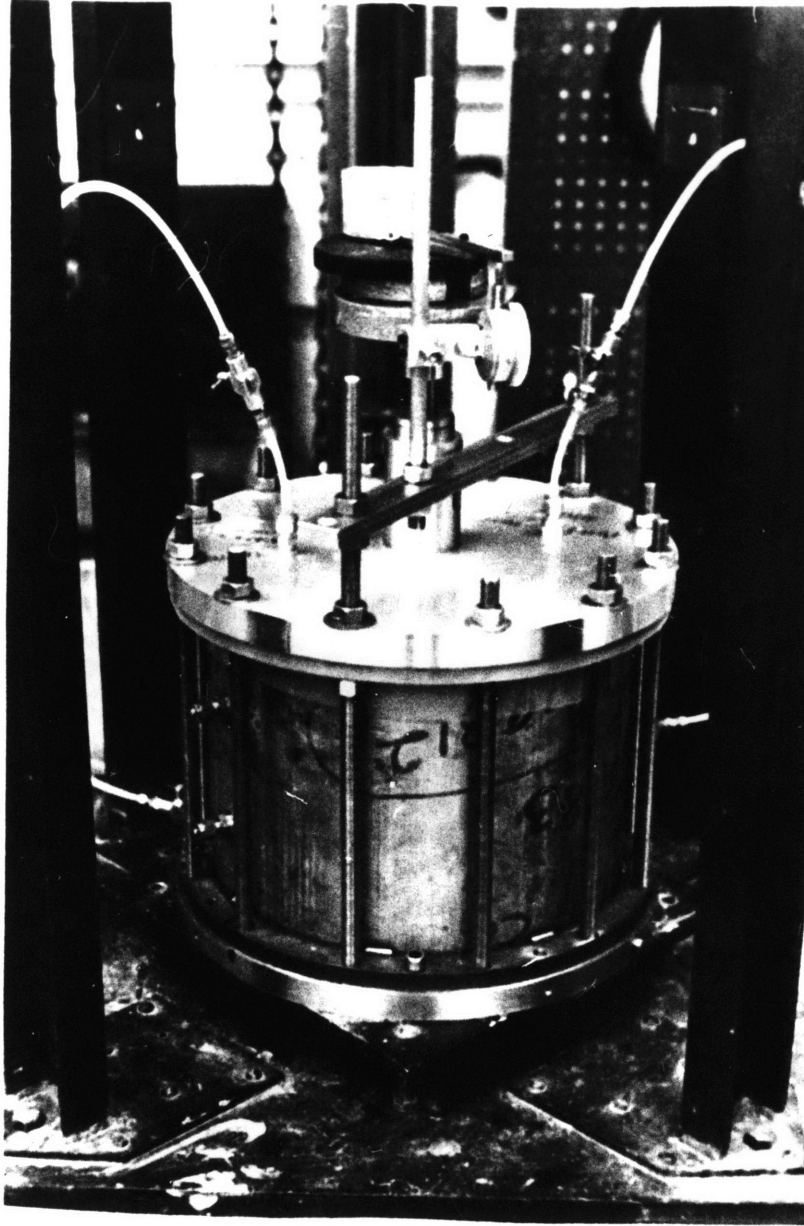


Surcharge Bag: Bin One

Figure B-4

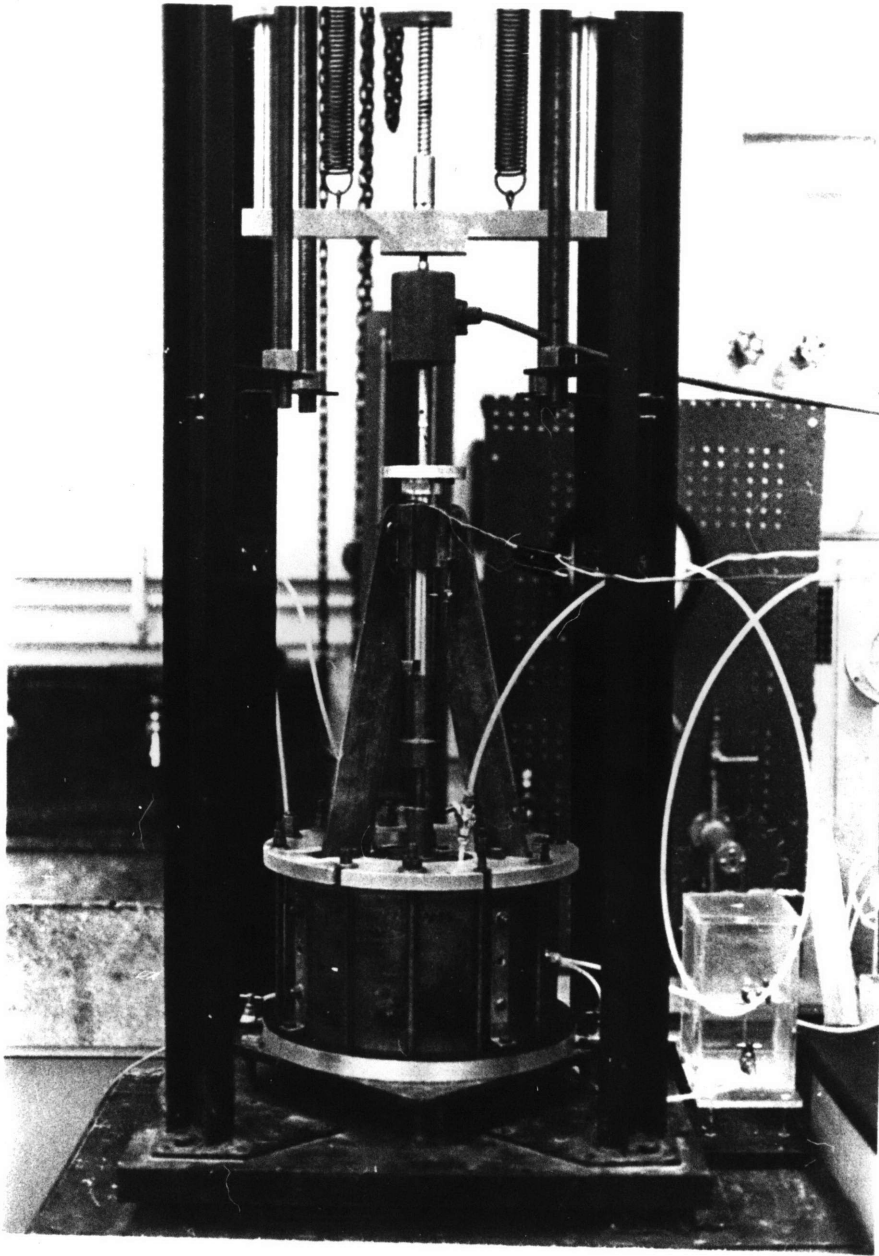


Surcharge Membrane: Bin Two



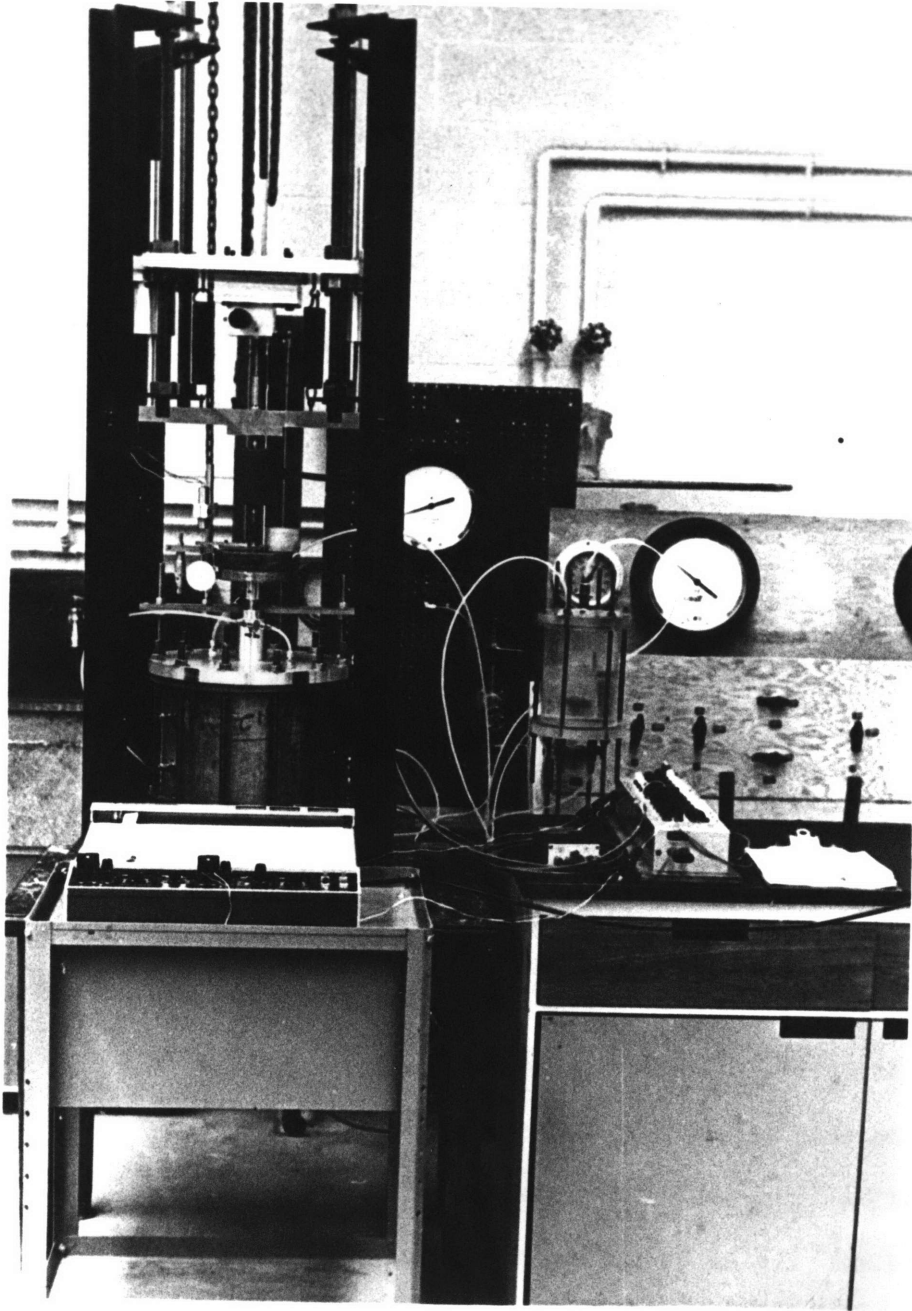
Final Consolidation: Bin Two

Figure B-6



Apparatus Arrangement At Time Of
Test: Bin One

Figure B-7



Apparatus Arrangement At Time Of
Test: Bin Two

Figure B-8

APPENDIX C
TABULATED TEST RESULTS AND OTHER INFORMATION ON
MODEL FOOTING TESTS

This appendix contains tabulated results of the model footing tests and other miscellaneous data.

The normally consolidated tests are numbered 100 through 108. The two tests with an overconsolidation ratio of two are numbered 200 and 201. Numbers 400 through 402 were assigned to the tests with an overconsolidation ratio of four. The basic data for each test have been tabulated in terms of ρ/B and $\sigma/\bar{\sigma}_{vc}$. These tabulations may be found immediately after the text of this appendix. Test 402 was conducted with Bin Two. The other tests were performed with Bin One.

The consolidation history of each test is summarized in Table C-1. A composite plot of $e - \log \bar{\sigma}_{vc}$ data from the test series is shown in Figure C-1. The average C_c value for the tests is 0.366. This compares favorably with the range of values reported for other samples of Boston Blue Clay obtained at the M.I.T. campus, Ladd and Luscher (1965). The results for test 107 show that Boston Blue Clay having an equivalent pore fluid salt concentration of 16 g/l NaCl and an initial water content of 100 percent, exhibits a straight line $e - \log \bar{\sigma}_{vc}$ curve for the stress range of 0.25 to 3.38 kg/cm².¹

Values of the rate of secondary compression, C_α , for the

¹

The C_c value for test 107 is slightly higher than the average value.

last normally consolidated increment of each test are shown in Figure C-2. Since each batch was initially a dilute slurry, the usual definition of C_α as given by Ladd and Preston (1965) could not be employed. Accordingly, C_α in this report is defined, as the ratio of the change in sample height per log cycle of time during secondary compression, to the sample height at the end of primary consolidation for the last normally consolidated increment. Since the maximum difference between sample heights at $\bar{\sigma}_{vm}$ was only 15%, the C_α values computed in this manner can be compared to determine whether the rate of secondary compression in these tests varied with the magnitude of $\bar{\sigma}_{vm}$. No dramatic dependence of C_α on $\bar{\sigma}_{vm}$ is seen in the figure.

The times of secondary compression at $\bar{\sigma}_{vm}$ were approximately constant for most tests. The values are summarized in Table C-2 along with the values of T_s/T_p .¹ The combined effect of the time for secondary compression and the value of C_α for each test are shown in Figure C-3 where the change in void ratio during secondary compression, Δe_s , is plotted versus $\bar{\sigma}_{vm}$. The value of Δe_s was approximately constant for all tests.

Water contents were taken throughout each batch of clay after the model test was conducted. Much of the apparatus had to be disassembled before the water contents could be taken. This normally took 15 to 30 minutes, during which time a change in the water content distribution in the immediate vicinity of the footing was possible. Comparisons of the water contents among the batches were made using two values. The first, called the final average water content,

¹ The values of T_s/T_p are comparable to the range of values which exists for the plane strain tests.

consisted of the average of 10 to 12 determinations made throughout the depth of the soil and out radially to within about one inch of the bin wall. The second value was determined from the average of the water contents made at depths from $\frac{1}{2}$ to two inches and for distances up to two inches from the centerline of the footing. This quantity, called the water content near the footing, was probably not affected very much by the aforementioned post test water content redistribution. The two water content values for each test are listed in Table C-3.

The values indicate that the experimental procedures employed in this program lead to remarkably reproducible results for each $\bar{\sigma}_{vm}$ and stress history. The slightly high water contents of the 200 series tests, relative to the 400 series tests is not considered serious. The final average water content is seen to be greater than that near the footing. This is explained by the fact that the final average included samples from locations near the bin walls which may have been influenced by side friction. Secondly, samples in this average taken from depths near the porous stone may have swelled during disassembly of the equipment.

TABULATED RESULTS
MODEL FOOTING TEST

100

$\bar{\sigma}_{vc} = 2 \text{ kg/cm}^2$

OCR = 1

$T_s = 56.4 \text{ hrs}$

$\sigma/\bar{\sigma}_{vc}$	ρ/θ
.274	.0001
.34	.0003
.423	.0006
.505	.0008
.589	.0014
.672	.0017
.755	.0020
.838	.0034
.92	.0042
1.002	.0056
1.087	.0073
1.17	.0092
1.252	.0148
1.297	.0184
1.336	.0307
1.354	.0407
1.36	.0686
1.37	.0965

TABULATED RESULTS
MODEL FOOTING TEST

101

$$\bar{V}_{vc} = 2 \text{ kg/cm}^2$$

$$\text{OCR} = 1$$

$$T_s = 50.9 \text{ hrs}$$

V/\bar{V}_{vc}	P/B
.1848	.0005
.222	.0014
.292	.0016
.37	.0018
.444	.0027
.5175	.0034
.591	.0037
.665	.0046
.74	.0051
.812	.0062
.886	.0068
.96	.0083
1.035	.0097
1.108	.0116
1.182	.0149
1.22	.0175
1.257	.0208
1.29	.0243
1.33	.0319
1.348	.0383
1.36	.0462
1.376	.0621
1.39	.0780
1.408	.1017

TABULATED RESULTS
MODEL FOOTING TEST

102

$\bar{\sigma}_{vc} = 2 \text{ kg/cm}^2$

OCR = 1

$T_s = 53.9 \text{ hrs}$

$\sigma/\bar{\sigma}_{vc}$	P/B
.0754	.0001
.151	.0003
.226	.0007
.28	.0011
.302	.0012
.377	.0014
.452	.0021
.529	.0023
.603	.0027
.68	.0034
.755	.0041
.83	.0052
.905	.0064
.976	.0075
1.054	.0096
1.13	.0122
1.205	.0156
1.243	.0178
1.28	.0215
1.32	.0274

$\sigma/\bar{\sigma}_{vc}$	P/B
1.328	.0342
1.34	.0411
1.35	.0479
1.36	.0547
1.368	.0616
1.372	.0684
1.381	.0753
1.392	.0821
1.394	.0889
1.395	.0999

TABULATED RESULTS
MODEL FOOTING TEST

103

$\bar{\sigma}_{vc} = 2 \text{ kg/cm}^2$

OCR = 1

$T_s = 56.6 \text{ hrs}$

$\sigma/\bar{\sigma}_{vc}$	ρ/B
.375	.0003
.438	.0005
.52	.0011
.564	.0016
.625	.0019
.688	.0021
.75	.0026
.813	.0032
.875	.0042
.939	.0051
1.0	.0058
1.062	.007
1.128	.0089
1.19	.0108
1.22	.011
1.251	.0141
1.28	.0165
1.311	.0184
1.345	.0218
1.365	.0287

$\sigma/\bar{\sigma}_{vc}$	ρ/B
1.37	.034
1.38	.0424
1.38	.0478
1.386	.0531
1.397	.0584
1.40	.0743
1.414	.0849
1.42	.0955
1.42	.0997

TABULATED RESULTS
MODEL FOOTING TEST

104

$$\bar{\sigma}_{vc} = 2 \text{ kg/cm}^2$$

$$\text{OCR} = 1$$

$$T_s = 55 \text{ hrs}$$

$\tau / \bar{\sigma}_{vc}$	ρ / σ
.1408	.0012
.2115	.0019
.2805	.0028
.282	.0028
.352	.0033
.423	.0039
.4925	.0046
.563	.0050
.644	.0056
.713	.0062
.775	.0070
.845	.0076
.915	.0084
.985	.0096
1.058	.0108
1.128	.0127
1.198	.0152
1.231	.0170
1.269	.0194
1.3	.0231

$\tau / \bar{\sigma}_{vc}$	ρ / σ
1.324	.0263
1.351	.0341
1.361	.0418
1.361	.0495
1.361	.0573
1.371	.0650
1.38	.0728
1.39	.0805
1.39	.0882
1.4	.0997

TABULATED RESULTS
MODEL FOOTING TEST

105

$\bar{\sigma}_{vc} = 1 \text{ kg/cm}^2$

OCR = 1

$T_s = 57 \text{ hrs}$

$\sigma/\bar{\sigma}_{vc}$	P/B
.181	.0001
.289	.0008
.322	.001
.465	.0014
.606	.0025
.75	.0035
.82	.0042
.89	.0045
.963	.0053
1.035	.0061
1.105	.0072
1.178	.0085
1.248	.010
1.32	.0115
1.372	.0144
1.44	.0216
1.46	.0288
1.468	.0332
1.46	.0361
1.44	.0432

$\sigma/\bar{\sigma}_{vc}$	P/B
1.43	.0505
1.43	.0577
1.445	.0649
1.442	.0721
1.442	.0793
1.445	.0865
1.445	.099
1.445	.1081

TABULATED RESULTS
MODEL FOOTING TEST

106

$$\bar{q}_{vc} = 1 \text{ kg/cm}^2$$

$$\text{OCR} = 1$$

$$T_s = 63.6 \text{ hrs}$$

q/\bar{q}_{vc}	P/B
.109	.0001
.179	.0005
.250	.0008
.294	.001
.32	.0011
.391	.0012
.46	.0017
.531	.0021
.6	.0024
.673	.0029
.742	.0033
.812	.0036
.883	.0044
.953	.0049
1.023	.0056
1.092	.0064
1.164	.0075
1.233	.0086
1.302	.0103
1.374	.0127

q/\bar{q}_{vc}	P/B
1.43	.0161
1.45	.0198
1.44	.0268
1.44	.0321
1.44	.0428
1.44	.0535
1.445	.0642
1.452	.0749
1.455	.0856
1.468	.0963

TABULATED RESULTS
MODEL FOOTING TEST

107

$\bar{\sigma}_{vc} = 3.38 \text{ kg/cm}^2$

OCR = 1

$T_s = 50.8 \text{ hrs}$

$\tau / \bar{\sigma}_{vc}$	ρ / θ
1.234	.0195
1.269	.0243
1.293	.0301
1.3	.0365
1.316	.0422
1.328	.0495
1.348	.0585
1.349	.0649
1.351	.0732
1.36	.0829
1.369	.0932
1.372	.1

Data Listed for $\rho / \theta > .019$

TABULATED RESULTS
MODEL FOOTING TEST

108

$\bar{v}_{vc} = 3.38 \text{ kg/cm}^2$

OCR = 1

$T_s = 65.3 \text{ hrs}$

v/\bar{v}_{vc}	ρ/θ
.138	.0003
.2065	.0005
.276	.0009
.344	.0013
.413	.0020
.481	.0023
.551	.0029
.619	.0031
.69	.0043
.758	.0051
.827	.0061
.895	.0072
.965	.0088
1.062	.0119
1.15	.0163
1.202	.0207
1.239	.025
1.269	.0294
1.285	.0338
1.296	.0382

v/\bar{v}_{vc}	ρ/θ
1.308	.0426
1.315	.047
1.319	.051
1.328	.0558
1.33	.0602
1.34	.0690
1.357	.0777
1.36	.0865
1.37	.0909
1.378	.10

TABULATED RESULTS
MODEL FOOTING TEST

200

$\bar{v}_{vc} = 1.69 \text{ kg/cm}^2$

OCR = 2

$T_s = 50.0 \text{ hrs}$

v/\bar{v}_{vc}	p/θ
.270	0
.403	.0004
.539	.0009
.672	.0013
.809	.0018
.943	.0024
1.077	.003
1.21	.0036
1.346	.0044
1.48	.0053
1.617	.0063
1.75	.0075
1.885	.0089
2.02	.0108
2.155	.0135
2.28	.0169
2.37	.0211
2.42	.0254
2.445	.0296
2.46	.0338

v/\bar{v}_{vc}	p/θ
2.46	.038
2.461	.0423
2.465	.0465
2.47	.0503
2.48	.0550
2.485	.0634
2.49	.0719
2.505	.0803
2.52	.0888
2.53	.0951
2.535	.0998
2.538	.106

TABULATED RESULTS
MODEL FOOTING TEST

201

$\bar{\sigma}_{vc} = 1.69 \text{ kg/cm}^2$

OCR = 2

$T_s = 63.8 \text{ hrs}$

$\sigma / \bar{\sigma}_{vc}$	ρ / θ
.26	.0004
.39	.0009
.52	.0014
.65	.002
.78	.0025
.91	.003
1.039	.0036
1.17	.0042
1.3	.0049
1.43	.0058
1.56	.0067
1.69	.0079
1.82	.0091
1.95	.0108
2.08	.0128
2.2	.0157
2.26	.0172
2.32	.0197
2.345	.0221
2.38	.0246

$\sigma / \bar{\sigma}_{vc}$	ρ / θ
2.40	.0295
2.39	.0344
2.39	.0393
2.39	.0442
2.4	.0541
2.41	.0639
2.42	.0737
2.43	.0835
2.45	.0934
2.455	.1

TABULATED RESULTS
MODEL FOOTING TEST

400

$\bar{\sigma}_{vc} = .854 \text{ kg/cm}^2$

OCR = 3.96

$T_s = 60.5 \text{ hrs}$

$\sigma/\bar{\sigma}_{vc}$	P/B
.196	.0002
.332	.0005
.604	.0013
.875	.0021
1.146	.0028
1.42	.0035
1.69	.0043
1.96	.0054
2.235	.0066
2.5	.0081
2.775	.0099
3.045	.0123
3.32	.0152
3.59	.019
3.82	.0236
3.92	.0262
4.05	.0315
4.11	.0367
4.15	.0419
4.15	.0472

$\sigma/\bar{\sigma}_{vc}$	P/B
4.16	.0524
4.165	.0577
4.17	.0629
4.19	.0682
4.195	.0734
4.22	.0813
4.25	.089
4.25	.0944
4.27	.0996

TABULATED RESULTS
MODEL FOOTING TEST

401

$\bar{\sigma}_{vc} = .844 \text{ kg/cm}^2$

OCR = 4

$T_s = 61.5 \text{ hrs}$

$\sigma/\bar{\sigma}_{vc}$	ρ/θ
.26	0
.457	.0006
.655	.001
.854	.0019
1.05	.0025
1.249	.0033
1.445	.0039
1.645	.0045
1.84	.0052
2.04	.0060
2.24	.0068
2.44	.0079
2.64	.009
2.83	.0104
3.02	.0121
3.22	.014
3.42	.016
3.62	.0184
3.82	.0217
4.01	.026

$\sigma/\bar{\sigma}_{vc}$	ρ/θ
4.15	.0302
4.22	.0329
4.3	.0384
4.34	.044
4.35	.0494
4.35	.0549
4.35	.0604
4.355	.0659
4.36	.0714
4.37	.0768
4.39	.0823
4.4	.0878
4.415	.0933
4.425	.099
4.44	.107

TABULATED RESULTS
MODEL FOOTING TEST

402

$\bar{\sigma}_{ve} = .845 \text{ kg/cm}^2$

OCR = 4

$T_s = 107.2 \text{ hrs}$

$\sigma/\bar{\sigma}_{ve}$	ρ/B
.2751	.0001
.5502	.0003
.8253	.0008
1.1	.0014
1.373	.0021
1.65	.0031
1.925	.0045
2.2	.0061
2.475	.0079
2.751	.010
3.02	.013
3.3	.016
3.58	.02
3.84	.026
4.02	.032
4.145	.04
4.15	.046
4.147	.052
4.15	.064
4.155	.075
4.2	.1

TABLE C-1 (1)

SAMPLE PREPARATION HISTORY

Test No.	Consol. stress (kg/cm ²)	Sample HT. end of increment (in)	Time for primary (hr)	Total time for increment (hr)	Initial slurry w/c %	Final Avg. w/c %	Remarks (Hts, in)
100	Vacuum			83			
	.062			5.3			
	.25	5.349	~ 10.3	10.3	96.0	33.74	(2.282)
	.50	4.996	< 10.8	10.8			
	1.5	4.576	16.7	28.6			
2.0	4.422	21.4	77.8				
101	Vacuum			42			
	.062			9			
	.19			14.5	97.4	33.63	(2.129)
	.50	4.292	21.7	41.6			
	1.25	4.119	23.5	74.4			
2.0							
102	Vacuum			40			
	.062			6			
	.25	-		16.6	98.9	33.1	(2.176)
	.50	-		7.9			
	1.25	4.352	28.4	45.8			
2.0	4.181	19.2	72.7				
103	Vacuum			43.5			(2.109)
	.062			3.4			
	.25	4.929	7 66.7	66.7	93.9	34.10	Sample HT. ~ 90%
	.50	4.616	7 28.4	28.4			Sample HT. for 90%
	1.25	4.291	16.7	43.4			
2.0	4.099	20	76.6				

TABLE C-1 (2)

Test No.	Consol. stress (kg/cm ²)	Sample HT. end of increment (in)	Time for primary (hr)	Total time for increment (hr)	Initial slurry w/c %	Final avg. w/c %	Remarks (H _s , in)
104	Vacuum			37			(2.059)
	.062			6			
	.25	4.941	> 89.5	89.5	96.6	34.18	Sample HT > T ₉₀ , < T ₁₀₀
	.50	4.513	27.6	45.8			
	1.25	4.198	13.3	28			
2.0	4.029	21	76				
105	Vacuum			40			(1.919)
	.062			2			
	.149	4.765	> 52.5	52.5	94.4	38.26	Sample HT for 90%
	.5	4.176	33.6	41.9			
	1.0	3.954	21.7	78.7			
106	Vacuum			36.5			(2.053)
	.07			3			
	.25	4.687	> 70.6	70.6	98.6	37.0	
	.50	4.398	< 44.8	44.8			
	1.0	4.161	28.4	92			
107	Vacuum			38			(2.143)
	.07			3.5			
	.25	4.898	~ 63.4	72.3	102.25	31.1	
	.50	4.663	~ 23.4	25.1			
	1.0	4.406	15.3	21.1			
	1.5	4.268	18.3	21.9			
	2.5	4.097	11	20.8			
3.38	4.003	18.3	69.1				

TABLE C-1 (3)

Test No.	Consol. stress (kg/cm ²)	Sample HT. end of increment (in)	Time for primary (hr)	Total time for increment (hr)	Initial slurry w/c %	Final avg. w/c %	Remarks (Hs, in)
108	Vacuum			40			
	.07	4.895	> 72.1	4.9			(2.12)
	.25	4.637	> 31.3	72.1			
	.50	4.406	18.4	40.2	98.8	32.13	31.3 FOR 90%
	1.0	4.267	< 24.2	24.8			
	1.5	4.120	11.7	24.2			
	2.5	4.014	27.4	25.6			
3.38			92.7				

TABLE C-1 (4)

Test No.	Consol. stress (kg/cm ²)	Sample HT. end of increment (in)	Time for primary (hr)	Total time for increment (hr)	Initial slurry w/c %	Final avg. w/c %	Remarks (Hs, in)
200	Vacuum						(2.08) Sample HT. for ~ 90%
	.07			~ 48			
	.25	4.872	>70.5	3.25			
	.50	4.568	26.6	70.5			
	1.0	4.338	<25.1	47.6	99.7	32.47	
	1.5	4.191	20.0	25.1			
	2.5	4.039	8.34	24.6			
	3.38	3.937	11.7	16.6			
	2.5	3.942	~ 1	61.5			
	1.69	3.955	~ 2	11.2			
201	Vacuum						(2.00)
	.07			29.5			
	.25	4.699	>72	72			
	.50	4.397	26.7	70.7			
	1.0	4.172	18.4	24.0	98.8	32.5	
	1.5	4.041	16.7	20.4			
	2.5	3.858	~ 10	94.4			
	3.38	3.78	31	94.6			
	1.69	3.80	~ 2	29.6			

TABLE C-1 (5)

Test No.	Consol. stress (kg/cm ²)	Sample HT. end of increment (in)	Time for primary (hr)	Total time for increment (hr)	Initial slurry w/c %	Final avg. w/c %	Remarks (H _s , in)
400	Vacuum			18			(1.997)
	.07	4.637	> 86.2	6.5			Sample HT. 785
	.25	4.330	> 27.4	96.2			Sample HT. 790
	.50	4.084	18.3	27.4	96.4	32.05	
	1.0	3.957	16.7	22.1			
	1.5	3.823	~ 9.3	24.7			
	2.5	3.730	12.2	17.2			
	3.38	3.741	~ 1	72.7			
	2.0	3.772	5.4	3.7			
	.854			22.2			
401	Vacuum			17.3			(2.033)
	.07	4.781	> 67	3.7			Sample HT. for 85%
	.25	4.435	> 24.2	67			Sample HT. > 90%, < 100%
	.50	4.243	~ 23	24.2	97.31	32.09	
	.75	4.041	14.5	23			
	1.5	3.886	8.3	26.2			
	2.5	3.795	10	21.4			
	3.38	3.806	> 1	71.5			
	2.0	3.839	3.3	2			
	.844			22.9			
402	0-2.5	3.837	13.3	40			Records incomplete (2.004)
	2.5	3.762	20.8	128	99.3	32.3	Rebounded at constant V _v by increase back pressure
	3.38	3.768	2.3	233			
	2.38	3.776	2.9	4			
	1.69	3.804	4.8	23.8			See small
.845							

Table C-2

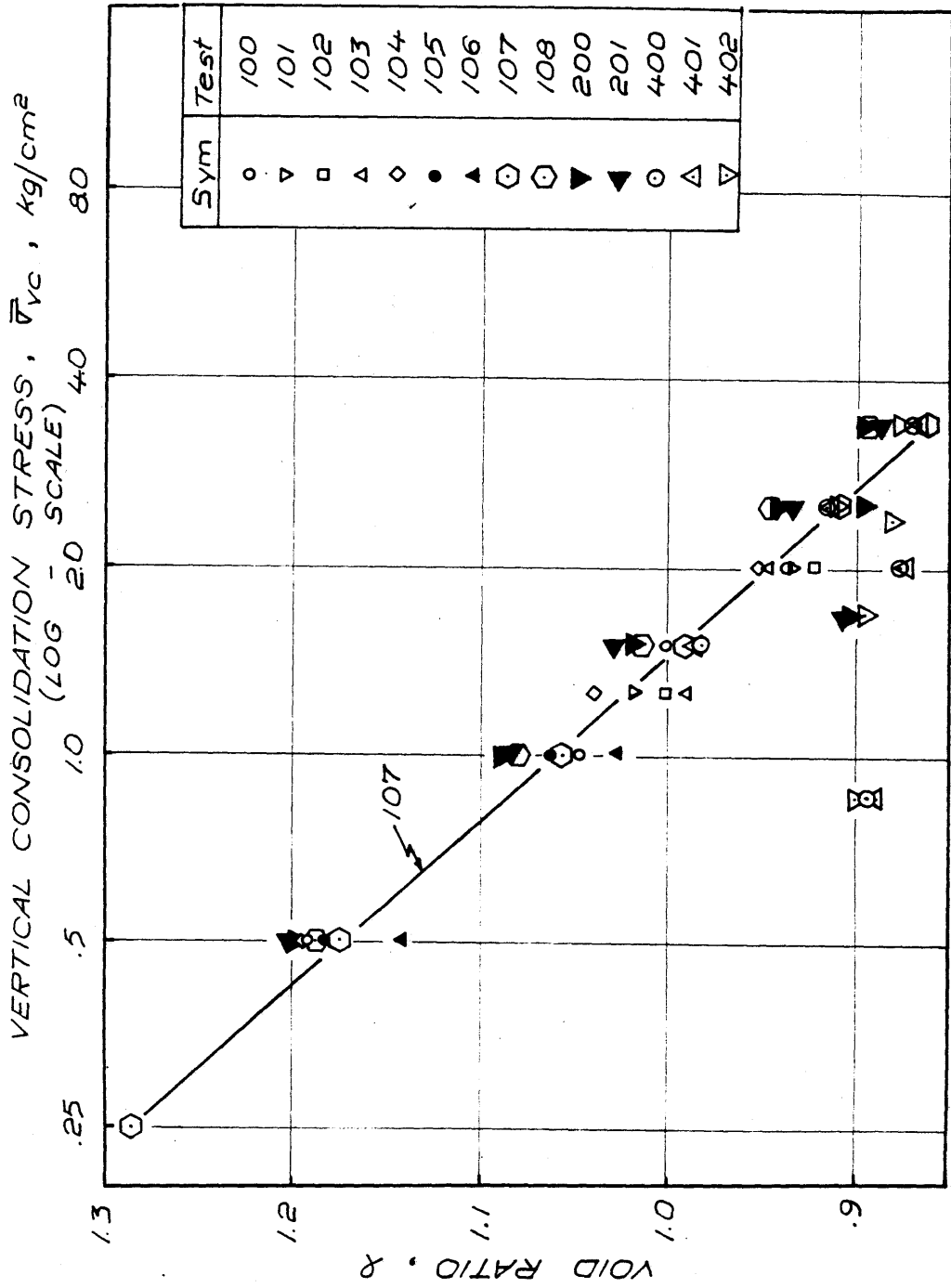
ELAPSED TIME FOR SECONDARY COMPRESSION FOR
THE LAST NORMALLY CONSOLIDATED INCREMENT

Test	Elapsed Time for Secondary Compression	$\frac{\text{Time for Secondary}}{\text{Time for Primary}}, \frac{T_s}{T_p}$
100	56.4	2.64
101	50.9	2.16
102	53.9	2.80
103	56.6	2.83
104	55	2.62
105	57	2.63
106	63.6	2.24
107	50.8	2.78
108	65.3	2.38
200	50.0	4.28
201	63.8	2.06
400	60.5	4.95
401	61.5	6.15
402	107.2	5.15

Table C-3

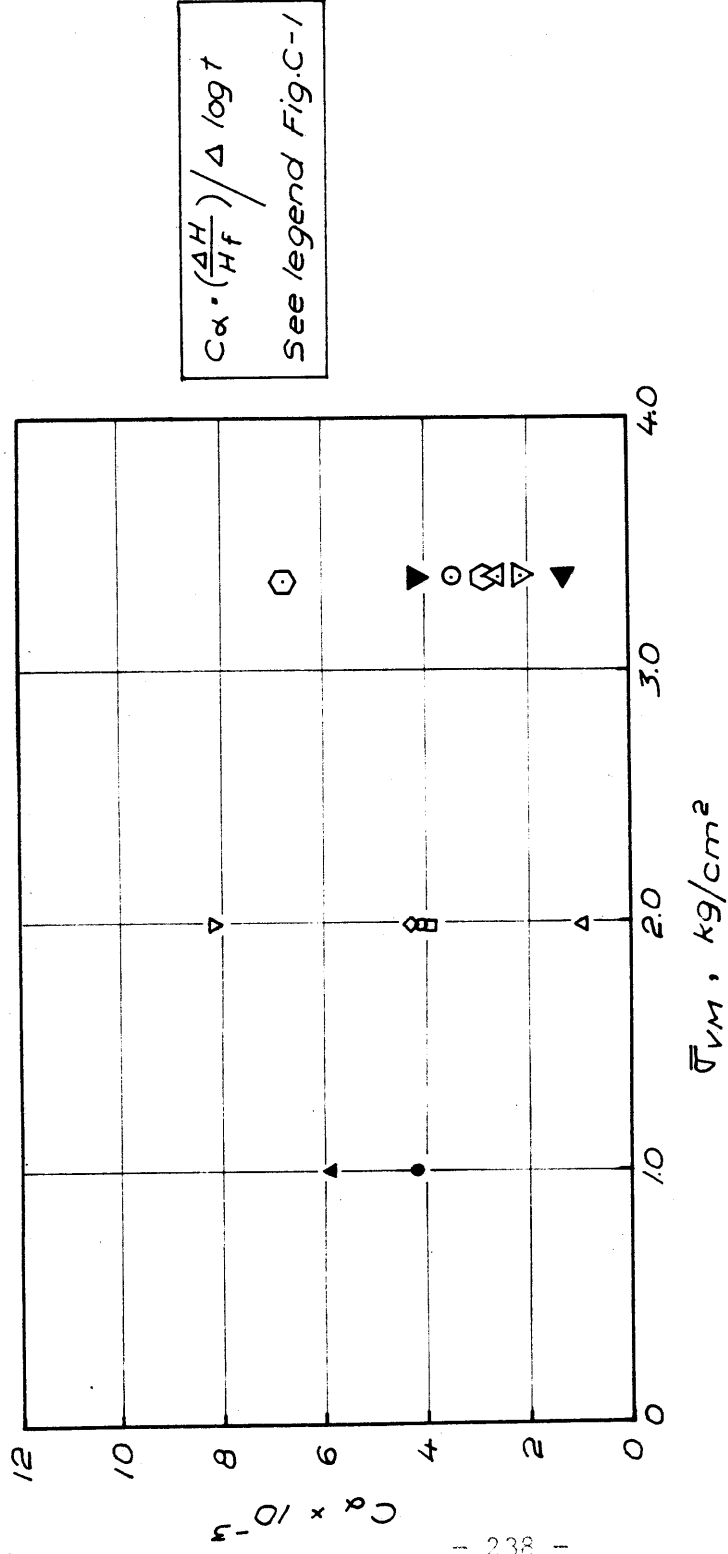
MODEL TEST WATER CONTENTS

Test	Final Average Water Content %	Water Content Near Footing %	$\bar{\sigma}_{vm}$ (kg/cm ²)	$\bar{\sigma}_{vc}$ (kg/cm ²)
100	33.74	33.22	2.0	2.0
101	33.63	32.76	2.0	2.0
102	33.14	31.88	2.0	2.0
103	34.10	33.35	2.0	2.0
104	34.18	33.41	2.0	2.0
105	38.26	37.52	1.0	1.0
106	37.83	37.0	1.0	1.0
107	31.02	31.0	3.38	3.38
108	32.13	31.5	3.38	3.38
200	32.47	32.0	3.38	1.69
201	32.5	32.0	3.38	1.69
400	32.05	31.7	3.38	.854
401	32.09	31.6	3.38	.844
402	32.31	31.97	3.38	.845



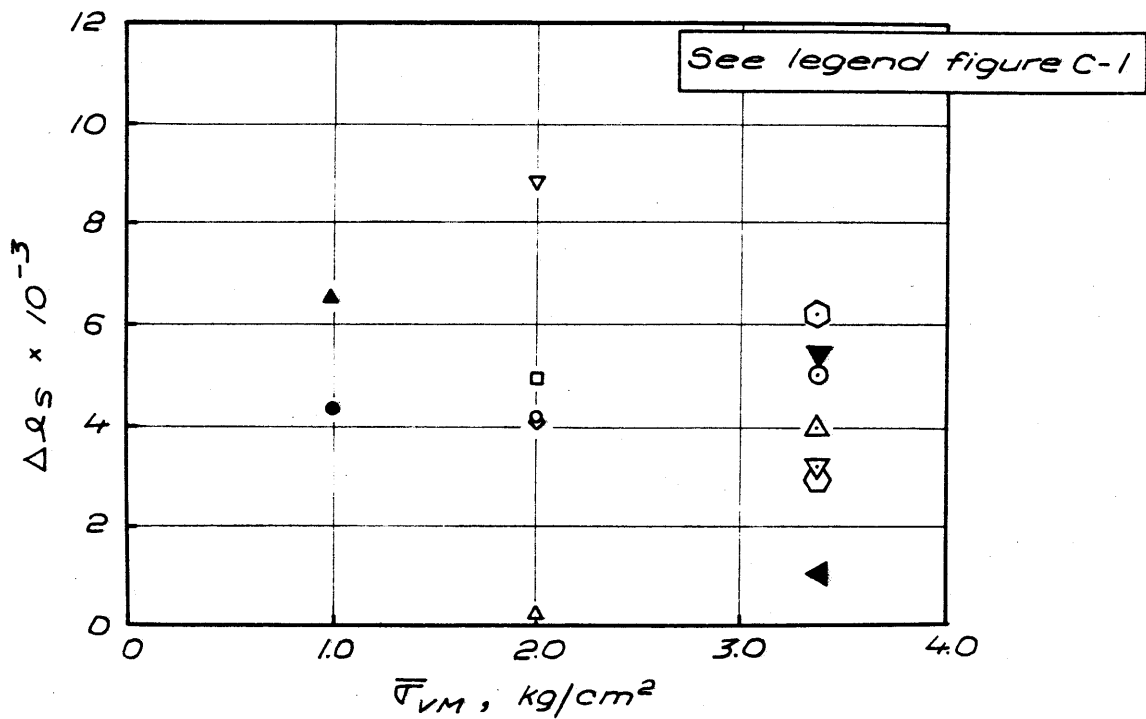
VOID RATIO VERSUS VERTICAL CONSOLIDATION STRESS FOR
MODEL LOADING TESTS

FIGURE C-1



C α VALUES FOR THE LAST NORMALLY CONSOLIDATED INCREMENT OF EACH TEST

FIGURE C-2



CHANGE IN VOID RATIO DURING SECONDARY COMPRESSION OF THE LAST NORMALLY CONSOLIDATED INCREMENT VERSUS VERTICAL CONSOLIDATION STRESS

FIGURE C - 3

APPENDIX D

MISCELLANEOUS INFORMATION ON PLANE STRAIN TESTS AND MEASUREMENTS OF K_0

This appendix contains miscellaneous information on the stress-strain-strength characteristics of Boston Blue Clay determined in plane strain for overconsolidation ratios of one, two, and four. Summaries of K_0 measurements from several sources are also given here.

Tabulated summaries of the tests are given in Table D-1. Stress-strain curves for several of the tests are shown in Figures D-1 through D-6. Except for test A-8, only those tests have been plotted that experienced at least 16 hours of consolidation after removing the side platens for the last normally consolidated consolidation increment. For the passive tests, the ordinate $\frac{\sigma_h - \sigma_v}{\bar{\sigma}_{vc}}$ refers to the difference between the horizontal and vertical insitu stresses. Therefore, no distinction need be drawn, in the figures, between horizontal and vertical K_0 tests. Curves of the normalized secant modulus, $E_s / \bar{\sigma}_{vc}$ versus applied shear stress ratio, $\Delta q / \Delta q_f$ for several tests are shown in Figures D-7 and D-8.

Table D-2 presents summary data of K_0 determinations from several sources.

TABLE D-1 (1)

SUMMARY OF PLANE STRAIN ACTIVE TESTS ON BOSTON BLUE CLAY

Test	OCR	$\bar{\sigma}_{vc}$	Wf %	Wi %	TS	B %	K ₀	At ($\sigma_1 - \sigma_3$) max				At ($\bar{\sigma}_1 / \bar{\sigma}_3$) max				Remarks Equipment Used & Batch No.		
								ϵ_v %	$\frac{q}{\bar{\sigma}_{vc}}$	$\frac{q}{p}$	A	$\bar{\sigma}_1 / \bar{\sigma}_3$	ϵ_v %	$\frac{q}{\bar{\sigma}_{vc}}$	$\frac{q}{p}$		A	$\bar{\sigma}_1 / \bar{\sigma}_3$
A-2	1.0	3.62	30.1	33.6	0.5	85	.49	1.5	.338	1.216	1.24	3.34	1.95	.333	1.198	1.46	3.50	P 150
A-3	1.0	3.92	29.2	34.6	1.3	55	.50	1.7	.356	1.36	1.012	3.45	3.45	.355	1.356	1.165	3.83	P 160
A-4	1.0	3.88	28.1	35.9	15.7	72	.47	0.42	.350	1.354	0.601	2.90	3.42	.318	1.234	1.91	3.42	P 300
A-6	1.0	3.80	29.5	36.5	16.0	91	.55	0.56	.335	1.272	0.95	2.90	2.75	.295	1.12	2.35	3.70	P 700
A-10	1.0	3.96	30.1	39.1	21	100	.51	0.216	.32	1.266	0.86	2.60	3.99	.264	1.042	-	3.64	B 1200
A-8	2.04	1.96	32.6	38.7	6	95 ^{±5}	.71	1.17	.578	1.132	0.34	3.8	5.04	.487	0.955	0.595	4.3	P 1200
A-9	2.0	2.00	32.3	37.1	16	98	.73	1.38	.561	1.126	0.34	3.53	2.90	.533	1.065	0.432	3.80	B 1200
A-5	3.94	0.73	31.2	36.9	23.2	94	.89	1.77	.903	.661	0.081	3.45	9.56	.835	0.611	0.21	4.25 and rising	P 400
A-7	4.0	1.46	29.6	36.5	21.7	74	.894	1.74	.99	1.45	0.182	4.7	1.45	.98	1.43	0.197	4.8	P 1000

All stresses : kg/cm²

- Hours after removal of side platens ; at $\bar{\sigma}_{vm}$ for O.C. tests
- Equipment used : P - Prototype, B - model B

TABLE D-1 (2)

SUMMARY OF PLANE STRAIN PASSIVE TESTS ON BOSTON BLUE CLAY

Test	OCR	$\bar{\sigma}_{vc}$	W _i %	W _f %	TS ¹	B %	K ₀	At ($\sigma_1 - \sigma_3$) max				At ($\bar{\sigma}_1 / \bar{\sigma}_3$) max				Remarks Equipm. used Batch No.			
								ϵ_v %	$\frac{q}{\bar{\sigma}_{vc}}$	$\frac{q}{p}$	A	$\bar{\sigma}_1 / \bar{\sigma}_3$	ϵ_v %	$\frac{q}{\bar{\sigma}_{vc}}$	$\frac{q}{p}$		A	$\bar{\sigma}_1 / \bar{\sigma}_3$	
P-1	1.0	4.51	34.7	27.1	3.82	80	.52	2.3	.165	0.75	0.971	2.81	-	-	-	-	-	Note a P 150	
P-2	1.0	3.85	34.7	27.1	14.7	71	.51	2.26	.178	0.687	0.923	2.49	-	-	-	-	-	Note a P 160	
P-4	1.0	4.03	33.6	26.1	22.8	89	.52	5.85	.214	0.864	0.963	4.55	6.2	.213	0.863	1.35	0.966	4.58	Horiz K ₀ P 6.50
P-10	1.0	3.98	43.4	30.9	21	96	.498	4.73	.178	0.709	1.098	4.6	-	-	-	-	-	-	Note b. B 1100
P-9	2.01	2.10	38.2	30.7	24	94	.662	3.22	.381	0.80	0.638	3.6	-	-	-	-	-	-	Questionable behavior after ($\sigma_1 - \sigma_3$) max. P Hor: K ₀ 1200
P-12	4.0	1.01	38.5	32.7	24	99	.84	3.0	.578	0.584	0.505	4.60	-	-	-	-	-	-	Hor: K ₀ Note b. B 1200

- Hours after removal side platens; at $\bar{\sigma}_{vm}$ for O.C. Tests
- Equipment used: P - Prototype, B - model B

Notes: a. ($\sigma_1 - \sigma_3$) max taken at point of inflection $\sigma - \epsilon$ curve
 b. Defined failure at $\bar{\sigma}_1 / \bar{\sigma}_3 = 4.6$

All stresses: kg/cm²

Table D-2 (1)

K_o DETERMINATIONS

Plane Strain Tests ^{a.}

K_o Value	OCR	$\bar{\sigma}_{vc}$ (kg/cm ²)	$\bar{\sigma}_{vm}$ (kg/cm ²)	No. of Determinations
.513 (.497 -.545)	1	2.0	-	7
^{b.} .513 (.498 -.525)	1	4.0	-	9
.703 (.662 -.730)	2	2.0	4.0	4
^{b.} .867 (.80 -.897)	4	1.0	4.0	5
^{b.} .85	4.25	.908	3.86	

a. All K_o values based on applied cell pressure

b. K_o value with membrane correction

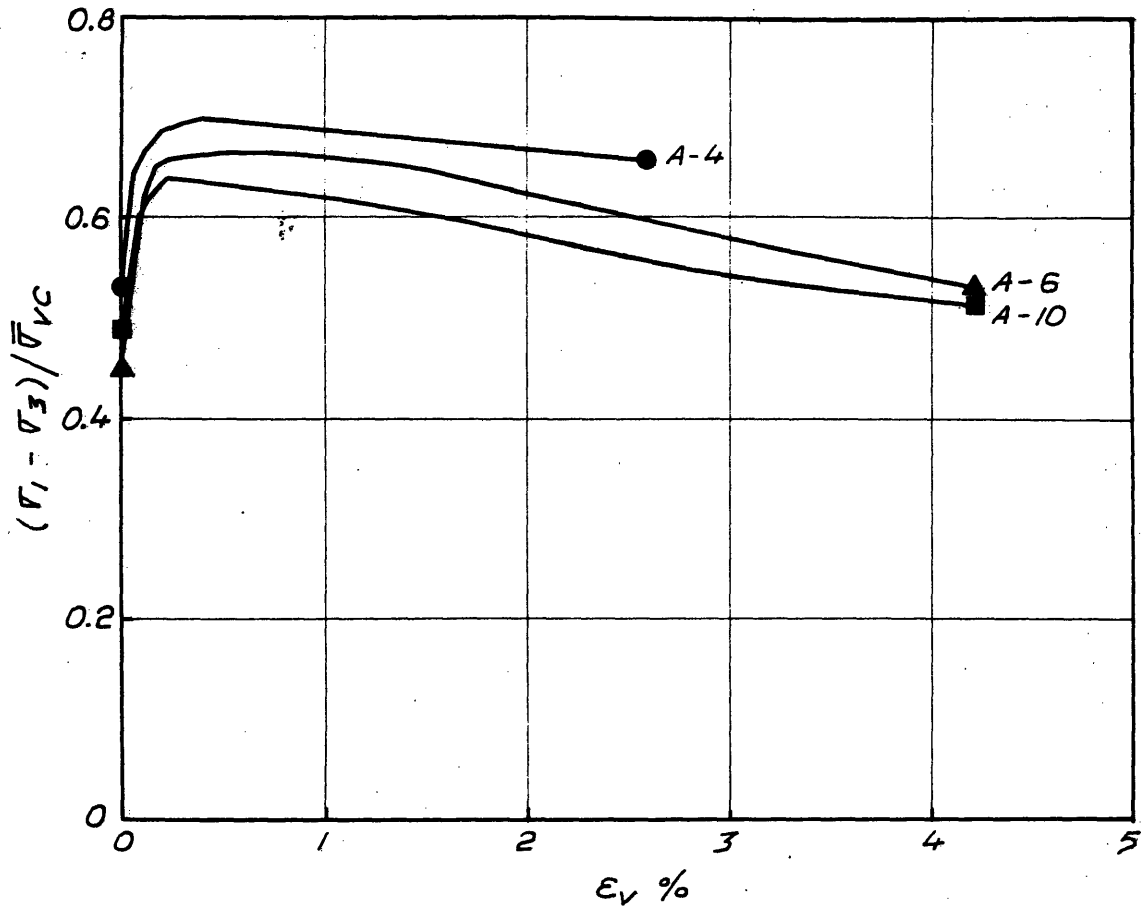
Other values without correction: $\Delta K_o + .004$ to $+ .007$

Table D-2 (2)

CK U Triaxial Tests

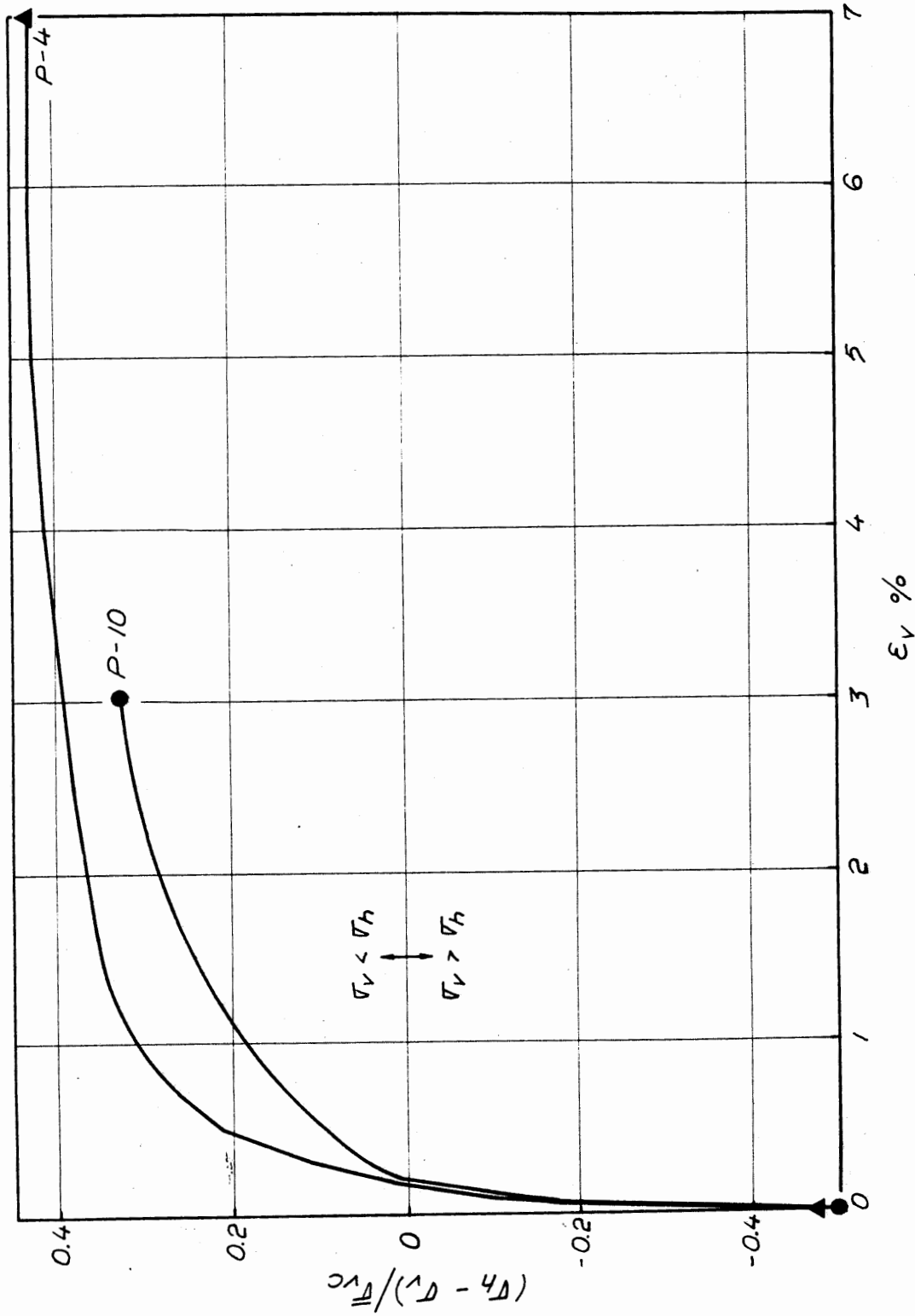
Source	K _o Value	OCR	$\bar{\sigma}_{vc}$ (kg/cm ²)	No. of Determinations
Braathen (1966) ¹	.501 (.493 - .502)	1.0	6.0	7
Earth Physics ¹ (1968)	.521 (.509 - .535)	1.0	3.0 and 4.0	18
	.74 .747 .748 .928 1.0 1.0	1.89 2.01 2.0 3.68 4.00 4.01	} $\bar{\sigma}_{vm} = 4.0$	
Ladd and Varallyay (1965) ¹	.531 (.528 - .536)	1.0		4.1 to 6.15

¹ See Appendix E for Soil Properties

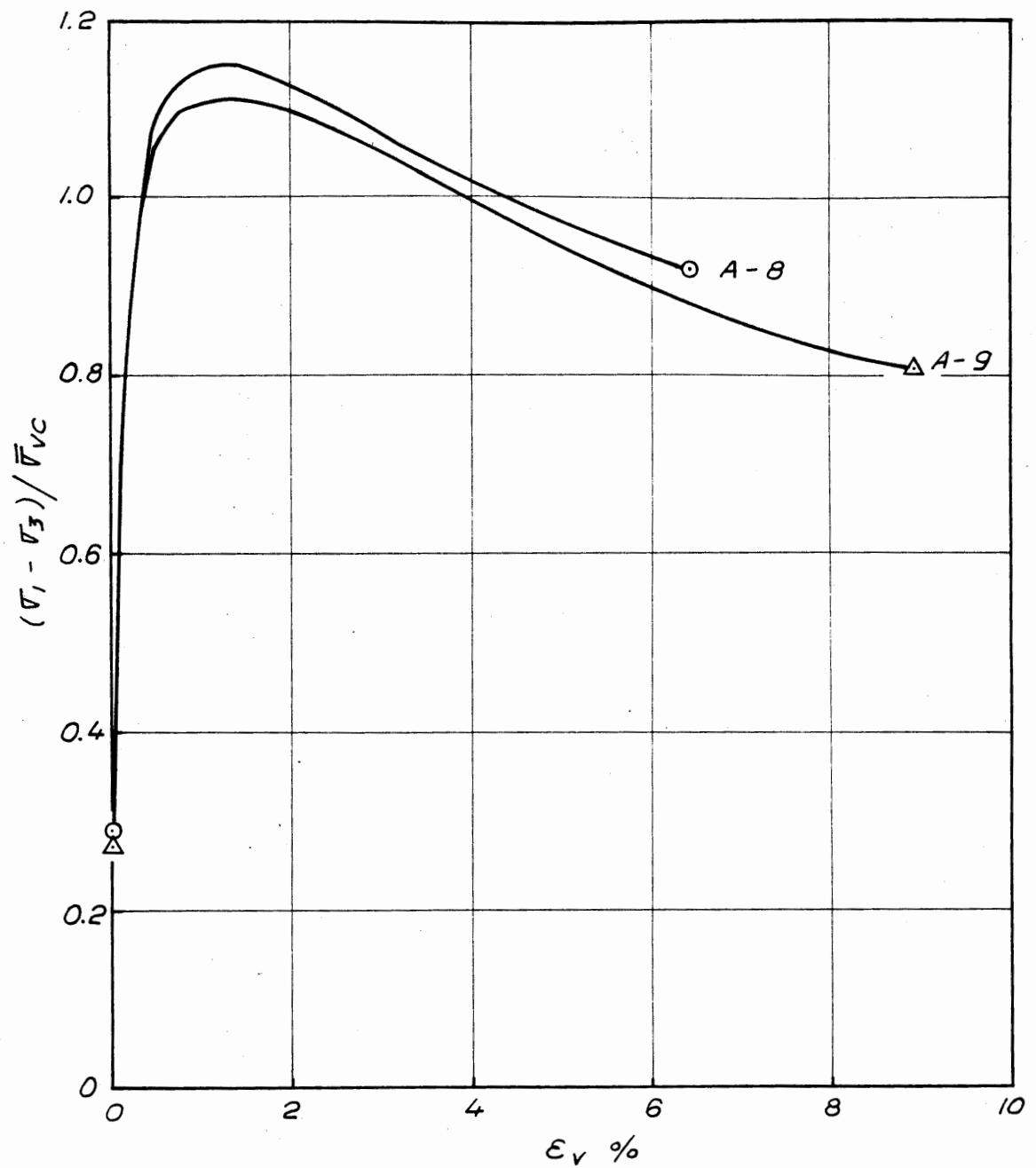


STRESS-STRAIN CURVES NORMALLY CONSOLIDATED PLANE STRAIN ACTIVE TESTS BOSTON BLUE CLAY

FIGURE D-1

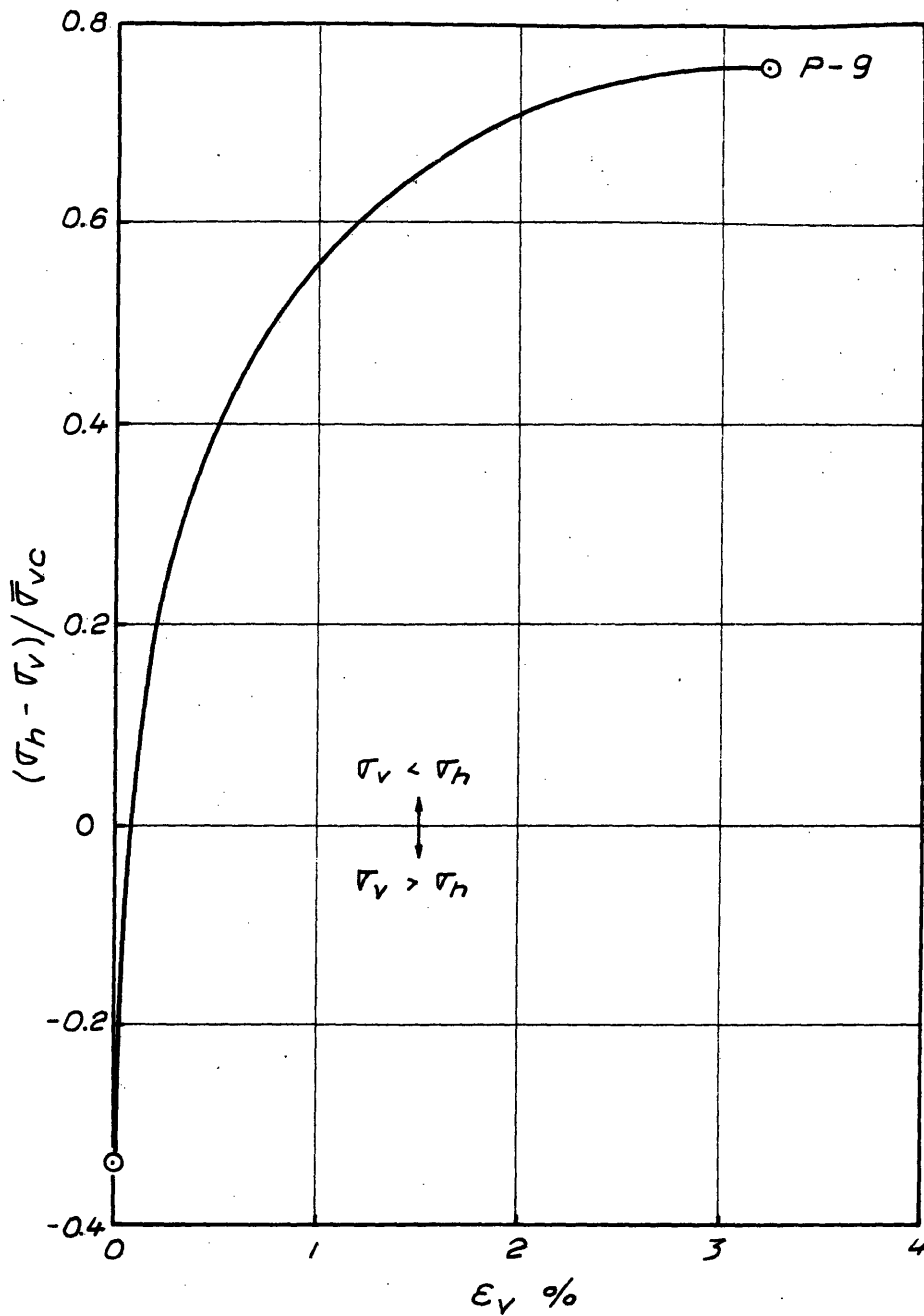


STRESS-STRAIN CURVES NORMALLY CONSOLIDATED PLANE STRAIN PASSIVE TESTS
 BOSTON BLUE CLAY
 FIGURE D-2



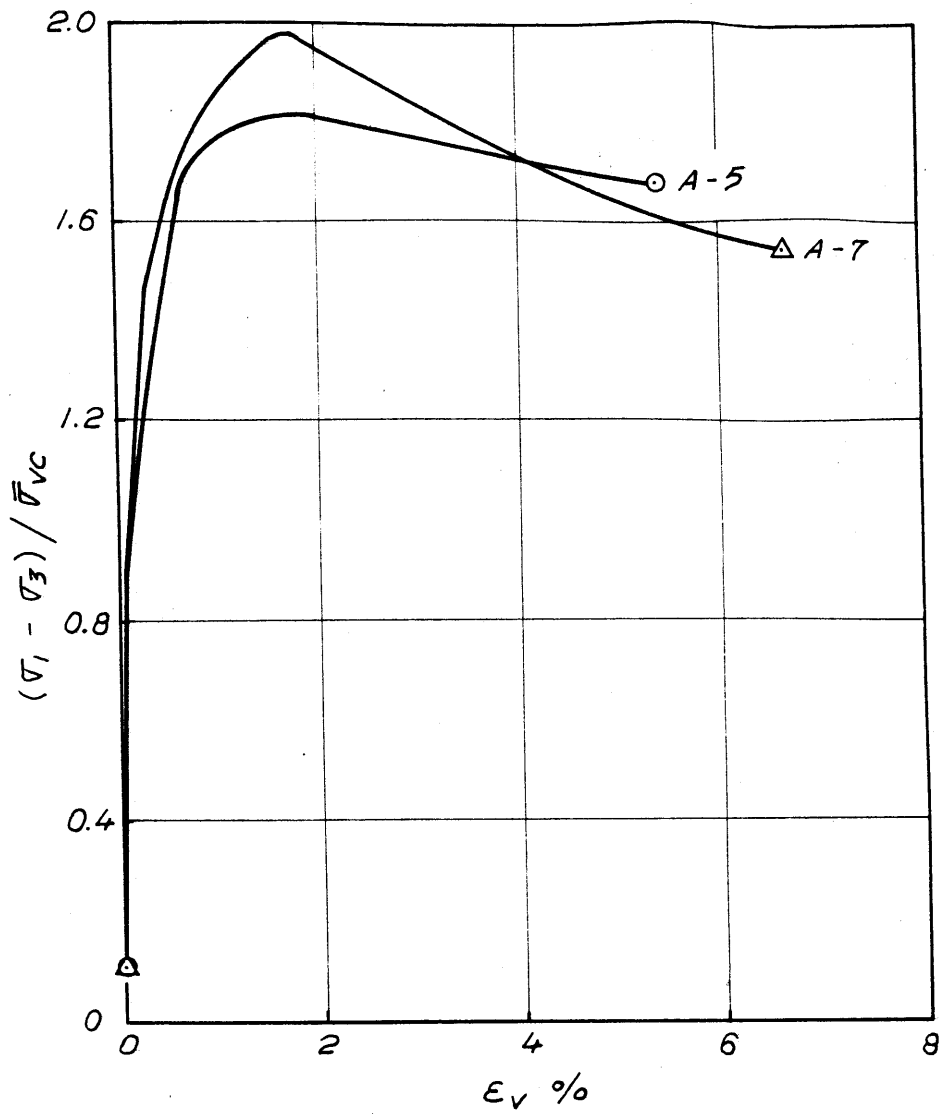
STRESS-STRAIN CURVES PLANE STRAIN ACTIVE TESTS
 BOSTON BLUE CLAY OCR = 2

FIGURE D-3



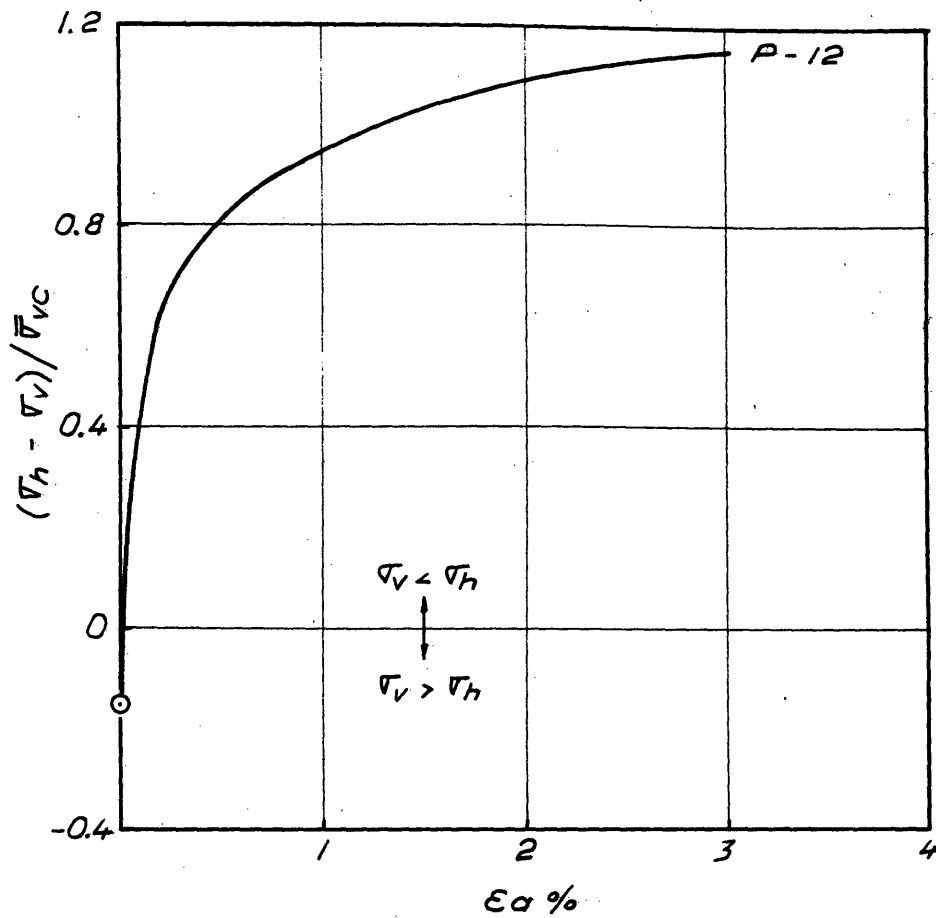
STRESS-STRAIN CURVE PLANE STRAIN PASSIVE TEST
 BOSTON BLUE CLAY OCR = 2

FIGURE D-4



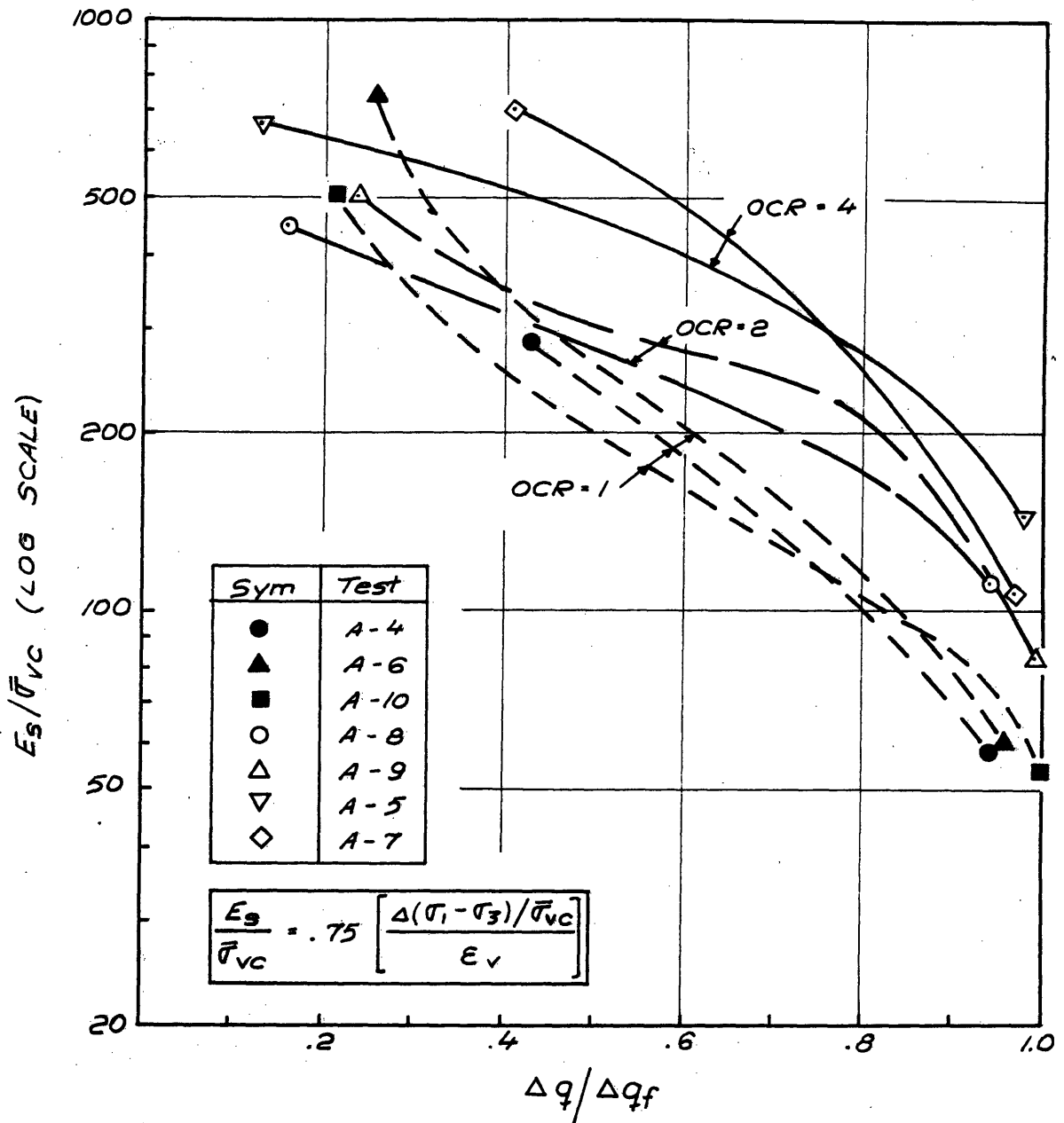
STRESS-STRAIN CURVES PLANE STRAIN ACTIVE TESTS
 BOSTON BLUE CLAY OCR = 4

FIGURE D-5

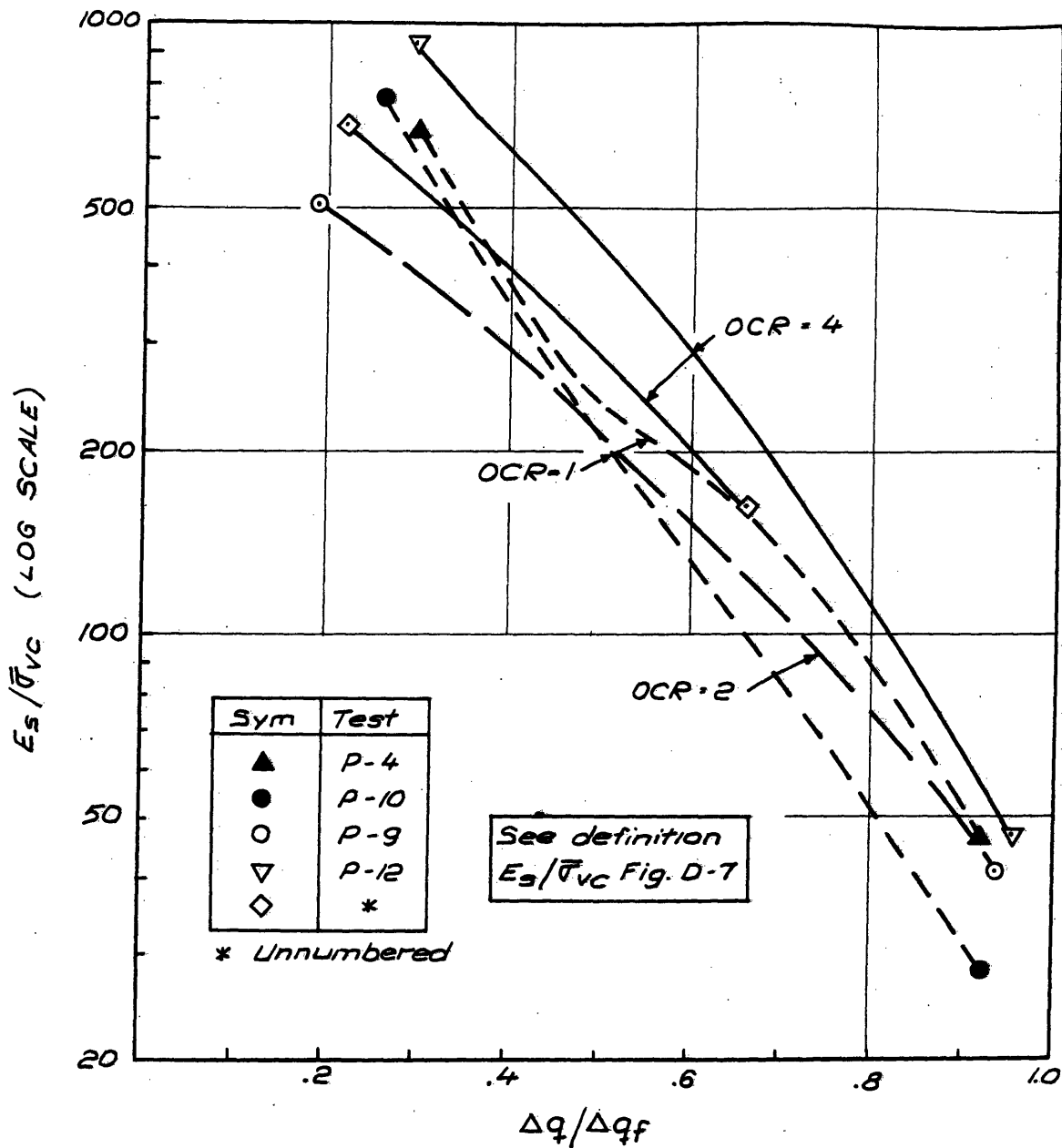


STRESS-STRAIN CURVE PLANE STRAIN PASSIVE TEST
 BOSTON BLUE CLAY OCR = 4

FIGURE D-6



NORMALIZED SECANT MODULUS VERSUS APPLIED SHEAR STRESS RATIO FOR PLANE STRAIN ACTIVE TESTS WITH BOSTON BLUE CLAY



NORMALIZED SECANT MODULUS VERSUS APPLIED SHEAR STRESS RATIO FOR PLANE STRAIN PASSIVE TESTS WITH BOSTON BLUE CLAY

APPENDIX E

MISCELLANEOUS INFORMATION ON \overline{CU} TRIAXIAL COMPRESSION TESTS

This appendix presents miscellaneous information on the \overline{CIU} and \overline{CK}_0U triaxial compression tests presented in this report. Table E-1 presents information on index properties, batch preparation, and pore fluid salt concentrations for the triaxial tests studied. Table E-2 presents summary information on triaxial tests discussed in this report that have not been reported elsewhere. Table E-3 gives summary information from Bailey (1961), and Table E-4 presents summary data from Braathen (1966). Figure E-1 shows the normalized secant modulus values, $E_s / \bar{\sigma}_{vc}$ for the tests reported by Bailey (1961) for two very different salt concentrations. No dramatic environmental effects are evident in the figure.

Table E-1

MISCELLANEOUS INFORMATION ON CU TRIAXIAL TESTS: BOSTON BLUE CLAY

Source	Description	Pore Fluid Salt Concentration of Slurry (g/l NaCl)	w _L %	w _p %	Activity	G _s	Avg. Water Content After Batch Preparation %
Bailey 1961	Water Samples	< 3	30	17.5	.31	2.77	-
	Salt Samples	35	34.7	17.7	.42	2.77	-
Ladd and Varallyay 1965		16	32.8 -	20.3 -		2.78	30.5
			33.3	20.4			
Braathen 1966		16	42.7	23.9			38.5
			23	23.2			
Earth Physics Research 1968		16	41.5±	19.5±		2.78	33

All batches 1-D consolidated to 1.5 kg/cm² from dilute slurries at initial water contents of 70 to 140 percent.

w_L and w_p determined at pore fluid salt concentration

TABLE E-2
SUMMARY OF \overline{CK}_0 TRIAXIAL COMPRESSION TESTS ON BOSTON BLUE
CLAY - 1968 EARTH PHYSICS RESEARCH

Test	W _i %	W _f %	$\overline{\sigma}_{vc}$	OCR	K ₀	$\frac{T_s @ \overline{\sigma}_{vc}}{\overline{\sigma}_{vc}}$	B %	At ($\sigma_1 - \sigma_3$) max				At ($\overline{\sigma}_1 / \overline{\sigma}_3$) max				Remark		
								E _v %	q	\overline{p}	A	$\overline{\sigma}_1 / \overline{\sigma}_3$	E _v %	q	\overline{p}		A	$\overline{\sigma}_1 / \overline{\sigma}_3$
T-1	32.5	29.0	3.90	1.0	.524	1.4	95	0.33	1.19	2.93	0.585	2.37	Not reached					
T-4	32.9	29.0	3.97	1.0	.519	1.5	98.3	0.32	1.25	3.00	0.511	2.435	Not reached					
T-2	33.2	30.0	1.062	3.68	.928	1.55	99.8	2.63	0.825	1.686	0.079	2.92	0.654	0.677	1.357	0.216	2.92	T _s @ $\overline{\sigma}_{vm}$
T-9	32.9	31.2	.998	4.0	1.0	1.5	100	1.44	0.79 (4.05) (5.00)	1.55	0.151	3.097	1.018	0.745	1.438	0.200	3.150	T _s @ $\overline{\sigma}_{vm}$

All stresses : kg/cm²

Strain rate: 1%/hr

TABLE E-3 (1)

SUMMARY OF CIU TRIAXIAL TESTS ON BOSTON BLUE CLAY - BAILEY (1961)

All stresses in kg/cm²

1 Test No.	Wi %	Wf %	$\bar{\sigma}_c$	OCR	Ts days (B)	At ($\sigma_1 - \sigma_3$) max					At ($\bar{\sigma}_1 / \bar{\sigma}_3$) max					Re-mort
						ϵ_v %	$\frac{q}{\bar{\sigma}_c}$	$\frac{q}{\bar{p}}$	A	$\bar{\sigma}_1 / \bar{\sigma}_3$	ϵ_v %	$\frac{q}{\bar{\sigma}_c}$	$\frac{q}{\bar{p}}$	A	$\bar{\sigma}_1 / \bar{\sigma}_3$	
W-1	26.9	20.6	6.0	1.0	5 (67)	2.1	.294	1.76	0.97	2.36	8.4	.28	1.68	1.27	2.95	
W-2	25.4	22.2	3.0	1.0	6 (94)	2.1	.336	1.01	0.81	2.48	8.3	.30	0.90	1.13	2.86	
W-3	25.3	20.5	6.0	1.0	4 (~90)	2.4	.297	1.78	0.97	2.39	7.4	.296	1.78	1.14	2.82	
W-4	25.6	23.6	2.0	1.0	3 (98)	1.4	.33	0.66	0.77	2.32	7.3	.275	0.55	1.31	2.91	
W-5	26.0	22.0	4.0	1.0	4 (99)	1.9	.282	1.13	1.02	2.33	8.6	.265	1.06	1.38	2.99	
W-7	24.8	22.0	3.0	1.0	46 (100)	1.9	.394	1.18	0.66	2.65	6.7	.366	1.10	0.86	2.98	
W-8	25.7	22.3	3.0	1.0	2 (?)	2.6	.347	1.04	0.83	2.64	5.7	.346	1.04	0.91	2.92	
W-9	25.1	22.0	4.0	1.0	5 (?)	2.2	.298	1.19	0.99	2.44	6.5	.292	1.17	1.18	2.89	
W-10	25.1	21.7	1.0	6.0	3 (?)	7.3	1.08	1.08	-0.032	3.02	7.3	1.08	1.08	-0.032	3.02	
W-11	25.2	22.6	0.5	12.0	4 (?)	4.3	1.48	0.74	-0.12	3.18	3.8	1.44	0.72	-0.10	3.23	
W-12	25.1	22.9	0.25	24.0	3 (?)	10.0	2.0	0.50	-0.23	3.06	1.9	1.28	0.32	0	3.46	

TABLE E-3 (2)

All stresses in kg/cm²

1 Test No.	Wi %	Wf %	$\bar{\sigma}_c$	OCR	Ts days (B)	At ($\sigma_1 - \sigma_3$) max				At ($\bar{\sigma}_1 / \bar{\sigma}_3$) max				3 Re-mark		
						Ev %	$\frac{q}{\bar{\sigma}_c}$	$\frac{q}{\bar{p}}$	A	$\bar{\sigma}_1 / \bar{\sigma}_3$	Ev %	$\frac{q}{\bar{\sigma}_c}$	$\frac{q}{\bar{p}}$		A	$\bar{\sigma}_1 / \bar{\sigma}_3$
S-1	28.6	25.8	2.0	1.0	7 (99)	1.8	.355	0.71	0.78	2.60	7.0	.35	.70	0.98	3.26	
S-2	29.0	23.9	4.0	1.0	4 (96)	2.2	.302	1.21	1.03	2.61	8.3	.30	1.20	1.23	3.29	
S-3	28.1	22.9	6.0	1.0	2 (98)	2.1	.292	1.75	1.04	2.47	8.0	.30	1.80	1.20	3.14	
S-4	28.4	25.1	3.0	1.0	3 (97)	2.5	.337	1.01	0.91	2.74	7.4	.333	1.00	1.04	3.12	
S-5	28.8	24.3	1.0	6.0	3 (86)	10.5	1.12	1.12	-0.027	3.11	10.5	1.12	1.12	-0.027	3.11	
S-6	29.0	24.6	0.5	12.0	2 (99)	9.0	1.78	0.89	-0.14	3.38	2.1	1.22	0.61	0.016	3.54	
S-8	29.1	23.9	1.0	6.0	2 (100)	7.8	1.12	1.12	-0.022	3.23	7.8	1.12	1.12	-0.022	3.23	
S-9	29.3	25.0	3.0	1.0	6 (68)	2.1	.314	0.94	0.99	2.64	8.0	.31	0.93	1.17	3.24	
S-10	29.2	24.6	3.0	1.0	4 (97)	1.9	.336	1.01	0.88	2.68	8.0	.32	0.98	1.09	3.29	

1. W = "Water"; S = "Salt"

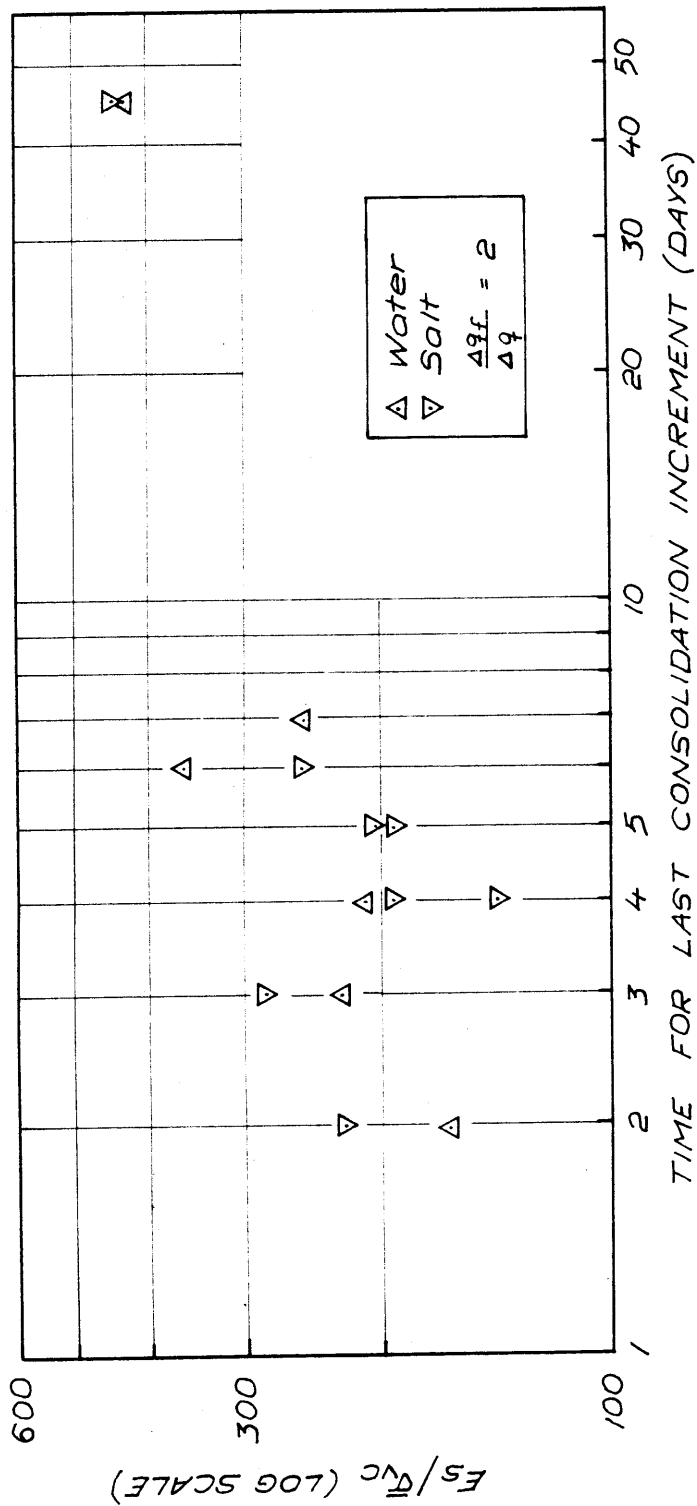
2. Ts at $\bar{\sigma}_c$ all tests

3. Strain rate ~ 1%/hr

TABLE E-4
SUMMARY OF CU TRIAXIAL TESTS ON BOSTON BLUE CLAY - BRAATHEN (1966)

All stresses kg/cm²
Strain rate 1 ± %/hr

Test No.	W _i %	W _f %	$\bar{\sigma}_{vm}$	$\bar{\sigma}_{vc}$	OCR (T _s) of $\bar{\sigma}_{vm}$ days	At ($\sigma_1 - \sigma_3$) max				At ($\bar{\sigma}_1 / \bar{\sigma}_3$) max					Rmts (g/L)	
						E _v %	q/ $\bar{\sigma}_{vc}$	q/ \bar{p}	A	$\bar{\sigma}_1 / \bar{\sigma}_3$	E _v %	q/ $\bar{\sigma}_{vc}$	q/ \bar{p}	A		$\bar{\sigma}_1 / \bar{\sigma}_3$
CU-1	42.0	31.6	6.0	6.0	1.0 (4)	4.03	.28	1.68	1.25	2.88	-	-	-	-	-	(23)
CU-2	42.6	31.1	6.01	6.01	1.0 (7)	3.04	.339	2.04	1.0	3.14	-	-	-	-	-	(23)
CU-3	42.4	31.1	5.98	5.98	1.0 (6)	1.78	.324	1.94	0.97	2.76	-	-	-	-	-	(23)
CU-4	38.4	30.7	6.06	6.06	1.0 (4.9)	3.60	.308	1.87	1.17	3.20	-	-	-	-	-	(16)
CU-5	41.7	32.7	6.0	1.48	4.06	9.08	.9	1.33	.282	3.75	-	-	-	-	-	(23)
CU-6	42.5	33.0	6.0	0.74	8.1	10.1	1.57	1.16	-0.039	3.73	12.66	1.55	1.15	1.98	0.035	(23)
CKU-1	42.8	33.8	6.0	5.49	1.09 (5)	0.37	.364	2.0	0.53	2.76	0.95	0.346	1.9	3.82	0.90	(23)
CKU-2	42.9	33.5	6.0	5.99	1.0 (1.7)	0.43	.322	1.93	0.85	2.71	-	-	-	-	-	(23)
CKU-3	41.5	32.1	5.99	5.99	1.0 (1.8)	0.35	.334	2.0	0.66	2.72	-	-	-	-	-	(23)
CKU-4	42.6	34.4	6.04	0.75	8.05	4.48	1.51	1.13	-0.05	3.59	0.97	0.656	0.67	1.02	0.224	(23)
CKU-5	42.8	36.8	5.98	1.5	3.99	3.37	.92	1.38	0.145	3.64	6.35	0.905	1.36	2.34	0.189	(23)



NORMALIZED SECANT MODULUS VERSUS TIME FOR LAST CONSOLIDATION INCREMENT FOR NORMALLY CONSOLIDATED \bar{c}_{iu} TRIAXIAL COMPRESSION TESTS (BAILEY 1961)

FIGURE E-1

APPENDIX F

MISCELLANEOUS INFORMATION FOR CONSTANT VOLUME

GEONOR DIRECT - SIMPLE SHEAR TESTS

This appendix contains a tabulated summary of constant volume direct-simple shear tests performed on Boston Blue Clay. This summary is given in Table F-1. A brief description of a limited number of special overconsolidated tests is also given here. The results of these tests are presented in Table F-2.

Three special tests were conducted in which the samples were consolidated to a maximum past pressure of 4 kg/cm². They were then rebounded to an OCR = 8. This was followed by reconsolidation, herein termed recompression, to a lower overconsolidation ratio as shown for each test in Table F-2. Constant volume tests were then performed.

The sample recompressed to an OCR = 1 exhibited a $(\tau_h)_{\max}/\bar{\sigma}_{vc}$ value that was only a few percent greater than any of the conventional normally consolidated tests. This sample had a lower preshear void ratio than first existed at the maximum past pressure. It exhibited a $\bar{\sigma}_v/\bar{\sigma}_{vc}$ ratio that was higher than most of the conventional tests. This is analogous to a lower positive excess pore pressure development.

The recompressed OCR = 2 sample had a $\frac{(\tau_h)_{\max}}{\bar{\sigma}_{vc}}$ ratio that was only 91 percent of the conventional OCR = 2 samples. It also exhibited a smaller strain to failure and a lower $\bar{\sigma}_v/\bar{\sigma}_{vc}$ ratio than the two conventional tests. The latter behavior is analogous to the development of greater positive excess pore pressure. The behavior of

the recompressed sample relative to the conventional samples is attributed primarily to the higher void ratio that should have existed during this test relative to the conventional samples. Reference to the consolidation chapter of any standard soil mechanics text will illustrate this point. The lack of a final water content, however, precludes making a direct comparison of the void ratios of the three samples.

Similar statements are appropriate for the recompressed OCR = 4 sample. Its strength at $(\tau_h)_{\max} / \bar{\sigma}_{vc}$ was only 90 percent of the conventional OCR = 4 samples.

The normalized pseudo-secant moduli from the recompressed OCR = 1 test fell within the high range of the conventional normally consolidated tests. The modulus ratios for the overconsolidated recompressed specimens were from 0 to 30 percent lower than the values for the corresponding conventional stress history.

The above observations on strength and modulus for the overconsolidated recompressed samples have important practical application. On jobs where low factors of safety are anticipated, the engineer is advised to determine whether any overconsolidated strata are of the rebounded or recompressed variety.

TABLE F-1 (1)

RESULTS OF CONSTANT VOLUME DIRECT - SIMPLE SHEAR TESTS ON BOSTON BLUE CLAY

All stresses in kg/cm²

Test No.	$\bar{\sigma}_{vc}$	OCR	W _i %	W _f %	At T_h max						At $(T_h/\bar{\sigma}_v)$ max						Remarks
					δ %	$T_h/\bar{\sigma}_{vc}$	$\bar{\sigma}_v/\bar{\sigma}_{vc}$	$T_h/\bar{\sigma}_v$	$\bar{\phi}$	δ %	$T_h/\bar{\sigma}_{vc}$	$\bar{\sigma}_v/\bar{\sigma}_{vc}$	$T_h/\bar{\sigma}_v$	$\bar{\phi}$			
CU 201	4.00	1.0	38.7	28.6	6.2	0.205	0.546	0.819	20.6	31.0	0.127	0.195	0.507	33.1	$\frac{d\delta}{dt} = 2.5\%/hr$		
CU 202	4.00	1.0	37.4	28.6	6.0	0.210	0.566	0.843	20.4	32.5	0.128	0.198	0.512	32.7			
CU 203	4.00	1.0	39.4	28.6	5.5	0.206	0.579	0.823	19.6	32.7	0.111	0.183	0.446	31.4	$\frac{d\delta}{dt} = 10\%/hr$		
CU 204	4.00	1.0	37.2	29.0	5.2	0.208	0.600	0.833	19.2	35.3	0.106	0.155	0.425	34.4	$\frac{d\delta}{dt} = 20\%/hr$		
CU 301	3.005	1.0	37.0	30.4	4.5	0.199	0.575	0.597	19.1	33.1	0.098	0.141	0.294	34.8			
CU 303	8.00	1.0	35.6	27.0	6.2	0.193	0.565	1.549	18.8	29.8	0.110	0.210	0.884	27.7			
CU 410	2.00	2.0	35.5	29.1	7.1	0.381	0.915	0.763	22.6	32.3	0.239	0.386	0.478	31.8			
CU 311	1.00	4.0	31.9	29.4	8.5	0.644	1.317	1.829	26.1	30.0	0.422	0.591	0.422	35.5			
CU 310	1.00	8.0	37.3	27.4	9.7	0.937	1.852	0.937	26.8	31.2	0.530	0.834	0.530	32.4			

TABLE F-1 (2)

All stresses in kg/cm²

1 Test No.	$\bar{\sigma}_{vc}$	OCR	W _i %	W _f %	At T_h max					3 Remarks
					δ %	$T_h/\bar{\sigma}_{vc}$	$\sigma_v/\bar{\sigma}_{vc}$	$T_h/\bar{\sigma}_v$	$\bar{\phi}$ °	
$\bar{c}U1001A$	0.5	8.0 ₂	37.5	-	10.6	0.993	1.87	0.416 0.935	28.0	} Test stopped before ($T_h/\bar{\sigma}_{vc}$) max
$\bar{c}U1301$	4	1.0	35.2	31.9	5.4	0.187	0.567	0.749 2.265	18.3	
$\bar{c}U1302$	2	2.0	35.6	33.1	5.44	0.344	0.925	0.689 1.85	20.4	
$\bar{c}U1303$	8	1.0	35.6	30.0	9.03	0.196	0.531	1.57 4.25	20.3	
$\bar{c}U1304$	1	4.0	35.8	32.65	7.74	0.555	1.23	0.555 1.23	24.4	

1. Tests from batches 200, 300, 400 from Edgers (1967)

All others from Earth Physics research in 1969

See appendix A for soil properties and batch information

2. $\bar{\phi}$: ARCTAN $T_h/\bar{\sigma}_v$

3. $\frac{d\delta}{dt}$: 5%/hr unless otherwise noted

TABLE F-2

CONSTANT VOLUME DIRECT-SIMPLE SHEAR TESTS ON RECOMPRESSED,
OVERCONSOLIDATED SAMPLES OF BOSTON BLUE CLAY

Test No.	$\bar{\sigma}_{vc}$	Preshear OCR	W _i %	W _f %	$\frac{\partial \delta}{\partial t}$ %/hr	At τ_h max				$\bar{\phi}$	Stress history
						δ %	$\tau_h/\bar{\sigma}_{vc}$	$\bar{\sigma}_v/\bar{\sigma}_{vc}$	$\tau_h/\bar{\sigma}_v$		
CU1004A	4.0	1.0	-	29.3	5	5.49	.214	0.592	.858 2.37	19.8	0 → 4 → $\frac{1}{2}$ → 4
CU1003A	2.0	2.0	37.2	-	5	5.1	.315	0.805	.63 1.61	21.3	0 → 4 → $\frac{1}{2}$ → 2
CU1002A	1.0	4.0	37.2	-	5	7.0	.526	1.11	2.1 4.44	25.3	0 → 4 → $\frac{1}{2}$ → 1

$\angle : \bar{\phi} = \text{ARCTAN } \tau_h/\bar{\sigma}_v$
All stresses kg/cm²

APPENDIX G

FACTORS INFLUENCING FINITE ELEMENT CORRELATIONS

The reliability that can be attached to the correlations obtained with finite element analyses and model footing tests is dependent on many factors. Good quality model footing tests are desired. Likewise, it is desirable that good undrained shear test data be available for choosing soil parameters for the finite element predictions. The quality of the finite element analyses must also be considered. Some of the factors affecting their reliability are discussed in this appendix. This discussion is limited to the observations made with an existing program, FEAST III, D'Appolonia (1968).

Emphasis in this discussion is placed on a comparison of three basically different finite element grids, numbers 1, 2, and 4.¹ Certain improvements were made in grid 4 with an additional grid, number 4A. Grid 4A is considered in the following discussion where appropriate, and is discussed in some detail at the end of this appendix. The grids are illustrated in Figures G-1 through G-4.² Grid 1 is very similar to that employed by D'Appolonia (1968) in

¹ Grid 3 did not differ appreciably from grid 2 and is not discussed here.

² The term "Reflection Boundary" has been applied to the right hand boundary in each grid to denote a boundary that is rigid with regard to lateral displacement and frictionless in the vertical direction.

earlier correlation efforts.

The first factor to be considered is the overall size of the finite element grid relative to the dimensions of the loaded area. Drawing on the experience of D'Appolonia (1968), grid depths and widths of at least five and four times the width of the footing, respectively, were employed. These compare to relative depths and widths in the model tests of 6.5 and 8.0 respectively. The grid dimensions employed, particularly in grids 4 and 4A, resulted in the zones of yielding being no closer than three footing widths from the fixed or reflected boundaries at normalized footing displacements of about 0.02. It will be shown, that beyond this normalized displacement, the finite element correlations should be considered with some reservation.

The vertical elastic stress distributions with depth under the edges of the footings in grids 1, 4, and 4A are compared in Figure G-5. These distributions were made for cases in which the footings were uniformly loaded and flexible. Also shown for comparison is the vertical stress distribution predicted for the same loading conditions and a Poisson's ratio equal to 0.5, by Poulos (1967) for a soil layer underlain by a rough rigid base at a depth of five footing widths. The stress distributions from grids 1 and 4 are adversely affected by triangular elements as seen by the irregularities in the stress distribution curves. These observations demonstrate that the use of triangular elements should be avoided as much as possible. If triangles are employed in transition zones between elements of different size, the triangles should be located as far as possible from zones of high stress

gradients. Quadrilaterals rather than triangles were used as transition elements in grid 4A. Irregularities in the vertical stress distribution were thus eliminated. Unsatisfactory performance of triangular elements for axisymmetric problems is reported by N.G.I. (1969).

Using a finite element grid having four elements under the half width of the footing, D'Appolonia (1968) demonstrated that the load-settlement behavior of rigid and flexible footings is almost identical. A uniform displacement was applied to the rigid footing and the average resisting stress computed. Nodal loads yielding a uniform applied stress were applied to the flexible footing and the footing displacement was monitored. Hoëg, et al. (1968) present similar results for a homogeneous soil using a lumped parameter model. A verification of these observations for grid 4 is shown in Figure G-6. Grid 4 had eight elements under the half width of the footing. The exercise was performed using soil parameters corresponding to an overconsolidation ratio of four for Boston Blue Clay. In Figure G-6 it is seen that the two methods of solution gave essentially identical results up to $\sigma/\bar{\sigma}_{vc} = 3.25$. The centerline displacement of the flexible footing has been plotted. Based on these observations, the two methods of solution should give similar results in terms of load-settlement behavior, for overconsolidation ratios of one and two.

The fact that the stress distribution under the rigid footing can be erratic is illustrated in Figure G-7. Stress distributions for grids 2 and 4 are compared for the row of soil elements adjacent to the rigid footing. The soil parameters used for the two runs correspond to

those for normally consolidated Boston Blue Clay. The only significant difference in the parameters for the two runs was the value of $E/\bar{\sigma}_{vc}$. The run for grid 4 employed $E/\bar{\sigma}_{vc} = 400$, whereas a value of 300 was used for grid 2. D'Appolonia (1968) illustrated that the displacement of a footing predicted by finite elements is inversely proportional within about 5 percent to $E/\bar{\sigma}_{vc}$ in the area of contained plastic flow. Using proportionality, the normalized displacements, ρ/B , for grid 4 noted in Figure G-7 have been adjusted to correspond to $E/\bar{\sigma}_{vc} = 300$.

Another observation that can be made from Figure G-7 is that the distribution of vertical stress in the elements immediately under the footing is more erratic in grid 2 than in grid 4. Triangles were placed in the grid 2 at a depth of $B/4$, whereas rectangles existed at the same depth in grid 4. This observation provides more justification for employing triangles as sparingly as possible. No comparative run was made with grid 1 for a uniformly displaced rigid footing. The location of triangles in this grid would almost certainly lead to an erratic distribution of vertical stress under the footing. Carrier (1968) investigated the vertical stress distribution under a rough rigid plate. He used a finer mesh than those employed here. As expected, the distribution of vertical stress which he observed under the footing was more uniform than those observed in this investigation.

Good agreement between finite element predictions and measured load settlement behavior might be achieved. However, these correlations should be considered in the light of the reasonableness of the pattern of subsurface movements and plastic yielding. No laboratory observations

in this area were made. However, the reasonableness of the finite element solutions can be assessed.

On the basis of the above discussion one might expect that a different confidence factor would be applied to the correlations obtained with the three grids. A discussion of the relative behavior of the three grids for approximately constant normally consolidated soil parameters will be presented first. This will be followed by consideration of the behavior of grid 4 for varying soil parameters.

The soil parameters used in the comparative study of the three grids for the normally consolidated case are given in Table G-1. Limited nodal displacement output was employed for the grid 2 run having the anisotropic undrained shear strength. Comparison of subsurface movements among the grids has therefore been made with the grid 2 run having the isotropic undrained strength. This difference in soil properties is not considered to adversely effect the qualitative conclusions that have been drawn. Comparisons of yielded zones among the grids have been made using the grid 2 run with the anisotropic strength. For internal consistency, the footing displacements at which comparisons have been made have been adjusted, if necessary, by proportionality to correspond to $E/\bar{\sigma}_{vc} = 300$.

Comparison of the subsurface movements for the three grids is made by consideration of the lateral movements that were predicted at two hypothetical slope indicator locations. One slope indicator is located at the edge of the footing and the second at B/4 from the footing. The slope indicator at the edge of the footing is located in

an area having very large stress and strain gradients. Movements for the edge slope indicators are given in Figures G-8, G-9, and G-10 for grids 1, 2, and 4 respectively. Plots of the predicted slope indicator movements for the location B/4 to the side of the footing are shown in Figures G-11, G-12, and G-13 for grids 1, 2, and 4 respectively. In all these figures the parameter $\Delta R/\rho$ is plotted versus depth. The ratio $\Delta R/\rho$ is the ratio of the lateral movement of the node under consideration, to the vertical movement of the corner node of the footing. A uniformly loaded flexible footing was employed for grid 1. For grids 2 and 4 a rigid footing was used wherein the nodes at the interface of the footing and soil were uniformly displaced.

It should be noted that decreasing values of $\Delta R/\rho$ with increasing values of ρ/B do not indicate that the nodal point in question is moving toward the footing. The absolute movement of the node is coupled to the value of ρ/B . Unless otherwise noted, study of these data has shown that for the load increments considered all nodes except those in grid 1 experienced continued outward movement as the footing penetration increased. However, as is evident from these figures, this continued outward movement was not always uniformly varying.

The lateral movements under the edge of the footing in grid 1 are not satisfactory. The behavior of grids 2 and 4 at the same location are much better. Except for the second node below the footing, the pattern of displacements for grid 4 are uniformly varying for ρ/B up to 0.012. For the second load increment, the second node did move inward. Likewise there is some erratic behavior under the edge of the

footing in grid 2 for low values of ρ/B . For values of ρ/B equal to or greater than about 0.02, the behavior of grids 2 and 4 are different. In grid 2 the lateral movements to a depth of $B/4$ are very large relative to the lateral movements at greater depths. The interface between the square elements and the triangular transition elements is located at a depth of $B/4$ in this grid. The change in the relative magnitude of lateral movement for large values of ρ/B in grid 4 at a depth of about one footing width is associated with a transition from a zone of general yielding to a zone that had not experienced extensive yielding.

The lateral movements for normalized displacements up to 0.03 are well behaved for the three grids at the slope indicator position $B/4$ from the footing. The uniformly varying nature of the subsurface movements is seen to have broken down for large footing displacements with grids 1 and 4. It should be noted that the footing displacement shown for grid 4 is greater than seven percent of the footing width.

The erratic nature of the subsurface movements at both slope indicator positions for normalized footing displacements of greater than 0.02 does not mean that the finite element analysis is at fault. Small strain theory was employed in the development of the program. Strains of greater than 20 percent were observed in elements near the corner of the footing for normalized displacements greater than 0.03. This combination of large strains with a small strain theory formulation may be one of the principal factors that caused the observed behavior. This observation suggests that the results of finite element analyses for

the type of foundation problem considered in this report should be viewed with reservation for normalized displacements greater than about 0.025. Fortunately, the ultimate bearing capacity in the model tests was largely mobilized before this normalized displacement was reached.

Patterns of yielding in the three grids for two nominal values of ρ/B are shown in Figures G-14 and G-15. For clarity in Figure G-15, the yielded zones for grid 4 have been shaded. For the sake of comparison, the boundaries of these zones have not been "smoothed" out. There is general agreement in both figures between grids 1 and 2. The yielded zone for $\rho/B = 0.01$ in grid 4 does not extend as far laterally as do the zones for the other grids. The lateral growth of the yielded zones for other grid 4 normally consolidated runs were in closer agreement to those shown for grids 1 and 2.

For the larger ρ/B value, a yielded zone is seen to lie within an unyielded area for grid 4. Grid 4 is not entirely alone in this respect however, for similar behavior was observed for the grid 2 run having the isotropic undrained shear strength. See Figure G-16. There are 104 elements below the footing in grid 4 from the surface to a depth of $2B$. In the same region in grids 1 and 2 there are 76 elements. There are many triangles in this area for grids 1 and 2 but none there for grid 4.

On the basis of the observations made thus far, the following conclusions can be drawn concerning the reliability that can be attached to the correlations obtained with the three grids. The patterns of subsurface movements in grid 1 are poor enough to eliminate it from

further consideration. Other adverse factors associated with grid 1 are its vertical stress distribution with depth, and the almost certain highly erratic stress distribution under the footing.

Grid 4 had a less erratic stress distribution under the footing than grid 2. Although no specific run was made to check this factor, the vertical stress distribution with depth in grid 2 is considered to be less acceptable than that with grid 4, because of the triangular elements that existed in this mesh. Although both grids showed erratic subsurface movements under the edge of the footing, grid 4 exhibited better overall performance for all normalized displacements studied. At $B/4$ away from the footing, both grids were well behaved until large values of ρ/B .

Grid 4 was considered superior to grid 2. It was used in parametric studies concerning the effects that variations in soil parameters have on the load deformation behavior of normally consolidated and overconsolidated Boston Blue Clay. For the reasons discussed at the end of this appendix, Grid 4A was employed in making final correlations with the model test data.

How much difference does exist between the results obtained with different grids for the same soil properties? The answer to this question is illustrated in Figure G-17.

The soil properties used in the two runs were identical except for the values of $E/\bar{\sigma}_{vc}$. For grid 2, the value of $E/\bar{\sigma}_{vc}$ equaled 350. The normalized displacements for this run were adjusted to correspond to a value of $E/\bar{\sigma}_{vc}$ equal to 400 before they were plotted in the figure.

For values of $\sigma/\bar{\sigma}_{vc}$ less than 0.8, the grid 2 results lie above those of grid 4. For larger values of $\sigma/\bar{\sigma}_{vc}$, the grid 2 curve lies below that for grid 4. The percentage difference between the normalized displacements at $\sigma/\bar{\sigma}_{vc} = 0.6$ is about 35 percent. The absolute magnitude of difference between the two runs at this point is however, quite small. At $\sigma/\bar{\sigma}_{vc} = 1.2$, grid 2 has a ρ/B value 1.25 times that of grid 4.

Correlations with a given grid for different overconsolidation ratios require the specification of different initial stress states and soil parameters. The possibility was considered that acceptable subsurface movements, yielded zones, and load-settlement correlations could be obtained with grid 4 for the normally consolidated case, while unacceptable results would result because of these factors for the overconsolidated cases.

The soil properties for the overconsolidated runs to be discussed are given in Table G-2. Subsurface movements for the same slope indicator positions discussed earlier are given in Figures G-18 and G-19 for an OCR = 2 and in Figures G-20 and G-21 for an OCR = 4. It is observed that there has been an overall improvement in the conditions for an overconsolidation ratio of two. There is erratic behavior immediately under the footing, but the deviations from the average curve are less than for the normally consolidated case. The behavior is excellent for ρ/B values less than 0.01 at both slope indicators for the overconsolidation ratio of four. For all practical purposes, failure occurred in this run at $\rho/B = 0.015$. This explains the erratic subsurface behavior at the larger footing displacements.

Patterns of yielding near failure for these runs are shown in Figure G-22. Two small areas of contained "elasticity" existed for the OCR = 2 run as shown by the shaded areas. The depth of the yielded zone is seen to decrease with increasing overconsolidation ratio.

Another factor affecting the load-settlement behavior predicted by Feast III is the size of the imposed load increment. The elastic constants for an element are changed to the "yielded" values only if the specified yield stress is reached or exceeded during the latest load increment. After "yield" the shearing resistance of an element increases in accordance with the yielded modulus. If due to a large load increment, the specified yield stress is exceeded by a significant degree, the shearing resistance of the element for the remainder of the problem will be too large. The cumulative effect for many elements could affect the predicted load-deformation behavior.

The effect is illustrated in Figure G-23 for two runs with grid 4 employing soil parameters for normally consolidated Boston Blue Clay. Both runs were identical in every respect except that in the first, 19 load increments were used to achieve a $\rho/B = 0.01$, while in the second, only six increments were employed to reach the same footing displacement. The difference between the two runs is not large. Oddly enough the stresses for the two runs at $\rho/B = 0.01$ were almost identical. The prediction for which six increments were used should not be considered the limiting case. If only one increment had been used then an elastic solution would have resulted for this displacement and the footing stresses would have been much larger.

Prior to making final correlations with the model test data,

a reassessment of the performance of grid 4 was made. The following modifications to grid 4 were incorporated in grid 4A. The two rows of rectangles under the footing at a depth of approximately $2B$, which had a length to breadth ratio of six, were replaced by three rows having a ratio of four. All but three of the triangles in grid 4 were replaced by quadrilaterals in grid 4A. The improvement that this made in the vertical stress distribution with depth was discussed earlier (Figure G-5). Also, the behavior of quadrilaterals is considered to be superior to that of triangles when yielding occurs. The depth to width ratio of grid 4A was made equal to six, to be in closer correspondence with that existing in the model tests. The grid width was rounded out to $5B$. Comparative runs for the two grids were made. Identical normally consolidated soil parameters were used and the load increments were the same. The comparison is shown in Figure G-24.

Table G-1
 NORMALLY CONSOLIDATED SOIL PROPERTIES USED
 IN COMPARATIVE STUDY OF
 GRIDS 1, 2, AND 4

Grid	$s_{uv}/\bar{\sigma}_{vc}$	K_s	K_o	$E/\bar{\sigma}_{vc}$	ν
1	.335	.6	.5	300	.49
2	.33	1.0	.5	300	.495
	.342	.6	.5	350	.49
4	.32	.563	.53	400	.495

Bulk modulus maintained constant after yield by adjustment of yielded Poisson's ratio.

Yielded modulus ratio = .001

Table G-2

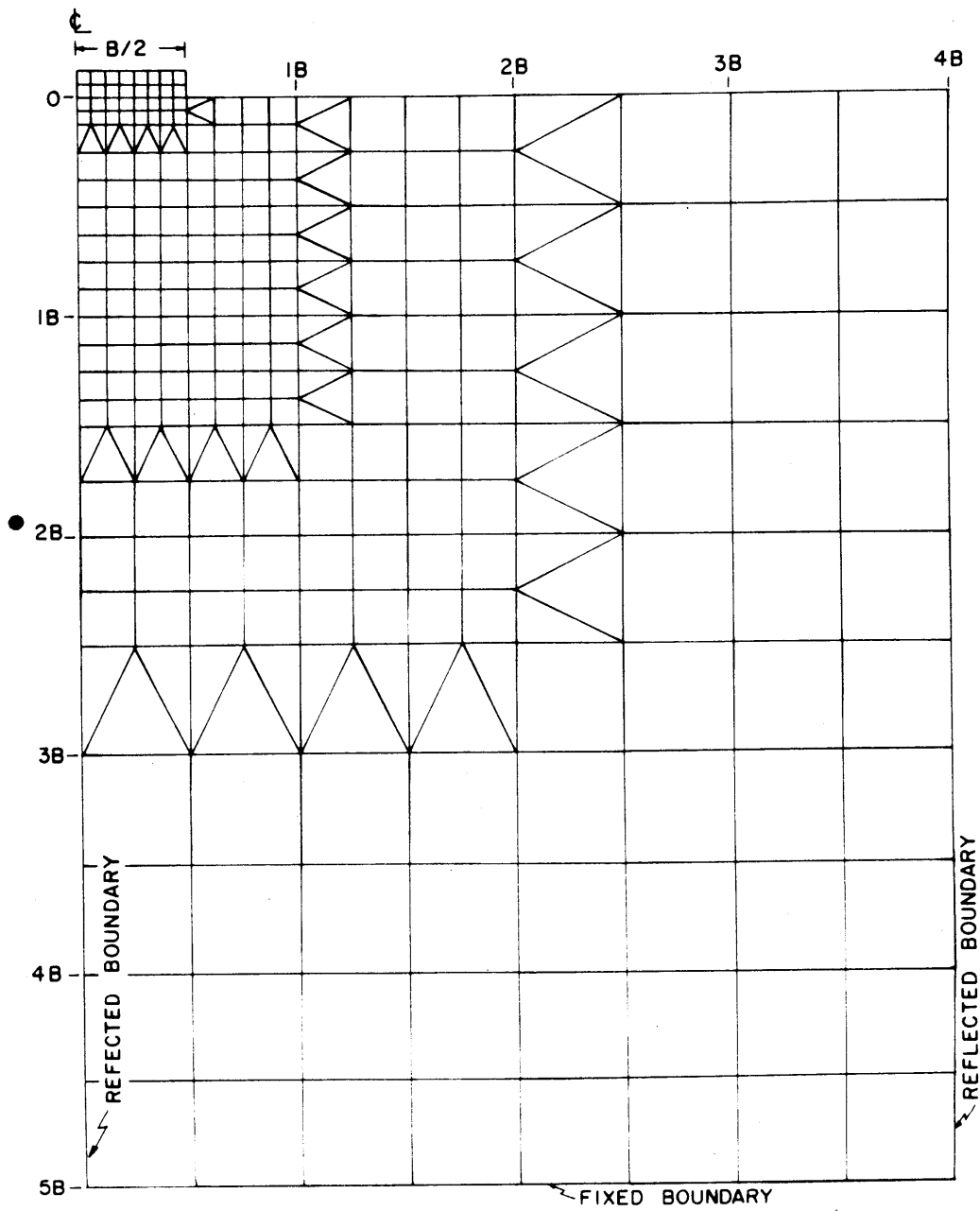
SOIL PROPERTIES FOR THE EVALUATION OF THE
PERFORMANCE OF GRID 4 FOR USE IN
OVERCONSOLIDATED CORRELATIONS

OCR	$s_{uv}/\bar{\sigma}_{vc}$	K_s	K_o	$E/\bar{\sigma}_{vc}$
2	.55	.688	.69	400
4	.9	.61	.89	300

$\nu = .495$

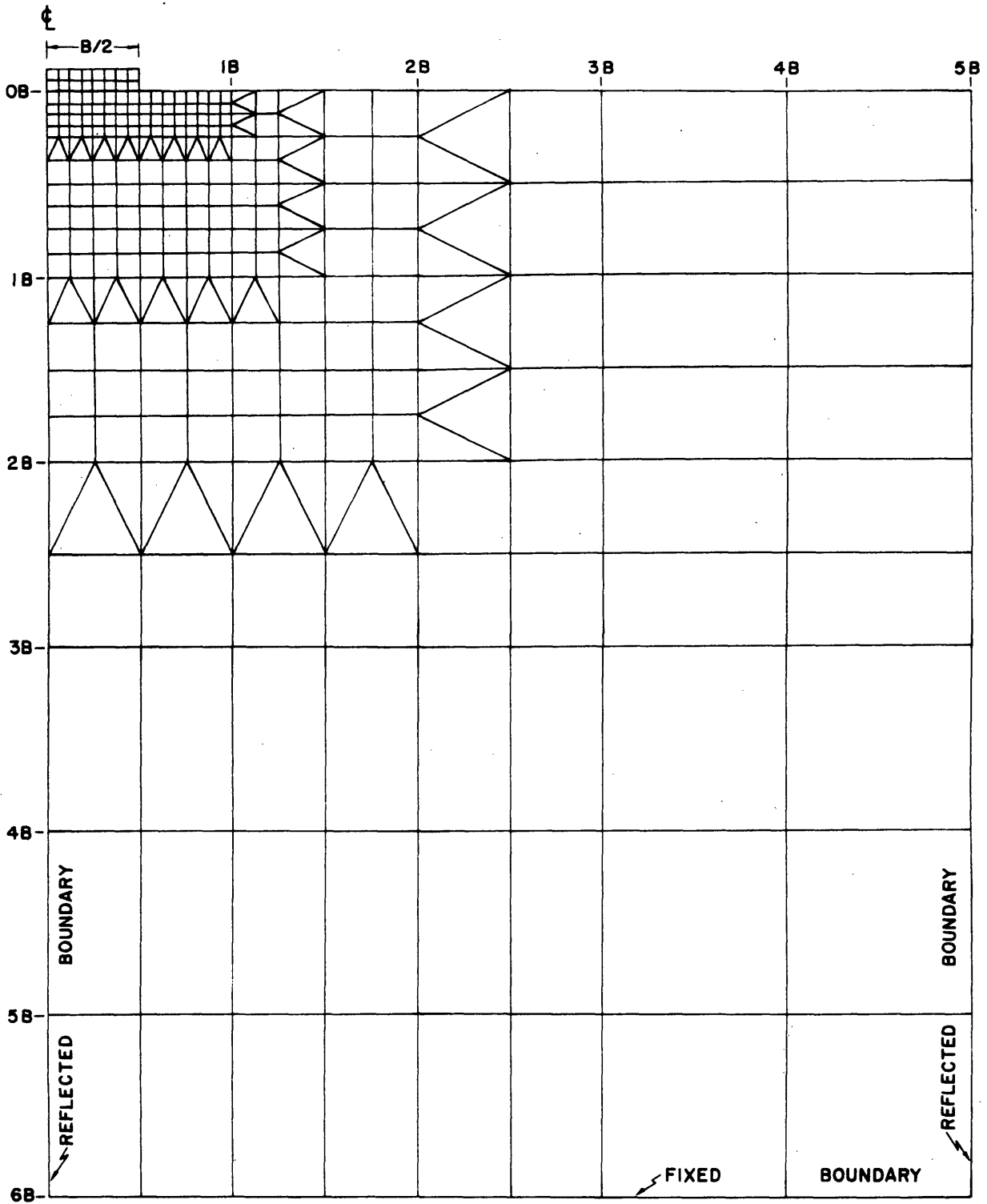
Bulk modulus maintained constant after yield by adjustment of yielded Poisson's ratio.

Yielded modulus ratio = .001



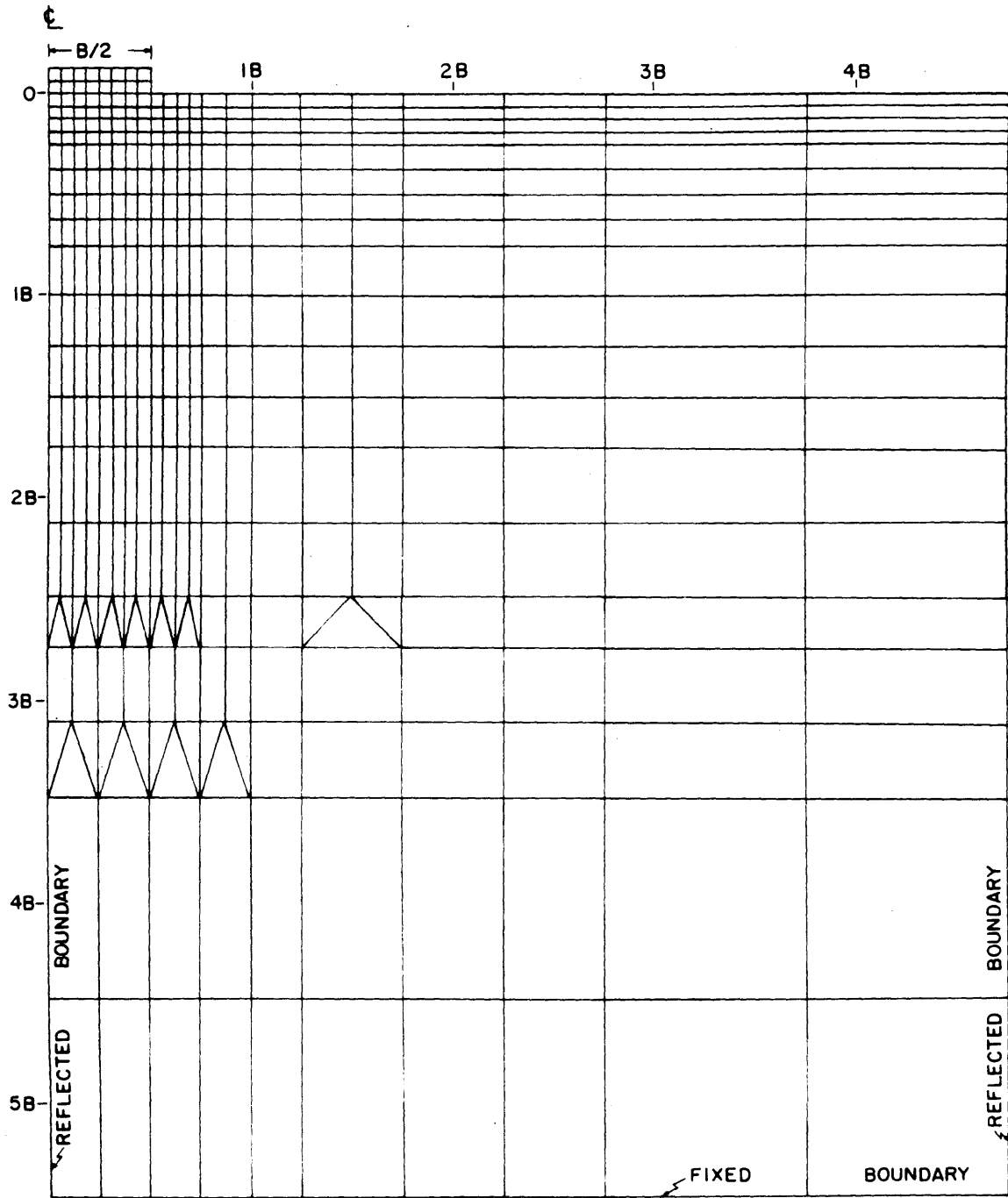
FINITE ELEMENT GRID I

FIGURE G-1



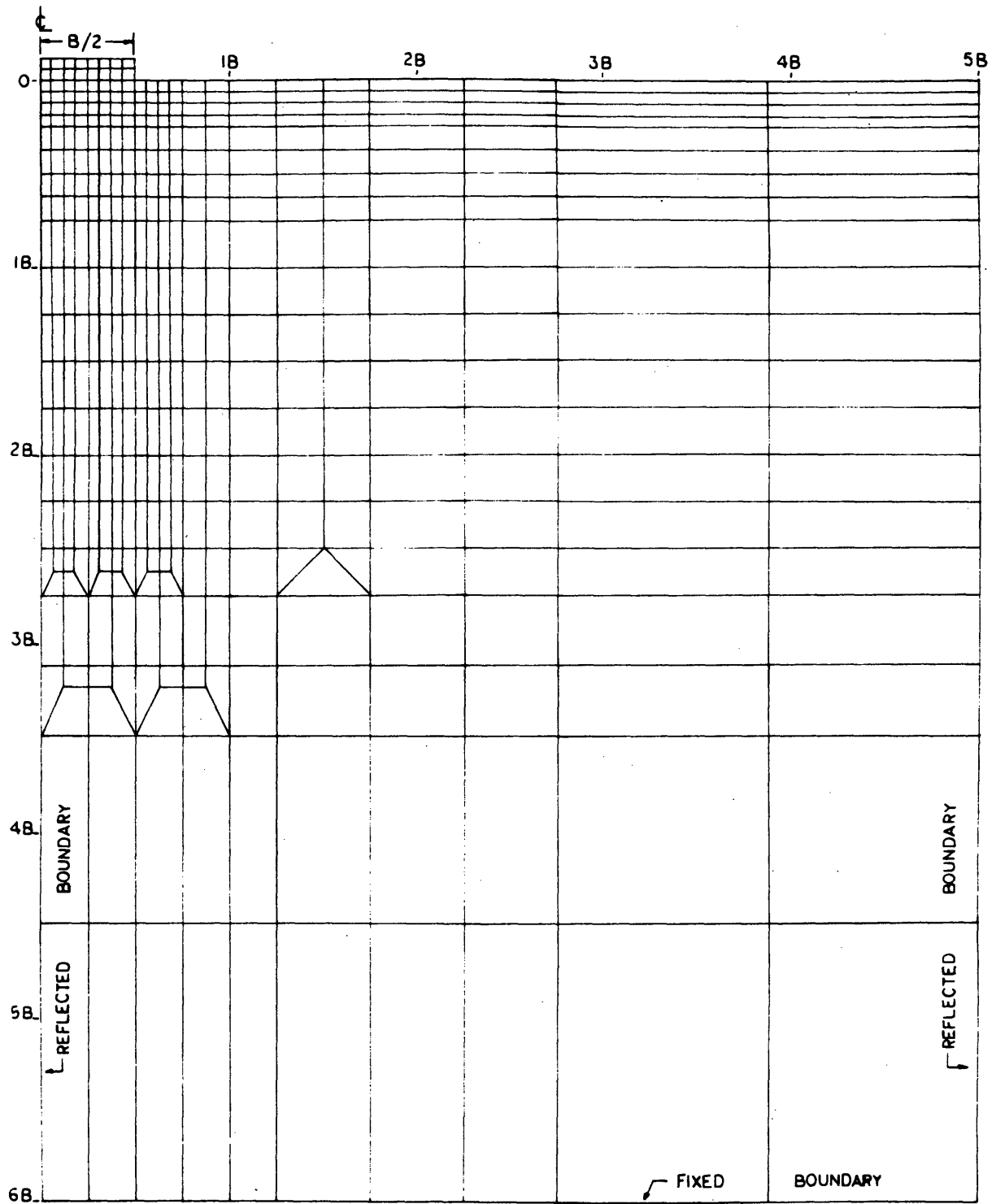
FINITE ELEMENT GRID 2

FIGURE G-2



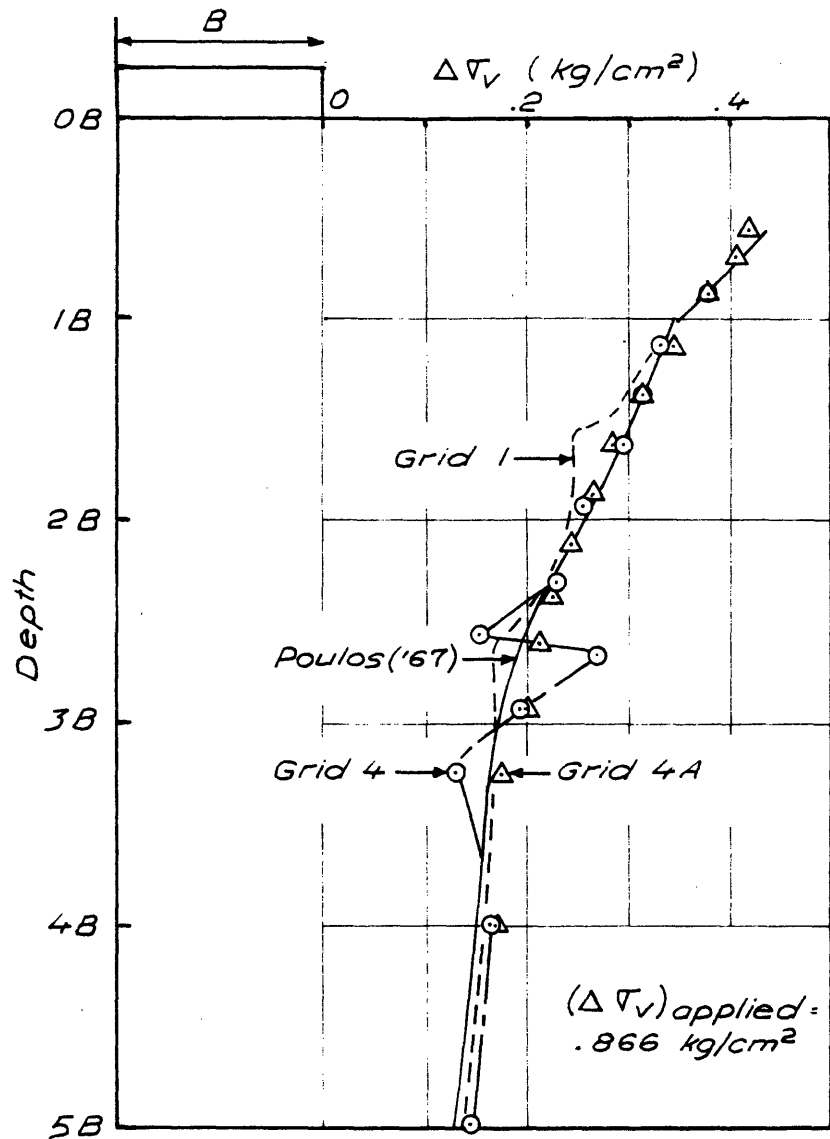
FINITE ELEMENT GRID 4

FIGURE G-3



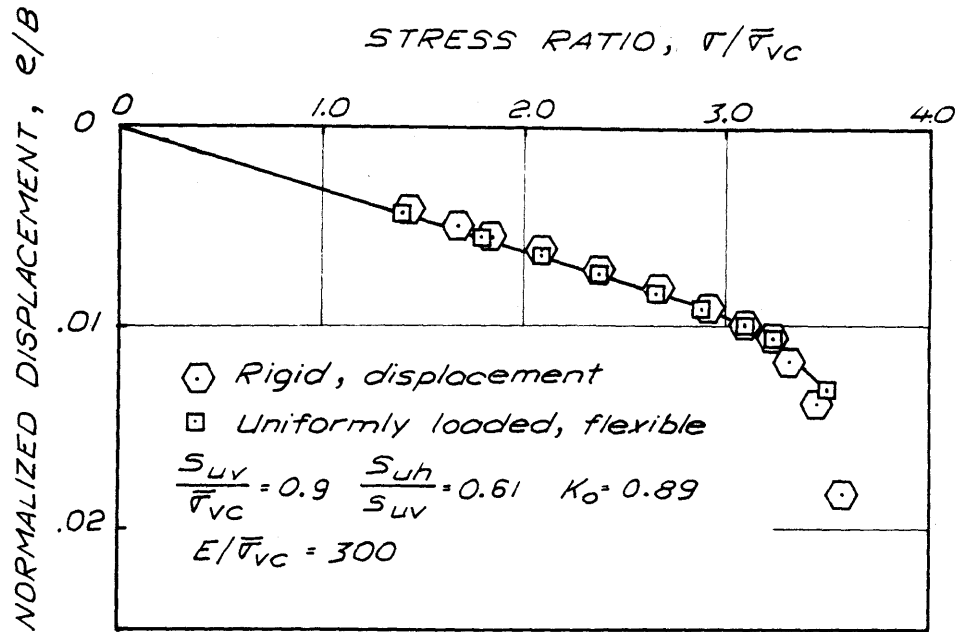
FINITE ELEMENT GRID 4A

FIGURE G-4



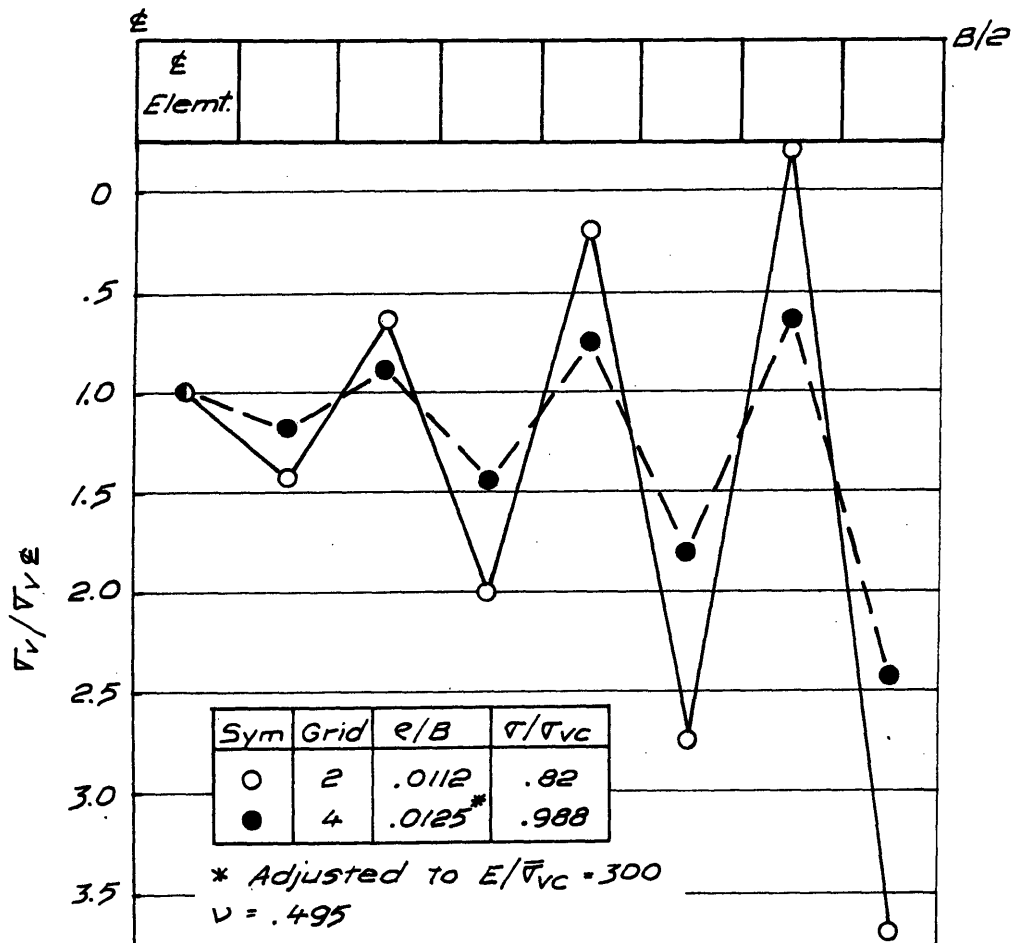
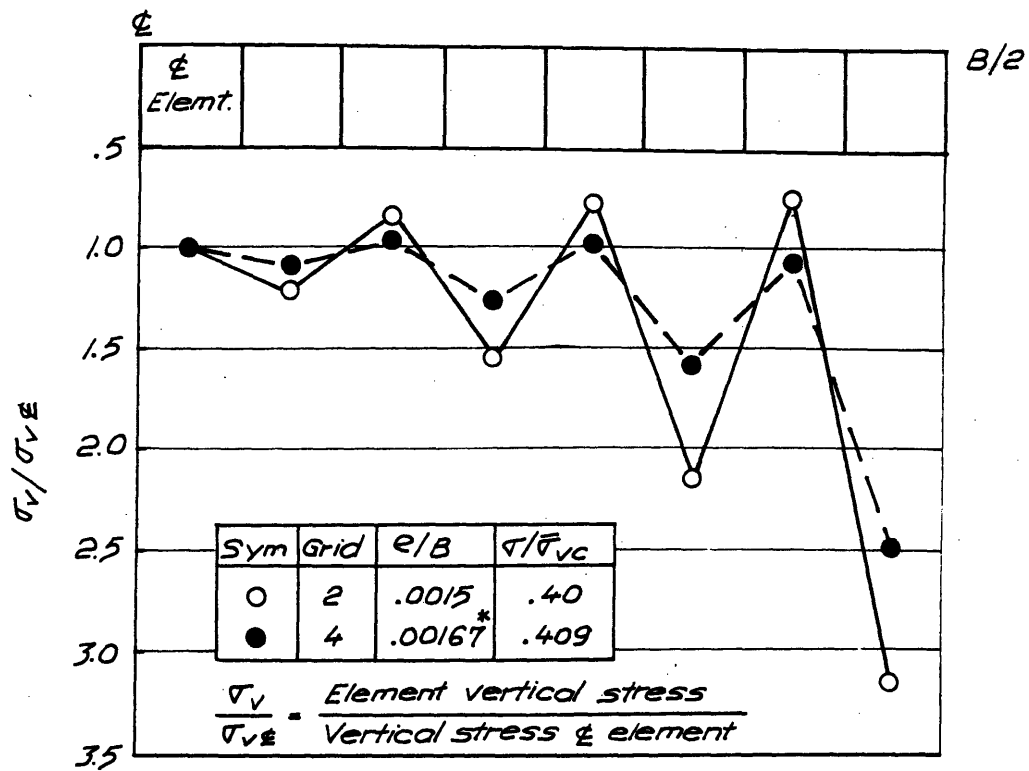
VERTICAL STRESS DISTRIBUTIONS UNDER THE EDGE OF A UNIFORMLY LOADED FLEXIBLE STRIP

FIGURE G-5

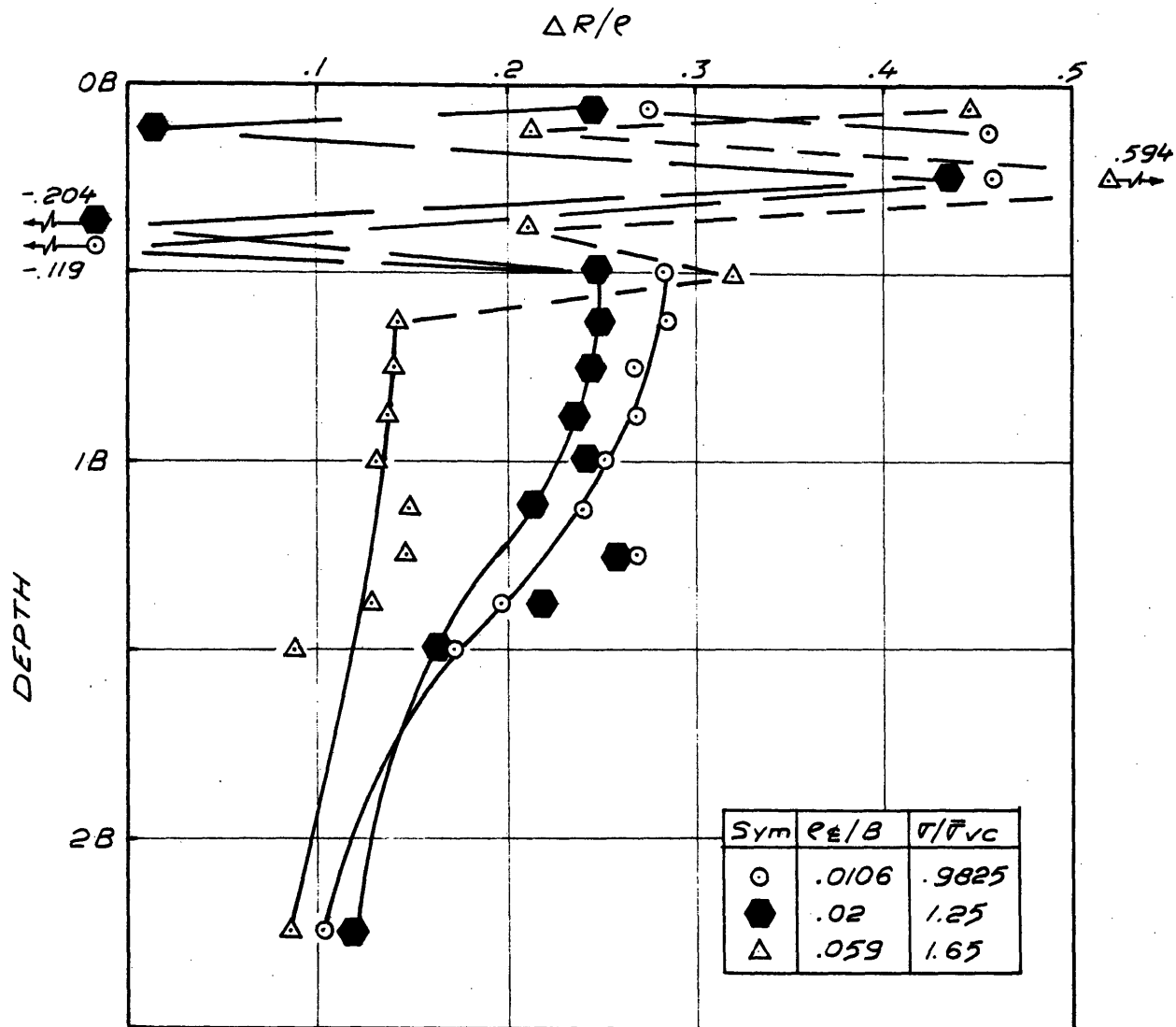


COMPARISON OF RESULTS OF FINITE ELEMENT PREDICTIONS EMPLOYING DISPLACEMENT AND STRESS CONTROLLED LOADING OF THE FOOTING, OCR = 4

FIGURE G-6

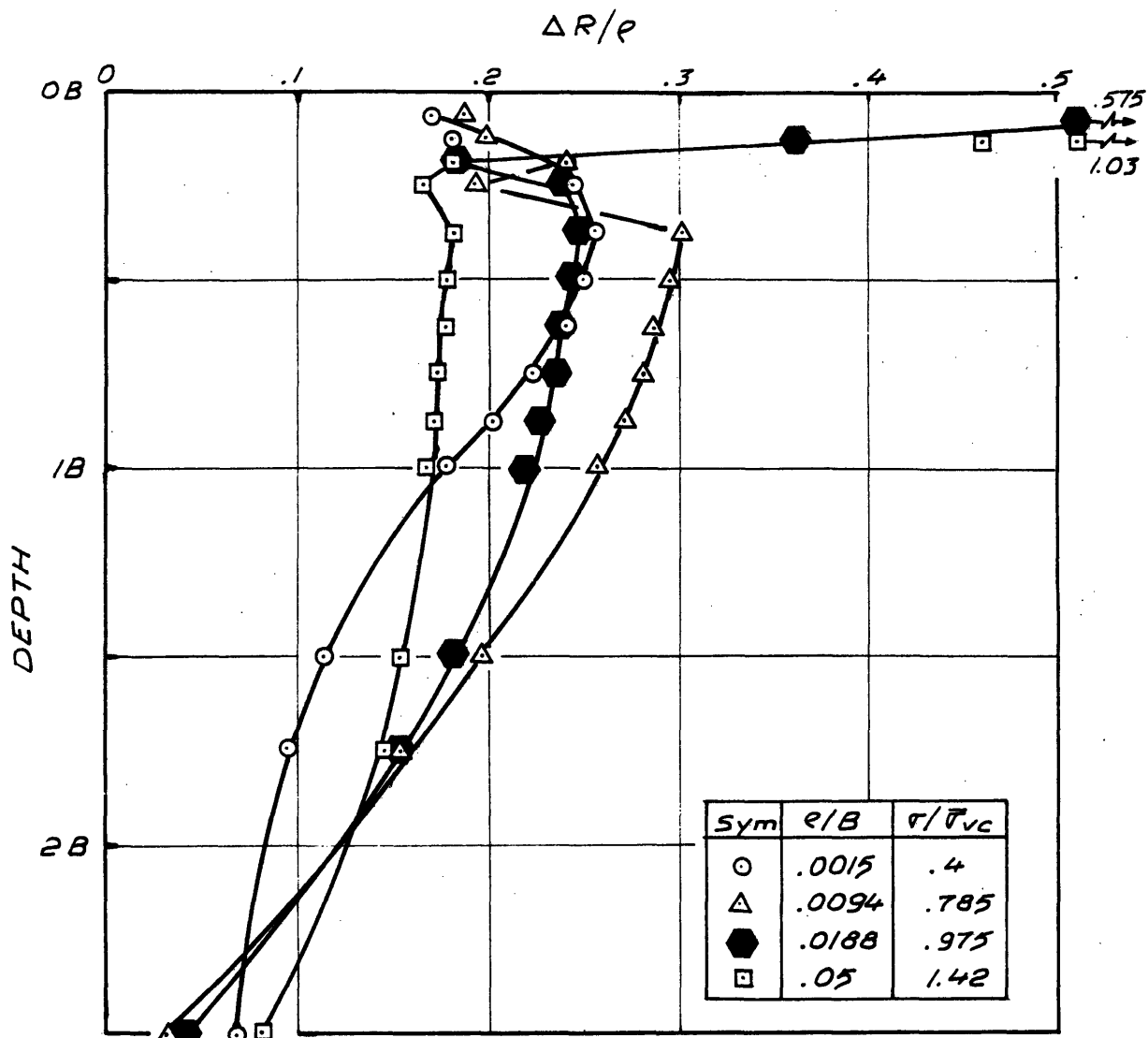


VERTICAL STRESS DISTRIBUTIONS UNDER FOOTING FOR TWO FINITE ELEMENT GRIDS FIGURE G-7

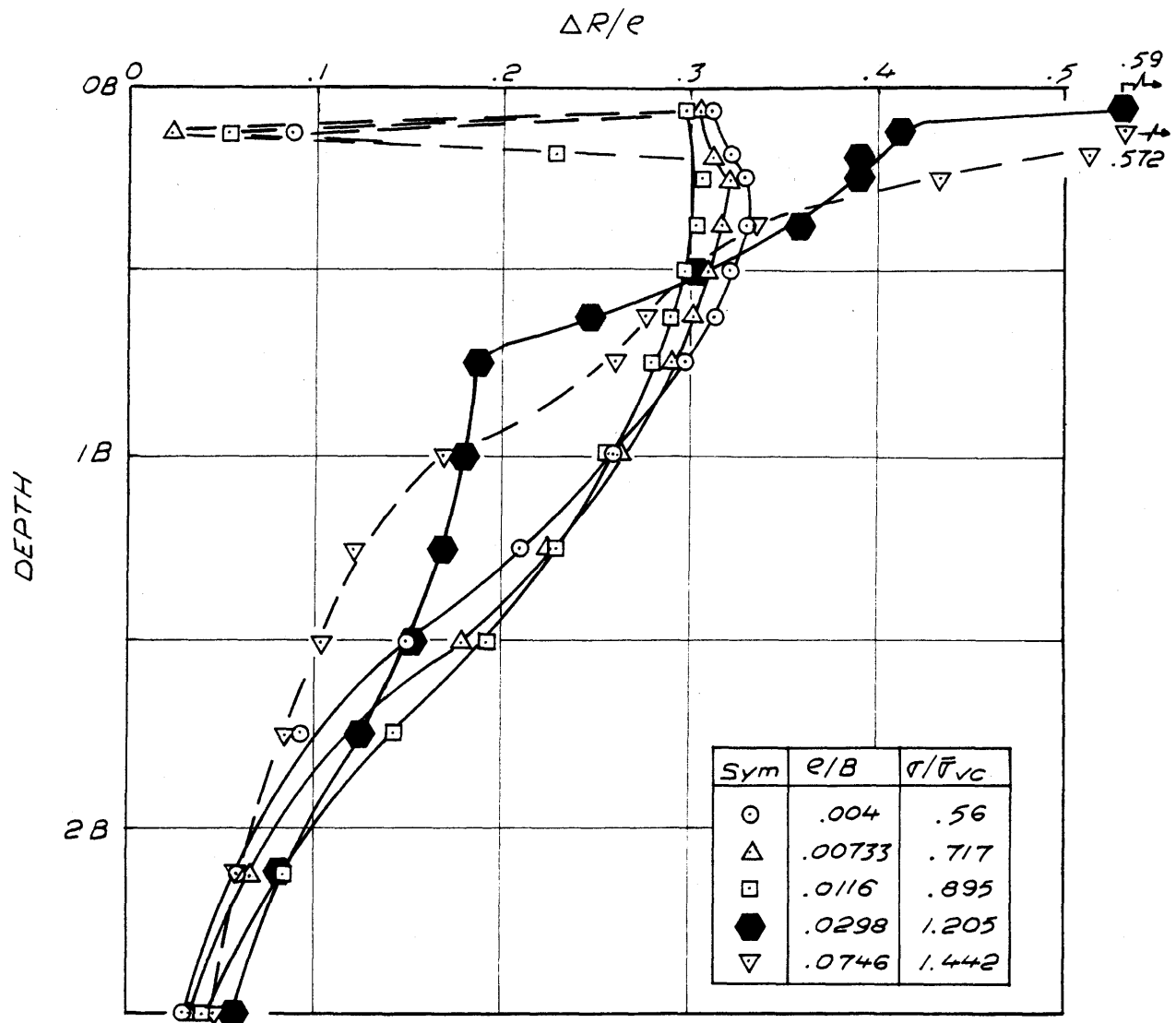


NORMALIZED LATERAL DISPLACEMENT WITH DEPTH FOR
 NODES UNDER EDGE OF FOOTING, GRID 1

FIGURE G - 8

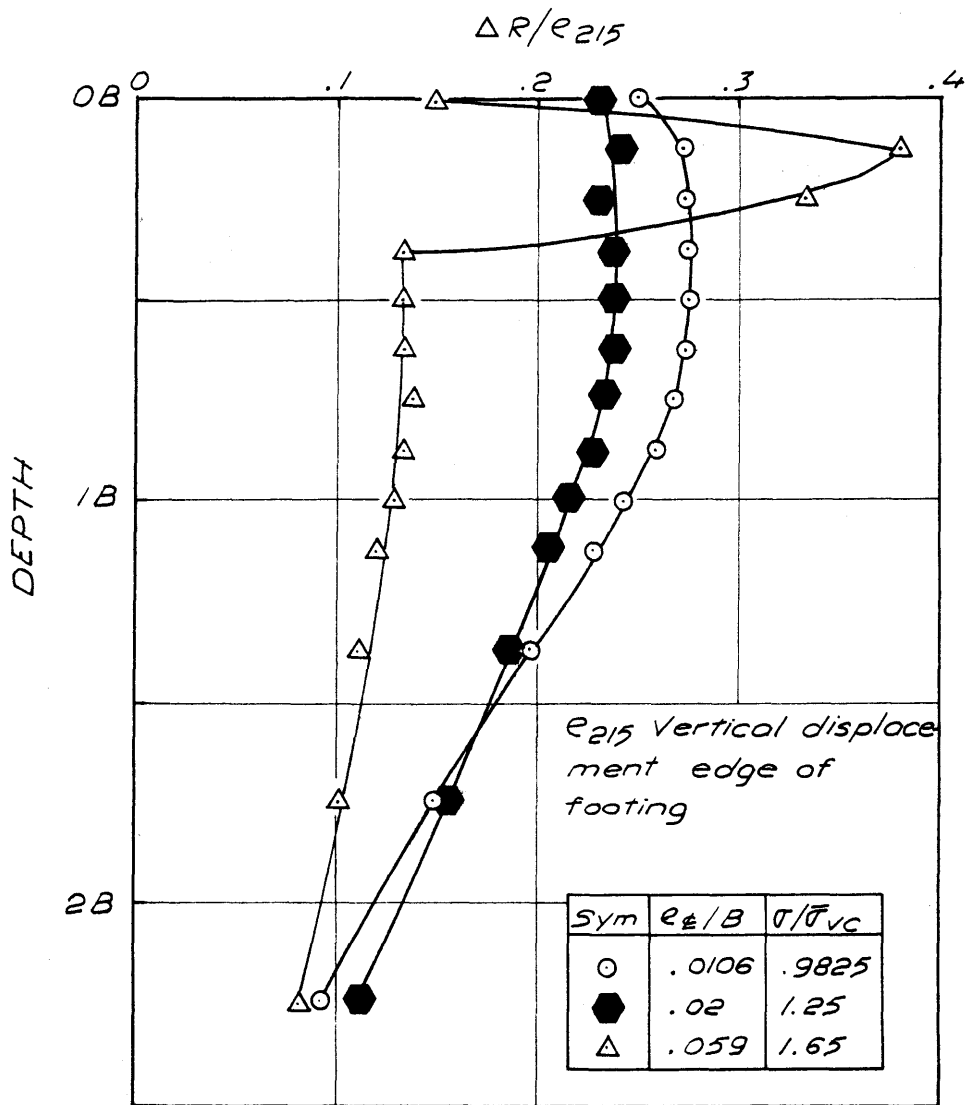


NORMALIZED LATERAL DISPLACEMENT WITH DEPTH FOR
 NODES UNDER EDGE OF FOOTING, GRID 2

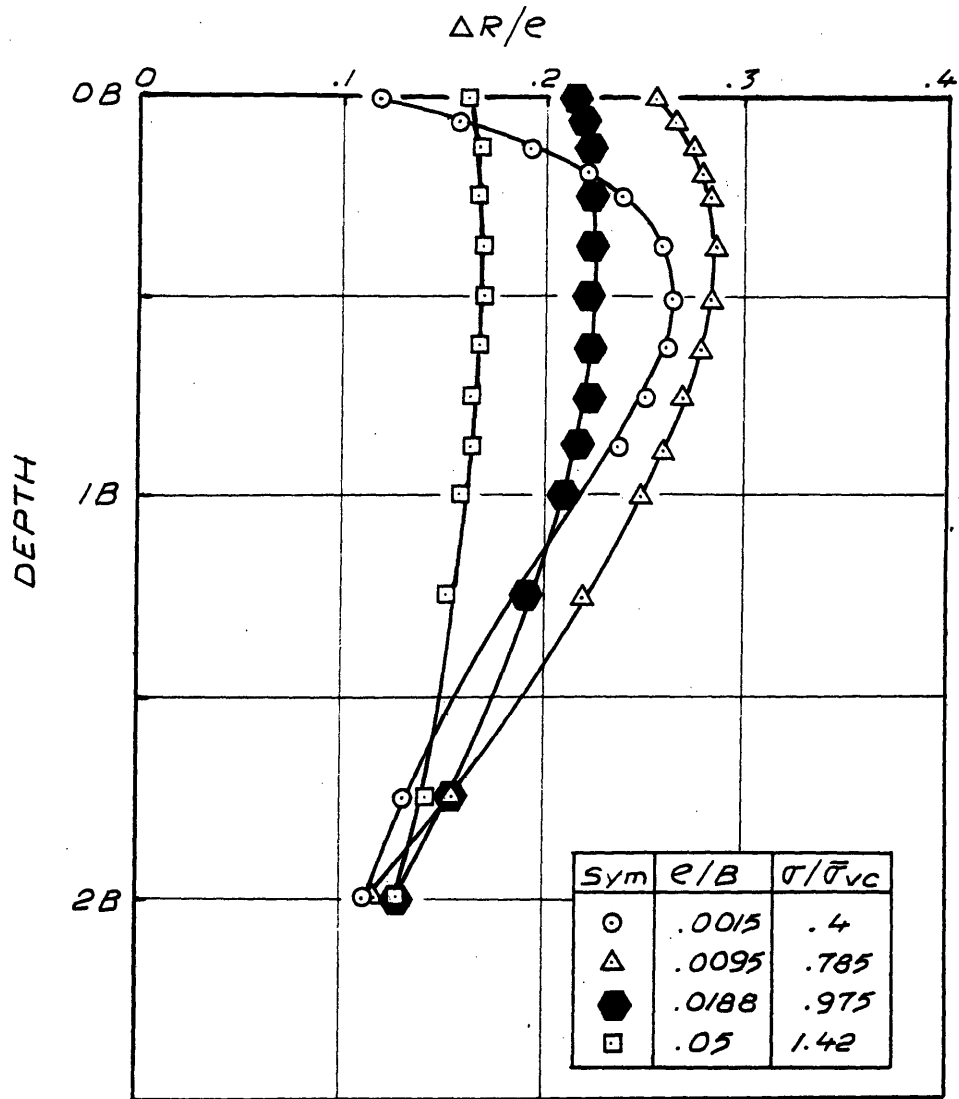


NORMALIZED LATERAL DISPLACEMENT WITH DEPTH
FOR NODES UNDER EDGE OF FOOTING, GRID 4

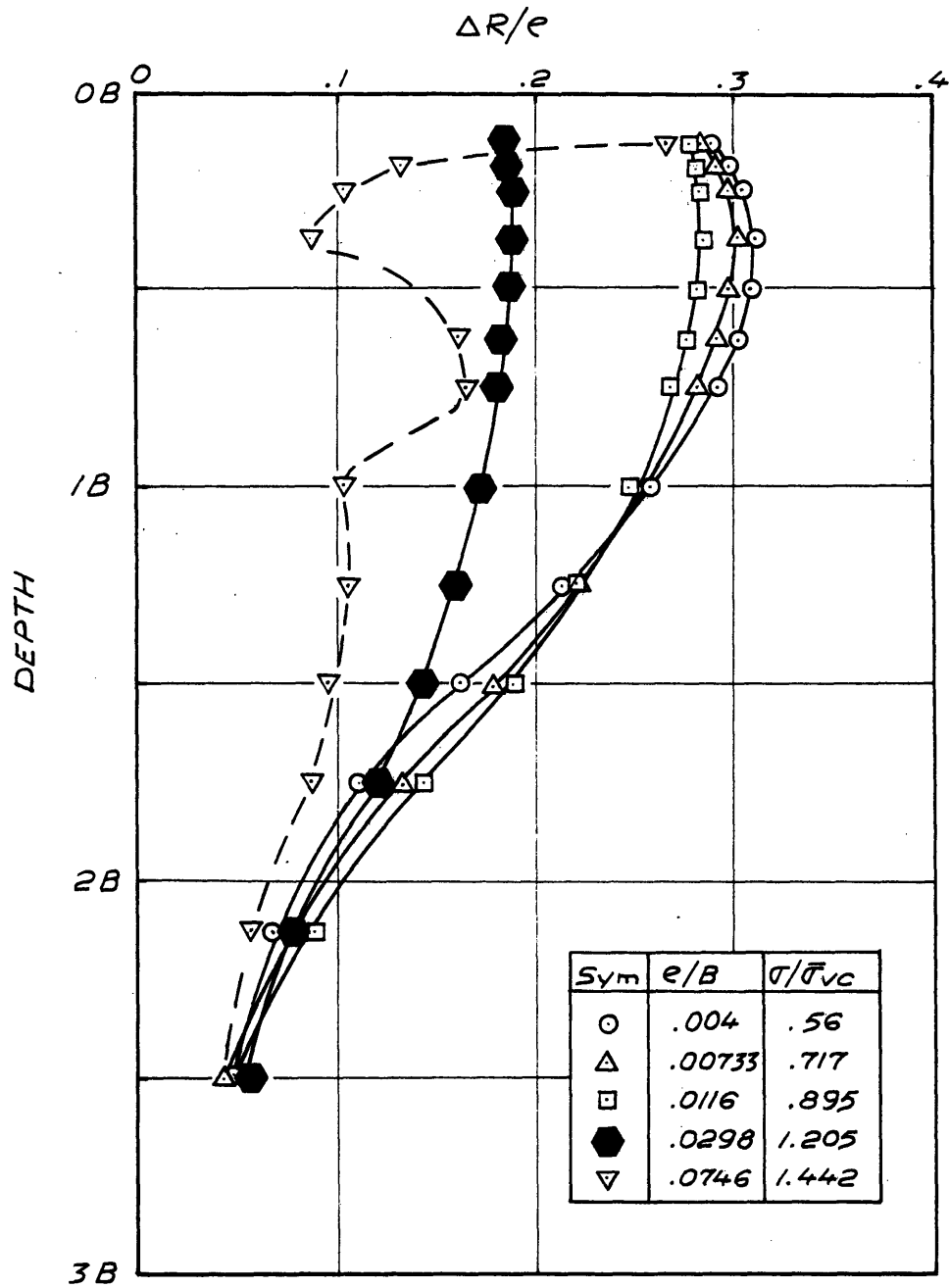
FIGURE G-10



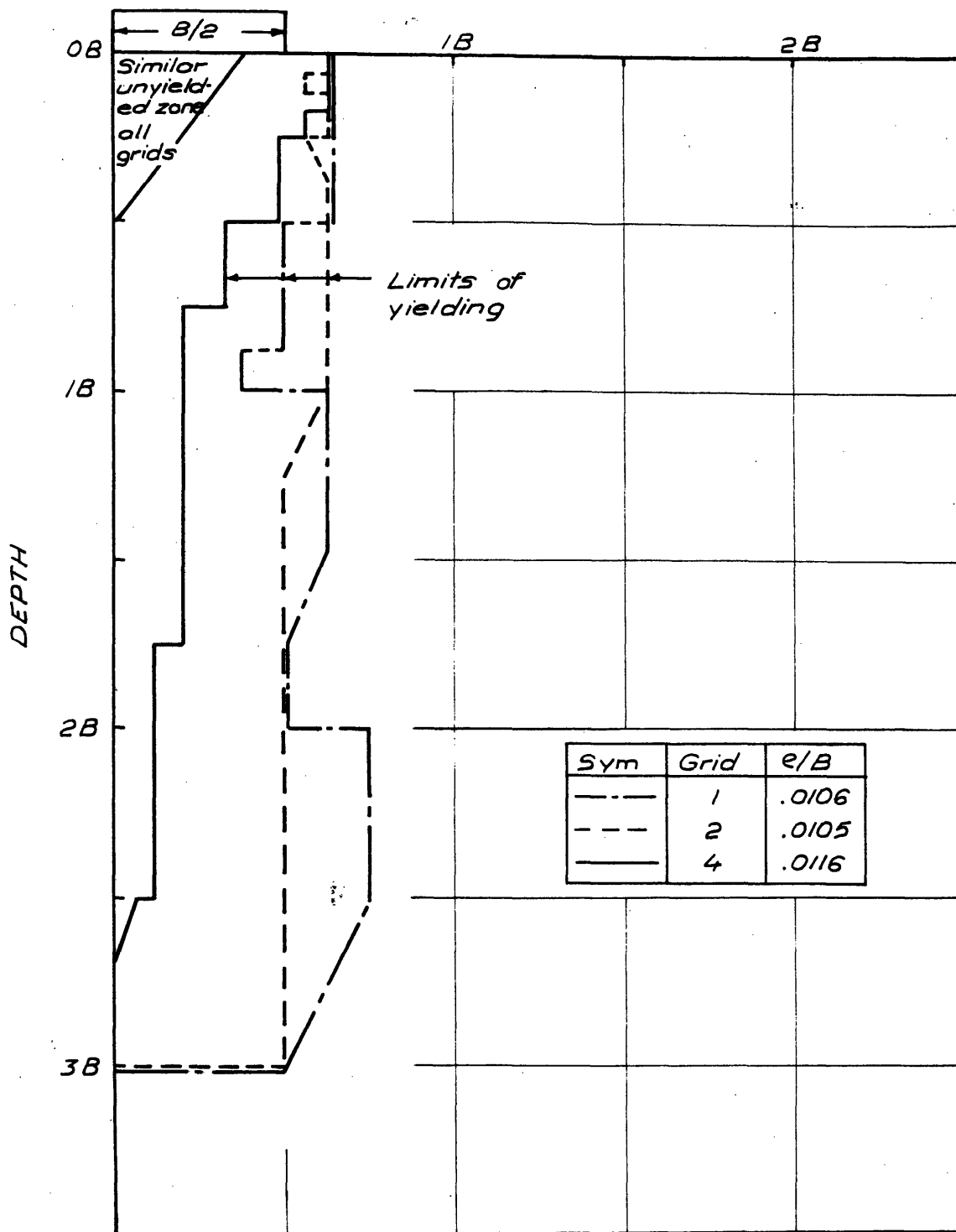
NORMALIZED LATERAL DISPLACEMENT WITH DEPTH
FOR NODES B/4 FROM SIDE OF FOOTING, GRID I



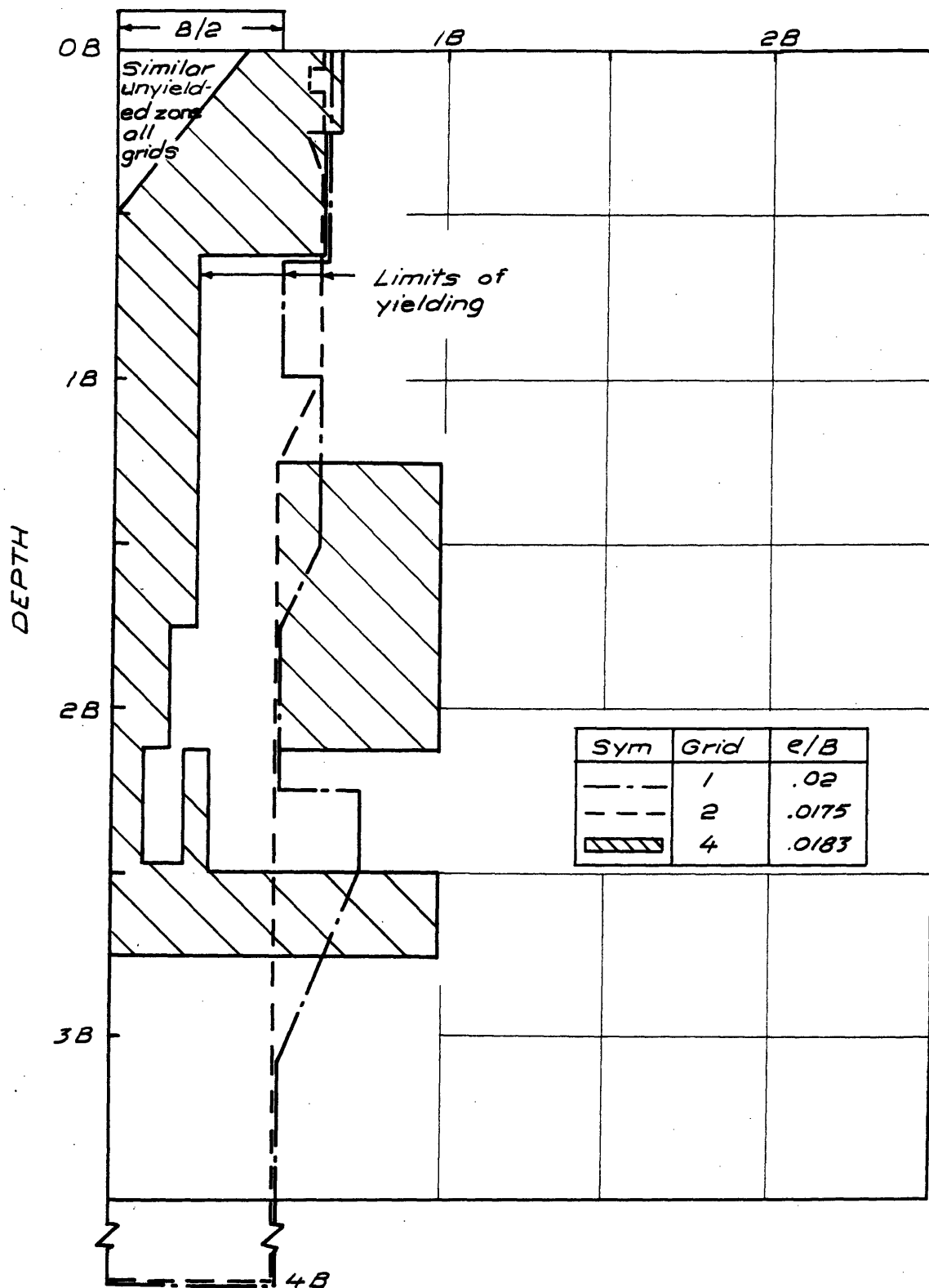
NORMALIZED LATERAL DISPLACEMENT WITH DEPTH
FOR NODES B/4 FROM SIDE OF FOOTING, GRID 2



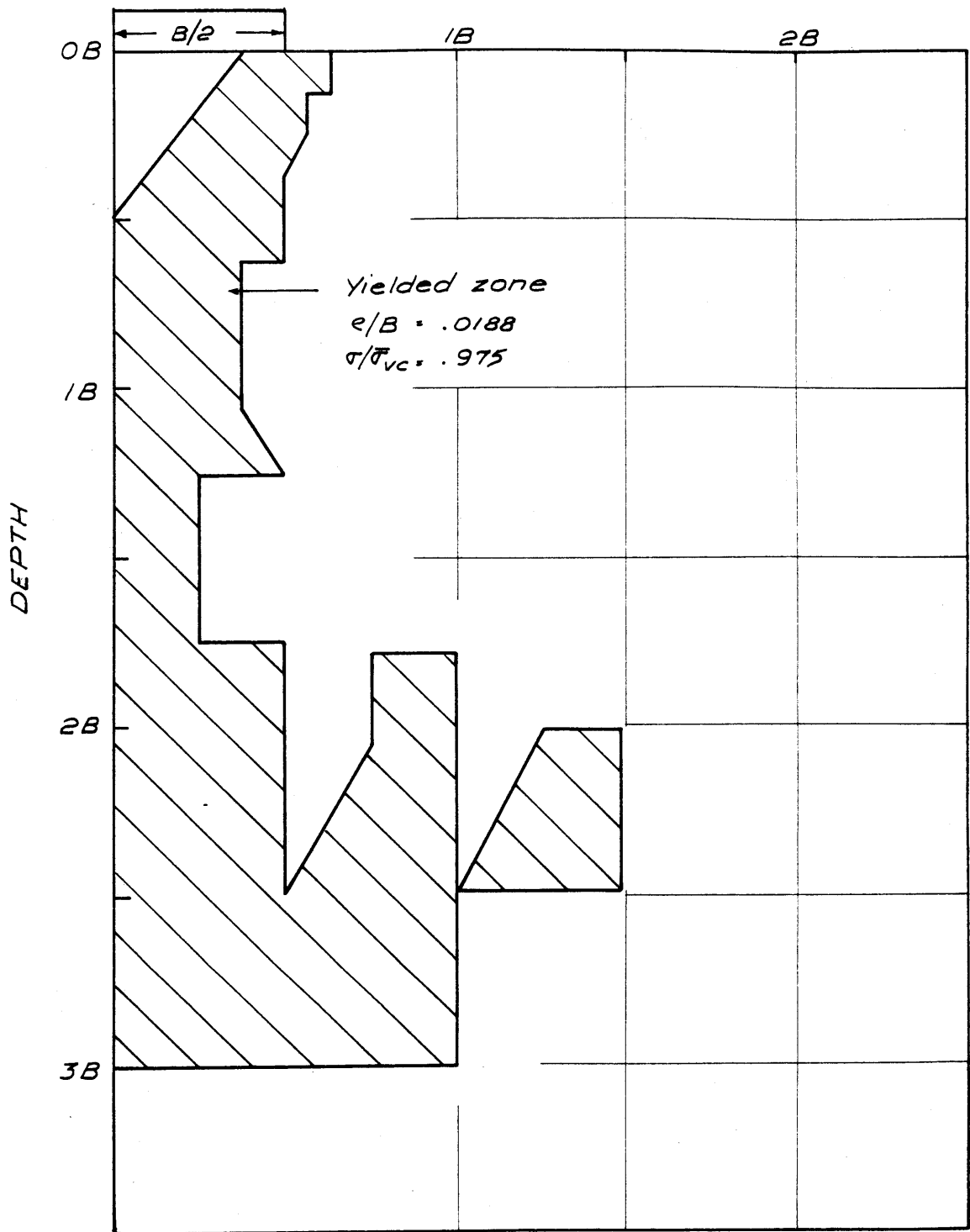
NORMALIZED LATERAL DISPLACEMENT WITH DEPTH
FOR NODES B/4 FROM SIDE OF FOOTING, GRID 4



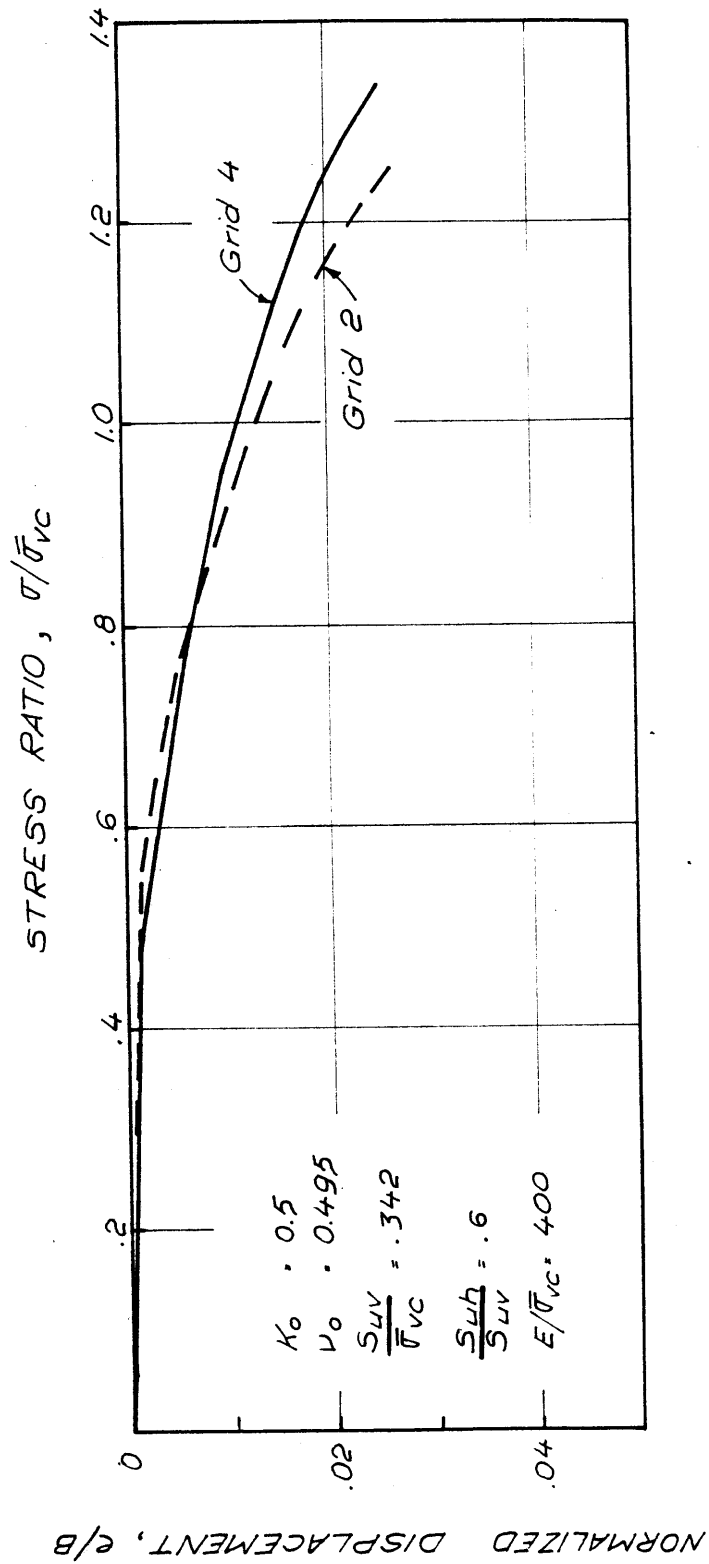
COMPARISON OF YIELDED ZONES FOR THREE FINITE ELEMENT GRIDS AT SIMILAR NORMALIZED DISPLACEMENTS FIGURE G-14



COMPARISON OF YIELDED ZONES FOR THREE FINITE
ELEMENT GRIDS AT SIMILAR NORMALIZED DISPLACE-
MENTS FIGURE G-15

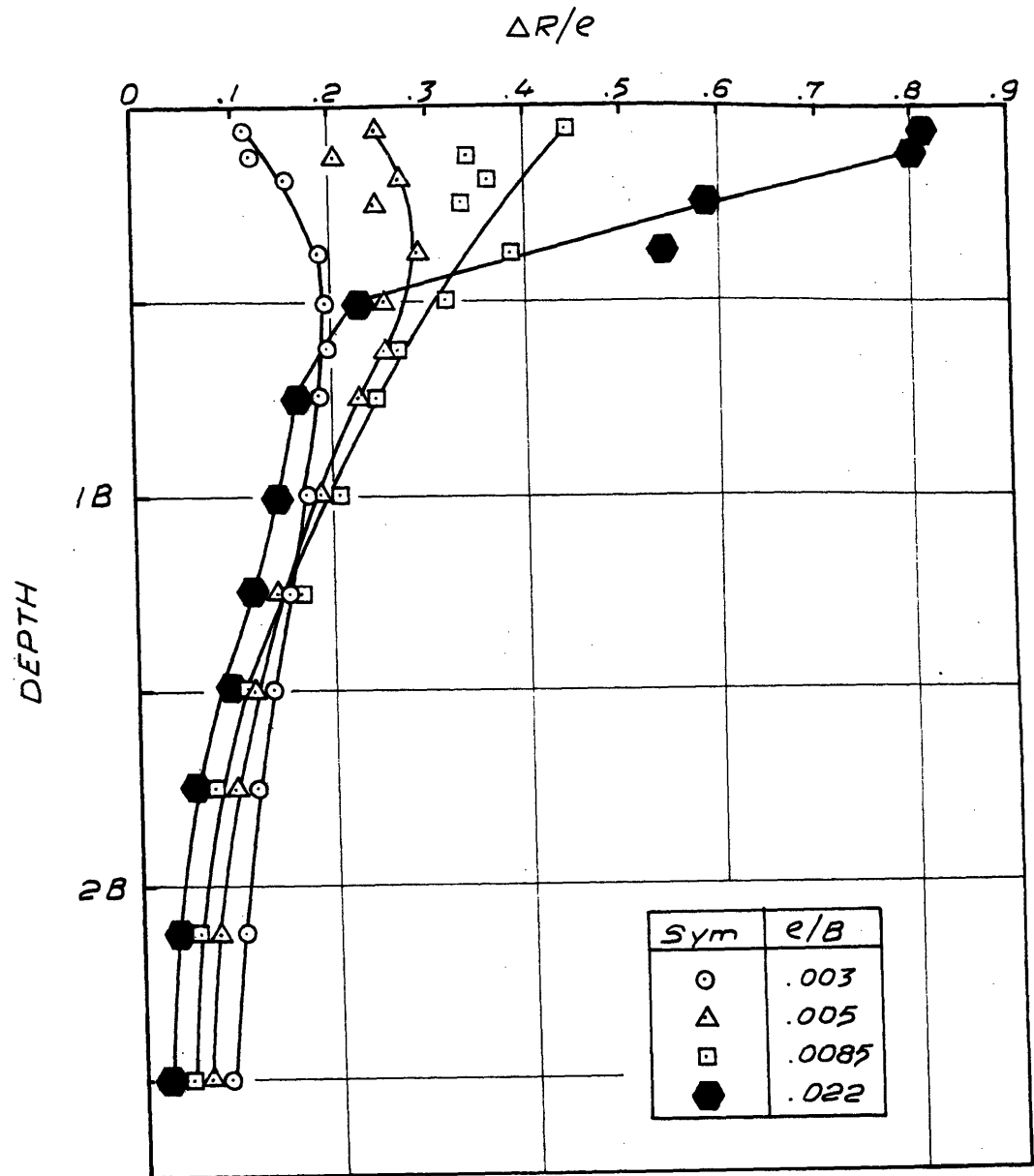


YIELDED ZONE FOR GRID 2 RUN WITH ISOTROPIC UN-
 DRAINED SHEAR STRENGTH

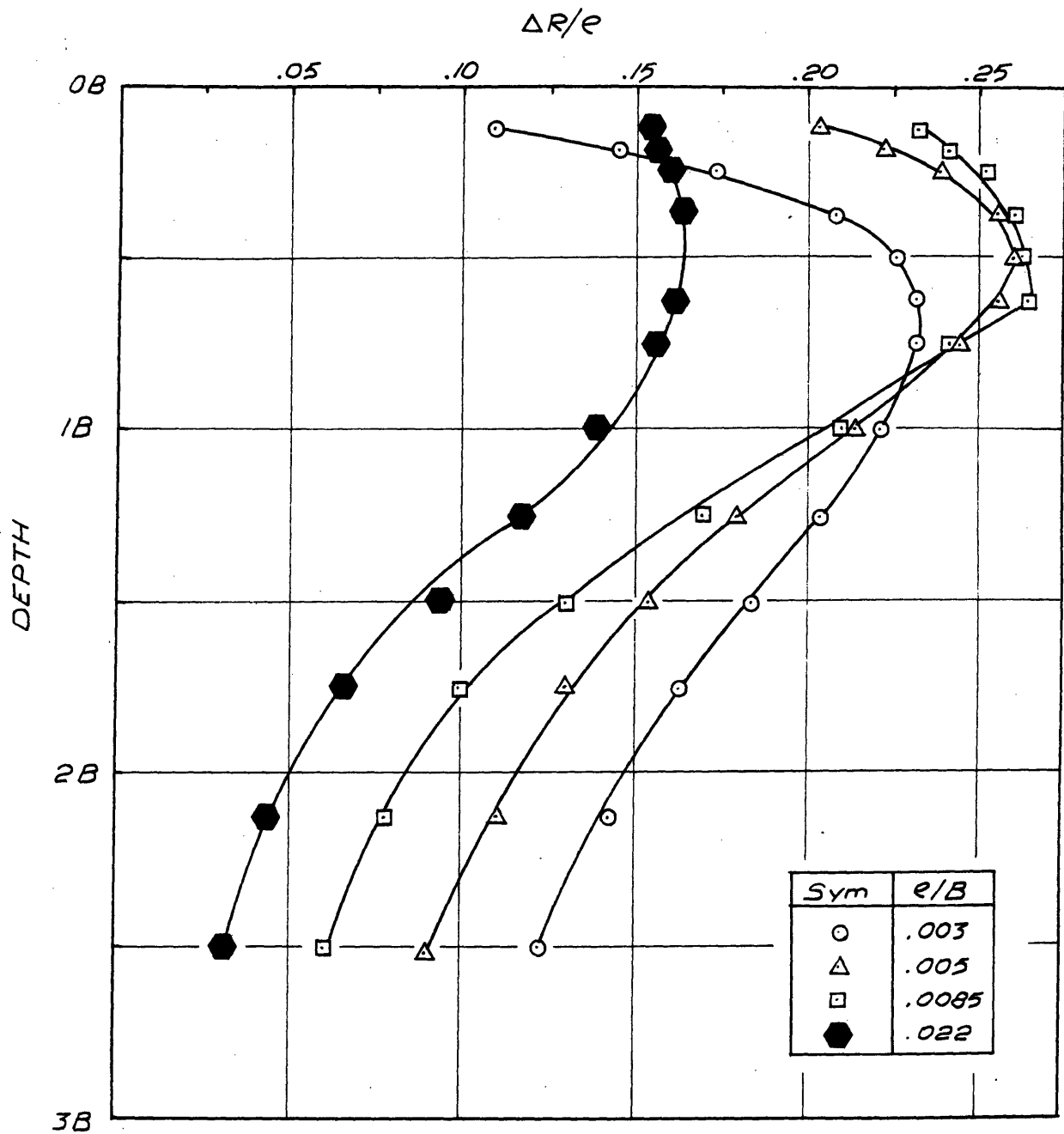


COMPARISON OF FINITE ELEMENT PREDICTIONS OBTAINED WITH DIFFERENT GRIDS USING THE SAME SOIL PROPERTIES

FIGURE G - 17

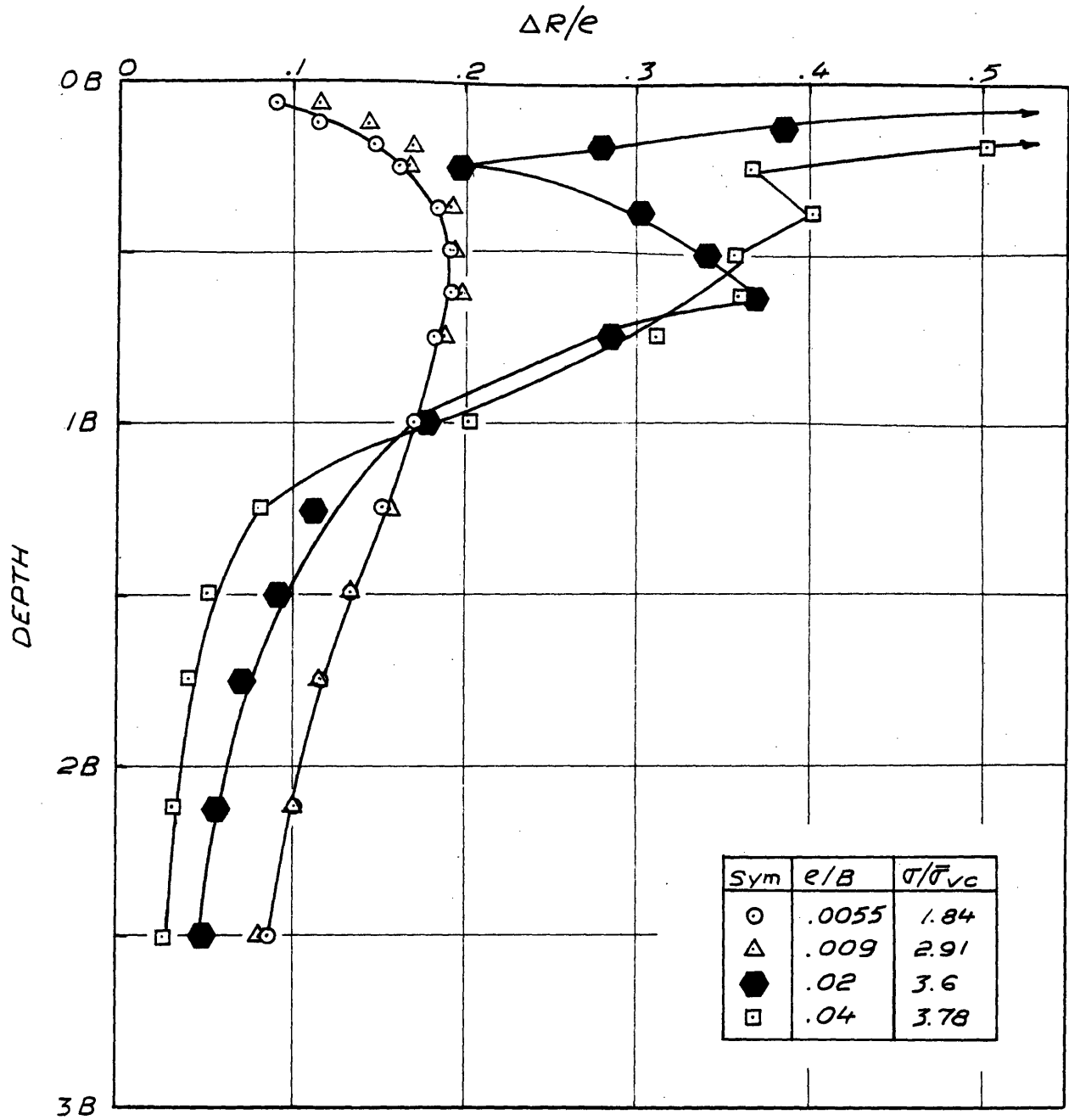


NORMALIZED LATERAL DISPLACEMENTS WITH DEPTH
 FOR NODES UNDER EDGE OF FOOTING, GRID 4,
 OCR = 2

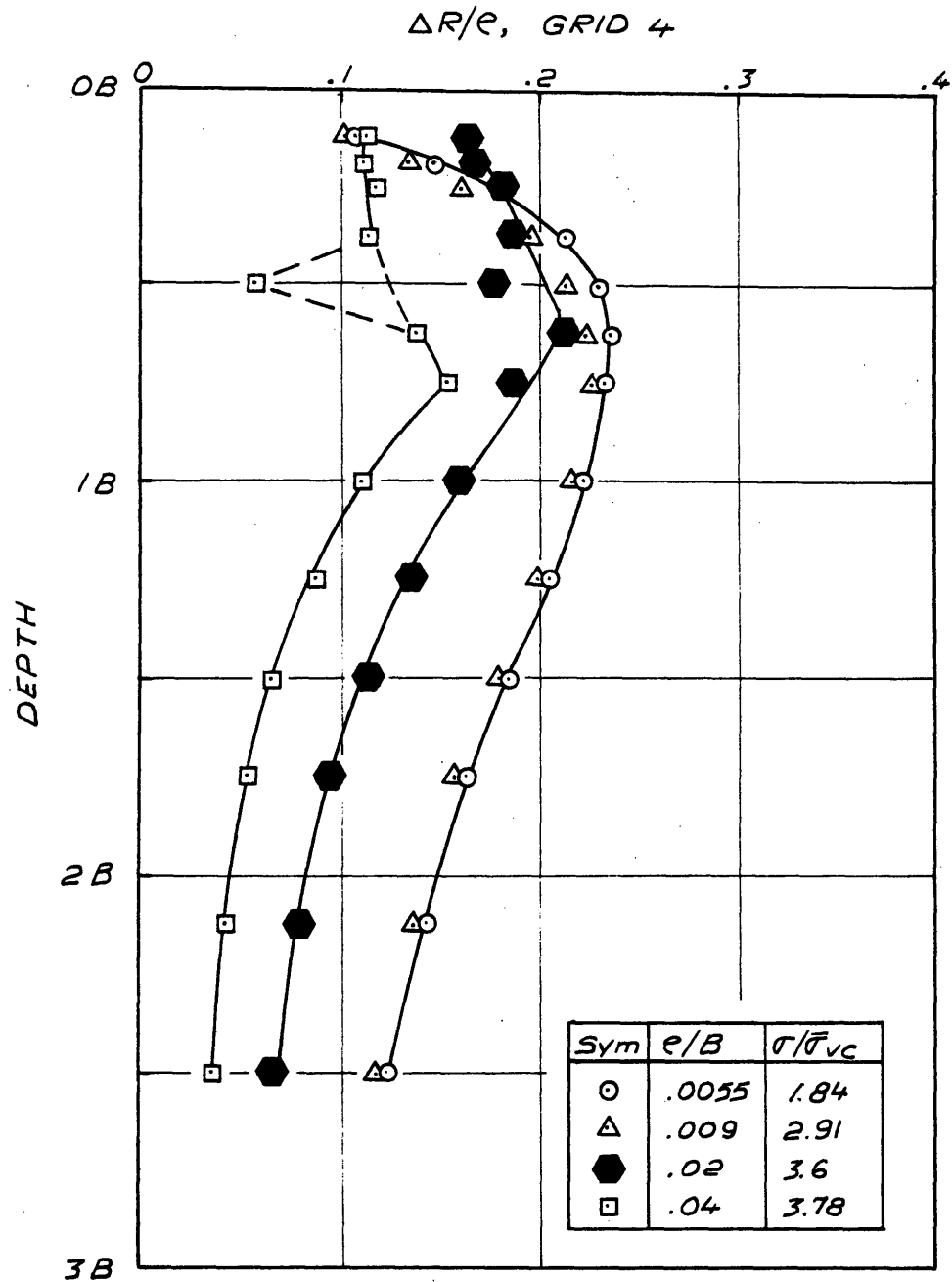


NORMALIZED LATERAL DISPLACEMENT WITH DEPTH FOR
 NODES B/4 FROM SIDE OF FOOTING, GRID 4, OCR = 2

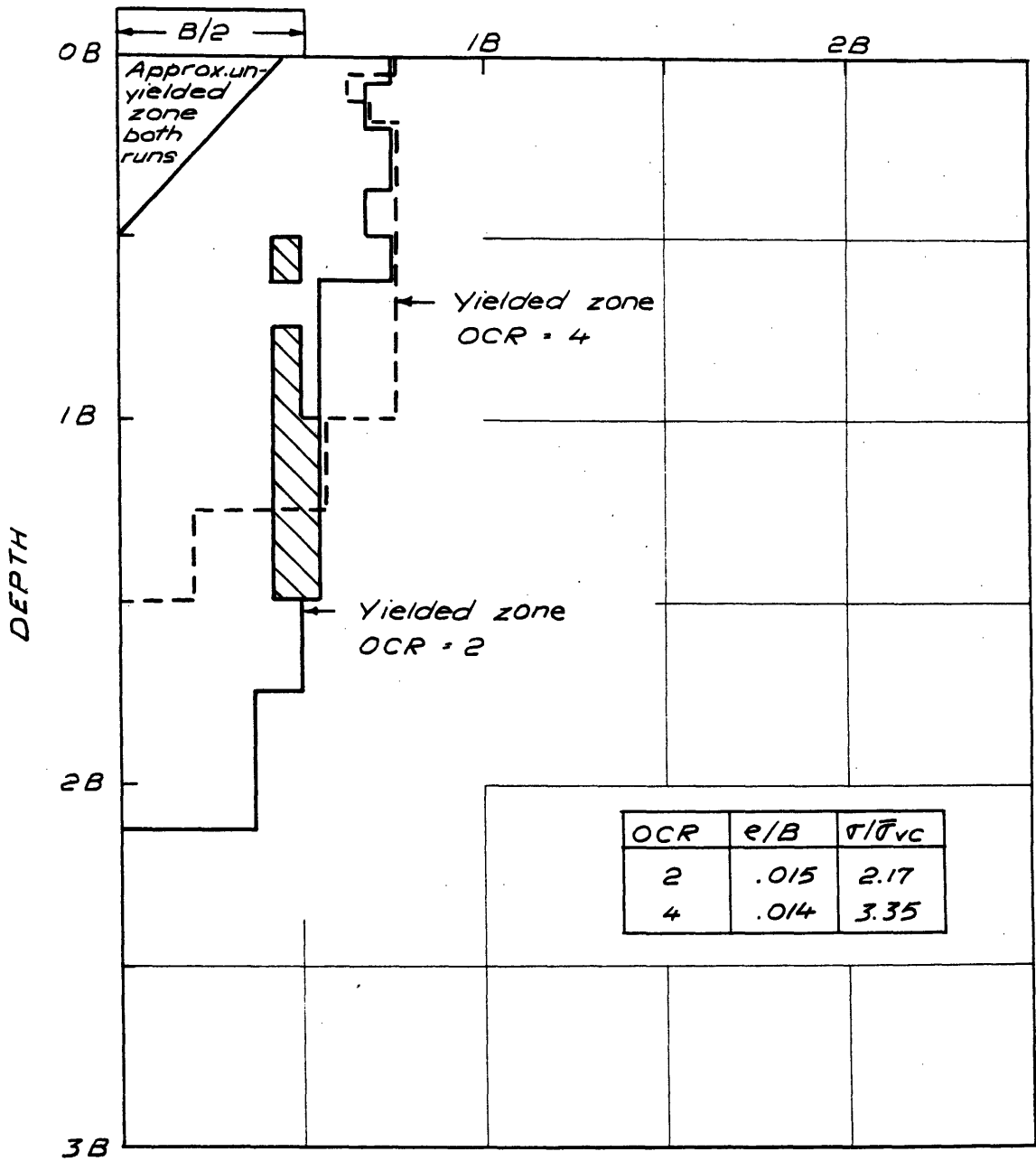
FIGURE G-19



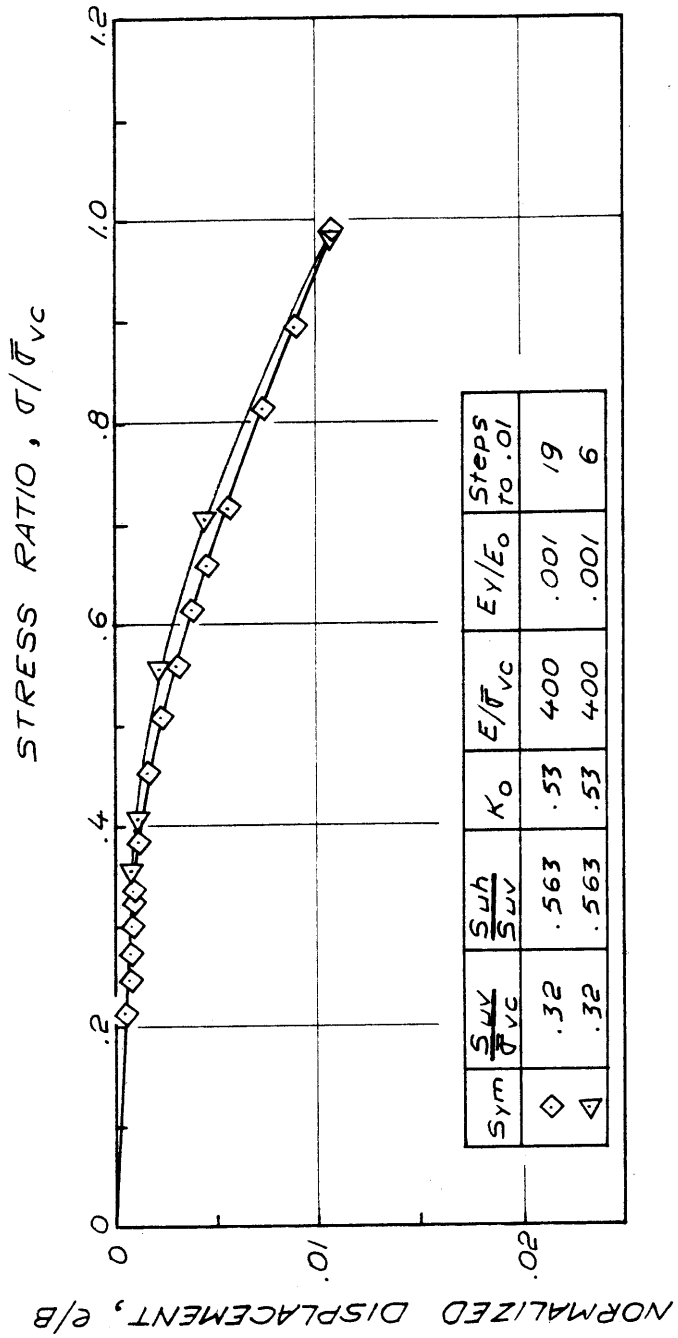
NORMALIZED LATERAL DISPLACEMENT WITH DEPTH FOR NODES UNDER EDGE OF FOOTING, GRID 4, OCR = 4



NORMALIZED LATERAL DISPLACEMENT WITH DEPTH FOR
 NODES B/4 FROM SIDE OF FOOTING, GRID 4, OCR = 4

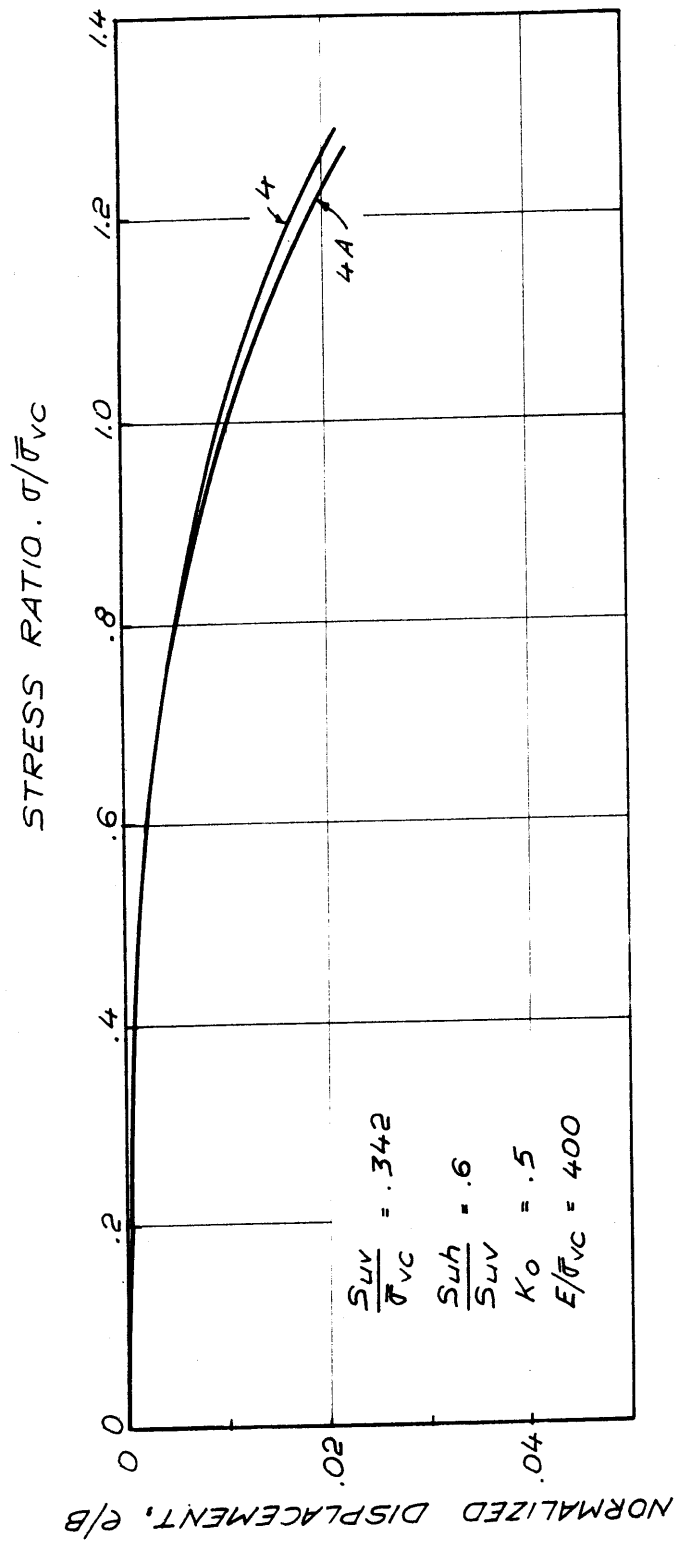


YIELDED ZONES NEAR FAILURE FOR OVERCONSOLIDATED CASES : GRID 4



INFLUENCE OF SIZE OF LOAD INCREMENT ON LOAD - SETTLEMENT PREDICTIONS USING FEAST III

FIGURE G-23



COMPARISON OF FINITE ELEMENT PREDICTIONS OBTAINED WITH GRIDS
4 AND 4A

FIGURE G - 24

BIOGRAPHICAL NOTE

Edward B. Kinner was born on July 15, 1939, in Herkimer, New York. He attended public schools in Herkimer and Lancaster, New York. He matriculated at Rensselaer Polytechnic Institute in September, 1957, and received the B.C.E. degree in June, 1961. During his four years' undergraduate study at Rensselaer he was the holder of two scholarships, the New York State Regents Scholarship and the U.S. Navy Holloway Plan N.R.O.T.C. Scholarship.

From June, 1961, to June, 1965, he served as an officer in the United States Navy. Assigned to sea duty, he worked in the areas of communications and marine propulsion.

He matriculated at Massachusetts Institute of Technology in September, 1965, and received the S.M. degree in January, 1967. He held a National Science Foundation Traineeship for one year and was a research assistant for the remaining period of his graduate work. He is a member of Sigma Xi and Chi Epsilon honorary societies and the American Society of Civil Engineers.

In addition to his military career his professional experiences include summer employment as a Research Engineer at M.I.T. and Soil Engineer at Haley & Aldrich, Inc. of Cambridge, Massachusetts.